SCALE-UP OF THE SEMI-CONTINUOUS CHROMATOGRAPHIC PROCESS

A Thesis submitted by R. E. Deeble, B.Sc., to the Faculty of Engineering, University of Aston in Birmingham for the Degree of Doctor of Philosophy.

Department of Chemical Engineering
University of Aston in Birmingham.

April, 1974.

Acknowledgements

The Author is indebted to the following:

Professor G. V. Jeffreys and the Department of Chemical Engineering for making available the facilities for research.

Professor P. E. Barker, who supervised the work, for his advice and encouragement.

Dr. A. B. Sunal, a fellow research worker, for many thought provoking discussions on both practical and theoretical aspects of the research topic.

Mr. M. F. Lea for construction of the electronic equipment.

Mr. N. Roberts, Mr. R. G. Evans and other members of the departmental technical staff who assisted in the manufacture and construction of the sequential unit.

Mrs. B. Davies for her diligence in typing this thesis.

The Science Research Council for provision of a scholarship.

Summary

A review is given of the reported experimental and theoretical work which has led to a better understanding of the gas/liquid chromatographic scale-up problem. The potential of several proposed process schemes for production-scale separations is discussed.

Column utilisation can be increased, with respect to the conventional batch process, by employing a counter-current movement between the solute-laden gas stream and the solvent-coated particulate solid to separate a continuous feed mixture into two fractions. A novel unit has been constructed in which this relative phase movement is simulated by sequencing the position of the input and output streams around a closed symmetrical system of twelve, fixed 7.6 cm-diameter columns. Mechanical movement, save the automatically timed opening and closing of proven reliability solenoid valves, has thus been eliminated.

The chemical system chosen for the study of the operating characteristics of the unit was an equivolume mixture of 1.1.2. trifluoro- 1.2.2. trichloro-ethane and 1.1.1. trichloro-ethane. The solvent phase was silicone oil DC 200/50 (25% wt./wt.) coated onto 500-355 m particles of Chromosorb P.

In the separating mode, the effects of the solute mixture feedrate, gas rate and apparent liquid solvent rate were primarily investigated by determination of the on-column concentration profiles. The operating limits for a successful separation were shown, in keeping with theory, to be reduced by both a concentration dependent absorption isotherm and column pressure drop. Measured H.E.T.P. values lay in the range 0.7 to 2.0 cm, the average value increasing with both solute concentration and gas

flowrate. Typically, purities in excess of 99.7% for both products have been achieved up to a feedrate of 0.7 $dm^3\ hr^{-1}$.

A computer simulation of the process scheme has been written which incorporates the concentration and pressure effects. The predicted and experimental concentration profiles are compared.

CONTENTS

CHAPTER 1

Introduction

Chromatography originates from the work of Tswett in 1906 (1) and Martin and Synge in 1941 (2). However it has been in the two decades following the successful demonstration of elution gas/liquid chromatography by James and Martin (3) that the technique has become firmly established as a powerful method for the resolution of chemical mixtures. These researchers packed a 3.35 m long capillary tube with kieselguhr onto which was coated a silicone oil containing 10% stearic acid to act as a solvent phase. Several mixtures selected from the range within the formic to dodecanoic members of the volatile fatty acid series were then injected into a stream of nitrogen flowing through the packed column. The resultant continuous absorption and desorption process caused the respective solutes to progress at different rates through the column. Separate 'peaks' were therefore monitored on elution of each acid in the injected mixture.

With the increasing demand for pure chemicals the potential of the chromatographic process not only for analysis but also as a separation technique at commercially viable throughputs was quickly realised. In 1955 Evans and Tatlow (4) published their work on the fractionation of fluorinated hydrocarbons in gram quantities on a 3 cm-diameter column. By 1969 the separation of m-xylene and p-xylene at a combined production rate of 45 million kg yr^{-1} on a 4.3 m diameter column was being proposed (5).

The technique is still not fully established amongst the range of separation processes available to the chemical engineer. Early optimism, which led to the use of such terms as 'production' and

'plant-scale' gas chromatography, has been tempered by the problem commonly associated with mass transfer operations; the resolving power is reduced with both increasing column diameter and throughput. Indeed it is this fact which has favoured the more rapid development of the technique for analysis.

Overcoming the inherent restriction on scale-up has provided a challenge to research workers. The various approaches pursued to improve large-scale column efficiency and increase column utilisation can be characterised by the three notional ways the gas and solvent phases may be moved to effect the relative direction of flow of the solutes; (i) co-currently, (ii) cross-currently and (iii) counter-currently.

(i) The most direct approach to scale-up is to increase the size of the analytical column in diameter and/or length. The solvent phase remains stationary while the gas phase flows through the column carrying the solutes. Provided separating efficiency can be maintained at a reasonable level, resolution of the injected feed into its multiple constituents is possible. Research and development work has concentrated on column design and packing techniques so now acceptable efficiencies can be achieved. However, throughput is still restricted by the batch nature of the process, a restriction only partially counteracted by the use of periodic injections of smaller volume.

(ii) The cross-flow mode of operation appears very attractive. Theoretically the movement of the gas phase and solvent phase at right angles to one another should enable the attainment of a continuous

'spectrum' of products as a consequence of the different resultant component velocities. Although several novel designs have been proposed to achieve this concept, none are amenable to large-scale operation.

(iii) The continuous fractionation of a feed mixture into two components or into two mixtures of different composition can be achieved by a counter-current movement, within limits set by solubility considerations, of the solvent and the gas phase. For a centrally located feed the solute(s) with least affinity for the solvent will be preferentially carried to the gas outlet while the solute(s) more strongly absorbed onto the solvent will move preferentially in the direction of the packing. The attraction of the application of counter-current chromatography at the production-scale is the prospect of higher throughputs for a given dimensioned column. The feed is continuous, utilising all of the available separating power of the column. Further, within the column, the respective component concentration profiles need only be partially offset to permit collection of resolved products at the column exits. This feature allows severe overloading by conventional batch chromatographic standards.

Following the pioneering work of Pichler and Schultz (6) and Scott (7), Barker and co-workers have actively developed this latter process (8 - 21). Its viability has been demonstrated by the successful fractionation of several mixtures of widely varying separation difficulty, including isomers and heat sensitive materials. A typical example was the recovery of 91% of 99 +% alpha-pinene from a crude turpentine feed (essentially a mixture of α-pinene, β-pinene and camphene) at a throughput of 66.5 cm^3 hr^{-1} on a 2.5 cm-diameter column (20).

As will be discussed in Section 2, during the development period until 1970 the form of the equipment used by Barker et al underwent several changes to overcome mechanical problems and improve resolving power. However, the largest column diameter utilised was 3.8 cm. The logical step was to increase this value, a step demanding a novel mechanical approach.

In originating the proposed new chromatographic separation unit the design was to be adaptable to any column dimension as well as mechanically reliable. Once constructed, the operating characteristics were to be investigated. In particular the importance of such parameters as the respective component absorption isotherms on the limitation of throughput were to be studied.

From the experimental observations a theoretical model of the process was to be attempted. Being akin to other counter-current mass transfer processes, either the traditional plate or transfer unit modelling approaches could be adapted to the development of a design procedure.

CHAPTER 2

Literature Survey

2.1 Scope

A measure of the spectacular growth of interest in the general field of chromatography following the work of James and Martin in 1951 (3) is given by the number of publications relating to the subject. Within a decade the number was approaching two thousand per annum and has continued to increase. The majority of these papers are concerned with analysis. Hence, after the introduction of the basic terminology and concepts, whose origins inevitably lie in the analytical field, this survey will necessarily be restricted to the application of gas/liquid chromatography as a chemical separation technique.

The problems which have faced those wishing to scale-up the basic chromatography process will be discussed in the light of theoretical knowledge. This will be followed by a section contrasting the practical solutions which have been developed, paying particular attention to their scale-up potential.

2.2 Basic Terminology and Relationships for Gas/Liquid Chromatography

The following subsection has been included to provide a basic understanding of the subject area. Further details may be found in several general texts (22, 23, 24, 25).

2.2.1 The Basic Process

Resolution is achieved in chromatography as a consequence of the different affinities of individual solutes within a mixture for a common solvent. In gas/liquid chromatography the non-volatile liquid solvent - the 'stationary phase' - is coated onto a particulate solid - the 'solid support'. The solutes are then brought into repeated contact with the solvent by 'carrying' them through the coated 'packing' in an inert gas stream. Solute zones are formed which move at a fraction, R, of the carrier gas velocity to be eluted in the order of least retarded first. At infinite dilution R may be defined as (23):-

(a) The relative solute band migration rate

(b) The probability that a solute molecule is in the gas phase

(c) The limiting fraction of time a molecule spends in the gas phase

(d) The fraction of molecules in the gas phase at equilibrium

The precise value of R applies only to the centre of the solute band; i.e. true equilibrium between the solute in the mobile and stationary phases occurs only at the point of maximum concentration in the migrating zone.

Figure 2.1 An Example of an Analytical Chromatogram

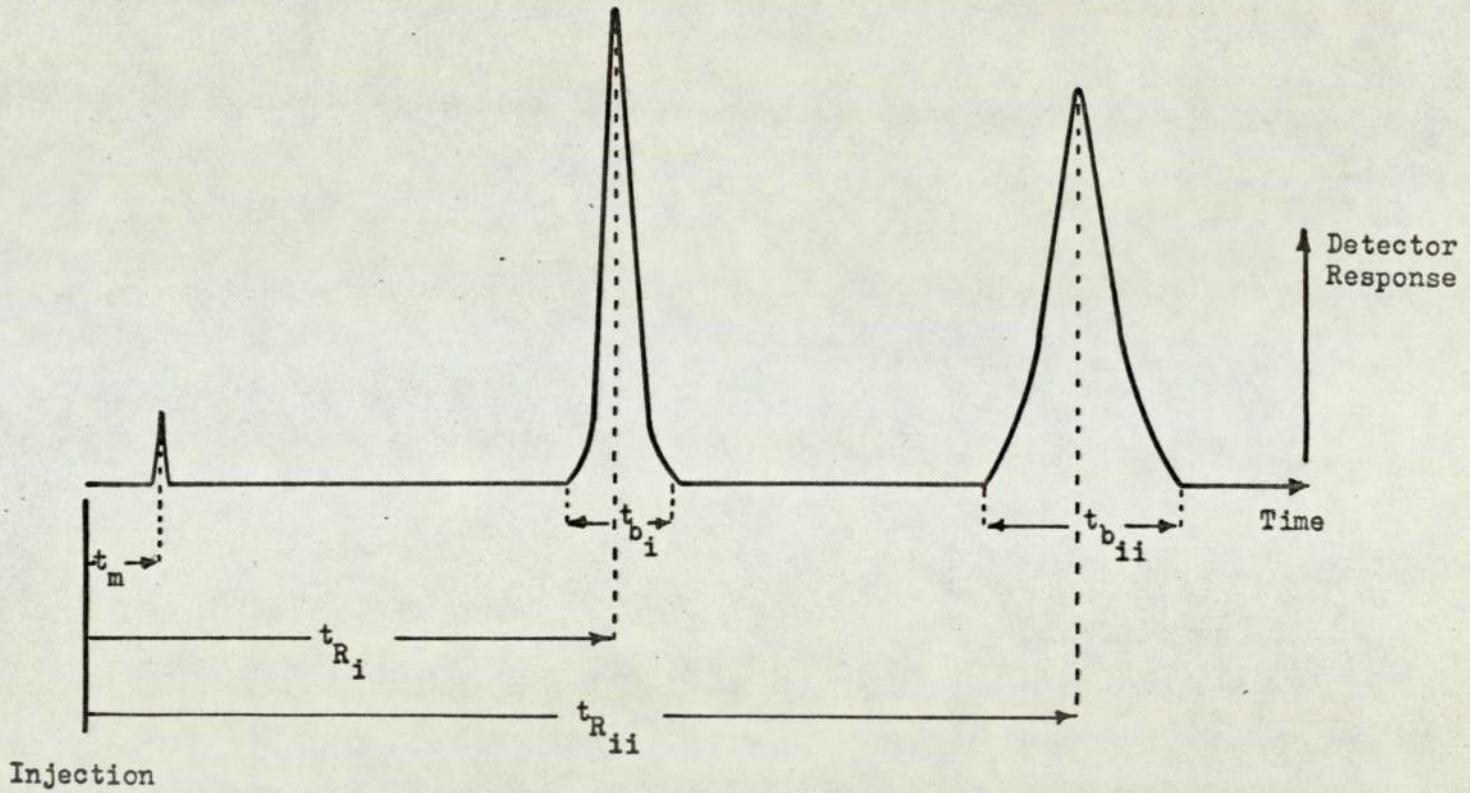

The chromatogram (elution curve) shown in Fig 2.1 is that obtained for two fully resolved components, i and ii, using a thermal conductivity cell - 'katharometer' - as detector. The first small peak is obtained for unabsorbed gas, often referred to as the 'air peak', while the second and third peaks have undergone the chromatographic process.

Thus: t_m = 'elution' or 'retention time' for an unabsorbed component and is therefore a measure of the gas hold-up in the column; i.e. the total interparticle volume in the column.

t_R = 'elution' or 'retention time' for a component.

t'_R = 'adjusted retention time'.

= $t_R - t_m$ and is therefore a measure of the effect of the chromatographic process on a component.

It should be noted that t_R and t_m include a contribution from the extra column apparatus, the injection and detection system, the sum of which is designated as the 'dead' time, t_D.

The respective times can be related to volumes through the gas phase velocity or flowrate. The average velocity of the carrier gas depends on the compressibility of the carrier gas in the column. To correct for the pressure gradient the 'compressibility factor', j, first deduced by James and Martin (3), is used.

$$j = 1.5 \, (P_{io}^{\,2} - 1) \, / \, (P_{io}^{\,3} - 1) \qquad 2.1$$

where P_{io} equals the ratio of inlet to outlet column pressures.

Hence the 'corrected retention volume', V_R^o, can be calculated from:

$$V_R^o = F \cdot \frac{T_c}{T_a} \cdot \frac{P_o}{P_a} \cdot j \cdot t_R \qquad 2.2$$

where : F = flowrate measured at ambient conditions

T_c = column temperature

T_a = ambient temperature

P_o = column outlet pressure

P_a = ambient pressure

The 'partition' or 'distribution coefficient', K, is defined as the equilibrium ratio of the solute concentration in the liquid solvent phase to the concentration in the gas phase. Hence it is a measure of the slope of a chord to the absorption isotherm, $\frac{q}{c}$. Generally, for analytical gas chromatography, the concentrations are sufficiently low to make the assumption of a linear 'absorption' or 'partition' isotherm realistic and the partition coefficient can be well approximated by the slope of the curve itself.

As the solutes can only progress through the chromatographic column when in the gas phase, K can be expressed in terms of measured volumes as

$$K = j.\frac{V_R'}{V_L} = \frac{V_R^o - V_G}{V_L} \qquad 2.3$$

where : V_G = the volume of the gas phase in the column = jV_m

V_L = the volume of the liquid phase impregnated on the support.

From a previous definition of the retention factor, R, K can also be expressed as

$$K = \frac{1 - R}{R} \qquad 2.4$$

Thus the partition coefficient is a measure, independent of the column on which it is measured, of the affinity of a solute for a solvent. It can therefore be used to define the potential resolution between two solutes i and ii, the 'separation factor'.

$$\text{Separation factor} = \frac{K_{ii}}{K_i} \qquad 2.5$$

It is customary to place the larger value of K in the numerator. As the separation factor approaches one the separation becomes more difficult.

While attention has been focussed on the most common elution technique, other forms of chromatography are possible. In particular should be mentioned 'frontal elution' chromatography, first applied to gas/liquid systems by Phillips et al (26, 27). Rather than a discrete sample, the solutes are continuously fed into the flowing carrier gas stream. The selective retardation process results in a chromatogram consisting of a successive series of 'S'-shaped steps, each step representing break through of a component in the feed. While this technique has little application for analysis it is important to both the study of concentration effects on resolution and large-scale separations.

2.2.2 Basic Theories

Two factors are important in determining whether a separation is obtained in elution chromatography:

(i) The centres of the solute zones should be as far apart as possible.

(ii) The zones must be kept narrow to eliminate or reduce overlap. The former, as shown above, is related to thermodynamic equilibrium. The latter is a function of column dynamics and it is this which the theories of chromatography attempt to define.

2.2.2.1 The Theoretical Plate Concept

Considering a mass transfer process as a series of theoretical plates or equilibration stages is a well established procedure. It is, therefore, not surprising that such a model was used for the first description of gas/liquid chromatography by James and Martin (3). The column was considered to consist of a series of discrete volumes, or plates, "such that the solution issuing from it is in equilibrium with the mean concentration of solute in the non-mobile phase throughout the layer". The mobile gas phase was regarded as discontinuous, consisting of a stepwise addition of volumes of mobile phase, each equal to the free volume per plate.

Two further fundamental assumptions were made:

(i) The partition coefficient was constant throughout the column, being independent of concentration; i.e. a linear absorption isotherm was assumed.

(ii) The exchange process was thermodynamically reversible. This implies that the equilibrium between solute and solvent was instantaneous - the mass transfer coefficient was infinitely high - and

diffusion processes could be ignored.

These assumptions have led to the use of the term 'linear ideal chromatography' for this type of model.

An equation was derived relating the concentration of solute to the plate number along the column, which allows calculation of the shape of the elution curve.

$$Q_{n+1} = \frac{1}{\sqrt{2 \cdot \pi \cdot n}} \cdot \left(\frac{V^o}{V^o_R} \right)^n \cdot e^{n\left(1 - V^o/V^o_R\right)} \qquad 2.6$$

where : Q_{n+1} = quantity of solute on $(n+1)$th plate

n = plate number from injection point

V^o = corrected carrier gas volume to plate n

V^o_R = corrected retention volume.

Gluekauf (28), by reducing the discrete volumes to infinitely small dimensions, derived a continuous model. The distribution of the eluted curve was found to be of the Poisson type which, as was subsequently pointed out by Van Deemter et al (29) and Young (30), could be approximated by a Gaussian distribution if the number of plates, N, was sufficiently large (say greater than 100).

The effect of the stagewise operation on the single pulse injection is, in the ideal case, to spread the solute zone into a Gaussian distribution curve, a curve characterised by the second moment or variance, σ^2. Therefore the height equivalent of a theoretical plate, H.E.T.P., can be considered as the rate of increase of the second moment per unit length of column.

$$H = \frac{l}{N} = \frac{d(\sigma_l^2)}{dz} \qquad 2.7$$

where (σ_l^2) is the length-based second moment and z is a measure of distance along the column of length l. An efficient column results in a narrow peak.

This may be related to the chromatogram presented as figure 2.1 as follows. The concentration/time profile has a standard deviation of σ_t in time-based units.

$$\text{Now} \qquad \sigma_t = \frac{\sigma_v}{R} = \text{appearance time for 1 standard deviation} \qquad 2.8$$

$$\text{Thus} \qquad N = \frac{l^2}{(\sigma_l)^2} = \frac{l^2}{(\sigma_t)^2 \cdot R^2} \qquad 2.9$$

But 1/R equals the elution time, t_R.

$$\text{Therefore} \qquad N = (t_R/\sigma_t)^2 \qquad 2.10$$

Considering the width of the peak at the base to be 4 σ_t, then

$$N = 16\left(\frac{t_R}{t_b}\right)^2 \qquad 2.11$$

The semi-empirical plate-theory has been superseded by models which include consideration of the fundamental mass transfer processes occurring within the chromatographic column. However, Klinkenberg and Sjenitzer (31), adopting a statistical approach, showed that the various factors contributing to band spreading, such as diffusion in both the gas and liquid phase and a finite mass transfer rate, could be individually described by the second moment of a Gaussian distribution.

A property of this quantity is that it is additive to give the total second moment of the eluted peak. H.E.T.P., although a misnomer, has remained as the term describing column efficiency.

2.2.2.2 Rate Theories

The idealised reversible process considered in the plate model is unattainable in practice. Van Deemter, Zuiderweg and Klinkenberg (29) developed a theory accounting for the contribution of certain, rate determining, kinetic processes to the diffuseness of solute bands. Individual terms for the effect of longitudinal diffusion in the gas phase, eddy diffusion resulting from the inhomogeneity of the packing and a finite rate of mass transfer(preventing the instantaneous attainment of equilibrium at all points on the solute curve)were combined to give the following equation for H.E.T.P.

$$H = 2\lambda . d_p + 2\gamma' . \frac{D_G}{u} + \frac{8}{\pi^2} \cdot \frac{k \cdot d_f^2 \cdot u}{(1+k)^2 . D_L} \qquad 2.12$$

where λ = eddy diffusivity factor; i.e. a characteristic quantity of the packing

d_p = mean particle diameter

γ' = labyrinth factor; i.e. factor to allow for the tortuous nature of the gas flow-path

D_G, D_L = molecular diffusivities in gas and liquid phases

u = interstial gas velocity

d_f = effective thickness of liquid film coating support

k = $F_g / K F_L$ = mass distribution coefficient or capacity ratio

F_G, F_L = fractional volume of a plate occupied by gas and liquid.

This equation is commonly written for simplicity as

$$H = A + \frac{B}{u} + C_L.u \qquad 2.13$$

where A = eddy diffusion term

B = longitudinal gas phase diffusion term

C_L = mass transfer resistance term, the liquid phase being assumed controlling for this model.

A review of the experimental determination of the terms in equations 2.12 and 2.13 has been given elsewhere (15, 22).

Since 1955 this basic equation has been extended and/or modified by many workers. Van Deemter (32) added an additional term to allow for the contribution to the plate height made by resistance to mass transfer in the gas phase. After Golay had developed the theory of capillary columns (33), Purnell (22) further modified the gas phase term to emphasise the effect of radial diffusion. The resultant equation was

$$H = 2\lambda.d_p + 2\gamma'.\frac{D_G^{\,o}}{u_o} + \frac{2}{3}\left[\frac{k.d_f^{\,2}}{(1+k)^2 D_L}\right]\bar{u} + \left[\frac{1 + 6k + 11(k)^2}{24(1+k)^2}\right] \times \left[\frac{d_p^{\,2}.X}{D_G^{\,o}}\right] u_o \qquad 2.14$$

where:

$D_G^{\,o}$ = gas phase diffusivity at column outlet pressure

u_o = gas velocity at outlet pressure

$\bar{u}$ = mean gas velocity; i.e. gas velocity corrected for compressibility

X = characteristic of packing interstices.

or, more simply,

$$H = A + \frac{B_o}{u_o} + C_L\bar{u} + C_G^{\,o}\,u_o \qquad 2.15$$

After studying the elution of acetone and benzene in nitrogen and hydrogen from columns containing three different 'Sil-O-Cel' support particle sizes (320, 160, 100 μm) coated with 20 per cent by weight polyethylene glycol, Bohemen and Purnell (34) concluded that $\lambda = 0.75$, $\gamma' = 1$ and $\chi = 1.5$.

An extensive theoretical study of chromatography has been undertaken by Giddings which is summarised in his, now standard, text (24). A stochastic approach - the 'random walk model' - gave an equation similar in form to equation 2.12. It differed only in that the labyrinth factors λ and γ' did not occur. A more rigorous approach - the 'generalised non-equilibrium theory'- was then developed. The basis of this theory is as follows.

Only the centre of the band moving through the chromatographic column represents true equilibrium between solute in the respective gas and liquid phases. As the rate of migration is proportional to the fraction of solute molecules in the gas phase, then the band is continually being widened by the velocity divergence within its boundaries. This local non-equilibrium can be described in terms of an effective diffusion coefficient, which can be used to determine the mass transfer, 'C', terms in equation 2.15.

Both the mass balance approach of Van Deemter et al and the random walk method depend on the additivity of the variance contributions of each term to the plate height. The implied

assumption is that all band spreading processes can be regarded as independent. However, it is believed that eddy diffusion and gas mass transfer effects are interdependent. Giddings (24), through his non-equilibrium approach, was able to introduce a 'coupling theory', the two effects being considered as acting in parallel. The simplified form of the extended rate equation was

$$H = \frac{1}{1/A + 1/\bar{C}_G\bar{u}} + \frac{\bar{B}}{\bar{u}} + C_L\bar{u} \qquad 2.16$$

The experimental results of Harper and Hammond (36) were most accurately described by this theory.

A strong theoretical base for the understanding of the operation of an analytical gas/liquid chromatographic column has been established. While values for the various constants in the expressions can be calculated from the chromatographic results themselves, it has recently been shown by Bethea and Bentsen (37) in an evaluation of nine plate height equations that prediction of H.E.T.P. purely from physical parameters is not generally accurate. In particular, satisfactory correlations for C_L and the complex gas phase flow pattern remain elusive.

The form of the equations presented do provide a guide to maximising analytical column performance; i.e. minimising the measure of the width of the eluted peak, H.E.T.P.

(i) Considering equation 2.13. As the value of the carrier gas velocity is increased from zero, it passes through a minimum (see Fig 2.2). This is a well established experimental fact.

Figure 2.2 Chromatographic Plate Height VS. Carrier Flow Velocity

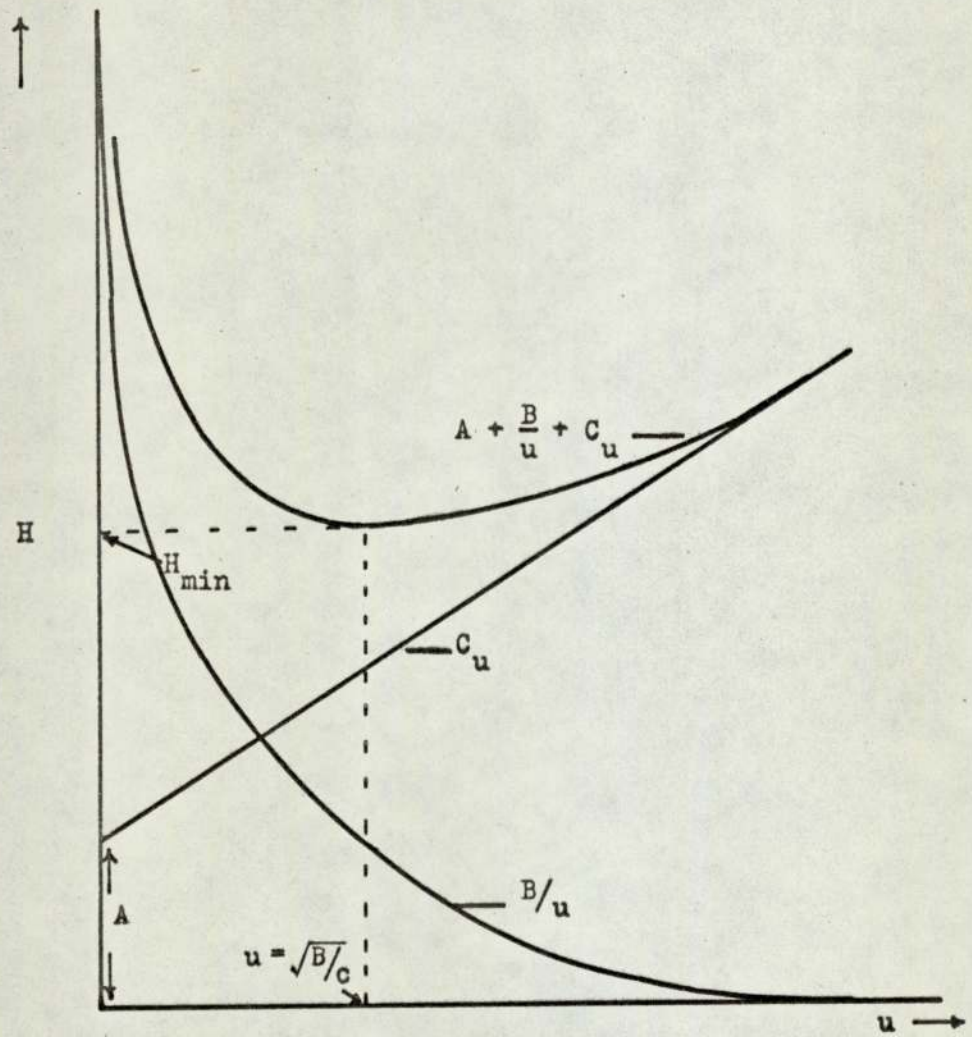

(ii) The particle size and mesh range should be kept at a minimum to reduce eddy diffusion. However, as the particle size is decreased, pressure drop will increase causing an increasing variation in the carrier gas velocity through the column. Only a short column section will be operating at or near the optimum value.

(iii) The particulate solid support should be evenly coated with a very thin film of the liquid solvent. Low solvent loadings can result in active sites on the support surface being free to adsorb the solutes. The resultant 'tailing' of the eluted peaks can be reduced by treatment with such chemicals as dimethyl-dichlorosilane, (D.M.C.S), which neutralises the sites.

(iv) The 'dead' volume, particularly in extra column fittings, should be kept to a minimum to reduce the contribution to H.E.T.P. made by gas phase diffusion.

(v) As the contribution of the C_G^o term is considered to be very much less than the C_L term in the analytical plate height expression, equation 2.15, then the attainable minimum H.E.T.P. is only slightly dependent on the identity of the carrier gas. However, Purnell (22) has shown that the optimum gas velocity increases almost in proportion to D_G^o, offering the possibility of faster analysis using hydrogen or helium as opposed to the more dense nitrogen or argon gases.

(vi) Column diameter should be kept to a minimum as the likelihood of efficient radial mixing giving a uniform solute band flow pattern through the column is reduced as the diameter increases. In keeping with this consideration the packing technique should give a uniform packed density.

(vii) The ideal injected sample has a narrow rectangular profile. Indeed a maximum allowable sample size (M.A.S.S.) exists beyond which the contribution of the width of the initial injection to the variance of the eluted peak will be significant (28, 29, 38).

$$V_{fG} \leqslant \frac{V'_R}{2\sqrt{N}} \qquad 2.17$$

As the column efficiency is increased, then the value of M.A.S.S. is reduced. Even if this criterion is met the peak concentration should be kept within the linear range of the partition isotherm.

(viii) Temperature does not appear directly in the plate height equations but is obviously crucial to the equilibrium relationship and speed of mass transfer. In practise a balance between analysis time and resolution is sort.

For the analyst, the introduction of such sensitive peak detection devices as the flame ionisation detector (39) has enabled the sample size to be reduced to a fraction of a cubic millimetre. Plate heights of less than 0.1 mm are therefore readily obtained with narrow bore columns (1-2 mm) packed with 150-125 μm support particles coated with only 1% (weight/weight) or less of the stationary phase.

2.3 The Scale-up of the Co-current Process

The discussion of the theory of the analytical process has underlined the problem facing those wishing to employ the unique resolving power of chromatography for separations at the laboratory ('preparative') or production-scale level. To be successful the rapid decline in separating ability with increased column diameter and solute concentration within the column must be reduced or counteracted. Again a theoretical understanding has been sought to suggest practical guidelines to the solution of this problem.

2.3.1 The Dynamics of Large Diameter Columns

In discussing ten factors which may detract from the performance of large diameter columns, Giddings (40) concluded that the observed variation in the point gas flow velocity across the column cross-section was of primary significance (41). The source of this variation is in the non-uniformity of the packed density. Using the conventional packing technique of vibrating or tapping of the column wall as the packing is poured into the column causes size segregation of the particles (42), the larger particles congregating near the wall. As the resistance of the packing to gas flow is therefore less at the wall Giddings argues that the solute band will become convex to the flow direction, the outside edge preceding the bulk by many centimetres.

In opposition to this theory several workers (41, 43, 44) have emphasised the significance of the 'wall effect' which has two distinct facets. The wall itself exerts a frictional drag, retarding the outermost gas molecules. However the path of least resistance is still

Figure 2.3 Flow Profile Through A Large Diameter Column

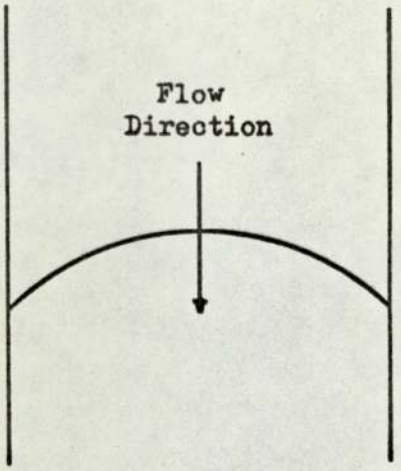

a) Postulated by Giddings (40)

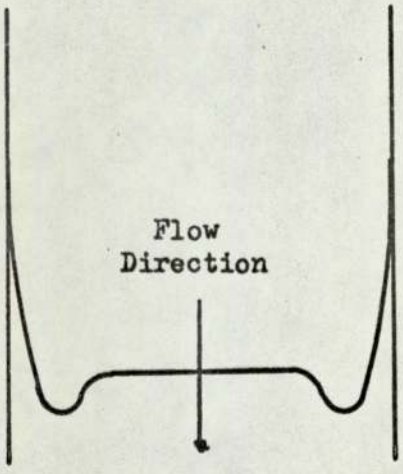

b) Postulated by Pretorius and De Clerk (44)

considered to be in the vicinity of the wall due to the misfit of the packed particles close to the cylindrical surface. Assuming the remainder of the bulk of the packing to be perfectly uniform the postulated cross-sectional flow profile is as shown in Fig 2.3. Also, Hupe (45) has experimentally shown that the centre of the solute band is relatively advanced in a 10 cm-diameter column. He attributed this fact to a faster exchange mechanism between mobile and stationary phase in the more densely packed central region. Hence the uniformity of the solvent phase loading is of fundamental importance.

The shape of the advancing solute band is further complicated by radial diffusion. This movement of solute molecules laterally to the flow direction can be beneficial. A more uniform band results from the repeated transfer of molecules back and forth from the respective points of high and low migration rate.

Attempts to formulate the additional band spreading occurring within large diameter columns have resulted in a further term, H_c, being added to the Van Deemter plate height equation. Huyten et al (41), Giddings (46, 47, 48), Higgins and Smith (49) and Rijinders (50), while adopting differing mathematical approaches, all derived a term of similar form.

$$H_c = f\left(\frac{r_c^2 \cdot u}{D_r}\right) \qquad 2.18$$

where : r_c = column radius

D_r = effective radial diffusivity

u = carrier gas velocity.

The exact interdependence of these parameters was dictated by the nature of the assumed velocity profile and/or the definition of the radial diffusivity.

For a quadratic profile, $u = \bar{u}\left[G_1 + G_2\left(\frac{r_x}{r_c}\right)^2\right]$, then(46)

$$H_c = \frac{G_2^2 \cdot r_c^2 \cdot \bar{u}}{96\,\gamma'_r \cdot D_G} \qquad 2.19$$

where G_1 and G_2 are dimensionless constants and r_x is a general point on the lateral axis of the column.

For an arbitrary profile, u(r), then (51)

$$H_c = \frac{2K^* \cdot r_c^2 \cdot \bar{u}}{\lambda_r \cdot d_p \cdot u + \gamma'_r \cdot D_G} \qquad 2.20$$

in which K^* is a complicated double definite integral of the velocity profile gradient, du/dx, being a general function of the particle to column diameter ratio. In the latter case D_r was considered to include the lateral movement resulting from the path of the gas through the packing, $\lambda_r d_p u$, in addition to the molecular diffusion in the radial direction, $\gamma'_r D_G$.

Giddings(48) tested the validity of the H.E.T.P. equation including an additional term of the above form (equation 2.19) by comparing 0.6 cm and 5.1 cm-diameter columns. He was able to show agreement between the theoretically predicted and experimentally measured values. In contrast Bayer et al (52), from experimental results obtained on a series of columns ranging from 1.3 cm to 10.2 cm, obtained a good fit to the equation

$$H = A + \frac{B}{u} + C_G u + C_L u + 2.83\,\frac{r_c^{0.58}}{u^{1.886}} \qquad 2.21$$

Pretorius and De Clerk (44) contest the assumption that all large diameter column band spreading mechanisms are scaled up in proportion to the radius. Considering the 'wall effect', the particle to column diameter ratio, d_{pc}, is of fundamental importance to the velocity profile. On this basis a semi-empirical expression for H_c was obtained (52):

$$H_c = \left(\frac{m}{2 . d_{pc}^{\,2} . D_r} \right) . d_p . u \qquad 2.22$$

where $$m = \frac{1}{100} \cdot \exp. \; -\left(\frac{1}{10\, d_{pc}} \right) \qquad 2.23$$

The above term was included in a dimensionless expression for the plate height;

$$\frac{H}{d_p} = 2\lambda + \left[\frac{1.2\ \varepsilon}{Sc_G(1 - \varepsilon)} \right] . \frac{1}{Re_p} + \left[\frac{1}{4} . \frac{k}{(1 + k)^2} \cdot \frac{d_f^{\,2}}{d_p} \cdot \frac{\nu_G}{\nu_L} \cdot \frac{1 - \varepsilon}{\varepsilon} \cdot Sc_L \right] . Re_p + H_c \qquad 2.24$$

where ε = void fraction

Sc_G, Sc_L = Schmidt number for the gas and liquid phase respectively
= $\frac{\nu_G}{D_G}$ and $\frac{\nu_L}{D_L}$

ν_G, ν_L = Kinematic viscosities of gas and liquid phase

Re_p = Reynolds number for packed columns
= $\frac{d_p . u}{\nu_G} \cdot \frac{\varepsilon}{1 - \varepsilon}$

According to this study, the plate height first increases with d_c (d_p being held constant), reaches a maximum when d_{pc} approximately equals 0.5 and then decreases as d_c is further increased. This hypothesis is experimentally supported (53, 54). Considering the significance of dimensionless groups to column performance it is interesting to note the experimental work of Charm et al (55) in the field of large-scale liquid chromatography. They concluded that provided dynamic similarity was maintained between two columns by maintaining the length to diameter ratios and Reynold's number constant then the separation characteristics would be the same.

In summary, a non-uniform velocity profile exists across the column cross-section. Its exact form and hence dependence on the column diameter, being complicated by packing defects, remains a matter of conjecture.

2.3.2 Finite Solute Concentration Effects

As the size of the injected sample is increased, the column efficiency in terms of the number of theoretical plates, is markedly reduced (see for example references 56, 57). The increased variance of the solute band can be attributed not only to the width of the injected sample as previously discussed (Section 2.2.2.2) but also to the effect of the comparatively high solute concentration on the chromatographic process.

The original derivation of terms in gas chromatography by James and Martin (3) was based on a model much simplified by the assumption of a 'linear ideal' process. While this assumption has some justification at the near infinite dilution conditions existing in an

analytical column it becomes increasingly unrealistic as the concentration is increased.

In addition to kinetic mechanisms, as the solute front proceeds through the column five possible factors affecting the retention, and therefore band broadening, can be pinpointed (58-63):

(i) The non-linearity of the absorption isotherm

(ii) Changes in the velocity of the gas phase caused by the flux of solute molecules across the gas/solvent interface wherever a concentration gradient exists.

(iii) The low thermal conductivity of the packing prevents the rapid transfer of heat emitted or absorbed during the chromatographic process (termed 'enthalpic overloading')

(iv) Gas phase non-ideality

(v) Liquid-surface and solid surface adsorption.

(iv) and (v) should be considered when applying chromatography to the accurate measurement of thermodynamic properties. (iii) can result in the occurrence of both axial and radial temperature gradients within a large diameter column. Further discussion of this phenomena is given in Section 6.1.2.4. (i) and (ii) are discussed below.

2.3.2.1 The Absorption Isotherm

The retention volume is the volume of gas required to move a zone of given concentration on the solute boundary through the chromatographic column. This can be related to a linear absorption isotherm by equation 2.3. For the general case the ratio of solute partitioning between the gas and liquid phase may vary with concentration; i.e. the isotherm is non-linear. A more correct definition of V^{o}_{R} was therefore

given by Helfferich (64) as

$$V_R^{\circ} = V_G + V_L \cdot \left(\frac{\partial q}{\partial c}\right)_c \qquad 2.25$$

Figure 2.4 shows the effect of the three commonest types of isotherm in the B.E.T. classification on the shape of the solute boundary (59). For a type 1 (Langmuir) isotherm, the retention volume and associated partition coefficient, $K = q/c$, decrease with increasing concentration. The leading edge of the solute peak is therefore sharpened while the trailing edge becomes diffuse. The converse is true for the effect of an anti-Langmuir isotherm. As the majority of systems in chromatography exhibit a non-linear isotherm then an increase in band width is to be expected at high solute concentration.

2.3.2.2 The Sorption Effect

Bosanquet (65, 66) was the first to describe the influence on the shape of the chromatogram of the variation in gas velocity with concentration. This results from the movement of molecules into or out of the gas phase as the solute boundary progresses. Conder and Purnell (60 - 63) subsequently included the sorption effect, corrected for gas phase compressibility, in their general retention volume equation. In its simplest form the equation can be expressed as

$$V_R^{\circ} = V_G + V_L \cdot (1 - jy_o) \cdot \frac{dq}{dc} \qquad 2.26$$

where y_o equals the mole fraction of solute in the gas phase as measured at the column outlet. As the concentration increases the

Figure 2.4 The Dependence of the Solute Boundary Profile on the Absorption Isotherm (59)

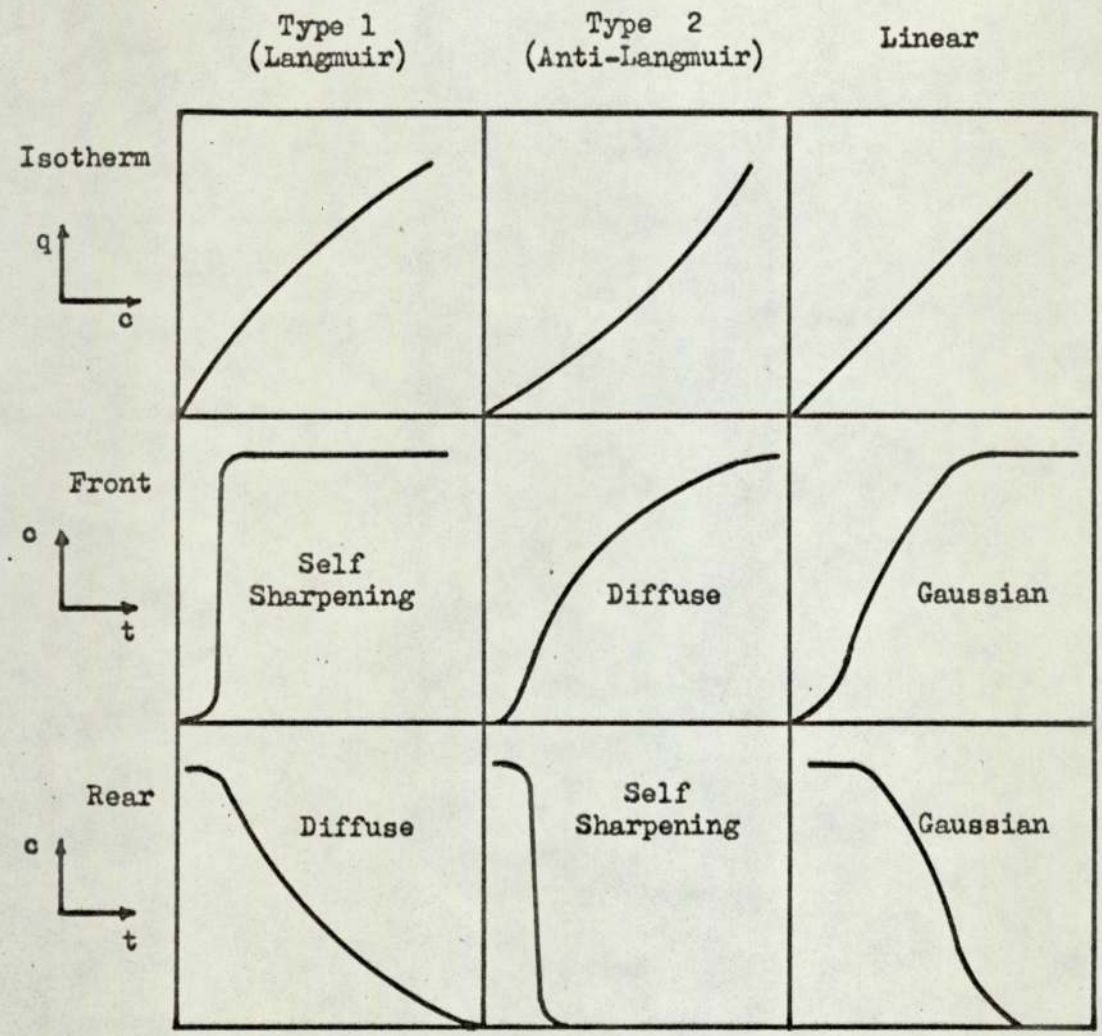

solute flowrate is increased giving a reduced retention volume. Hence the sorption effect always gives a self-sharpening leading edge and a diffuse trailing edge to the solute band, zones of high concentration moving faster than those at a lower level. The resultant effect of high concentration on band broadening is therefore dependent on whether the effects of the absorption isotherm and of sorption are naturally supporting or opposed. If opposed, a 'stationary front' can be formed, the band width becoming independent of column length (67 - 70).

2.3.3 Practical Solutions to the Scale-up Problem

Successful scale-up of the basic co-current process demands that the detrimental effects on capacity of a non-uniform velocity profile and finite solute concentration must be overcome. The practical solutions proposed may be classified into six categories; (i) multiple columns; (ii) columns of non-circular cross-section; (iii) flow distributors within the column; (iv) improved packing technique; (v) increased column length and (vi) repetitive injection. Each will now be discussed.

2.3.3.1 The Use of Multiple Columns

Utilizing several columns in parallel has the obvious advantage of allowing each individual column to be of narrow bore, while the total quantity of solvent phase remains substantial. Thus detrimental large diameter column effects are avoided without reduction in capacity. Johns et al (71, 72) compared a combination of eight parallel columns, each of 1.6 cm-diameter and 183 cm-length, with a single column of the same dimensions. Their experimental results showed the H.E.T.P. values

for the two systems to be equivalent even when the sample size for the parallel column array was increased by a factor of eight. This must be contrasted with the results of McCallum (73) who, for a similar experiment, observed very little gain in capacity.

The problem resides in the need to perfectly match the retention characteristics of each individual column. While the search for a reproducible packing technique has been moderately successful, the improved methods have been accompanied by a reduction to an acceptable level of the value of H.E.T.P. for large diameter columns (see Section 2.3.3.4). Difficulty is also experienced in even distribution of sample and gas flow through the inlet manifold. Hence, parallel columns have not found wide acceptance.

2.3.3.2 The Use of Columns of Non-Circular Cross-Section

Several column geometries have been proposed as a means of unifying the profile developed within a conventional circular tube. Oval (74, 75) and annular (76, 77, 78) cross-sectioned columns have been studied as well as the introduction of longitudinal fins (79, 80) or rods (81) within the column itself. Performance improvement is gained not only from improved column dynamics but also from better heat transfer properties. However, all the above work was carried out at an order of equivalent diameter of approximately 2 to 3 cm, save for the 7.5 cm hexagonal finned column of Reiser (80). Their difficulty of construction generally restricts application to the small preparative-scale where temperature programming may be successfully applied.

2.3.3.3 The Use of Flow Distributors Within The Column

Golay (82) recognised that maldistribution of the solute in the gas phase could be overcome by remixing the carrier stream at periodic intervals along the column, thus serving as an artificial radial diffusivity. He suggested that short column sections should be joined by a length of small diameter tubing in which diffusion may take place. The spacing of the remixing zone is critical. If too frequent, they could cause more band spreading than they eliminate.

This concept is of particular relevance to production-scale columns where the promotion of radial mixing is crucial to performance. In recent years homogenisers or baffles have been developed for insertion into such columns. At their simplest, these devices have taken the form of washers. By placing 'doughnut' type rings at 10 cm intervals, Bayer et al (83) achieved a plate height of less than 2 mm in a 10 cm-diameter column. Frisone (84) successfully retarded the normally advanced periphery of the solute band (wall effect) by the use of solid washers, soaked in stationary phase. A spacing of 30 cm was used in a column of 5 cm-diameter. In contrast, Verzele (85) was unable to obtain any beneficial effect with various shaped chemical washers.

The flow homogeniser patented by Carel and Perkins was of a more elaborate design (86, 87). It consisted of a plate with a single central hole sandwiched between two sintered discs. The outer discs servedto smooth flow variations while the central 'doughnut' promoted remixing. With the aid of such devices these workers were able to successfully scale-up throughput in direct proportion to cross-sectional

area when increasing column diameter from 1 to 30 cm (88). For the column of 30 cm-diameter, a single injection of 1475 cm^3 of a hydrocarbon mixture (n - C_6, C_7, C_8) was fully resolved. The column length was 2.44 m. Plate heights of 2 mm on a 10 cm-diameter column are commonly achieved (89), which compares favourably with the value of 3 mm observed by Verzele employing a four ring homogeniser in a column of only 7.6 cm-diameter (reported as private communication by Pecsar, 89).

Abcor Inc., Massachusetts, a company marketing production-scale chromatographs, favour the 'disc and doughnut' type baffling system associated with liquid-liquid extraction columns (5, 90 - 93). The disc, of diameter less than the column, forces the gas flow toward the column wall. The following 'doughnut' returns the flow to the centre, promoting mixing. An example of the few published experimental results obtained when using this type of baffling is the separation of 98.6% pure α-pinene from crude turpentine at a throughput rate of 900 $cm^3 hr^{-1}$. The column was 10 cm wide by 2.74 m long (91).

An economic feasibility study has been reported by Abcor for the separation of para-and meta-xylene at a combined production rate of 45.4 million kg yr^{-1}. (5). As a gas chromatographic process, two columns of length and diameter 4.26 m are envisaged, giving 99% pure products at a manufacturing cost of 4.4 ¢ per kg of p-xylene (U. S cents - paper published in 1969). This cost compares favourably with the normal crystallisation process.

The introduction of baffling has been a significant factor in improving the viability of chromatography as a production-scale process.

2.3.3.4 Improving Column Packing Techniques

Experimental results reported by Huyten et al (41) demonstrate the problem associated with packing columns of large diameter. Investigating the effect of the packing technique on 7.6 cm and 25.4 cm-diameter columns, they found that H.E.T.P. values of between 2 mm and 20 mm could be obtained on the same column by using different methods; pouring, pouring with tapping of the column wall, tapping, vibration and tapping with vibration. The source of this variation has been identified as the difficulty in obtaining a homogeneous packing. Pypker (42) was able to visually observe the particle size segregation resulting from the above listed methods by mixing green 841 - 425 μm 'celite' with red 212 - 125 μm 'Celite' in a 1 : 1 ratio (Fig 2.5).

The search for a reproducible packing technique giving columns of high efficiency has been extensive. In addition to the work of Huyten, Bayer (94), Frisone (84) and Higgins and Smith (49) have all investigated methods involving some combination of pouring, tapping and vibration with conflicting results. Huyten and Bayer concluded that tapping and slow filling produced the best columns. Higgins and Smith obtained the lowest H.E.T.P., a value of 1.0 mm for a column of diameter 2.5 cm, by allowing the packing to trickle from a funnel through a glass tube centred above the column. Frisone was unsatisfied by any of the three methods he employed; vibration plus vacuum, tamping plus vacuum and slurry-packing, finally resorting to the use of flow homogenisers.

Hupe et al (45) observed that a 10 cm-diameter column packed by

Figure 2.5 Particle Size Segregation Resulting From Various Packing Techniques (42)

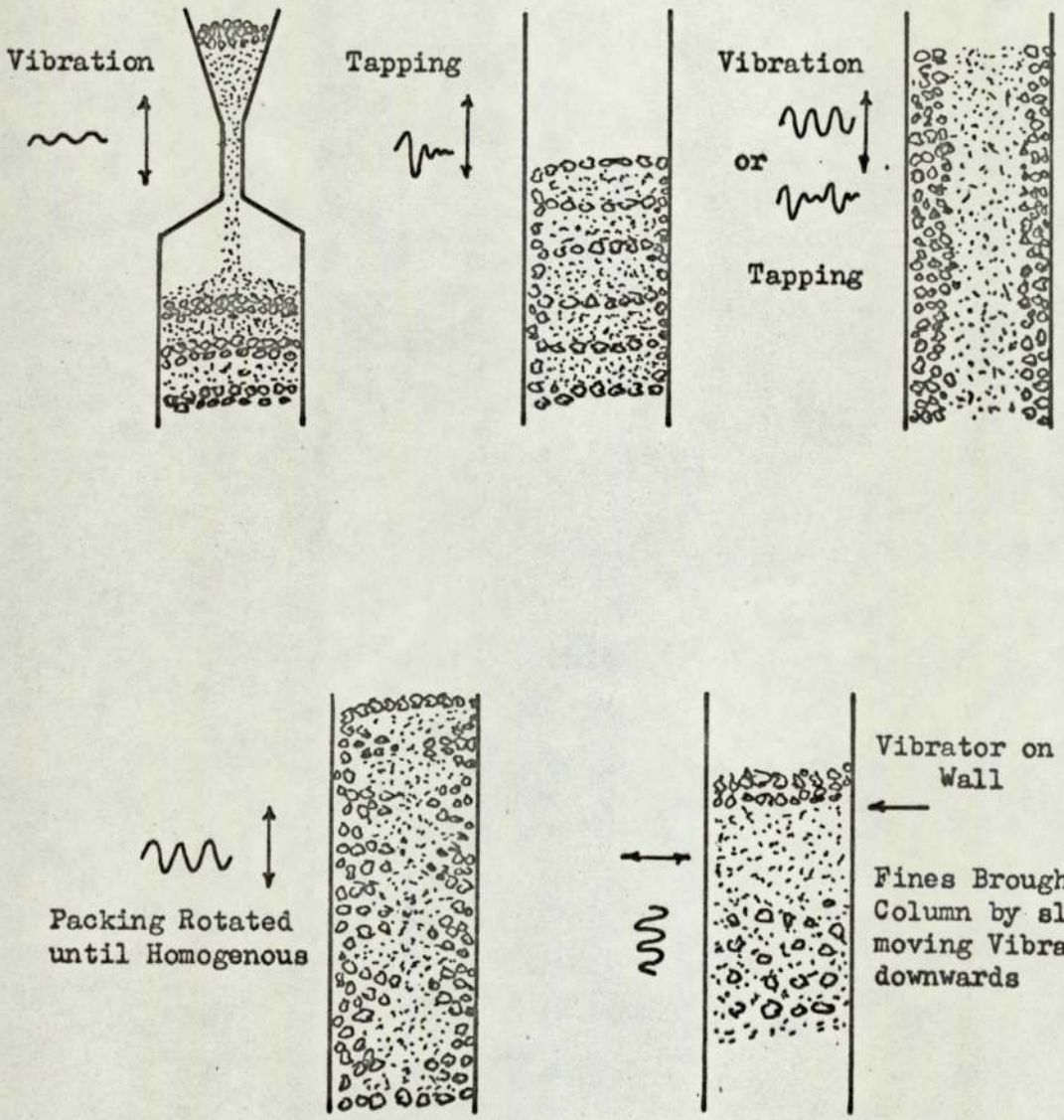

pouring and tapping gave a plate height of 6 mm. A study of the cross-sectional solute profile revealed that the profile was advanced at the point of highest packed density, the column centre line. The profile was corrected by increasing the peripheral packed density with a conical shaped plunger. An H.E.T.P. of 2.7 mm was then obtained.

Guillemin (95 - 98) and Pecsar (89) have demonstrated the high reproducibility in chromatographic performance of a fixed bed after fluidisation. H.E.T.P. values as low as 1.6 mm have been obtained with this technique on a 15.3 cm-diameter column. However, the resultant open packing structure, while giving a low pressure drop, is very susceptible to collapse by mechanical shock or vibration, with an increase in the plate height of 15-30%.

Following the work of Bayer and associates (83), Albrecht and Verzele (99) have recently developed a technique combining mechanical rotation and shaking with the continuous application of pressure. Packing is added in small quantities and the shake-turn-pressurise (S.T.P.) procedure repeated until the level within the column is constant. A 7.6 cm-diameter column yielded an H.E.T.P. of 1.2 mm which exceeds the performance obtained by any other method.

In summary, it can be said that those techniques which remove operator interaction are superior in terms of both reproducibility and low plate heights. For column diameters of several metres as envisaged for co-current chromatography at the full production-scale such techniques are unlikely to be applied, the preference being for some form of baffling.

Finally, in discussing packing techniques consideration must be given to the entrance and exit sections of the column. Several studies have shown that if these sections are left unpacked the expected efficiency loss from diffusion occurs (41, 100, 101). The design, type and degree of packing giving the best result is a matter of conjecture. Huyten et al (41), studying conical shaped inlet and outlets to a column of diameter 7.6 cm, concluded the conical angle had no effect. However, filling the entire exit cone with chromatographic packing gave a 40% efficiency increase. No advantage was gained by totally filling the inlet cone. For a 25.4 cm column a partially filled inlet cone gave the lowest column H.E.T.P. of 2.2 mm.

Albrecht and Verzele (101), in a similar study on a 7.5 cm-diameter column, found the lowest plate heightswere obtained for an inlet cone packed with inert glass spheres. The 250-210 μm spheres were thought to assist the even distribution of the injected solute across the column cross-section. Hupe et al (45) have experimentally shown the importance of this initial distribution. A non-uniform profile at the column inlet is unlikely to be corrected by the low natural radial diffusion experienced at large column diameters.

2.3.3.5 Increasing Column Length

From analytical theory, the maximum feed volume permissable if the intrinsic theoretical plate height of a column is not to be adversely effected, is given by equation 2.17, which may be written (30) as

$$V_{fG} \leqslant \frac{V'_R}{2\sqrt{N}} = \frac{V_m (1 + k)}{2\sqrt{N}} \qquad 2.27$$

If this equation is satisfied then Purnell (102) has shown that the number of plates required to exactly separate a pair of components (i.e. peak centres 6σ apart) is given by

$$N_{req} = 36 \left(\frac{\alpha}{\alpha - 1} \right)^2 \cdot \left(\frac{1 + k}{k} \right)^2 \qquad 2.28$$

where : α = the separation factor for a given column

$$= \frac{V'_{Rii}}{V'_{Ri}}$$

Thus, in the ideal case, the value of N in equation 2.27 is specified. To increase the permissable feed volume the adjusted retention volume must be increased. The quantity of stationary phase contained in the column must, therefore, be increased. In addition to increasing stationary phase loading and column diameter this can be achieved by increasing the column length. The advantage of such as approach is that intrinsic efficiency, in terms of plate height, can be maintained, provided the length is above a minimum value (40, 41, 103 - 109).

Conder and Purnell (110, 111) have extended the above ideal case to consider the effect of 'overloading'; i.e. exceeding the feed volume limitation imposed by equation 2.27. They concluded that the feed band width could be increased by a factor of twelve, giving a six-fold increase in throughput, by tripling the column length. Any further increase was unlikely to be economically justified.

Considering again equation 2.28, as the capacity ratio, k, is generally much greater than unity, then it is the separation factor, α, which largely dictates the minimum plate number and therefore column

length requirement. Hence Verzele (104 - 108) and Sakodynskii and Volkov (112, 113) have advocated that difficult separations (α approaching 1) are best achieved on very long, narrow bore columns. For a 75 m x 9 mm coiled glass column filled with a 30% loaded support, Verzele was able to successfully resolve dichloromethane, chloroform and tetrachloromethane from a single injection of 35 cm^3 (106). The pressure drop associated with columns of such length must be counteracted by the use of a coarser solid support. A particle size range of 1680 to 821 μm was used in the example quoted, representing a compromise with respect to mass transfer efficiency.

A mechanical technique for overcoming the pressure drop restriction is to circulate the solute bands around two or more columns, linked to form a closed cycle, before elution. Several schemes have been proposed (114 - 119), an interesting example being the three column system of Golay (119). A complete sequence of six cycles is illustrated in Fig 2.6. At any time two of the columns are linked to form the main separating section while the third is used to vent the more strongly absorbed component.

Long-narrow columns have the advantage of being more amenable to temperature programming. However, a long retention time is associated with the increased column length, placing a restriction on the throughput rate. Coupling this fact with the generally larger single sample capacity for wide columns suggests that short-wide columns are superior for production-scale applications. At the preparative-scale the choice of column dimensions is not so straightforward. Pecsar (89), following

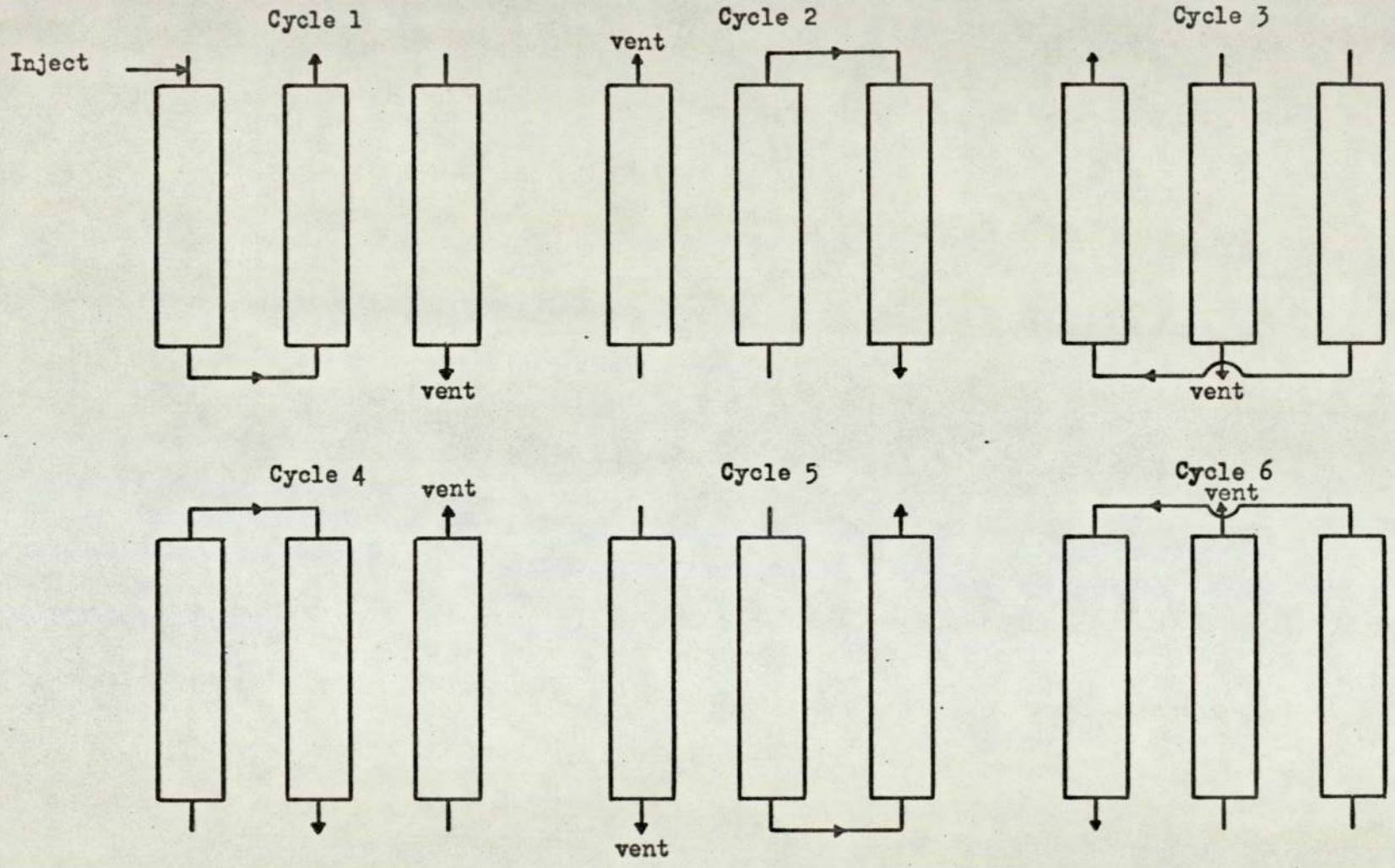

Figure 2.6 Recirculated Column Scheme Proposed by Golay (119)

a cost comparison (86, 120), concludes that long-narrow columns are to be preferred if the separation factor is less than 1.15.

2.3.3.6 Repetitive Injection

Analytical chromatography is a batch process. As the single injection migrates through the column the total width of the solute bands occupy only part of the available length at any one time. For practical scale-up, column utilisation and therefore throughput, is usually increased by introducing a 'repeated injection' technique. The batch samples are injected at as frequent an interval as the total on-column width of the preceding sample permits without extensive overlap. Synchronized automatic injections are used in conjunction with a peak sensing device,which diverts the individual eluting bands to separate fraction collection points.

As an example of the throughput gain,Ryan et al (91) observed that, for a 10 cm x 3.04 m column operating at carefully selected conditions, the feed of turpentine could be injected 1.8 times more frequently than for a single injection to give 99% resolved α- and β-pinene products.

The introduction of repetitive injection poses several questions regarding the optimum design and operating parameters for a co-current chromatographic separation process. Should the eluted peaks be fully resolved or can sample size, carrier gas velocity, injection rate or temperature be increased to reduce retention time and give overlapping peaks? In the latter case the contaminated fraction of the chromatogram needs to be 'cut out' and recycled. Which gives greater throughput, rapid small injections on a low loaded, small particle size

support or slower, large injections onto coarse support heavily coated with stationary phase? Theoretical and experimental studies have attempted to answer such questions.

2.3.4 Optimisation of Column Design and Performance

When applying chromatography as a separation technique the concept of minimising H.E.T.P. is inadequate as the sole guide to optimising column characteristics and operating conditions. The primary objective is the production of high purity components in least time (preparative-scale) or at least cost (production-scale). The expression for efficiency should therefore reflect the compromise between throughput and component resolution for a system of given separation difficulty.

The simpler case, where successive injections are made only on complete elution of the preceding solute bands, has been treated by Sawyer (38, 120). Equation 2.27 was expressed in terms of column parameters and combined with equation 2.28 to give an expression for the maximum throughput of a component in an ideal column containing the minimum required number of plates, Nreq.

$$\frac{V_{SL}}{\text{unit time}} = \frac{(x / 1 - x).k.\ \rho_p.f_L}{12.[a/(a-1)]\ .(1+k)^2.M_L}\left[\frac{\pi.r_c^{\,2}.M_i.u_o.j}{\rho_i}\right] \qquad 2.29$$

where : V_{SL} = volume of the sample as a liquid

x = mole fraction of solute in solvent

ρ_p, ρ_i = density of coated packing and sample component i respectively

f_L = fraction of total weight of packing which is solvent; i.e. stationary phase loading

M_L, M_i = molecular weight of the liquid solvent and sample components respectively.

Equation 2.29 enabled the following general observations to be made concerning the selection of column parameters for a separation process (38):

(i) Providing column efficiency can be maintained, throughput increases in proportion to cross-sectional area.

(ii) A solvent phase giving the largest separation factor should be employed to reduce the plate requirement.

(iii) A carrier gas velocity beyond the optimum value for minimum plate height is advantageous.

(iv) Mass throughput increases with sample molecular weight while decreasing with sample density.

(v) A high stationary phase loading is desirable.

From equations 2.28, 2.29 and a plate height expression the minimum column length required for a given separation, column diameter and carrier gas flowrate can be calculated.

The question of optimum column length was considered by Timmins et al (5). Defining efficiency in terms of column utilisation, $\eta = \frac{\text{moles produced per time}}{\text{column volume}}$, they derived:

$$\eta = \left(\frac{0.4}{R_s}\right).\left(\frac{P_i^o}{R_g.T_c}\right).\left(\frac{u_{in}.\phi}{l_{min}}\right).\left(\frac{l_{min}}{l}\right).\left(1 - \frac{l_{min}}{l}\right)^{1/2} \qquad 2.30$$

where : R_s = resolution

$$= \frac{t_{Rii} - t_{Ri}}{4\sigma_{ii}}$$

P^o_i = vapour pressure of the feed at column temperature

R_g = gas constant

T_c = temperature of column

u_{in} = carrier gas velocity at the column inlet

ϕ = porosity of the packed column

l_{min} = minimum column length required for separation of two components by 4σ

$$= H \times 16 (R_s)^2 . [\alpha/(\alpha - 1)]^2 . (k_{ii} + 1)/k_{ii}^{\ 2}$$

l = actual column length.

(Note: units for the above expression are feet, minutes, atmospheres, ^oR)

A plot of η versus l/l_{min} showed a maximum for l/l_{min} = 1.2 to 1.5. This range was therefore considered to represent the optimum balance between sample volume and column length. The range is considerably lower than the previously reported suggestion by Conder and Purnell (110, 111) that, for preparative columns, the minimum column length could be effectively increased by a factor of three. Equation 2.30 also confirms that a high feed vapour pressure, carrier gas velocity and permeability of the packing favour effective column utilisation. However, a larger particle size reduces the effect of gas compressibility at the expense of some mass transfer efficiency.

Pretorious and colleagues at the University of Pretoria have extensively studied the optimisation of preparative chromatographic performance for the more practical repeated injection case (44, 122 - 130). The basis of their approach was to define an efficiency term which relates production rate to separation difficulty and purity through the chromatogram. Thus for a two component system requiring two cuts per injected sample (two-fraction technique), De Clerk (44,130) defines the efficiency as (see Fig 2.7).

$$E = \frac{(m_i - \Delta m_i).u_o}{W_{to}.(1 + k_i)} \qquad 2.31$$

where : E = mass production rate of component i

m_i = mass of component i produced at the column outlet per sample injection

Δm_i = mass discarded during fraction cutting

W_{to} = total chromatogram width per sample at the column outlet inside the column.

Purity is inherent in the assumed distance between peaks. For Gaussian shaped peaks, a distance of four standard deviations, $4\sigma_{io}$, leads to a cross-contamination of about 2%.

Equation 2.31 has been related to packed column parameters to give the following expression for volumetric production rate (44).

$$E' = \frac{E}{\text{inlet concentration}} = F_i.r_c^2.Re_p.\left(1 - \frac{G_i.H}{l}\right)^{1/2} \qquad 2.32$$

with $F_i = \pi.\sqrt{2\pi}.(1 - \varepsilon).v_G.(1 + \text{erf}\sqrt{2}R_s)$

and $G_i = \dfrac{16(1 + k_i)^2 R_s^2}{k_i^2(\alpha - 1)^2}$

Figure 2.7 An Illustration of the Elution Chromatogram For a 2-Component System when Repetitive Injection is employed (44, 130)

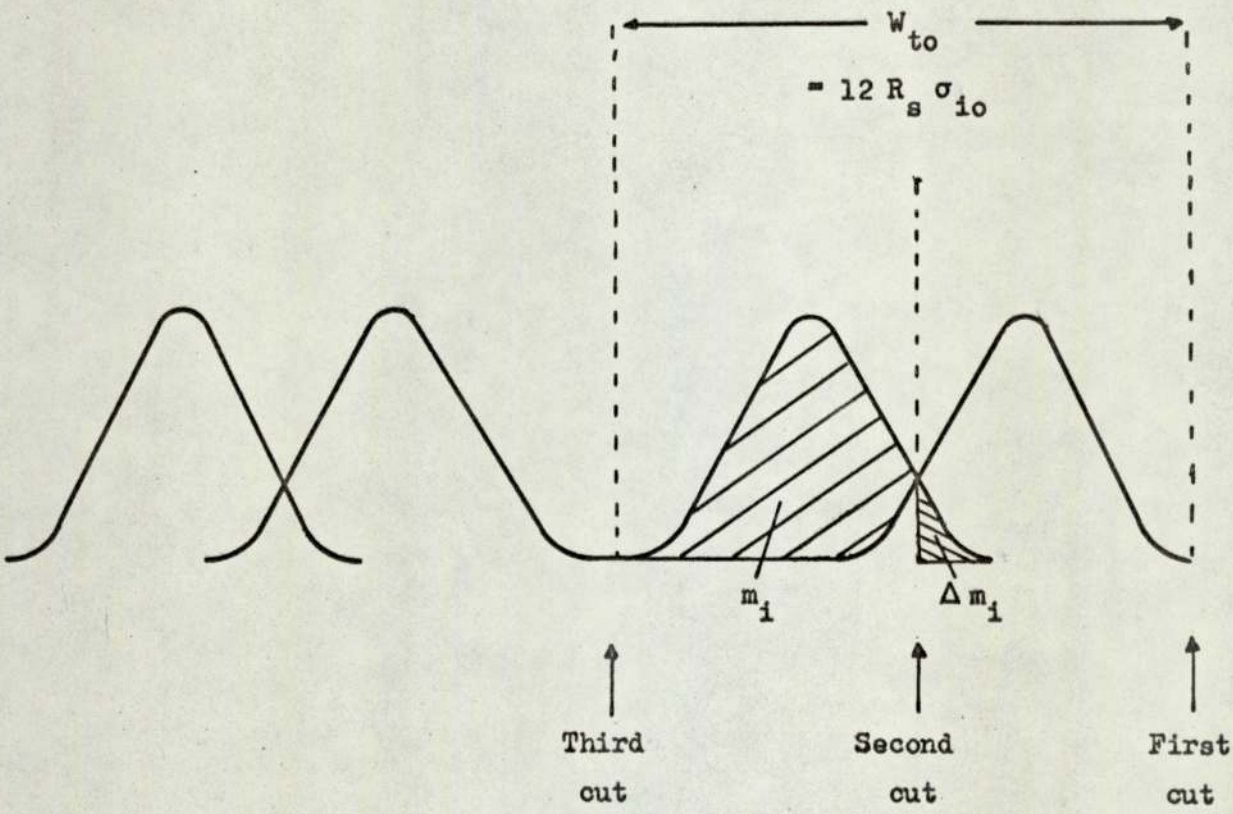

In addition to confirming the significance of such factors as separation factor and particle size, several important conclusions have been drawn from this work (44, 125 - 128, 130):

(i) Production rate is dependent only on the square root of the plate height, H. Hence, in contrast to analytical chromatography the importance of H at the preparative-scale is secondary.

(ii) The value of the partition coefficient does not significantly effect E'.

(iii) Carrier gas velocity appears implicitly in the terms Re_p and H. The dependence of efficiency on these terms at increasing velocity are opposed. Hence an optimum value of velocity exists for a column of given length and diameter which is greater than the analytical value. Gordon et al (125) have shown that for a three-fraction technique with two components ('heart-cutting') this optimum value may exceed the limit at which the required resolution can still be met.

(iv) An optimum sample volume exists for each component in a mixture. However, the production efficiency decreases quite slowly as the optimum value is exceeded.

(v) The dependence of production efficiency on column radius is complex as r_c appears both explicitly and implicitly in H. It is expected that for easily resolved mixtures the r_c^2 term will dominate, production efficiency increasing almost linearly with cross-sectional area. For more difficult separations the significance of plate height in the equation will increase and, therefore, an optimum column diameter will exist beyond which no significant gain in E' is achieved. In this

case Gordon et al (127) suggest a column diameter of approximately 10 cm will represent the optimum.

(vi) The maximum feed concentration should be used. Indeed the column could be operated in the non-linear isotherm region, peak skewing being tolerated for the gain in throughput.

(vii) Production efficiency increases almost linearly with length, the ultimate restriction being pressure drop (44, 126).

(viii) For a two-fraction technique there is an optimum stationary layer thickness, $\frac{d_f}{d_p} = 0.01$ (44). When heart-cutting, the loading should be the maximum that the support can hold without 'clogging'.

Thus, as expected, the optimum conditions for a preparative chromatographic column are radically altered by the introduction of a repetitive injection technique.

Craven (131) experimentally observed the existence of an optimum carrier gas velocity (4 cm s^{-1}) and sample volume (60 cm^3) for the separation of α- and β-pinene on a 10 cm-diameter column. An optimum temperature (125°C), some 35°C below the system boiling point, was also found to exist. Operating at these conditions with repetitive injection gave a throughput of 828 cm^3 hr^{-1}, recovering 98.6% β-pinene. While this is approximately 8% less than the throughput obtained by Ryan et al (91) for the same system, column diameter and stationary phase, the column used by Craven was only 2.03 m long, a decrease of 35% in length.

At the full production-scale a cost element must figure prominently in the optimisation expression. However, as a relatively new separation

process, available data is limited. Empirical equations projecting production cost as a function of column parameters must, of necessity, be extremely tentative.

The common approach has been to define as a criterion of performance the reciprocal of the total separation cost per unit mass of product; throughput, Q, divided by the total processing cost, including product recovery, per unit time, $\dot{S}^*$. Process variables should be selected to minimise this quantity.

The analysis of Conder (132) has been the most extensive to date. He combined a theoretically based equation for throughput in a repeated injection process with an empirical expression for cost based on data published by Ryan and Dienes (133) for the separation of α- and β-pinene on a 10 cm-diameter column. A summary of his conclusions is given below:

(i) For a 'heart-cutting' technique the optimum recovery of product per injected sample is 60%, the contaminated 40% being recycled. Columns should therefore be made deliberately short and operate at the maximum carrier gas velocity with long, rectangular shaped, feed injections.

(ii) With increasing column diameter, $Q/\dot{S}^*$ initially undergoes a rapid reduction. When the scale is large, the change in cost advantage is much slower. Hupe (134) empirically estimated the transition point in the slope of the cost curve to be at a column diameter of approximately 20 cm.

(iii) For large columns, say greater than 30 cm in diameter, it is important to achieve a low value for H.E.T.P. As the diameter is reduced the plate height becomes of less significance to throughput as previously reported.

(iv) Q/S^* is not very sensitive to the separation factor, although the stationary phase resulting in the easier separation should always be chosen. In addition the stationary phase loading has little effect on the economics, simply dictating whether small batches are frequently injected or large batches injected at longer intervals.

(v) The optimum temperature is at, or slightly above, the boiling point for thermally stable solutes as, at this temperature, the asymmetry resulting from finite concentrations is least.

(iv) and (v) are surprising observations. As the separation factor is a measure of the separation difficulty, it would seem logical to assume that, as for distillation with respect to relative volatility, the product cost would be very sensitive to this factor. With respect to temperature, Craven (131) has experimentally shown the optimum value for the throughput of α- and β-pinene on a 10 cm-diameter column to be some 35°C below the boiling point. A higher temperature would be detrimental to both operating cost and production rate.

Summarising, it is not possible to draw up a general set of recommended guide lines for column design and operation when applying gas/liquid chromatography as a separation technique. Conflict arises with the chemical system, the duty, and the injection plus product recovery technique.

At the preparative-scale the co-current system is now accepted as a general laboratory tool. The largest constructed unit reported is 30 cm in diameter. However, larger units extending into full production-scale have been economically justified for systems which are, at present, difficult to resolve to a high degree of purity.

2.4 Alternative Process Schemes

In describing practical solutions to the problem facing those wishing to scale-up the basic, batch, co-current process, it was shown that a repeated injection technique represented an increase in column utilisation and, therefore, throughput. Several researchers have devised mechanical schemes to enable the final step in this direction to be made, the introduction of a continuous feed. These may conveniently be divided in two groups as described in Chapter 1; (i) cross-current flow processes (ii) counter-current flow processes.

2.4.1 Cross-current Flow Processes

A scheme for the continuous separation of a multicomponent mixture by the lateral movement of the solvent phase relative to the carrier gas was proposed by Martin (135). The column was to be formed by packing the annular space between two concentric cylinders. While gas flowed through these cylinders they would be rotated past a fixed feed point. The solutes would therefore follow a helical path to elute, for collection, at a point relative to the feed dictated by their respective solvent affinities. The more strongly absorbed components would be carried farthest (Fig 2.8a).

A theoretical appraisal led Giddings (136) to conclude that this scheme was capable of better resolution and throughput than a conventional column of similar packed cross-section. Dinelli et al (137, 138) converted the concept to a working unit. To avoid both cross-contamination within the packing and construction difficulties, the annulus was replaced by 100, 6 mm x 1.2 m individual tubes arranged

Figure 2.8 Cross-current Flow Schemes

a) Helical Flow

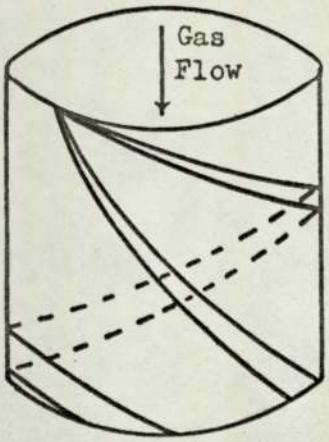

Principle

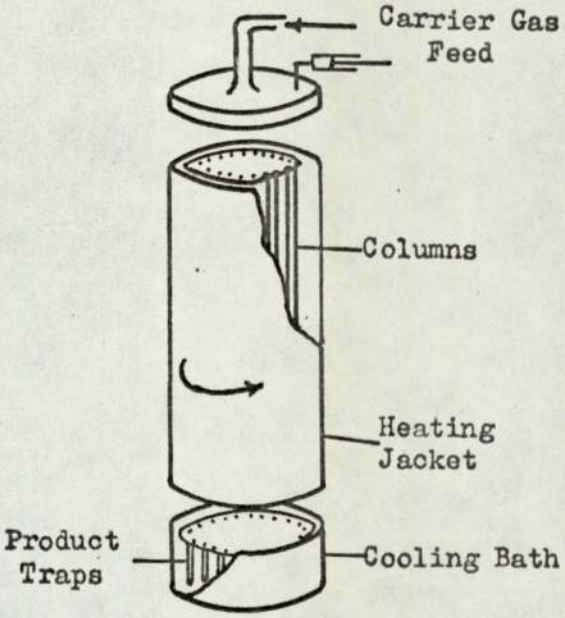

Multiple Column System of
Dinelli et al (137)

b) Radial Flow

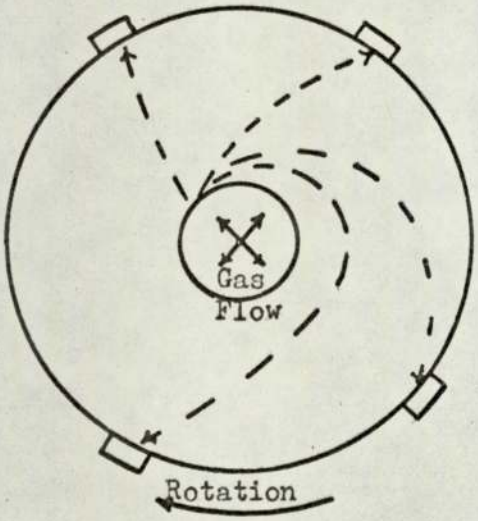

Principle

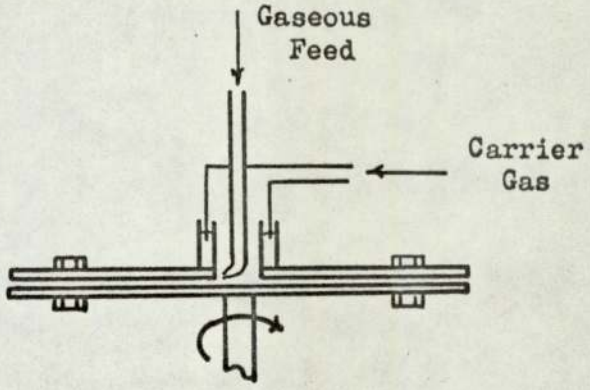

Parallel Disc System of
Sussman et al (145)

on a circular pitch. The tube bundle was enclosed in a heating jacket while the corresponding collecting traps were suspended below the unit in a cooling bath.

Optimum operating conditions have been determined (139). In practice, as the feedrate is increased, the number of traps in which a component appears increases until eventually overlap occurs. The feedrate, therefore, has a maximum for a given product purity. For the separation of benzene/cyclohexane on tricresyl phosphate as stationary phase the theoretical maximum throughput for 99.9% purity was predicted to be 220 cm^3 hr^{-1}. Experimentally it was found to be 200 cm^3 hr^{-1}. Examples of the separation of isomers and close boiling mixtures on a unit with greater column length have also been given (140-142).

The careful matching of column characteristics, the need for a reliable mechanical seal between the individual columns and the traps, and the physical movement of a large column bundle make it unlikely that a unit in this form will be applied at the production-scale.

Mosier (143) has patented a unit operating on the same rotating annular column principle. In this case the solutes move in a horizontal rather than vertical plane, travelling from the centre to the circumference of a wide annular packing (Fig 2.8 (b)). For a practical unit, Sussman et al (144, 145) replaced the packed annulus by two parallel discs (Fig 2.8 (b)), the adjacent surfaces being coated with solvent phase. Plastic spacers held the discs apart to form a capillary channel approximately 0.01 mm wide. With 60.8 cm-diameter

discs, the largest unit constructed, a throughput of 18.9 cm^3 min^{-1} was reported for the separation of a mixture of 55% butane and 45% methane. A theoretical study led the authors to claim that the gas throughput could be as high as 50 cm^3 min^{-1} on a 30.4 cm-diameter unit (145).

The primary application of this system is for the separation of gases which require only a short residence time between the plates for resolution. More difficult separations, requiring longer retention of the components, would lead to increased band spreading, each solute occupying a greater fraction of the coated disc surface. The throughput for successful resolution would therefore decrease.

Further scale-up is limited by two factors:

(i) The feed emanating from the centre of the disc must result in an inner band of very high solute concentration. Throughput is therefore restricted by the saturation of the solute phase in this zone. In scaling up the disc dimensions, available surface area will be lost to the necessary increase of the inside diameter of the annulus.

(ii) The manufacture of the discs and the seals between the disc circumference and solute collection ports requires a high degree of precision engineering.

The final scheme falling within the cross-current flow category remains, as yet, conceptual (146). It consists of a rectangular box whose four sides are constructed in porous metal (Fig 2.9). Filled with chromatographic support, the 'slab' is suspended inside another, solid wall, box. A plate set at each corner isolates the four sides of the slab. The feed mixture (i + ii) is introduced into one corner. The

Figure 2.9 'Chromatographic Slab' Proposed by Tuthill (146)

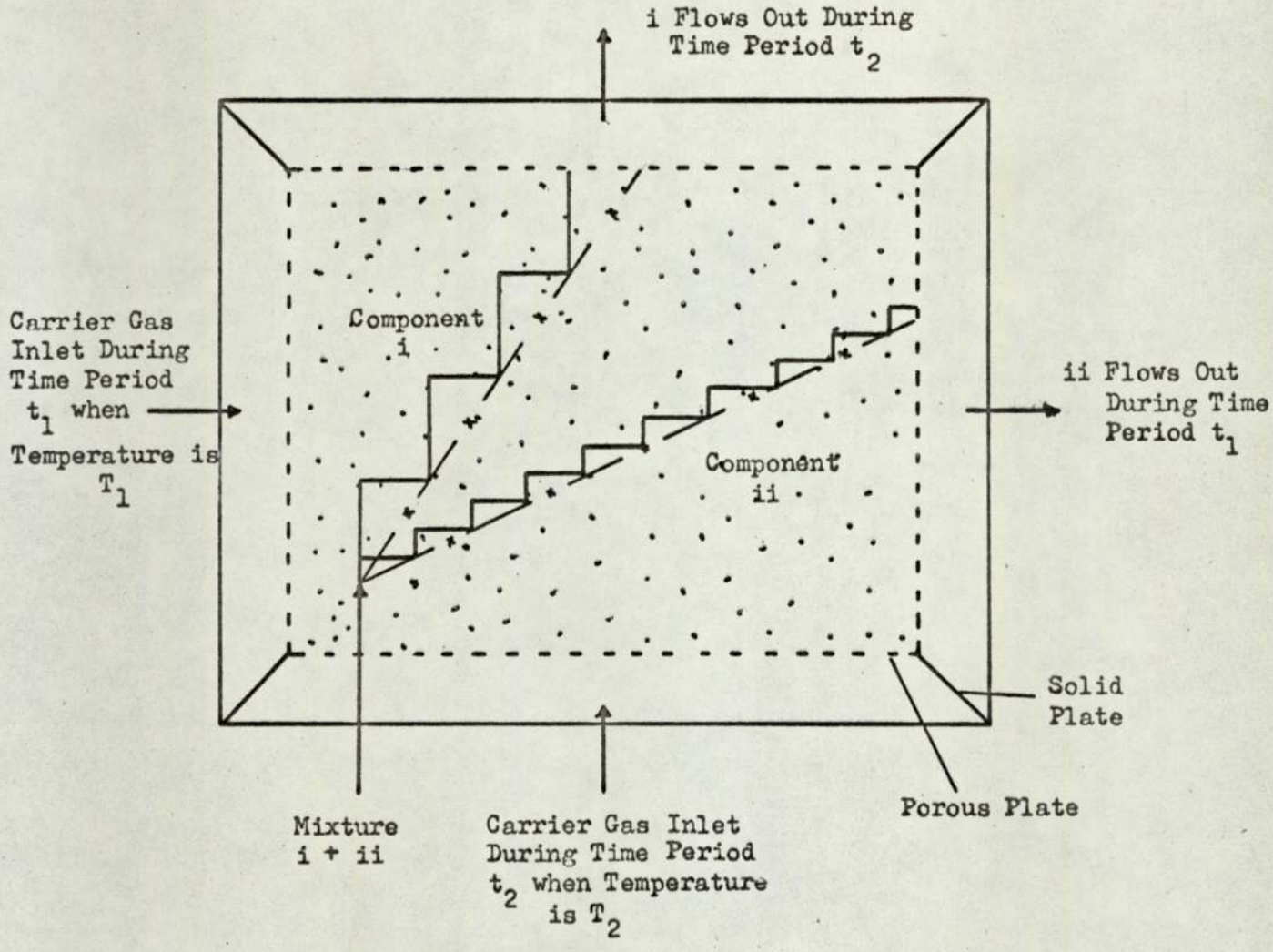

flow direction of the carrier gas is changed by alternate selection of the inlets placed on the two adjacent sides which together form that corner. When the carrier gas inlet point is switched, the slab temperature is also changed. The two solutes i and ii, as a consequence of their differing solvent affinity, progress at different rates in both the horizontal and vertical direction. Flowrate and temperature conditions can be selected such that the resultant velocity of solute i (lower solvent affinity; i.e. lower K value) is greatest in the vertical direction while solute ii preferentially moves in a horizontal direction. The resolved components will therefore elute from differing sides of the slab.

In concluding this subsection, it is interesting to note that neither of the units constructed on the cross-current flow principle have been used to exploit its major theoretical advantage, the ability to continuously resolve a multicomponent mixture in a one-stage operation.

2.4.2 Counter-current Flow Processes

The increased potential throughput for a counter-current flow scheme relative to a conventional co-current system can best be illustrated by considering Fig 2.10 in which the solute concentration profiles obtained for a binary separation are compared. If 'pure' products are to be collected in the batch process (Fig 2.10 (a)) then, either the eluted components must be fully resolved (X) or the central 'valley' fraction must be cut-out (YZ). As previously discussed (Section 2.3.4), the latter 'heart cutting' procedure appears most economically attractive, Conder (132) suggesting that the optimum recycle is 40% of the injected

Figure 2.10 Comparison of the Solute Concentration Profiles obtained for a Binary Mixture being separated by

a) a Repeated Batch Co-current Process

b) a Counter-current Flow Process

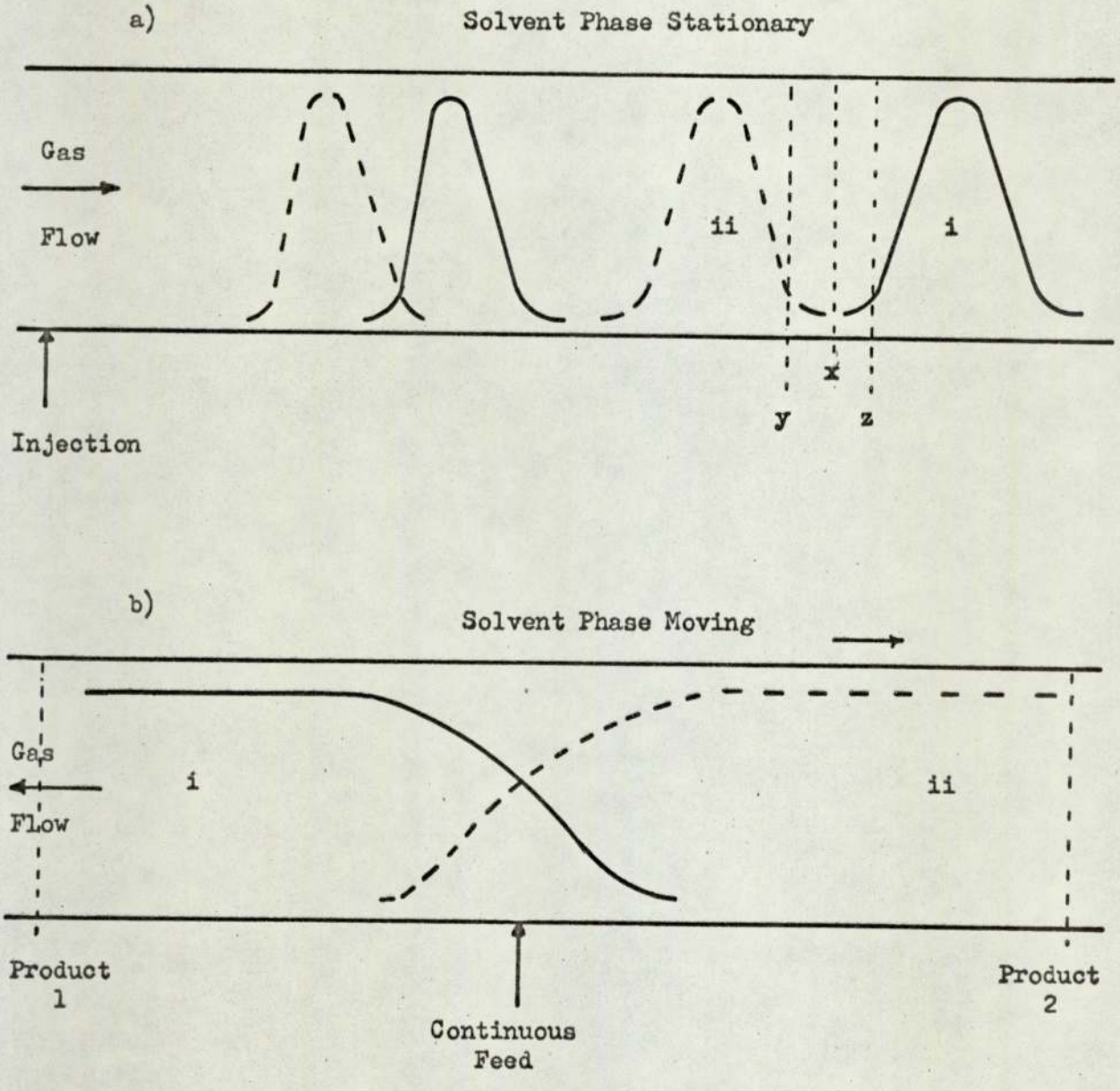

Note i = less strongly absorbed component (lower K value)

ii = more strongly absorbed component (higher K value)

sample.

In contrast, for the counter-current flow scheme (Fig 2.10 (b)), the solute concentration profiles need only be partially resolved within the chromatographic column to permit collection of pure products at the column exits (1, 2). The entire separating power of the column can be used to effect this partial resolution and therefore severe overloading, by co-current standards, of the solvent phase is permitted. Hence, in principle, a gain in throughput should be achieved.

The achievement of a mechanical system based on the principle of counter-current gas/liquid chromatography has undergone two main stages of development; (i) moving-bed and (ii) moving-column systems.

2.4.2.1 Moving-Bed Systems

A typical apparatus for moving-bed chromatography was that used by Barker and co-workers (8 - 11, 15, 21) which is illustrated in Fig 2.11. A vertical copper column of 2.5 cm-diameter was fed with solvent-coated solid support from a hopper. The solids flowed under gravity at a rate controlled by an orifice and rotating table at the column base. Vibration of the column wall ensured a continuous steady solids flow. On exiting from the column, the solids were returned to the hopper.

The column can be considered to consist of two parts; a main separating section into which the feed is pumped and a heated stripping section. Hot, dry, excess carrier gas entered the base of the stripping section to remove the more strongly absorbed component(s), ii, carried preferentially in the direction of solvent flow, as Product 2. Gas not removed from the Product 2 offtake port continued to flow through the

Figure 2.11 Moving-Bed Apparatus for Counter-current Chromatography (11)

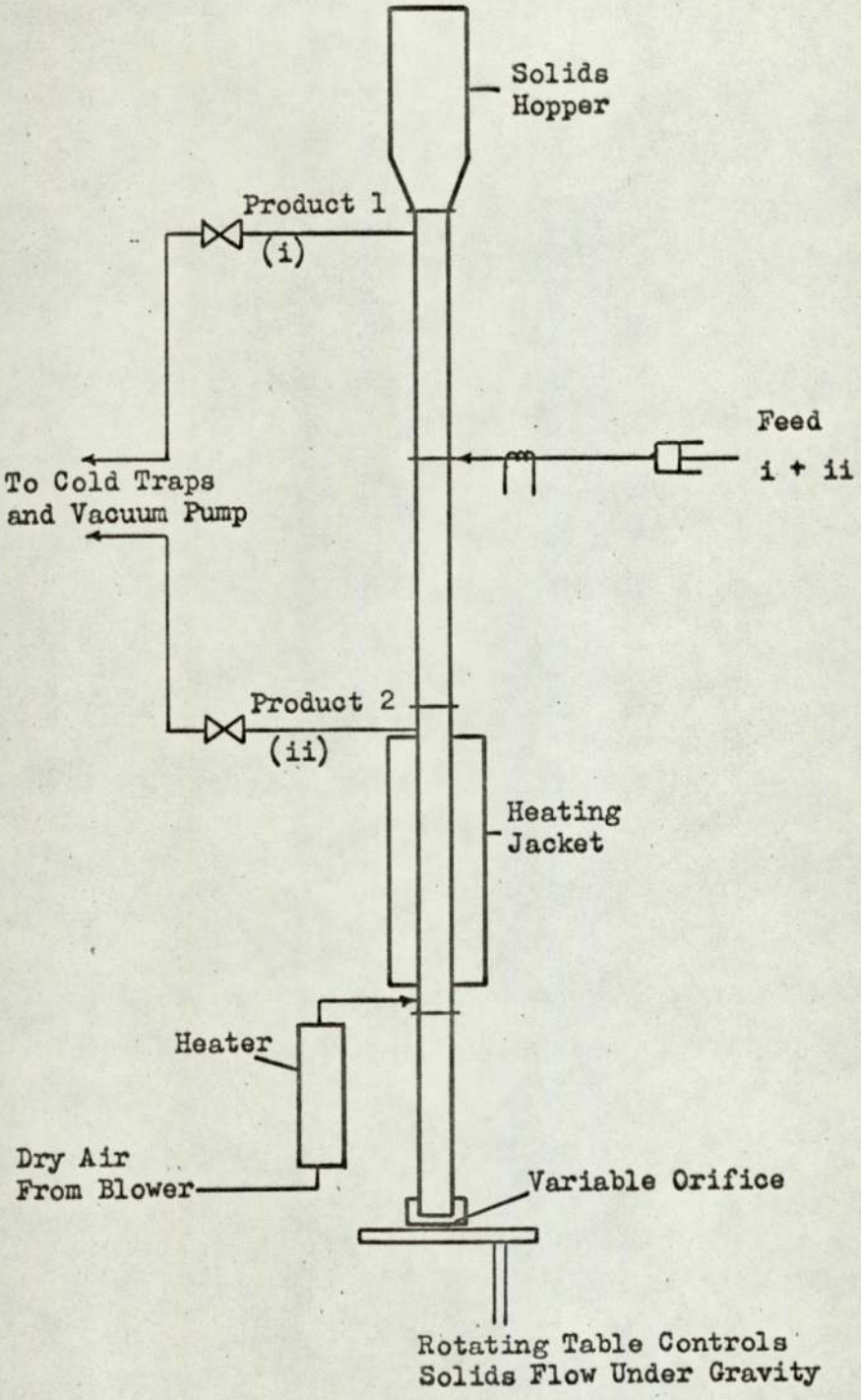

separating section to exit from the column, carrying the least strongly absorbed component(s), i, as Product 1. Components were recovered from the respective product streams by cold traps.

Barker and Lloyd (10 - 12) and Huntington (15) have studied the performance of the above described moving-bed unit with a series of equivolume binary mixtures selected from benzene, cyclohexane and methylcyclohexane. With air as carrier gas and operating the separating section at ambient temperatures, high separated product purities were obtained at throughputs of up to 30 cm^3 hr^{-1} of cyclohexane-methylcyclohexane. The chromatographic packing used was 29.6% by weight polyoxyethylene 400 diricinoleate coated onto 1680-841 μm particles of C22 Sil-O-Cel Firebrick (Johns Manville), a diatomaceous earth. The separation factor at 20°C for this system is 1.8. Evaluating column efficiency in terms of transfer units gave values for $H.T.U._{O.G.}$ of between 9 and 10 cm.

Schultz (147) investigated the separation of cis- and trans-butene-2 on a column 100 cm long and 1 cm in diameter. At a feedrate of 78 cm^3 hr^{-1}, consisting of 37.6% by volume trans and 62.4% cis, 32 cm above the feed point trans was 99.7% pure and 32 cm below cis was 99.4% pure. Purities in excess of 99.999% were claimed for the separation of 38.8 mole % dimethylbutane and 61.2 mole% cyclopentane at a feedrate of 21 g hr^{-1} on a larger column (2.6 cm x 138 cm). The column was operated at the boiling point of the materials.

Tiley and co-workers (148, 149) and Scott (150) have also reported successful separations on moving-bed columns of small diameter. Larger

scale operating data have been reported by the Phillips Petroleum Company (151). The 15 cm-diameter column, of length 2.54 m, was constructed with a separate stripping section. Carrier and stripping gas streams were independent. Regenerated packing was recycled to the head of the column by a gas lift. Using a packing of approximately 1.5 mm firebrick spheres coated with dioctyl phthalate, and hydrogen as carrier gas, 225 cm^3 min^{-1} of a 30% cyclohexane/70% benzene mixture was successfully separated at an operating temperature of 85°C. No product purities were quoted.

A sidearm of 1.27 cm-diameter was introduced in the lengthened separation section between the feed inlet and Product 2 offtake ports by Barker and Lloyd (12). Selecting differing values for the relative gas and liquid phase flowrates in the main separating section and sidearm enabled the continuous separation of a three-component mixture to be attempted. For the equivolume mixture cyclohexane-benzene-methylcyclohexane, at a feedrate of 12.6 cm^3 hr^{-1}, 99.5% pure cyclohexane was obtained as Product 1, 99.5% benzene as Product 2 while the sidearm product was methylcyclohexane (maximum purity 78.6%) contaminated with benzene (13, 15).

While industrial-scale units have been constructed for both gas/solid chromatographic systems and ion-exchange, the truly continuous moving-bed system presents three problems associated with solids flow:

(i) Accurate control of the solids flow is difficult to achieve.

(ii) Comparatively low, uneven packed densities are obtained, with a consequent efficiency loss.

(iii) Attrition of the expensive friable packing occurs, requiring a regular sieving and replenishing operation to be undertaken. The return of the solids to the feed hopper by air-lift would aggravate this problem.

In addition, the gas velocity within the column is limited to being less than the minimum fluidisation velocity. To overcome these problems, mechanical schemes based on rotation of a fixed bed within a moving circular column have been devised.

2.4.2.2 Moving-Column Systems

Three schemes have been proposed in which a closed circular column packed with coated support is rotated past fixed inlet and outlet ports, thus eliminating the disadvantages associated with solids flow. Within the main separating section, XYZ, the direction of carrier gas flow is counter-current to the direction of the column, and therefore solvent phase, rotation. (Fig 2.12)

The schemes differ in the flow direction in the stripping/purging sections and the means of controlling the flow direction generally within the column. Pichler (6), Gulf Research and Development Corporation (152), Glasser (153) and Luft (154) all proposed that the relative port positions and carrier gas flowrates be selected such that correct directional flow was maintained by balancing pressure drops. Barker (17) removed the consequent restrictions on column usage and flowrates by placing a cam-operated gas lock valve between the carrier gas inlet port and the Product 1 offtake. Gas flow is unidirectional, hence the column length available for separation is limited only by the requirement for the short

Figure 2.12 Circular Columns for Counter-current Flow Processes

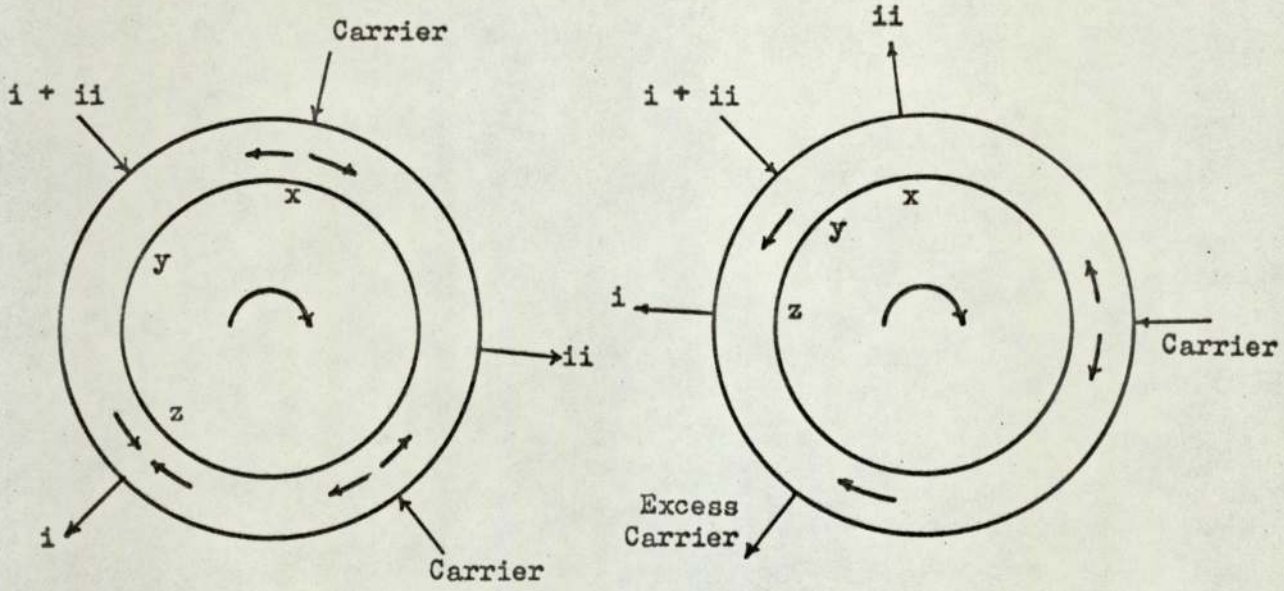

a) Pichler (6), Gulf Research (152) and Glasser (153)

b) Luft (154)

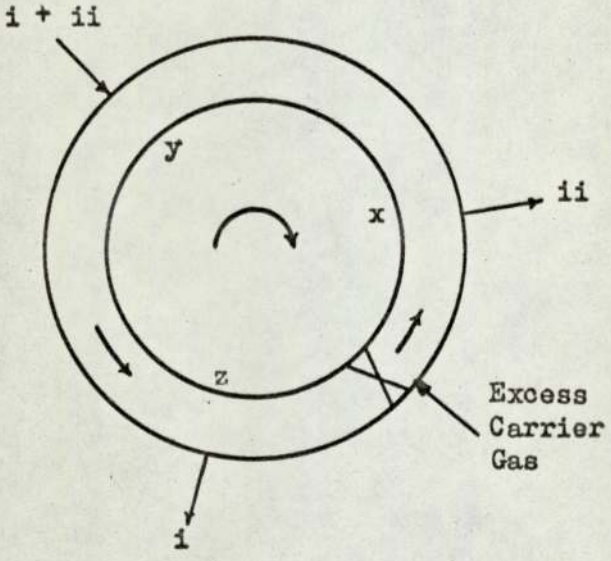

c) Barker and Universal Fisher Eng.Co.Ltd. (17)

stripping section and to provide a gas seal.

The unit constructed by Barker and Huntington (14 - 16), Fig 2.13, consisted of eight square cross-section chambers, 3.8 cm in diameter, linked through external valves to form a circle of 1.5 m diameter. Isolating one section by mechanically closing a consecutive pair of these valves provided an effective gas lock. Each section contained a copper helix through which a heating (or cooling) fluid could be passed. As the column rotated, the fluid was directed to the current stripping section by a system of cam-operated valves.

To permit gas flow into and out of the column 180 gas passages were equally spaced over the chamber face, each passage being normally closed by a self-sealing valve. These valves were automatically opened when they passed under one of the fixed inlet and product offtake ports. Spring loaded plates pressing onto 'O'-rings set in the toroid face prevented leakage to the atmosphere from the opened passages between port and column. The feed mixture entered the column in a vapour state. A 'bleed' of carrier gas was introduced behind the feed port to 'scavenge' any condensed liquid. A chain drive mechanism could rotate the column at between 1 and 10 revolutions per hour although, in practice, a rotational speed close to the lower end of the range was used.

A series of chemical systems were chosen to study the operating performance of the unit (14, 15, 20). Air was used throughout as carrier gas. The packing, as for the moving-bed system of Barker and Lloyd, was 1180-850 μm particles of Sil-O-Cel C22 firebrick coated with 30% by weight of polyoxyethylene 400 diricinoleate. An equivolume mixture of the

Figure 2.13 Circular, Moving-Column Chromatograph (17)

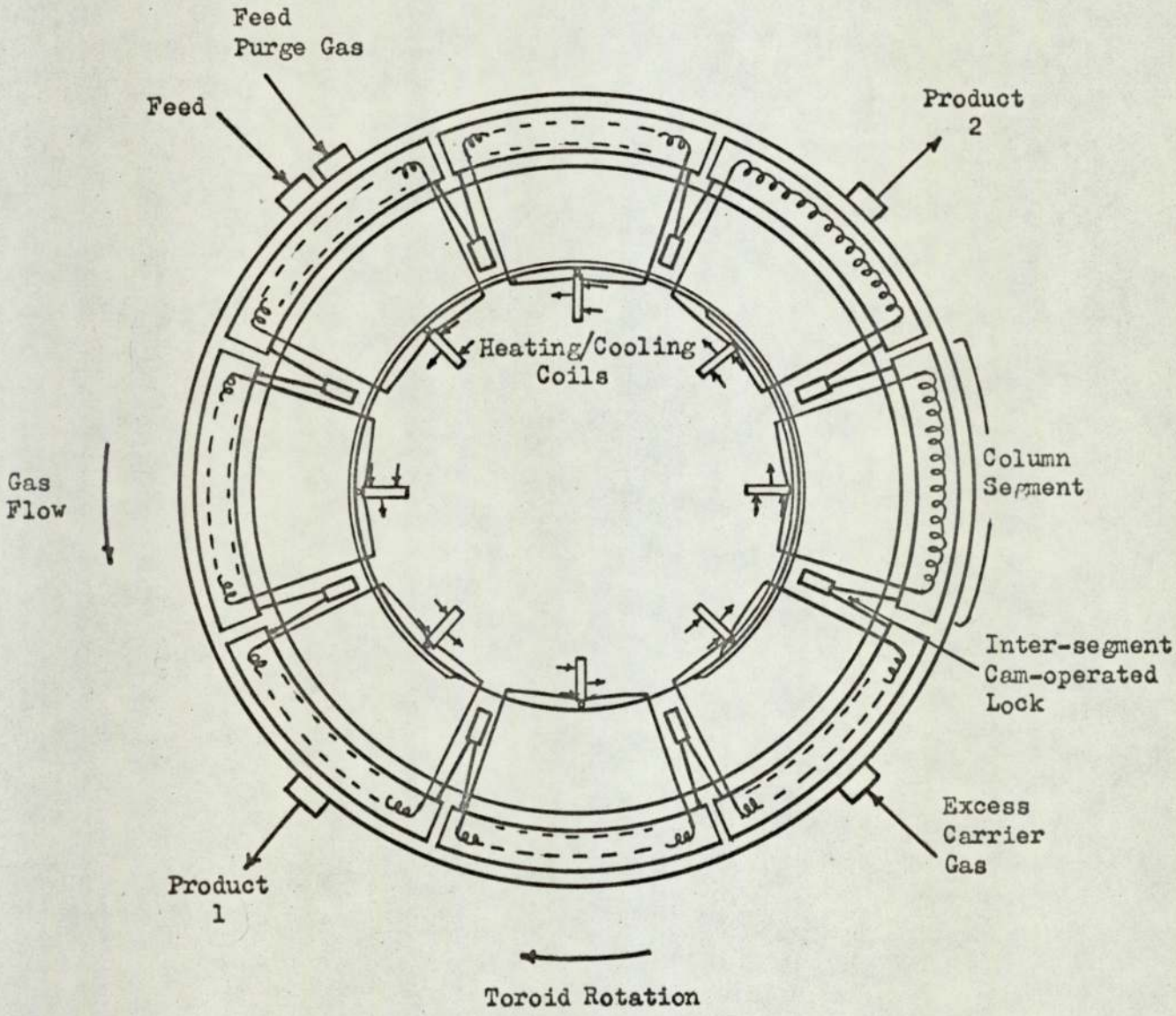

azeotrope cyclohexane-benzene was separated to high purity at throughputs up to 90 cm^3 hr^{-1}. A similar maximum throughput for pure products was obtained for the close boiling system dimethoxymethane/dichloromethane (separation factor = 2.8 at 20°C). For the removal of five impurities from a 97% pure cyclopentane fraction the feedrate was increased to 410 cm^3 hr. With a separating section of 2.72 m length, operating at ambient temperature more than 80% of the cyclopentane was recovered as 'pure' Product 2. The separation factor for this system is 1.52 at 20°C.

Column efficiency was expressed in terms of both H.T.U. and, following modification of an expression given by Tiley and co-workers (148), H.E.T.P. The latter term was not equivalent to that generally associated with chromatography. It more closely resembled the meaning of plate height as used in chemical engineering. For the benzene/cyclohexane system, calculated H.T.U.'s were as low as 2.2 cm (based on benzene above the feed zone) while H.E.T.P.'s ranged from 5 to 6.25 cm.

To increase the separating length of the 1.5 m diameter unit as designed would require the construction of an even larger, cumbersome unit. Barker, in collaboration with the Universal Fisher Group Ltd., Crawley (17), overcame this problem by forming the column from a cylindrical nest of 44, 2.5 cm-diameter by 22.8 cm long tubes linked alternately at top and bottom to give a closed loop (Fig 2.14). Stainless steel was the material of construction.

The tubes were held between two rings. Poppet-valves controlled transfer of gas between tubes in the bottom ring. As the column was rotated, at speeds between 0.2 and 2 rph, a fixed cam depressed at least

Figure 2.14 Compact Circular, Moving-Column Chromatograph (17)

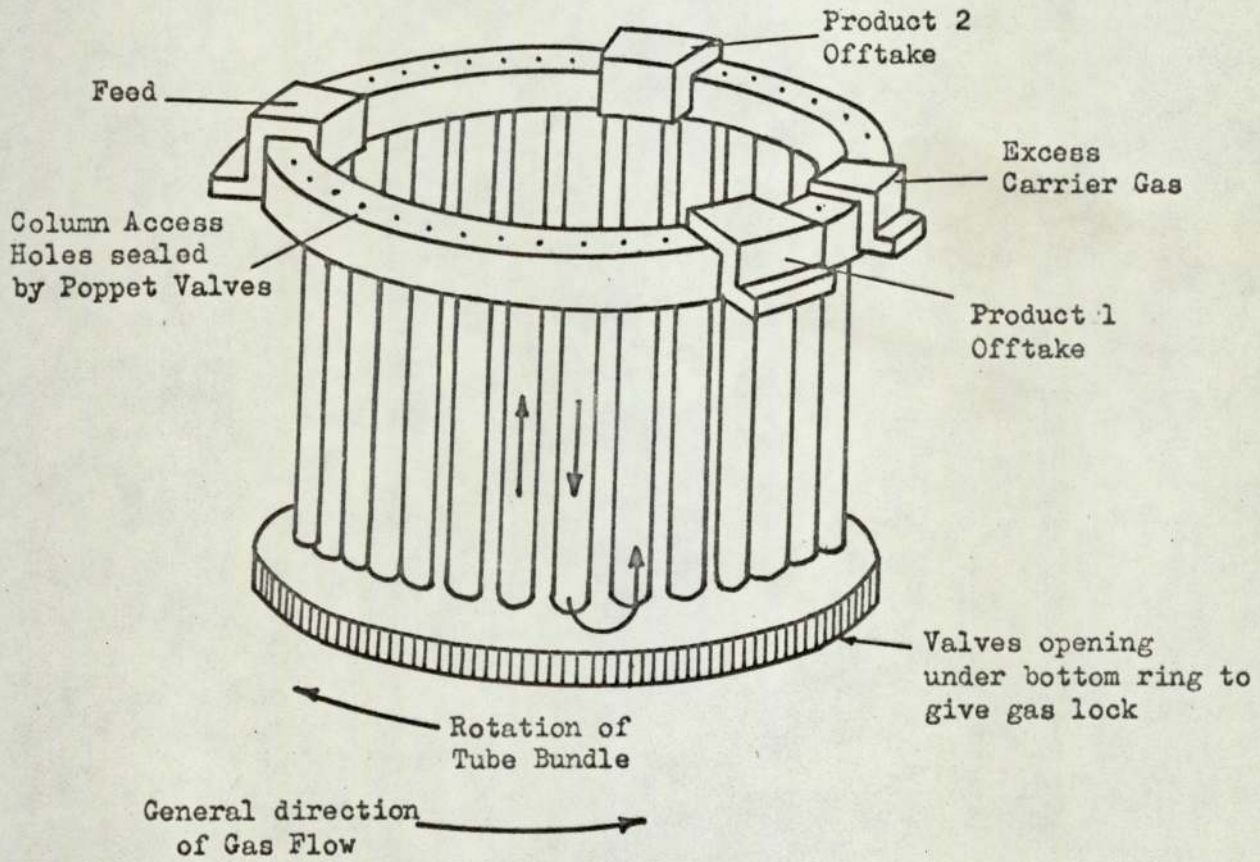

two of these valves to provide the required gas lock and hence maintain unidirectional flow.

Two sets of evenly spaced holes were drilled in the upper face of the top ring. One set provided access to the packed columns for vaporized feed the other serving for excess carrier gas inlet and Products 1 and 2 outlet. Poppet valves were again used to normally close these access points. As the column rotated under the four, fixed position ports, carefully positioned cams depressed the respective valve stems to permit flow to and from the tube bundle. Spring-loaded 'Graphlon' seals, held against the polished top ring face were used to prevent leakage from the ports when the valves were opened.

The entire unit was housed in a thermostatically controlled oven capable of operating up to 200°C.

Published experimental performance data demonstrate the improved separation power of this unit relative to the 1.5 m circular chromatograph (18 - 21). With the analytical chromatograph used, no detectable impurity was observed when refining a 97% pure fraction of cyclopentane at a throughput of 154.4 cm^3 hr^{-1}. The cyclopentane was almost completely recovered as pure Product 2. While throughput has been reduced by a factor of 3, in proportion to the reduction in cross-sectional area, the increased length of the separation section, 4.3 m relative to 2.75 m, enabled a considerable improvement in the purity and yield of the desired product to be achieved.

Selecting a further example from the range of systems studied, Barker and Al-Madfai recovered 91.3% of 99.5% pure α-pinene from crude

turpentine being fed to the unit at a rate of 66.5 cm^3 hr^{-1}. The packing was 500-355 μm particles of 'Celite' coated with 20% by weight polypropylene sebacate. The oven temperature was 113°C.

For a proportional scale-up, the quoted throughput is 20% greater, and the recovery and purity superior, to that found by Ryan et al (91) for a 10 cm-diameter column operating with repeated batch injections. As the column length, 2.74 m, and the operating temperature, 152°C, used by Ryan differ, the comparison is inconclusive.

Three mechanical factors restrict the direct scale-up of the compact circular chromatographic unit:

(i) Operating experience has shown the cam-operated 'poppet' valves, as designed, to be unreliable under the rigorous conditions of stress, temperature and corrosive chemicals. Two simplified versions of the unit have been constructed in which these valves have been replaced by a machined 'Graphlon' disc (155, 156) or annulus (157) held, under compression, against a metal face of the same geometry. Alignment of slots in the two plates as the tube bundle rotates, provide the inlet and outlet ports. Both units have been applied to preparative-scale liquid/solid chromatographic separations.

(ii) Successful operation of the moving-column system is heavily dependent on a reliable face-seal between the top ring and the fixed ports. Wilkinson (158) states that the two surfaces should be flat to within 0.1 μm for such a seal to be fully successful. The high precision engineering problems introduced by increasing the dimensions of such a seal makes this approach impractical.

(iii) Rotating a bundle of large diameter tubes would also present mechanical difficulties which were costly to overcome.

For advancement, a new mechanical approach which did not employ column rotation was required. The design and study of such a scheme forms the basis of the present work, part of which has been previously reported (159, 160).

CHAPTER 3

The Design and Construction of a New Sequential Chromatographic Separator

The experience gained from the moving-bed/fixed port circular chromatographic machines of Barker and co-workers led to the following two conclusions:

(i) In moving to large column diameters it was evident that physical movement of the column should be avoided.

(ii) A separate column section would be advantageous for the purging of the more strongly sorbed component(s), the purge fluid being independent of the carrier stream. Two main advantages result. The purging gas rate can be increased to such a level as to ensure the complete removal of product from the isolated section without increasing pressure in the separating section. Also, the carrier gas entering the main separating section is not contaminated with Product 2.

In designing a new unit three general factors had to be considered; reliability, flexibility and cost. As a continuously operating unit, the need for reliability is self-evident. Flexibility arises out of the future desire to be able to apply the design principle at all column diameters for all forms of chromatography. In addition, the facility to operate as a batch system was required for comparative purposes within the projected experimental program. Finally, for this research work, a capital budget of £1,000 was available for the construction of the new unit. The design, therefore, represents a compromise with respect to size and materials of construction.

3.1 Principle of Operation

Fig 3.1a schematically shows the distribution of two components within the system soon after 'start-up'. Carrier fluid enters the column at port C and flows through the solute coated packing. The least strongly sorbed component (component i) is preferentially moved towards the Product 1 offtake port, Cp. A section of the closed loop column is isolated by locks Tx and Txx, an independent fluid stream entering at port P and exiting from Pp.

In Fig 3.1b all the port functions have been advanced around the fixed column,co-current to the direction of mobile phase flow. The rate of port advancement is less than the velocity of the less strongly sorbed component through the packing but greater than that of the more strongly sorbed component (component ii). Consequently component ii is being 'held' preferentially on the solvent phase while component i is issuing from Cp as 'pure' Product 1.

Fig 3.1c represents the fully established operating condition of the system. The isolated section, now containing component ii, is being purged to give Product 2 and regenerate the packing ready to receive the advancing component i, at present issuing from Cp. It can be seen that the counter-current movement of solute laden carrier and solvent phase has been simulated by the movement of the ports, co-current to the direction of the carrier phase, past a fixed column.

A gas/liquid chromatographic separator based on the above principle was constructed at the 7.6 cm (3 inch) column diameter level. British and American Patent applications have been registered describing this equipment (161).

Figure 3.1 Diagramatic Representation of the Principle of Operation of the Sequential Chromatographic Separator

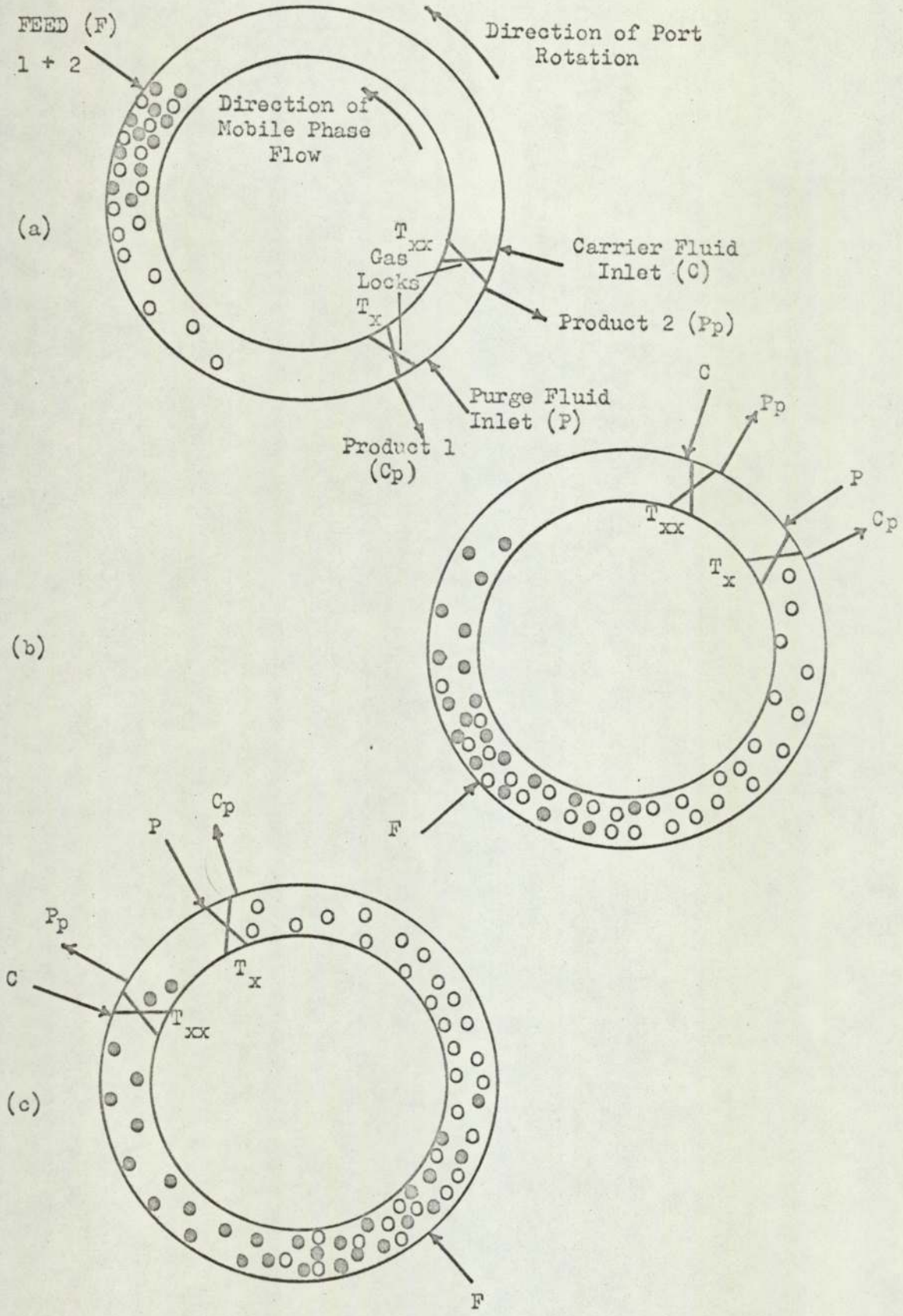

3.2 The Central Unit

3.2.1 Overall Description

From Fig 3.1 it can be seen that seven moving functions were required; feed inlet, carrier gas inlet and outlet, purge gas inlet and outlet and two gas locks. The unit was therefore designed in discrete sections, the column forming each section being provided with the necessary functions by solenoid operated valves.

Twelve packed columns were linked alternatively at top and bottom to form a closed symmetrical ring. Fig 3.2 shows three consecutive columns in diagramatic form. On each transfer line between the columns was situated a normally open solenoid valve (T). Energising a consecutive pair of these solenoids effectively isolates an individual column. The gas inlet and outlet ports, situated on the end cones of each column, were provided by four, normally closed, solenoid valves (C, Cp, P, Pp). A similar valve provided the inlet port for liquid feed (F).

The twelve ports of each type were connected to an independent, centrally situated, distributor system. Lines from the gas distributors then passed to the relevant control and measuring devices while the feed distributor was connected to a positive displacement pump.

The inlet and outlet solenoid valves (gas plus liquid feed) were electrically connected, in the required combinations of five, to twelve terminals. An additional rail of twelve terminals was provided for the transfer valves. The two terminal rails were interconnected, through a relay bank, such that when one terminal on the inlet/outlet valve rail was energised then two terminals on the transfer valve rail were also

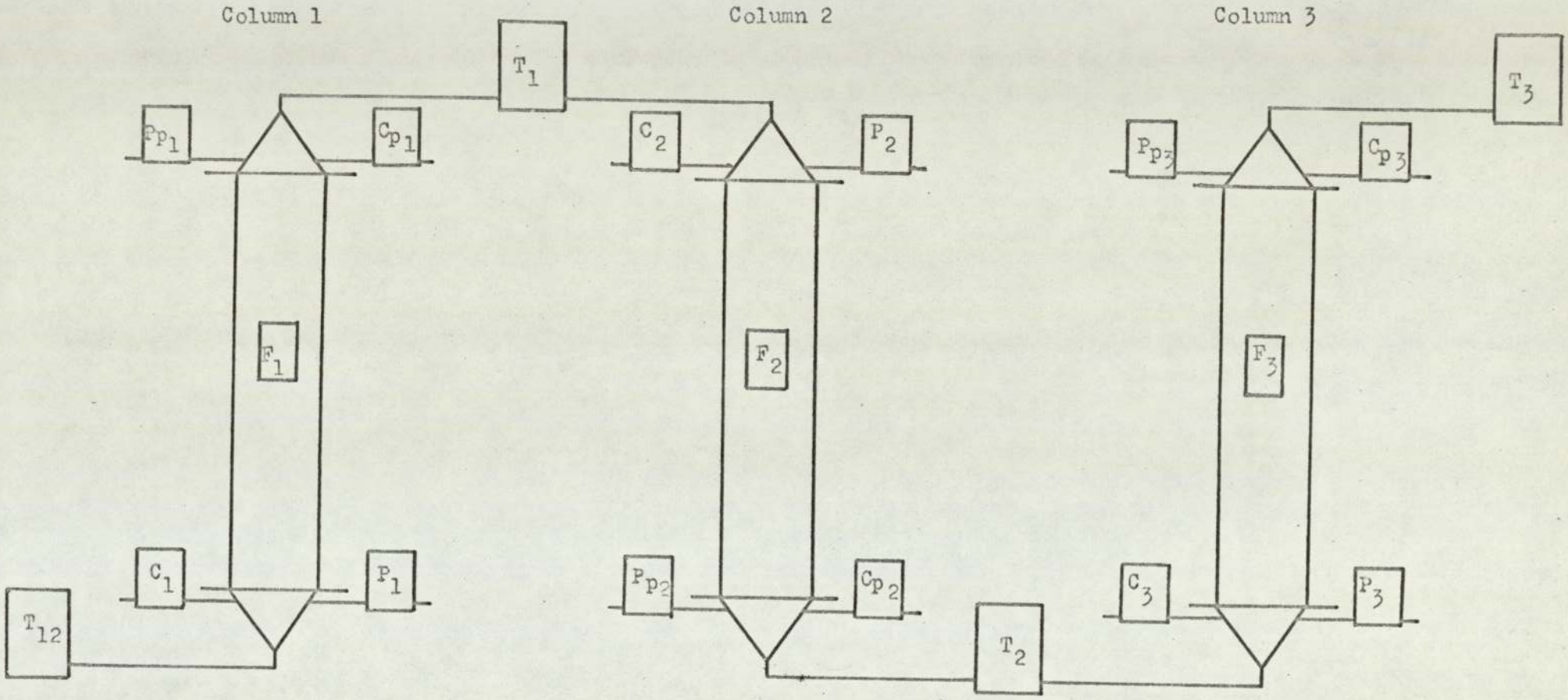

Figure 3.2 Schematic Diagram of Three Consecutive Columns showing Relative Positions of Solenoid Valves

Legend for Valves: T = transfer
C_p = carrier product (Product 1) outlet valve
P_p = purge product (Product 2) outlet valve
F = feed
C = carrier fluid (gas) inlet
P = purge fluid (gas) inlet

energised. Each of these terminal combinations were energised in turn, for a selectable time interval, by an automatic electronic timing device.

Assigning the numbers 1 to 12 to the individual columns; at a particular point in the cycle bed 2 would be isolated by energising the solenoid valves T_1 and T_2. The purge gas inlet, P_2, and outlet Pp_2 solenoids on bed 2 would be energised to open, effecting purging of the more strongly sorbed component. The carrier gas inlet solenoid on bed 3, C_3, would also be energised to open, carrier gas passing through eleven packed columns to exit from bed 1, as Product 1, where the carrier gas outlet solenoid, Cp_1, is energised. Feed would be pumped into an appropriate bed lying between 3 and 1, say 8, through the energised centrally positioned valve, F_8.

On sequencing, column 3 would be isolated by energising solenoids T_2, T_3. Purge gas now enters column 3, at P_3, to purge Product 2, issuing from Pp_3. Carrier enters column 4 at C_4 and flows round the unit to exit from the regenerated bed 2 through Cp_2. Feed would be entering bed 9, through F_9. 12 sequences complete the cycle which then resumes.

Details of the design and construction follows.

3.2.2 Detailed Design and Construction

3.2.2.1 The Columns

The individual column dimensions were selected as a balance of two factors, cost versus continuity. The 'ideal' system is truly continuous in operation, with the port functions being gradually rotated past the fixed column, giving a steady product concentration level. It was, therefore, desirable to limit the discrete nature of operation of the

sequential process. However, each packed column introduced into the system required a further six solenoids plus their respective pipe networks. In addition the format of the equipment demanded an even number of columns.

Within the given budget for the research, twelve copper columns of 7.6 cm-diameter were selected, representing a 9 : 1 scale-up factor over the unit constructed by Universal Fisher (17 - 20). In keeping with that unit a length/diameter ratio of 8 : 1 was chosen giving a packed length of 61 cm (24 in).

Plate 3.1 shows the assembled unit while Fig 3.3a is a detailed drawing of an individual column.

The end flanges of 1.3 cm (1/2 in) mild steel were silver soldered to the outer wall of the copper tube. The outside diameter of the flanges was 12.7 cm (5 in) with 4, 9.6 mm (3/8 in), bolt holes evenly spaced on a pitch circle diameter of 10.2 cm (4 in). This did not comply with B.S. 10, which specified a flange diameter of 18.4 cm (7.1/4 in) with 4, 1.6 cm (5/8 in) bolts as a p.c.d of 14.6 cm (5.3/4 in). However, as it was desired to keep the transfer lines to a minimum, smaller flange dimensions were selected.

The packing was retained in the column by a copper gauze, of nominal aperture size 150 μm (100 B.S.mesh), silver soldered onto an annular brass ring of 8.9 cm (3.5 in) inside diameter. The seals between the tube and flange, the gauze retaining ring and the end cone flange were provided by 2.4 mm (3/32 in) thick gaskets of 'Klingerit', an asbestos/rubber composite supplied by Richard Klinger Ltd., Warley, Worcs.

PLATE 3.1 The Columns - Side View

CD	Central distributor
F	Feed solenoid valve
FP	Solute mixture feed pump
G	Gas inlet/outlet solenoid valve
H	High pressure air line to transfer solenoid valve
PC	Fine pressure controller
SP	Septum sealed sample point
T	Transfer solenoid valve
TT	Timer unit rear terminals

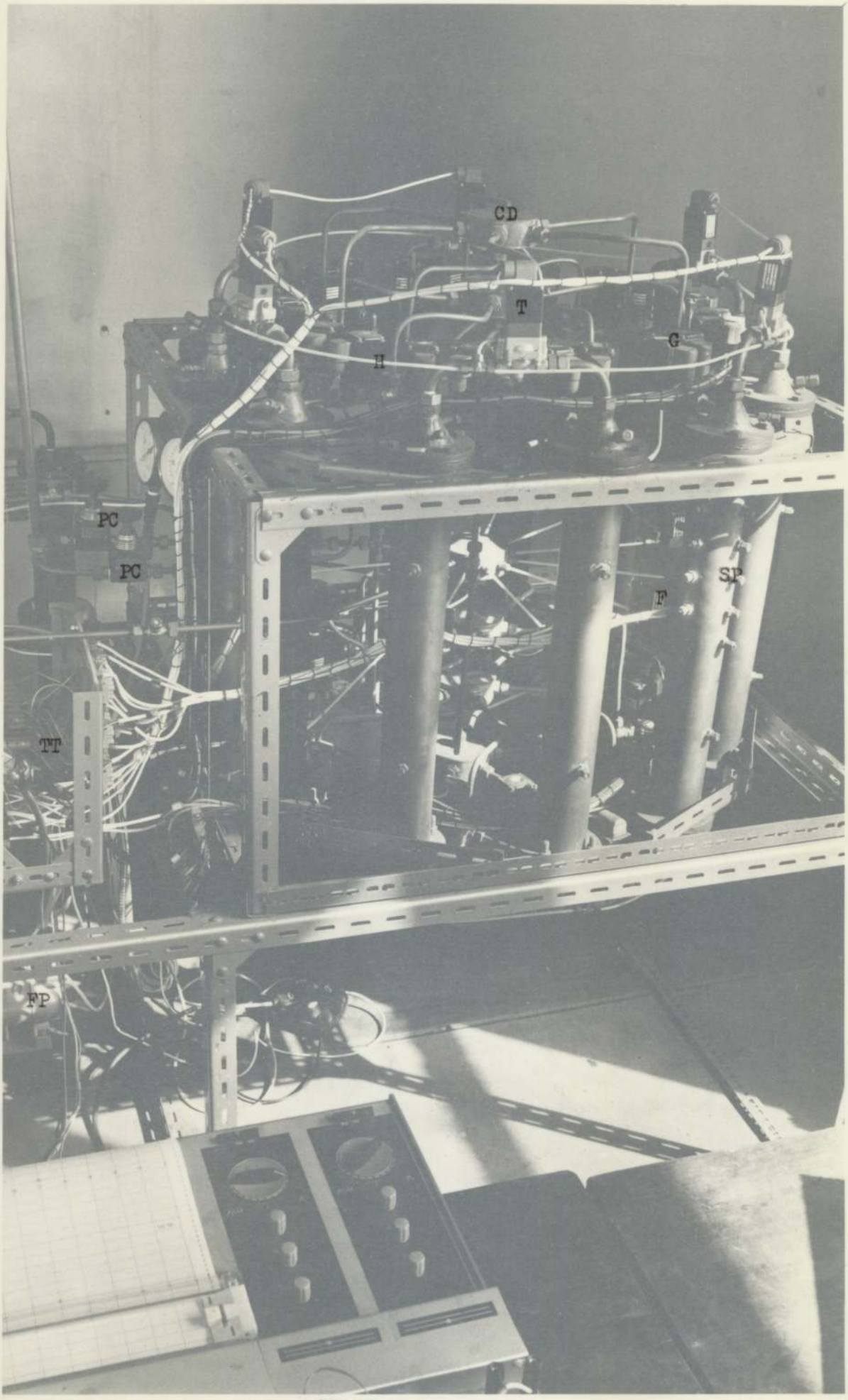

PLATE 3.1

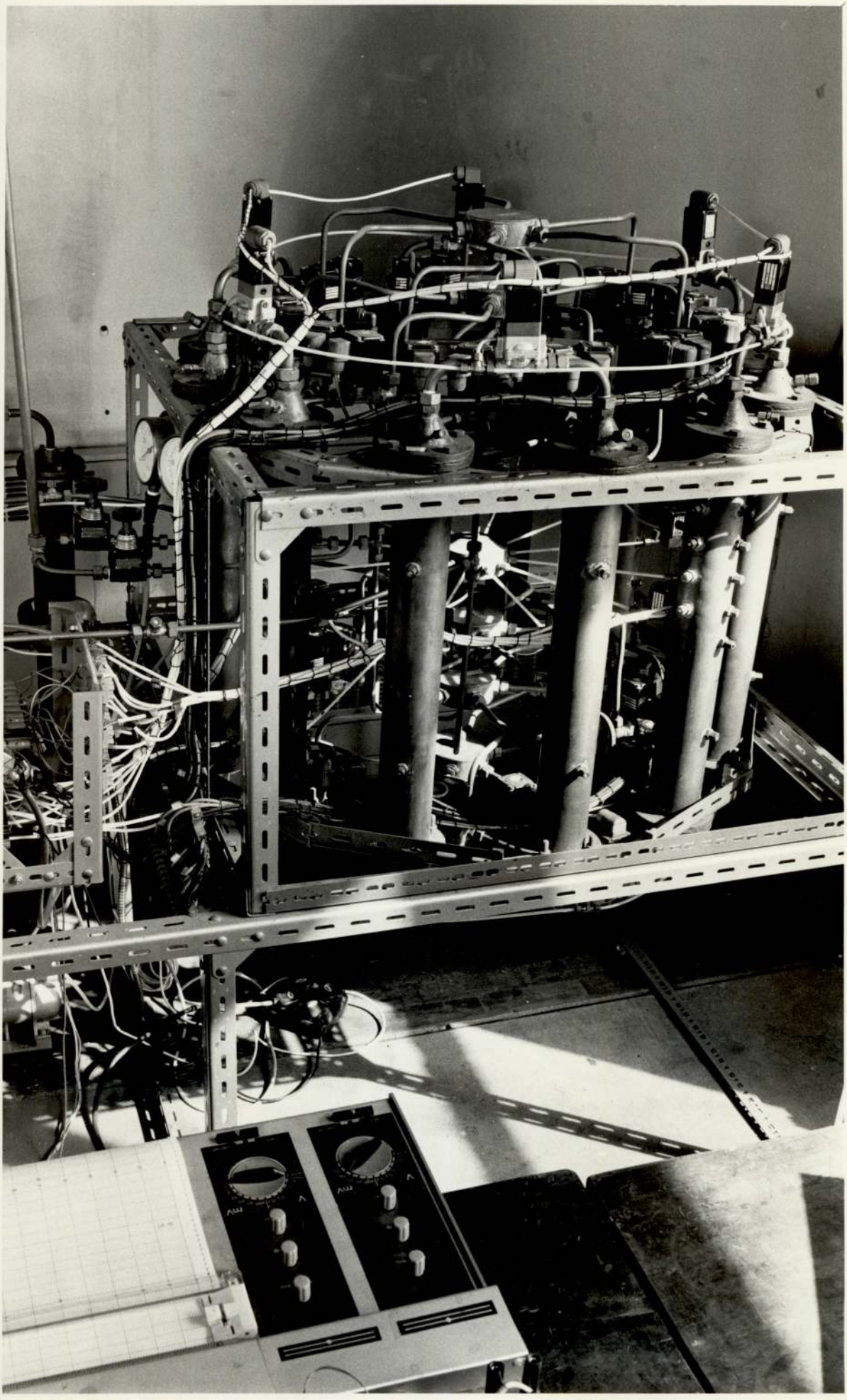

Figure 3.3 Design of an Individual Column

a) Overall Construction

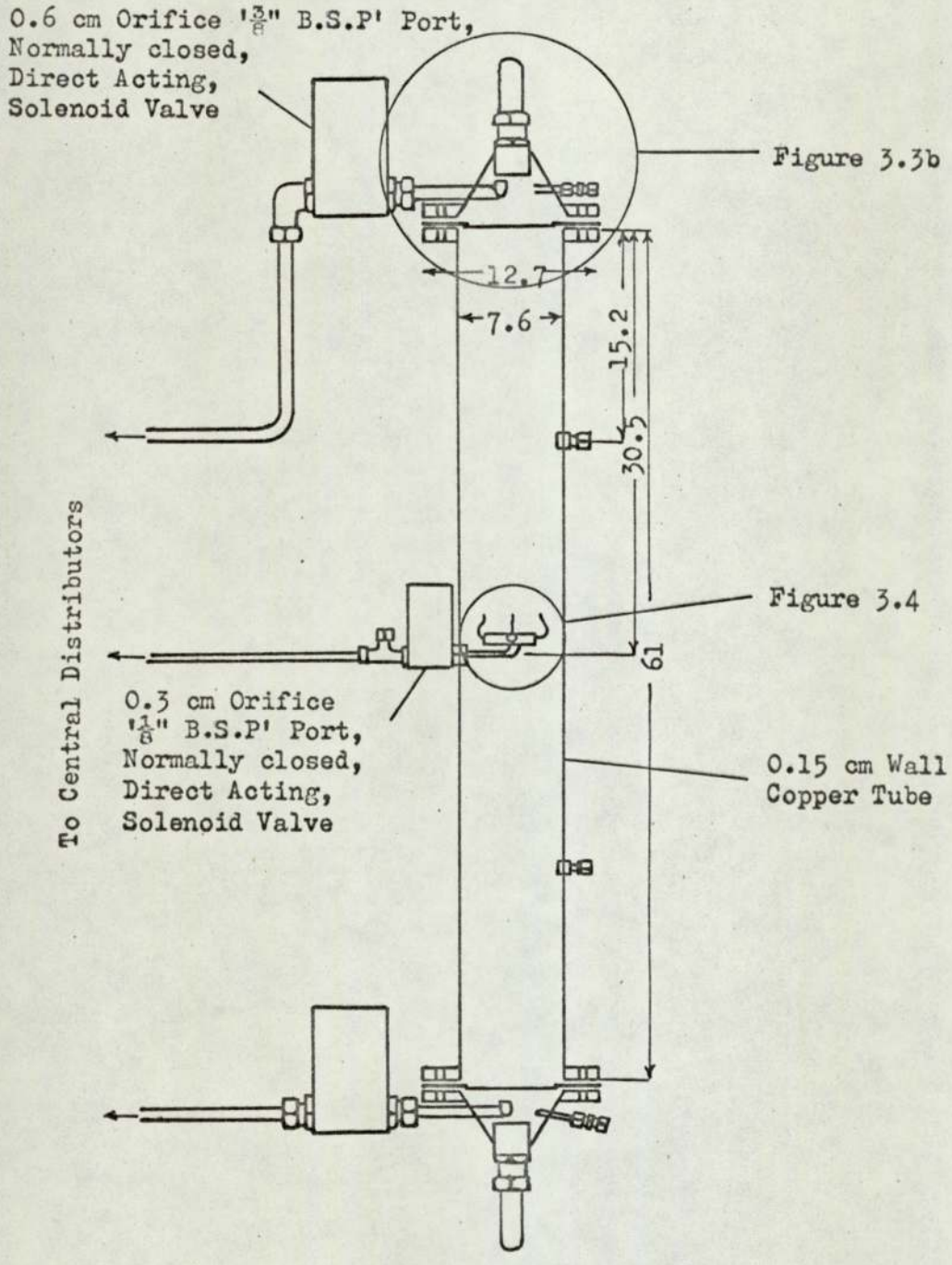

Note: i) dimensions given are in centimetres
ii) scale is 1/5th full size

Figure 3.3 (Cont'd.)

b) Column End Cones

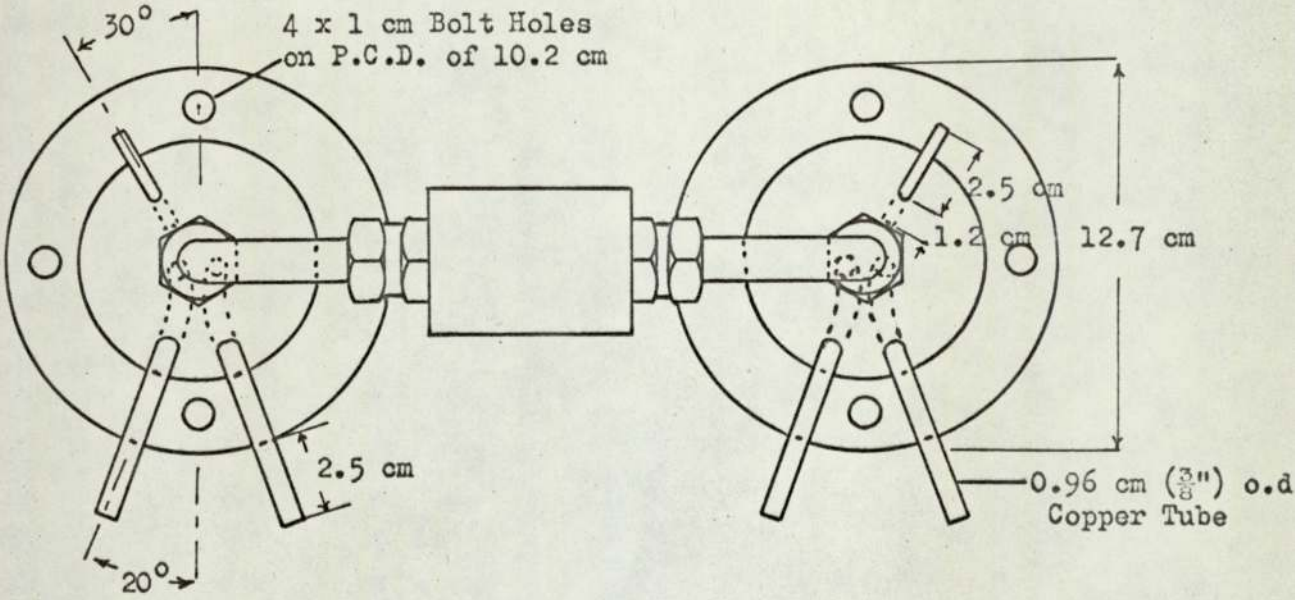

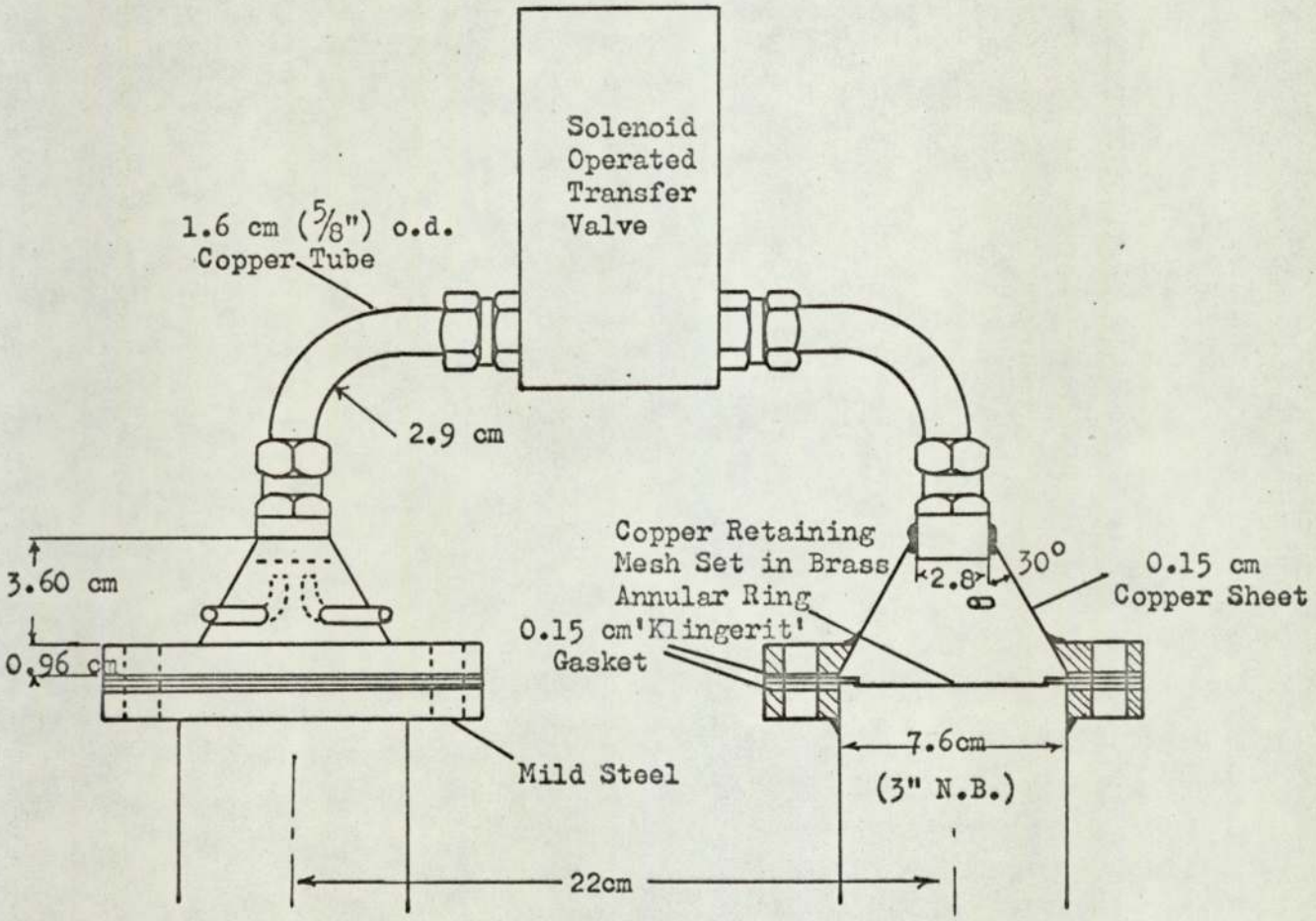

Note: Scale is 2/5th full size

It was found necessary to coat the gaskets with a sealing compound, 'Stag' (I.C.I. Ltd.).

The mild steel flanged copper end cones are shown in detail in Fig 3.3b. The truncated cones were formed from 1.6 mm copper sheet, the angle being approximately 60° and height 5.1 cm (2 in). A "5/8 in" B.S.P. brass parallel female stud coupling (all couplings were supplied by Simplifix, Wednesfield, Staffs.) was silver soldered into the apex of the truncated cone to receive the 1.6 cm o.d. copper transfer line from the isolating solenoid. The tube diameter for the lines is consistent with the inlet port diameter of the selected solenoids.

The gas inlet/outlet lines entering the cones were 9.5 mm o.d. copper tube, two being present in each cone. The length of these lines was kept to a minimum as their volume represents 'dead' space between the columns and the solenoid valves. Allowing the lines to extend 2.5 cm beyond the flange was sufficient to permit connection to the parallel male stud coupling from the normally closed solenoid valves. The ends of the inlet and outlet gas lines within the cone were turned in the direction of gas flow through the unit.

At construction the cones and transfer lines were packed with glass wool. This was removed during testing as strands were being carried in the gas stream onto the seating of the valves, resulting in unacceptable leakage.

The feed inlet was centrally positioned in each column. A '1/8 in B.S.P.', brass stud coupling was soldered into the tube wall, allowing the feed solenoid to be set as close as possible to the column.

Inside the column the feed line was split into four by a cross fitting (see Fig 3.4). A 1.6 mm o.d. tube, packed with glass wool, emanated from each arm of the cross and was turned in the direction of gas flow. Such an arrangement gave four feed exit points within the packed bed evenly spaced on a circular pitch with a diameter of approximately 4 cm. The intention was to assist even cross-sectional solute loading of the solvent phase while limiting the distributor volume. A large volume of liquid feed in the distributor after the feed solenoid was closed would slowly vapourise, possibly resulting in contamination of resolved products at a later stage in the cycle.

A sample point was set midway between the feed point and the end cones on each column. In addition, on four of the columns, regularly spaced around the unit, two rows of six sample points were set at right angles to each other between the feed point and the upstream end cone. Each column sampling point consisted of a '1/8 in' B.S.P. stud coupling soldered into the column wall and cut flush to the inside of the column. A silicone rubber septum (Perkin Elmer Ltd., Beaconsfield, Bucks.) set into the nut head provided a seal while permitting gas sampling by a syringe. A sampling tube, similarly fitted with a septum, was let into each end cone.

The twelve columns were connected, as shown in Fig 3.2 and Plate 3.1, to form a compact closed circle suspended in a frame. The distance between column centres was 21.6 cm, giving a diameter for the central unit of 90 cm. The column spacing was dictated by the space requirement of the transfer solenoids and associated lines, as well as the central

Figure 3.4 Internal Feed Distributor

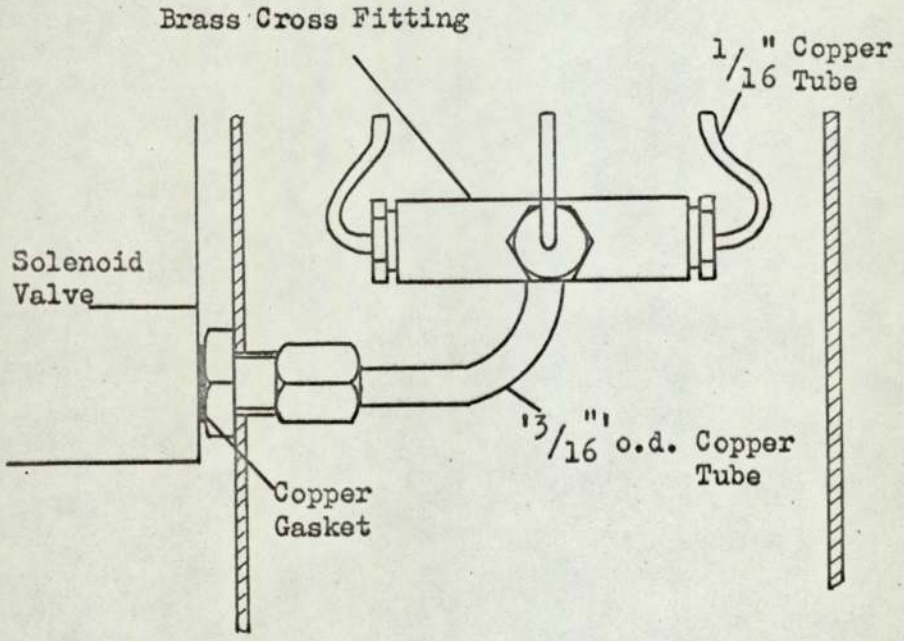

Note: Scale is full size

distribution pipe network for the inlet/outlet fluid lines. The orientation of the tubes and end cones was such that all inlet/outlet fluid access points faced to the centre of the circle, while all sample points faced outwards for access. The support frame, of 4 cm 'Handy Angle', had dimensions of 96.5 cm long by 96.5 cm wide by 58.5 cm high.

3.2.2.2 The Solenoid Valves

Careful selection of the valves was necessary as they must remain fully closed when possibly operating against a substantial 'back pressure'. This consideration results from the independence of the pressure in the isolated and main separating sections. The valves chosen, all of brass bodies with 'Viton' seats, were purchased from Burkert Contromatic Ltd. (Bowbridge, Stroud). They fall into two categories:

(i) The gas inlet and outlet ports (C, Cp, P, Pp) were provided by 6 mm orifice, '3/8 in B.S.P.' port, normally closed, direct acting solenoid valves. A similar valve but of 3 mm orifice, '1/8 in B.S.P.' port was used as the inlet port for the liquid feed (F). Both valves, on testing, withstood a differential back pressure in excess of 150 kN m^{-2} without the plunger being lifted against the spring to cause leaking. A value of 150 kN m^{-2} was considered to give adequate flexibility in the flow and pressure settings.

(ii) 13 mm orifice, '5/8 in B.S.P.' port, normally open, servo-acting solenoids were used for the transfer solenoids (T). To meet the selection criteria it was found necessary to modify these valves. An external high pressure air line, linked around the twelve solenoids, was used to seat the diaphragm in the energised state. (Fig 3.5).

Figure 3.5 Modification to 'Transfer' Solenoid Valves

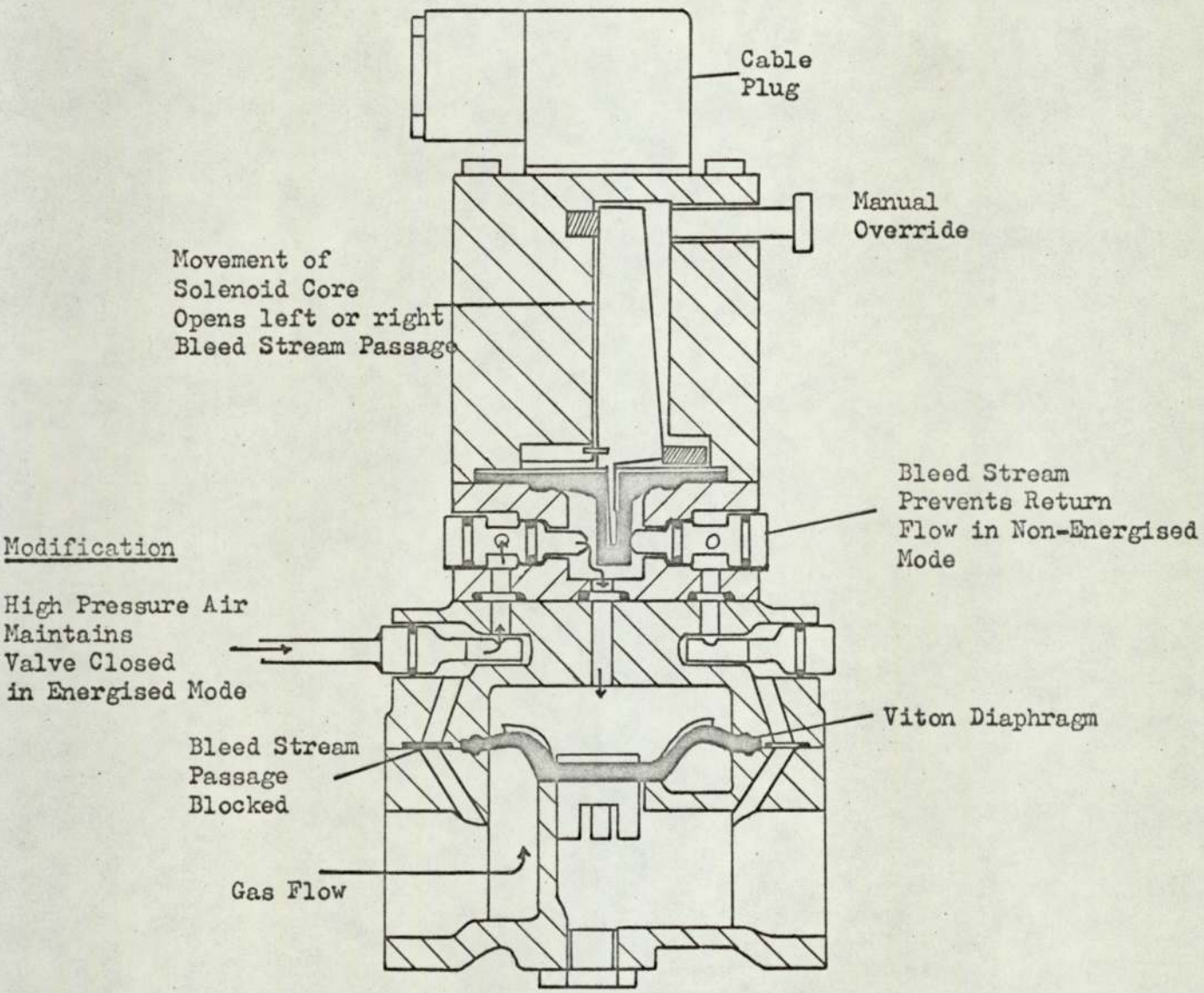

Note: Valve cross-section shown in energised state

All solenoid coils were fully encapsulated and fitted with a 'Burkert' cable plug. The connecting 5 A, 240 V cables from the solenoids to the automatic timed sequencing unit were harnessed together, according to valve function, to run tidily around the periphery of the unit. While the transfer solenoids were directly connected to the transfer valve terminal rail, in which two successive socket points are energised, the wiring for the inlet/outlet gas solenoid valves and for the feed solenoids was taken to two sets of connecting blocks. The neutral and earth lines within the two respective sets of connecting blocks were strapped together allowing a single line for each to be used to make the final connection to the 'timer'. Twelve live lines, each line combining four valves (C, Cp, P, Pp), were then connected to the single energised socket terminal rail. For flexibility, jack plugs were attached to the twelve live feed valve lines. These could then be plugged into the single energised socket rail, offsetting the feed location with respect to the isolated column as required.

A detailed description of the terminal, and hence solenoid, energisation pattern is given in Section 3.3.1.

3.2.2.3 The Central Distribution Network

A pipe network was constructed to separately distribute the five input/output fluid streams to each column. The five streams are; carrier gas inlet, carrier gas outlet (Product 1), purge gas inlet, purge gas outlet (Product 2) and the liquid feed. The nature of the separation unit, giving consideration to such factors as pressure drop in the gas lines, demands symmetry. Consequently nine distribution centres were required. The feed port is located at the mid-height of the column.

Therefore the liquid feed could be distributed by one distribution centre with twelve 'arms'. However, the position of the four inlet/outlet gas ports successively alternated from, say, the base of one column to the top of the next (Fig 3.2). Hence, two distributors having six arms were required for each gas port type.

The design of the distributors, constructed in brass and copper, took three forms (Fig 3.6):

(i) The liquid feed distributor (Fig 3.6a and Plate 3.2) was essentially a closed cylinder of diameter 10.2 cm (4 in) and wall height 3.8 cm (1.1/2 in) with a shallow coned base. Twelve '3/16 in B.S.P.' parallel male stud brass couplings were silver soldered into the circumference of the copper cylinder at an even spacing. A spring loaded '3/16 in B.S.P.' brass tap, of a simple cock type (Simplifix, Wednesfield, Staffs.) was similarly soldered into the centre of the brass base and top plates. The lower tap enabled isolation of the distributor from the feed pump and control of drainage of the feed pipe network at the end of a run. The purpose of the top plate tap was to permit displacement of air from the distributor during start-up (see Section 8.1). This tap was subsequently replaced by a nut and septum because of leakage.

(ii) The four gas outlet distributors had the same dimensions as the feed distributor. The six evenly spaced 'arms' were formed by '3/8 in B.S.P.' parallel male stud couplings. The same sized coupling was soldered into the top plate to accept the inlet gas line. In case of condensation of any of the products in the lines a gas tap was set in the base plate cone. For the chemical system chosen for study in this work this was superfluous but may prove valuable in the future.

(iii) The four gas inlet distributors (Fig 3.6c) are as described in (ii) but with a flat base plate. The provision of a drainage tap is obviously unnecessary.

The nine distributors were set vertically on the axis of the cylinder formed by the twelve columns (Fig 3.7). Their order was set by two factors; the need for symmetry and the prospect of studying in the future a chemical system which may condense in the product lines. Hence, the lines from the product ports must have a generally downward run. As the purged product is normally the least volatile this was placed in the lowest position of the two sets of four gas distributors. The pairs of like function distributors were linked by 9.6 mm o.d. copper tubing to the line running to the relevant central device by an equal 'tee' coupling. The spacing between distributors, although kept to a minimum, was set by the sharpness of angle through which the linking pipe could be turned.

The tubing connecting the feed solenoids to the feed distributor was of white 4.8 mm o.d. nylon. This material was chosen for its transparency. A small steel ball-bearing held in the line between two wire stops could be observed as a check on the correct functioning of the feed solenoid valves during operation of the unit. A 'tee' fitting was also placed in the line immediately preceding the valve to enable all air to be displaced from the feed lines before start-up. The vertical stem of the 'tee' was initially capped with a gas tap but this was also subsequently replaced by a nut and septum to eliminate slight leakage.

The tubing pattern for the 9.6 mm copper gas lines from the solenoid valves to the distributors was largely dictated by the width of the valves. Symmetry was of course maintained (Fig 3.8 and Plate 3.3).

Figure 3.6 Central Distributors

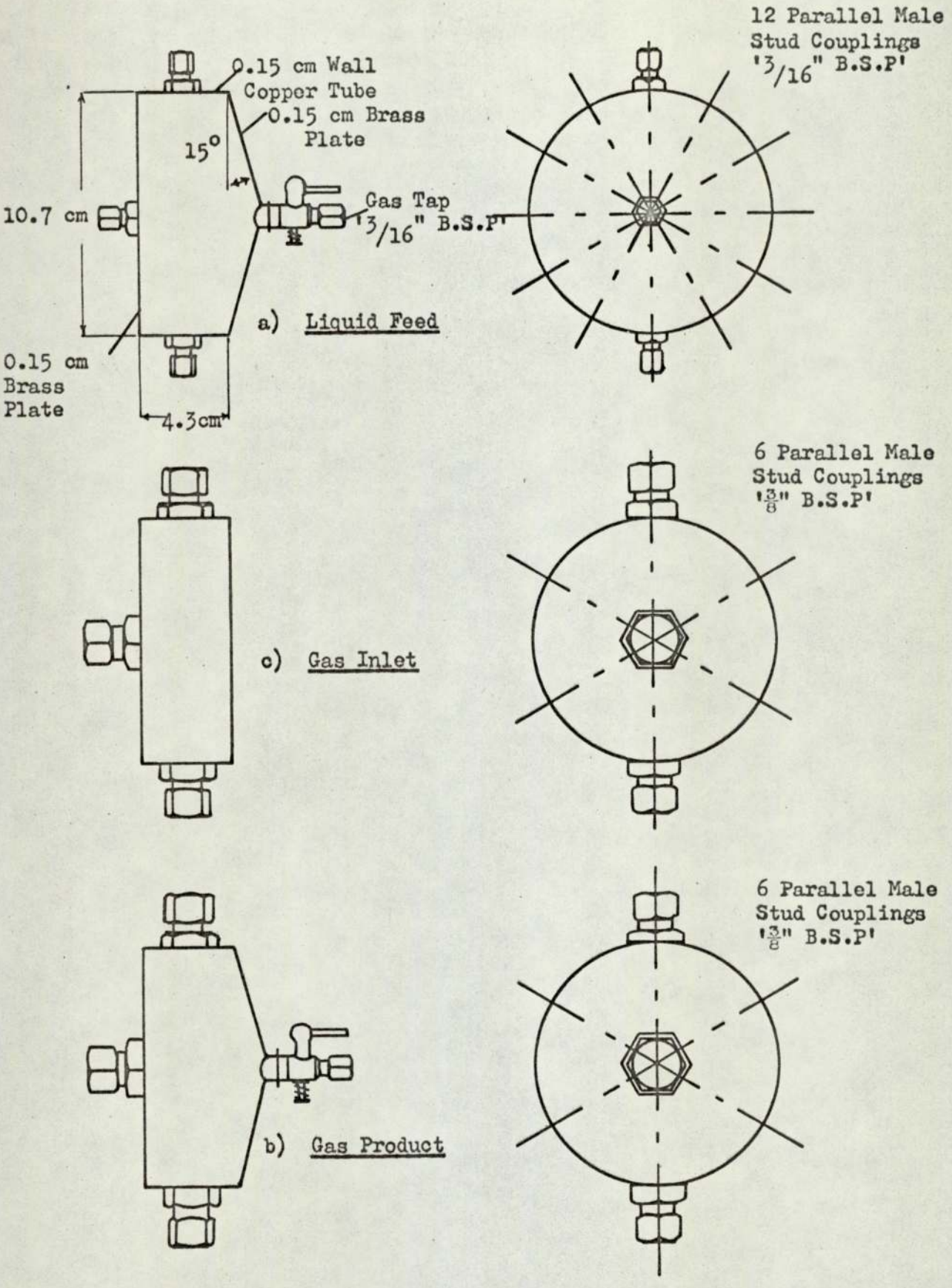

Note: Scale is 2/5th full size

Figure 3.7 Vertical Order of Central Distributors

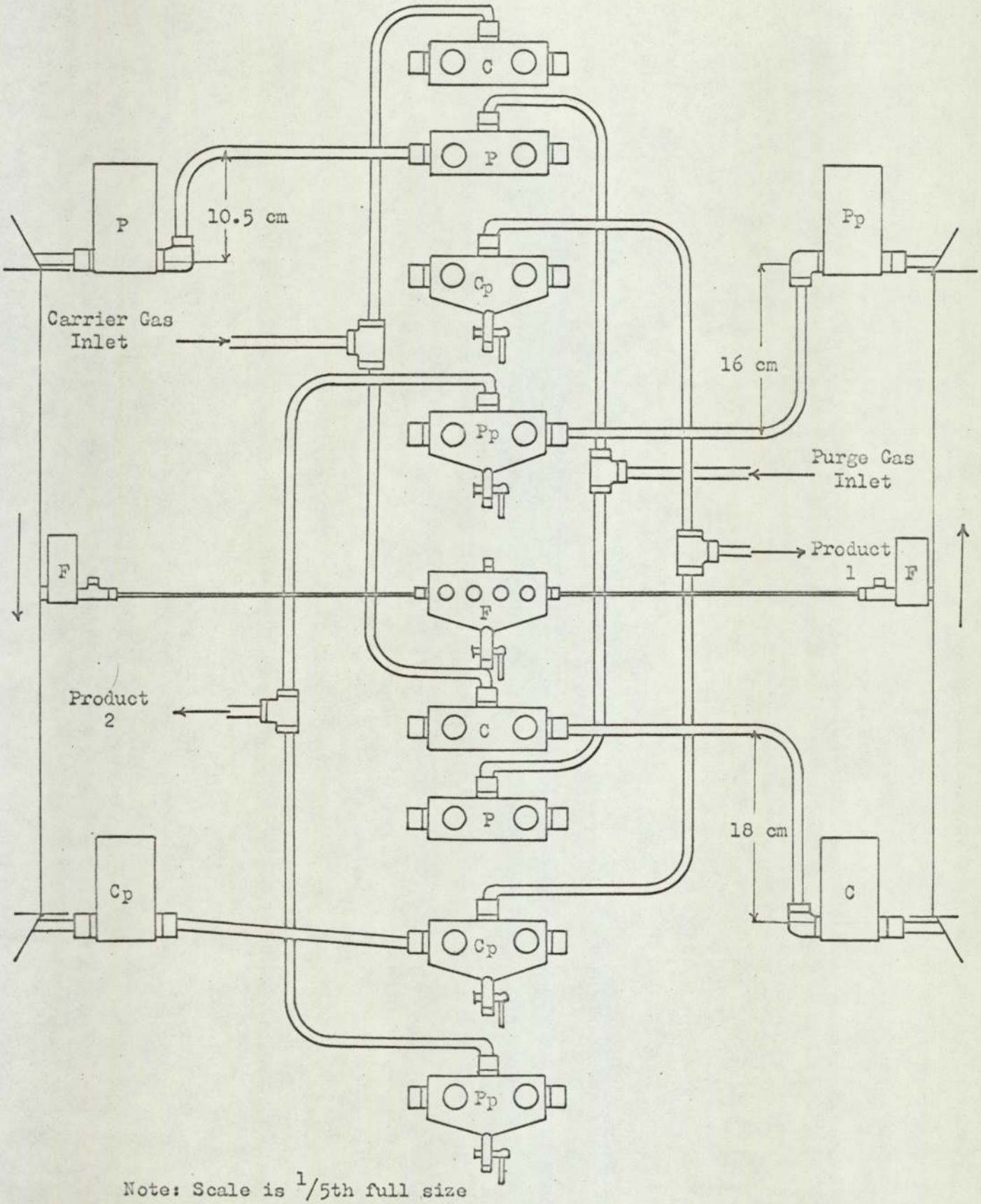

Note: Scale is $^{1}/_{5}$th full size

Figure 3.8 Diagram to show Pipework Connection Pattern from Columns to Central Distributors

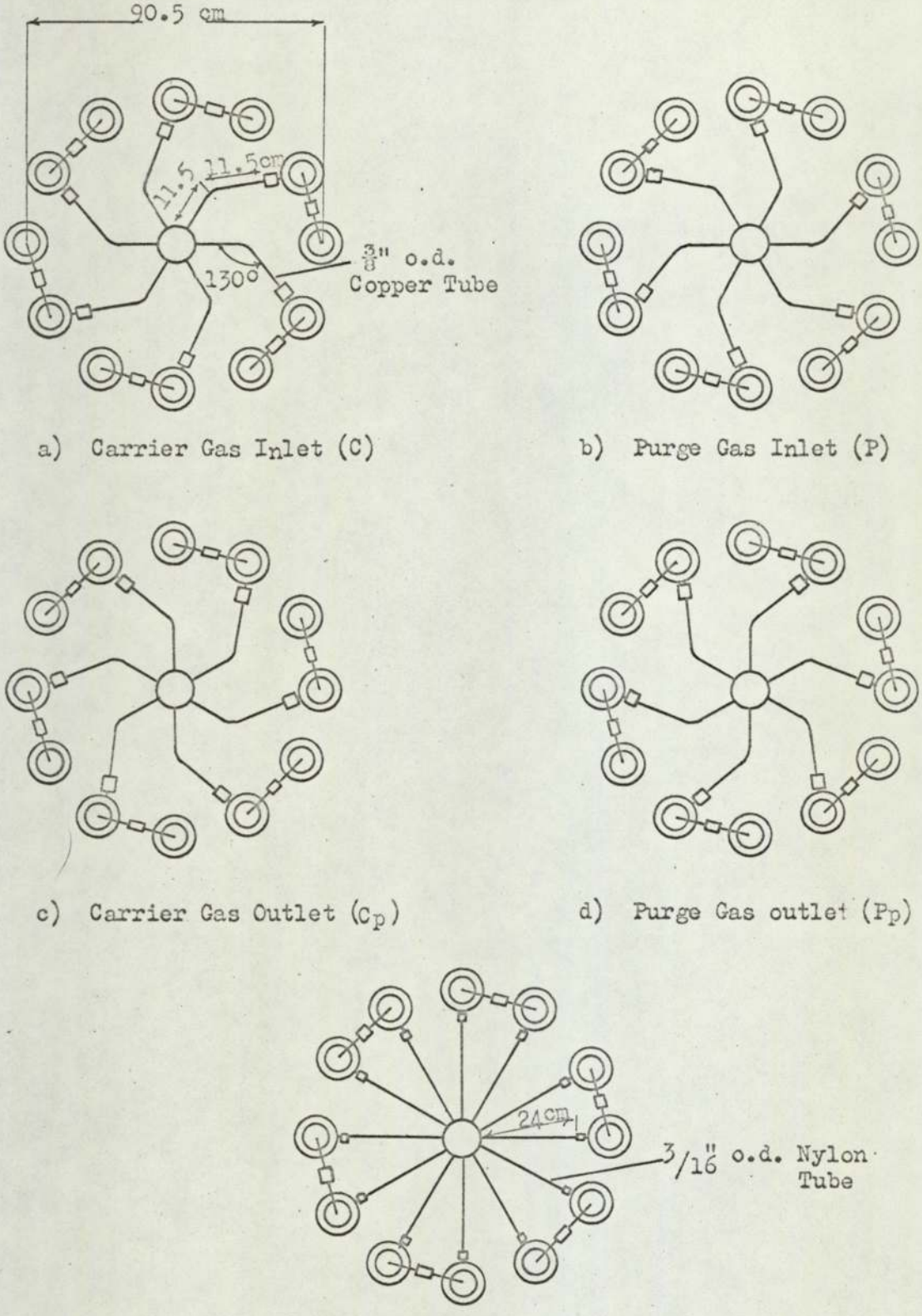

a) Carrier Gas Inlet (C)

b) Purge Gas Inlet (P)

c) Carrier Gas Outlet (C_p)

d) Purge Gas outlet (P_p)

e) Feed (F)

PLATE 3.2 Central Distributor

C	Carrier gas inlet
F	Solute feed
N	Nylon tube (3/16" o.d.)
P_p	Purge product (Product 2)

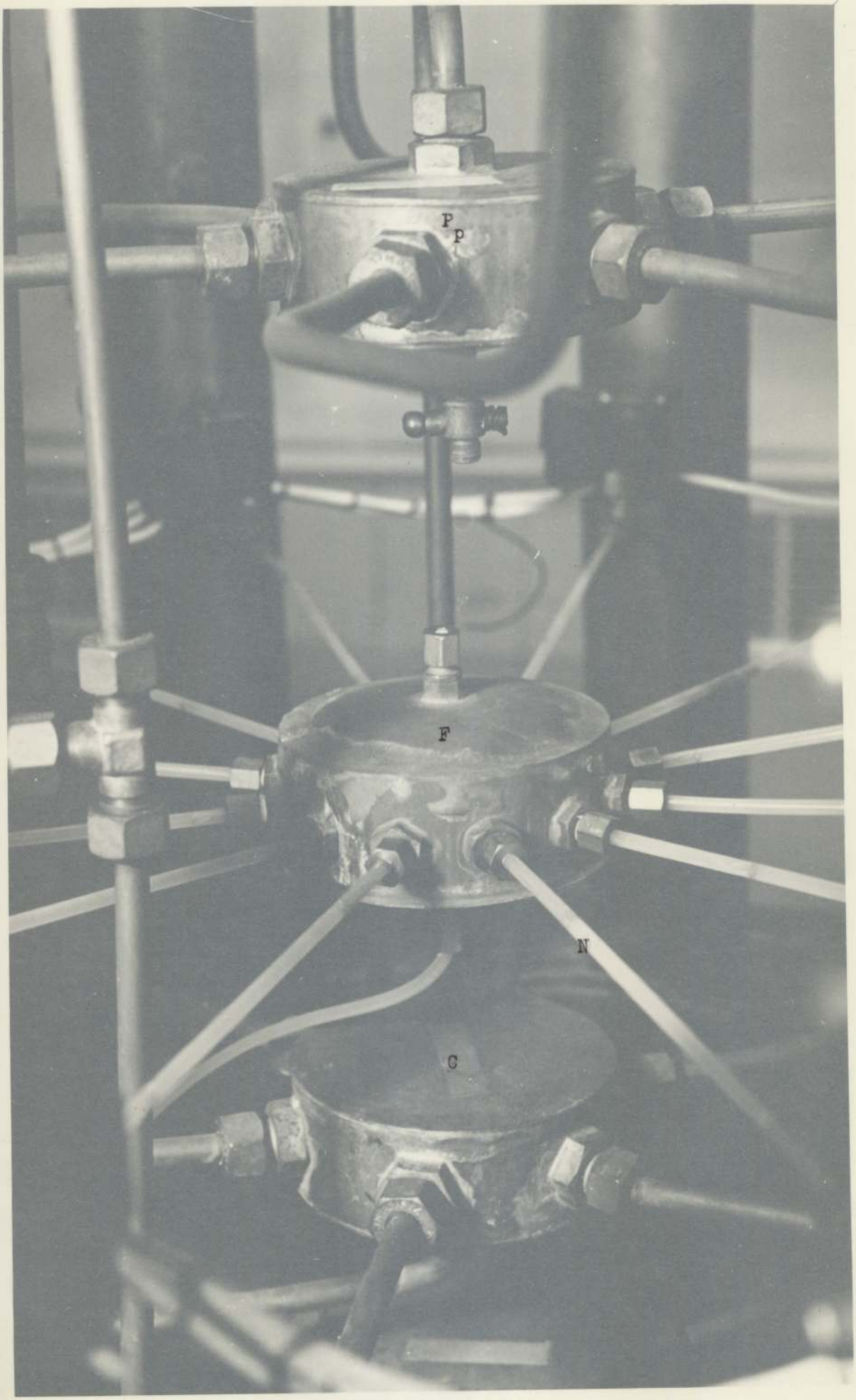

PLATE 3.2

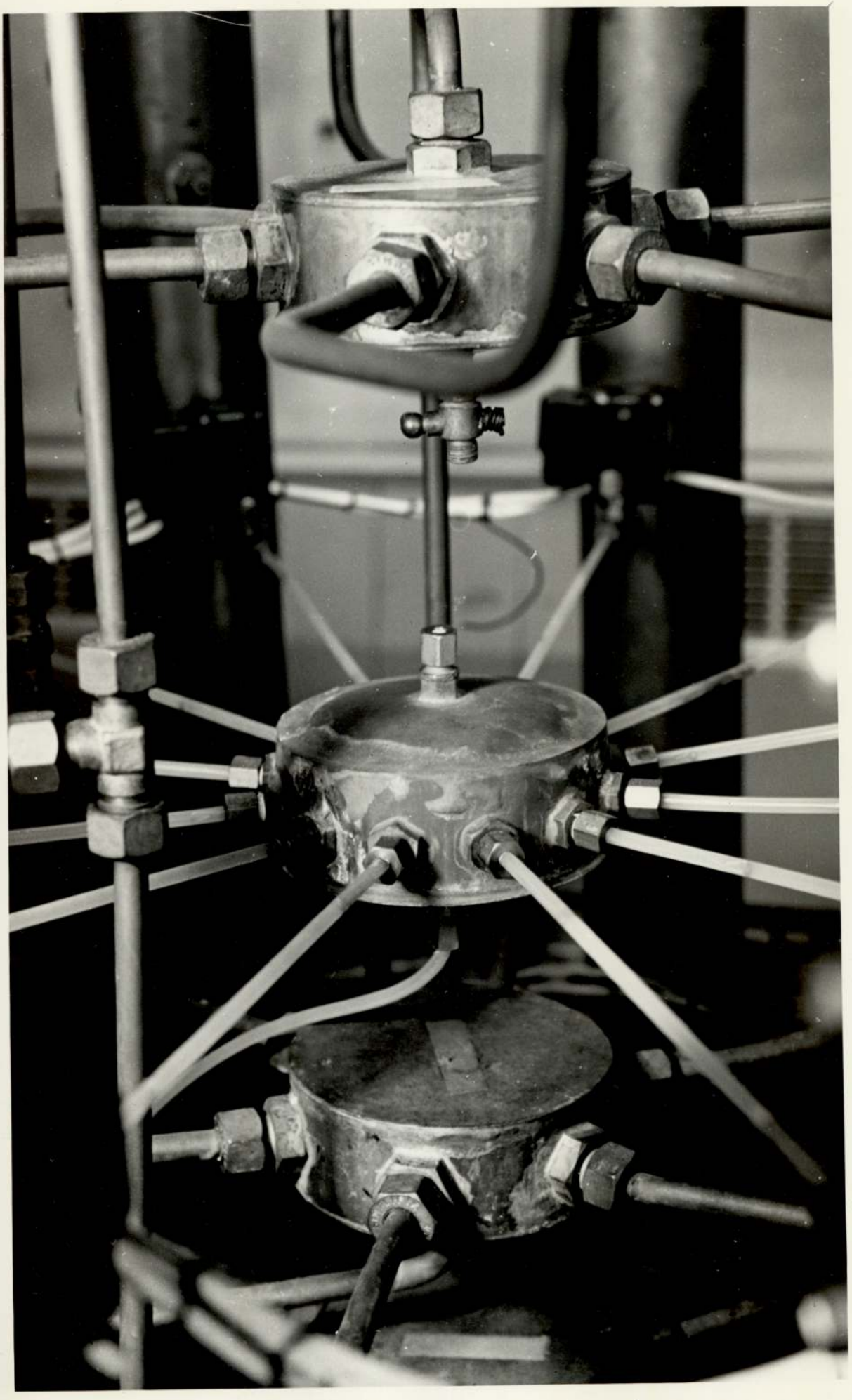

PLATE 3.3 The Columns - Plan View

AD	Silica gel air drier
C	Carrier gas inlet solenoid valve
C_p	Carrier product (Product 1) solenoid valve
CD	Central distributor
CPR	Coarse pressure regulator
F	Fine air filter
H	High pressure air line
P	Purge gas inlet solenoid valve
P_p	Purge product (Product 2) solenoid valve
T	Transfer solenoid valve
3-C	3-way cock valve

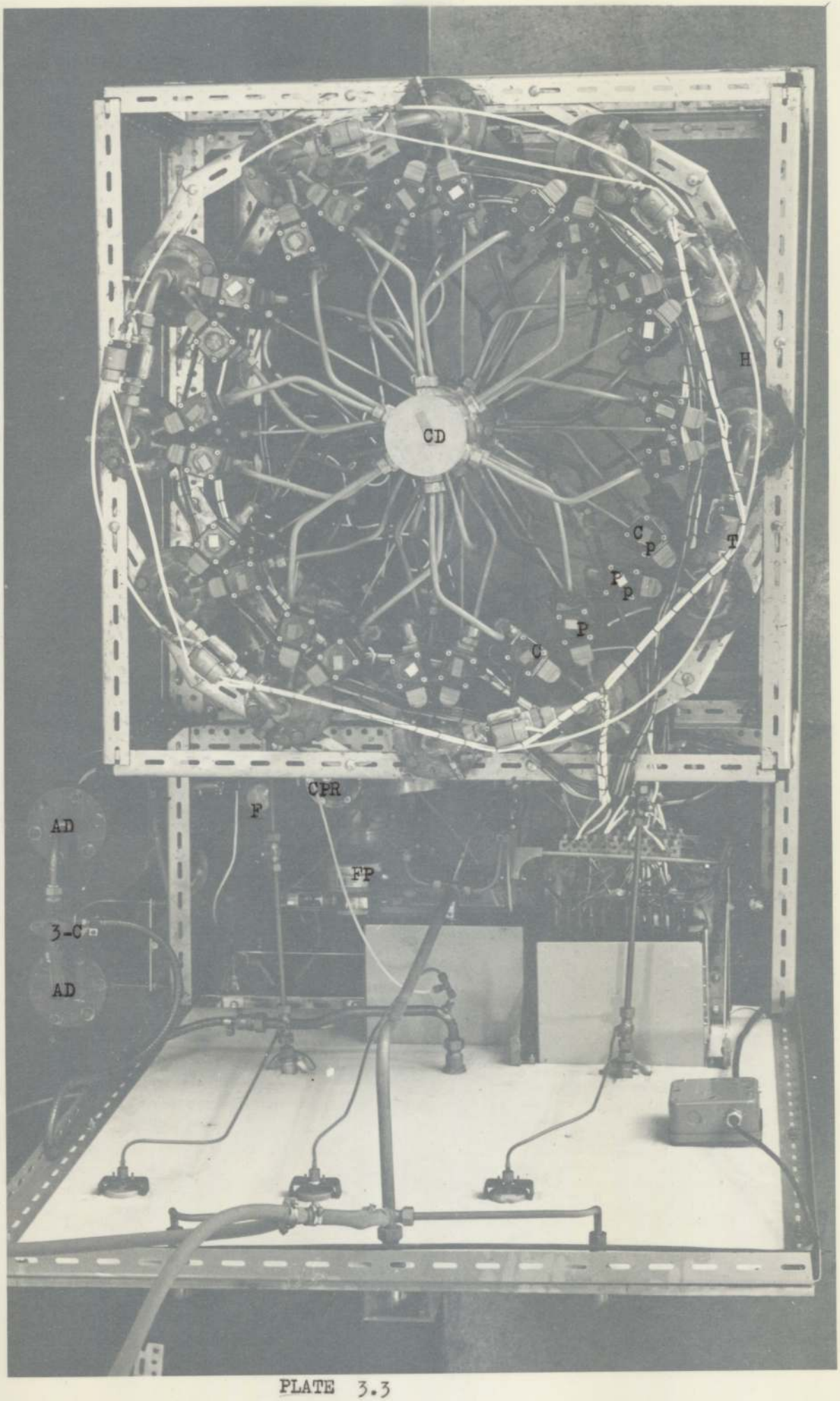

PLATE 3.3

3.3 Control, Measuring and Peripheral Functions

3.3.1 The Automatic Timed Sequencing Unit

The unit used for the switching of the solenoid valves in the required pattern was designed and constructed by the departmental electronics technician, M.F. Lea. Fig 3.9a schematically shows the operating principle while Figs 3.9 (b - d) give the circuit diagrams.

Considering Fig 3.9c, 12 V dc. from a stabilised power supply (detailed in Fig 3.9b) charged three parallel 100 μF capacitors at a rate determined by the settings of variable resistances R1 and R2. R2 was pre-set while R1 could be adjusted by a calibrated dial on the front panel. When the capacitor charge was at a sufficient value, the unijunction, U, was triggered, allowing current to flow through the relay, RL1. Switching from A to B energised the solenoid, S, of the uniselector, which then stepped through one of the twenty-five sets of four contacts. At the same time, the now short-circuited clock, reset.

The switching of the uniselector continued for twenty-four time periods, giving two complete sequencing cycles for the separation unit. At the final, twenty-fifth contact, it'homed' to contact 1 and restarted. As the switching action of the uniselector was electro-mechanical, a spark-quenching circuit, Q, was included. The scaling of the clock-circuit gave a time period of 1 - 10 minutes, a calibration curve against R1 dial setting is given in Appendix 1. A switch, O, permitted the circuit to be 'frozen' while a contact button, K, when pressed, caused the uniselector to switch rapidly.

Fig 3.9d shows the wiring pattern from the uniselector contacts to two independent banks of twelve relays, RLX and RLXX respectively. The

Figure 3.9 Circuit Diagrams for the Automatically Timed Switching Unit

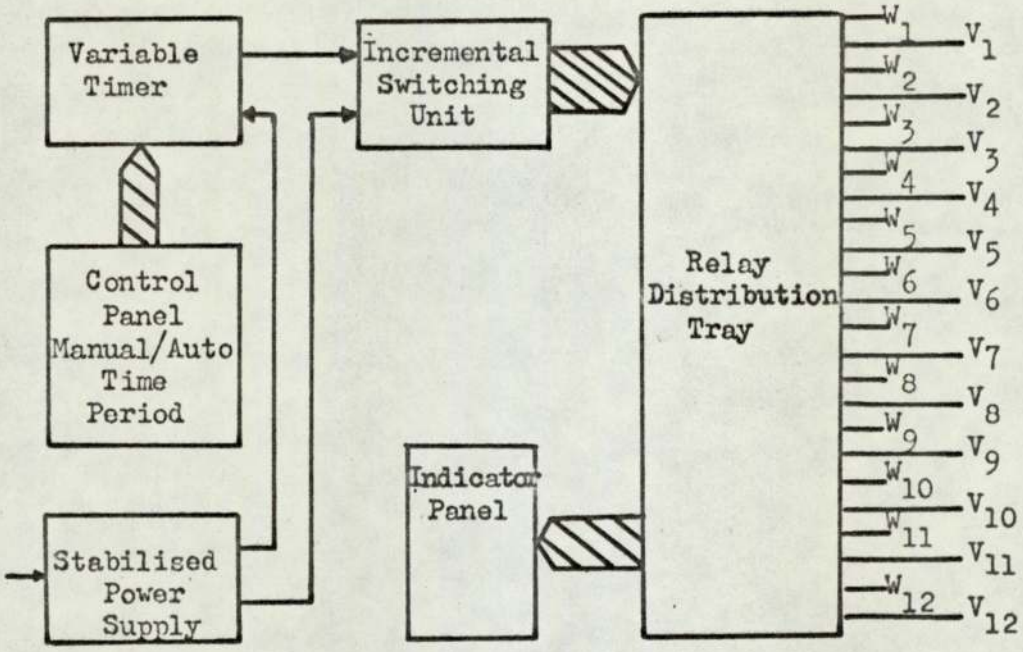

3.9a Overall Scheme of Operation

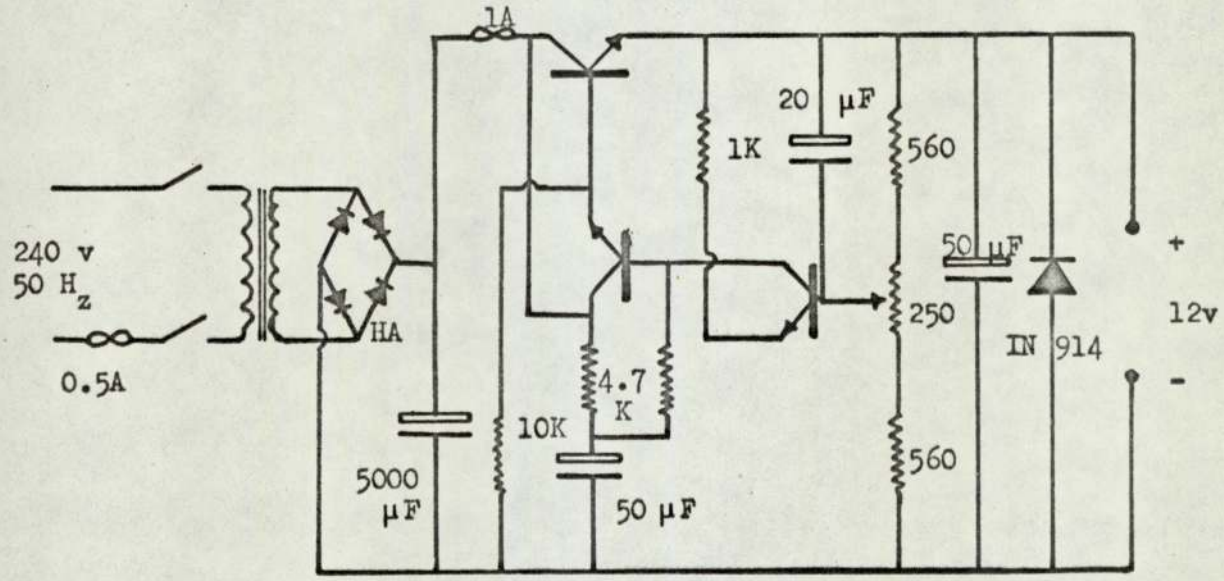

3.9b Regulated Power Supply

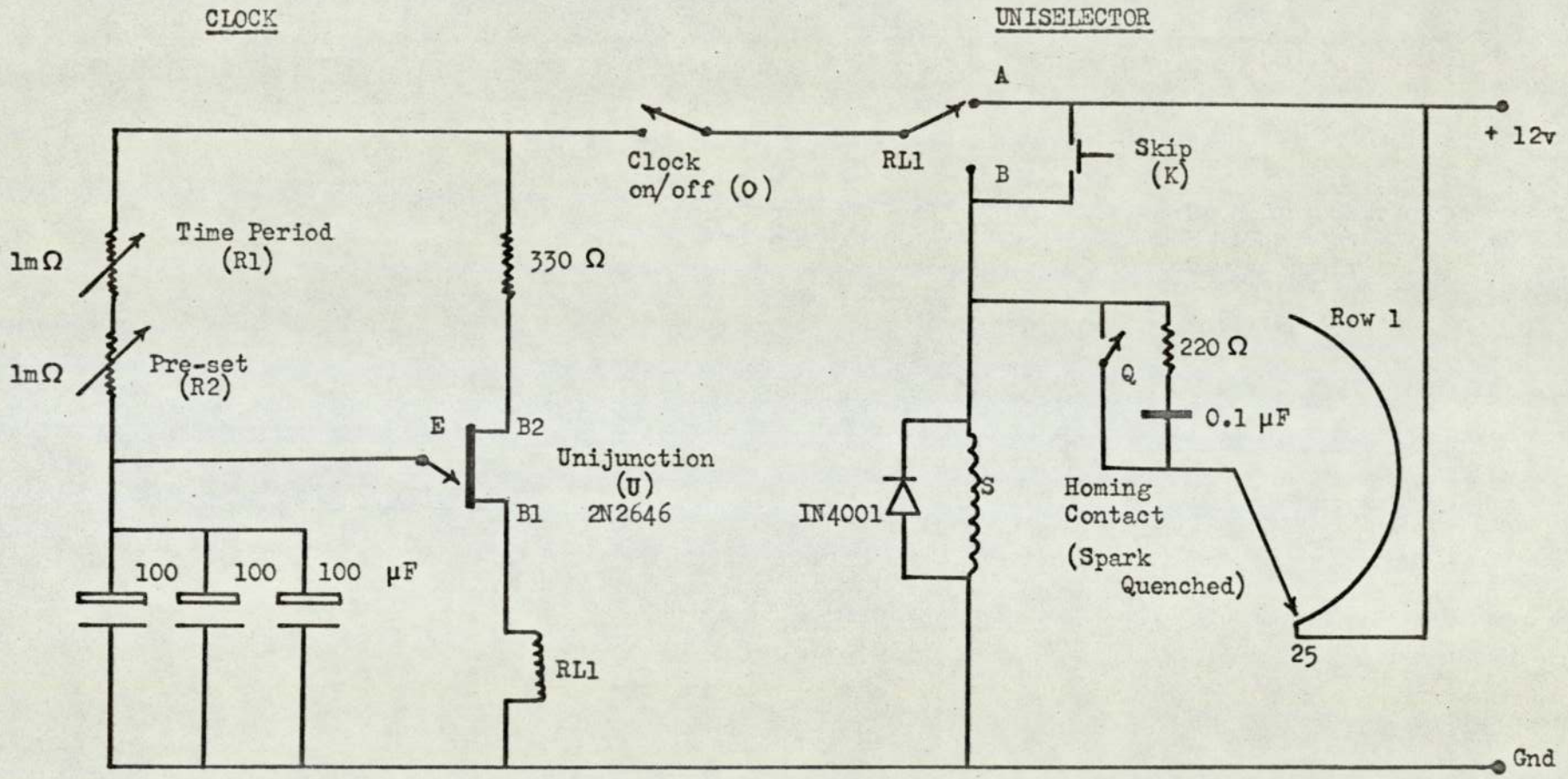

Figure 3.9c Central Timing/Sequencing Segment

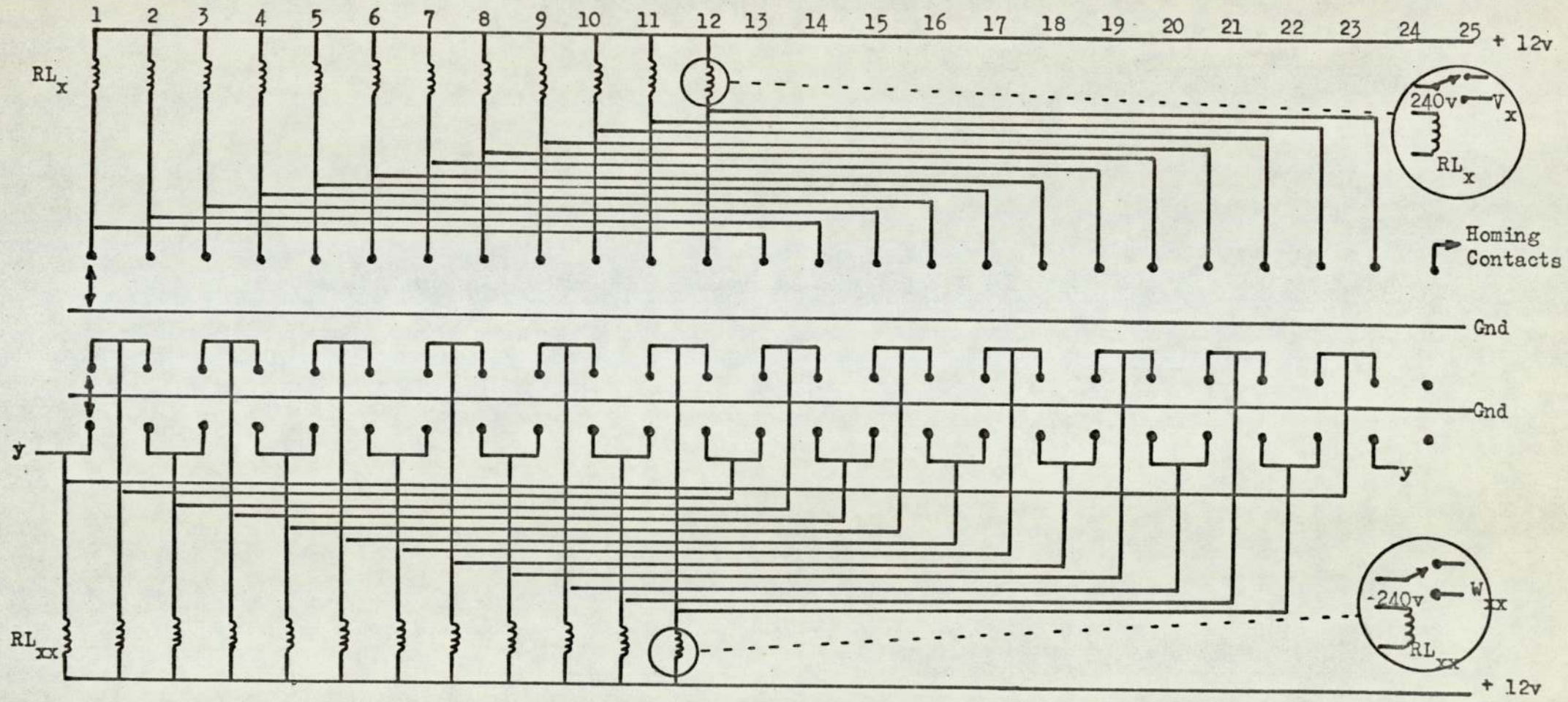

Figure 3.9d Wiring Pattern from 25 Contact Uniselector to Single and Paired Energised Sockets (V_x, W_{xx})

Fig 3.10 Solenoid Valve Connection Pattern to the Terminals of the Automatically Timed Sequencing Unit

Column Isolated (Assigned Number)	1	2	3	4	5	6	7	8	9	10	11	12
Terminals Energised In Rail W_{xx}	W_{12} W_1	W_1 W_2	W_2 W_3	W_3 W_4	W_4 W_5	W_5 W_6	W_6 W_7	W_7 W_8	W_8 W_9	W_9 W_{10}	W_{10} W_{11}	W_{11} W_{12}
Transfer Valves Energised	T_{12} T_1	T_1 T_2	T_2 T_3	T_3 T_4	T_4 T_5	T_5 T_6	T_6 T_7	T_7 T_8	T_8 T_9	T_9 T_{10}	T_{10} T_{11}	T_{11} T_{12}
Terminals Energised In Rail V_x	V_1	V_2	V_3	V_4	V_5	V_6	V_7	V_8	V_9	V_{10}	V_{11}	V_{12}
Inlet/Outlet Valves Energised	C_2 Cp_{12} P_1 Pp_1 F_7	C_3 Cp_1 P_2 Pp_2 F_8	C_4 Cp_2 P_3 Pp_3 F_9	C_5 Cp_3 P_4 Pp_4 F_{10}	C_6 Cp_4 P_5 Pp_5 F_{11}	C_7 Cp_5 P_6 Pp_6 F_{12}	C_8 Cp_6 P_7 Pp_7 F_1	C_9 Cp_7 P_8 Pp_8 F_2	C_{10} Cp_8 P_9 Pp_9 F_3	C_{11} Cp_9 P_{10} Pp_{10} F_4	C_{12} Cp_{10} P_{11} Pp_{11} F_5	C_1 Cp_{11} P_{12} Pp_{12} F_6

Note Solute feed shown entering centre of main separating section.

relays separately switched 240 V A.C. supply across two rails of terminals, V_X and W_{XX} at the rear of the unit. It can be seen that, at any time, only one terminal connection in the rail V_X was 'live' while there were two consecutive 'live' terminals in the rail W_{XX}. Thus in operation, the unit energised terminals W_{12}, W_1 and V_1 together and then, after a selected time interval, de-energised terminals W_{12} and V_1 and energised terminals W_2 and V_2 so that terminals W_1, W_2 and V_2 were energised. After a further time interval terminals W_1 and V_2 are de-energised and terminals W_3, V_3 energised, and so on until the cycle is completed. Repetition of the cycle continues automatically.

Two indicator panels of neon lights fed by signals from the relay distribution tray provided an instantaneous indication of the terminals energised.

The connection pattern of the various sets of solenoid valves to the terminals is tabulated in Fig 3.10. The feed point is set at the middle of the separating section. Numbering of the columns was related to the panel of neon lights such that the isolated column corresponded to the terminal number in the single energised terminal rail, V.

3.3.2 Inlet and Outlet Gas Control and Purification

The overall flow diagram of the system is given in Fig 3.11. Plate 3.4 shows the front control panel.

As no carrier gas recycle system was incorporated, economics dictated the use of the University mains air supply. Opening of the 2.5 cm butterfly type isolating valve permitted air of approximate pressure 650 kN m^{-2} to pass through a'1.1/2 in B.S.P.T.' port industrial 5 μm filter (Norgren, West Bromwich) to a cylindrical surge tank of

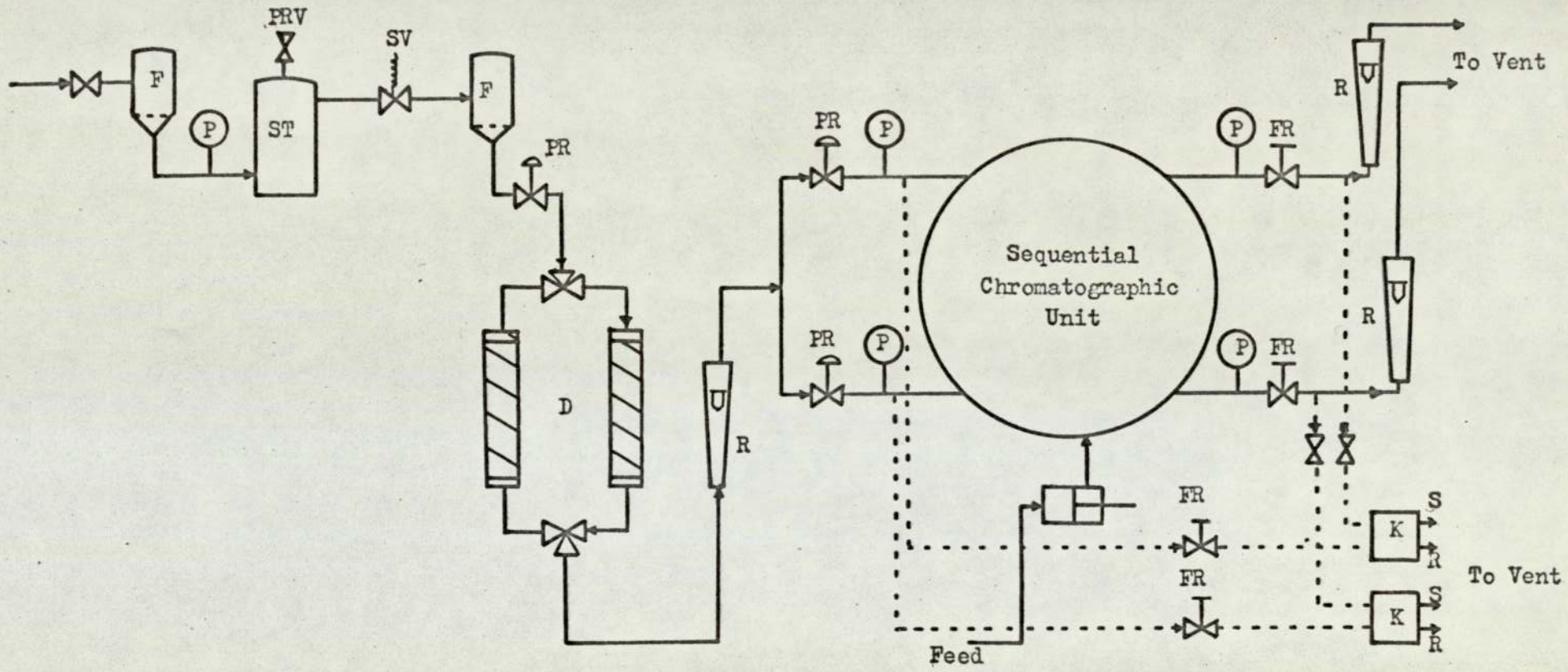

Figure 3.11 Line Flow Diagram for Complete System

Legend: R = Rotameter, P = Pressure Gauge, D = Silica Gel Driers,
PR = Pressure Regulator, FR = Flow Regulator, PRV = Pressure Relief Valve
SV = Solenoid Operated Valve, F = Filter, K = Katharometer,
S = Sample Stream, R = Reference Stream.

PLATE 3.4 The Control Panel

B	Solute feedrate measuring burette
BR	Katharometer bleed stream flow regulator
FP	Solute mixture feed pump
FR	Solute mixture feed reservoir
FR1, FR2	Flow regulator for product streams 1 and 2 respectively
K1, K2	Katharometer for product streams 1 and 2 respectively
KC1, KC2	Katharometer control box for product streams 1 and 2 respectively
P	Perspex panel to cover live terminals at rear of timer unit
P1R, P2P	Product 1 (14K) and Product 2 (18K) outlet rotameter respectively
P1P, P1P	Product 1 and Product 2 outlet pressure gauges, tapping taken before flow regulators
S	Overall on/off switch
TIR, TIP	Total inlet gas rotameter and pressure gauge respectively
T.U.	Automatically timed sequencing unit
V	Vent to extractor fan

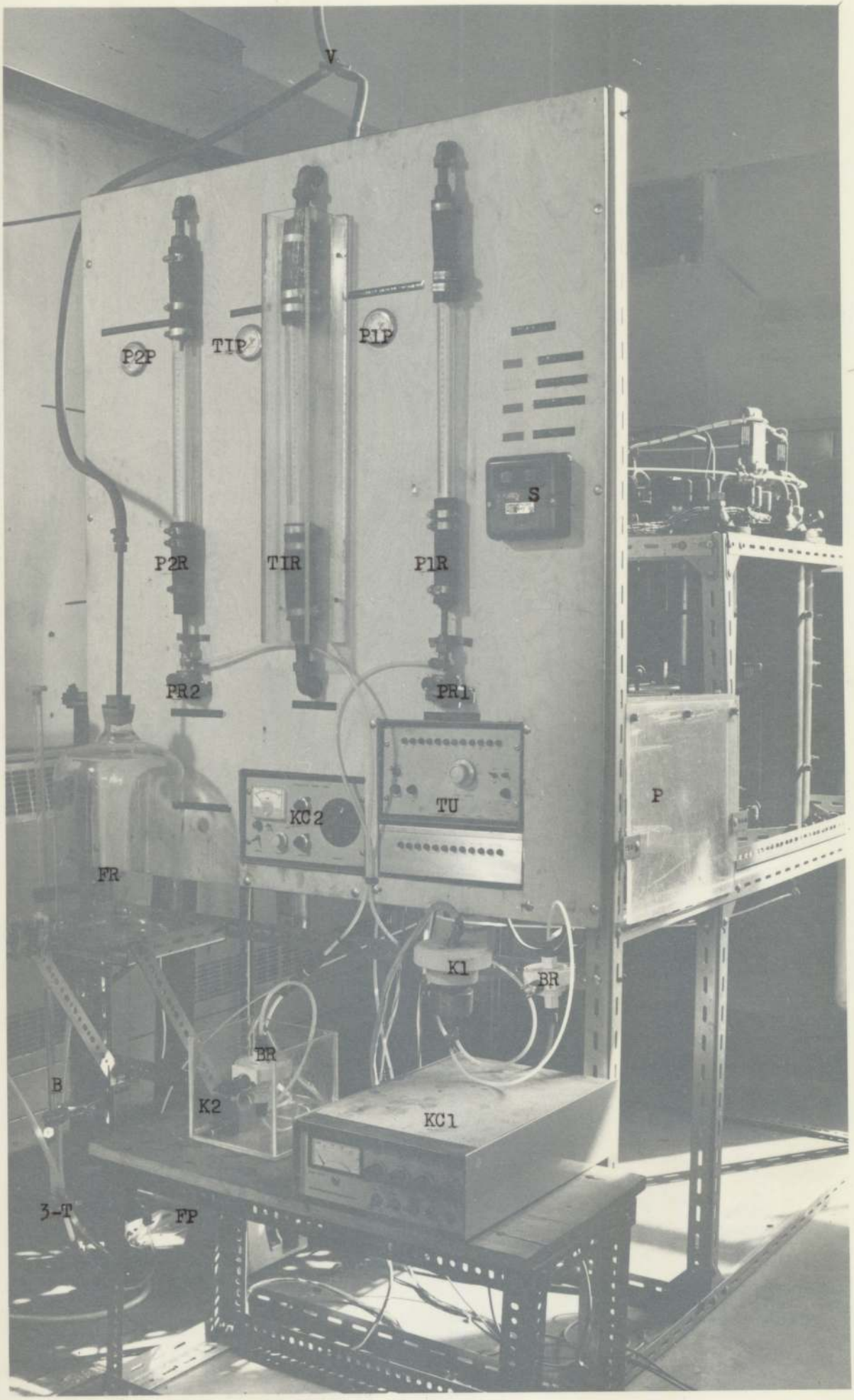
V
P2P
TIP
P1P
S
P2R
TIR
P1R
PR2
PR1
KC2
TU
P
FR
K1
BR
BR
B
K2
KC1
3-T
FP

PLATE 3.4

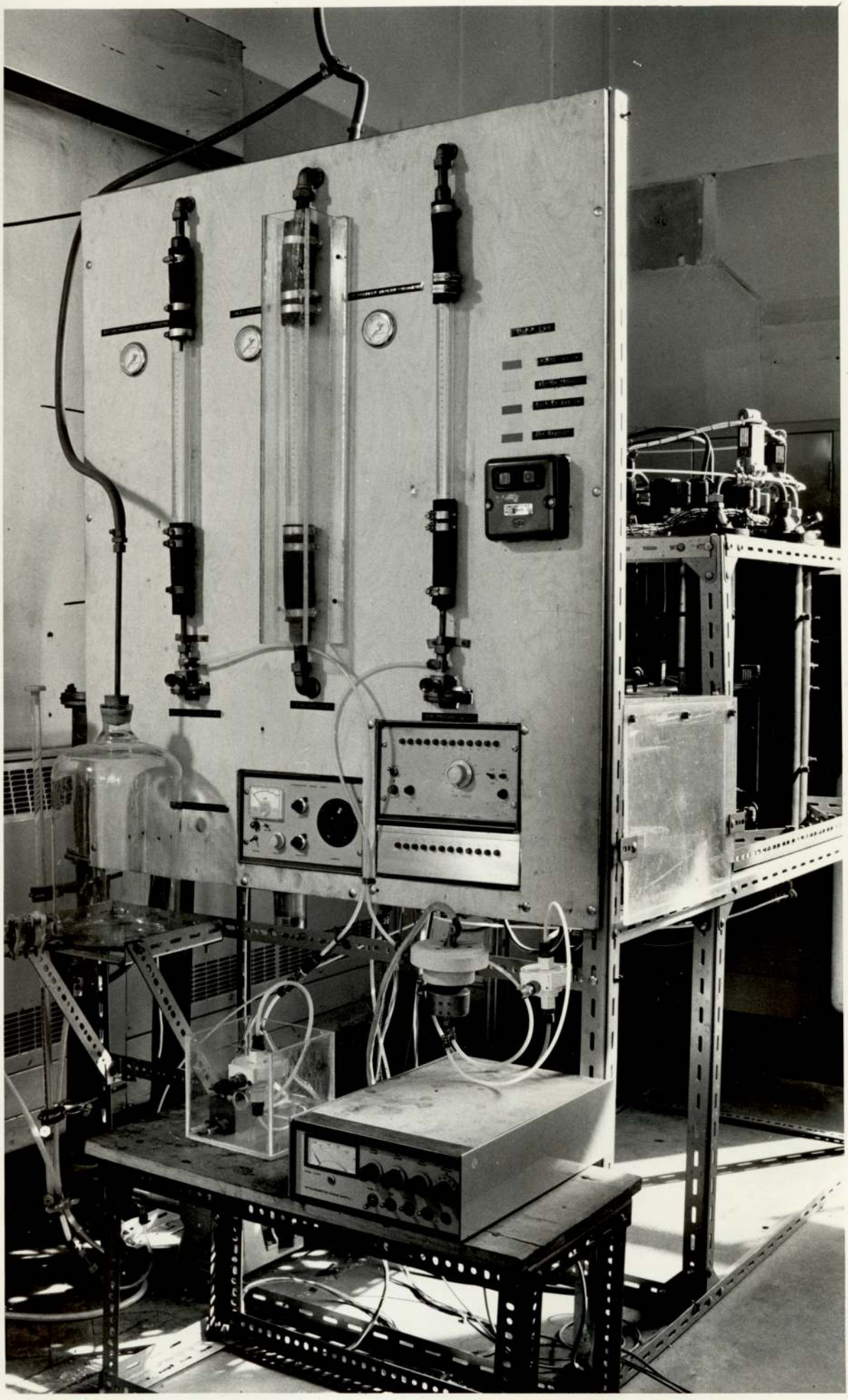

capacity 0.126 m^3 volume. The tank could be emptied through a gas tap fitted near the base. A flexible, reinforced P.V.C., 6.3 mm bore tube was used to connect the tank to the subsequent filtering and pressure regulation stage. This consisted of a Norgren, '3/8 in B.S.P.T.' port, 'Ultraire' filter connected to a coarse pressure regulator. The pressure was regulated to approximately 500 kN m^{-2}, being monitored further upstream.

The final drying stage consisted of two beds of silica gel (D), individually selectable by two brass 3-way cock valves positioned in line as shown in Fig 3.12. The dimensions of the flanged columns proved adequate to each give at least six hours drying operation without regeneration. For a longer run, replacement of the spent silica in the 'off line' column was possible without interruption of air flow.

Before splitting the inlet air line into the carrier and purge streams, the flowrate was monitored by a 24 A Rotameter (Rotameter Manufacturing Co. Ltd., Croydon, Surrey.). This rotameter, plus the associated 100-520 kN m^{-2} (0-60 psig) pressure gauge proved valuable for pressure testing the unit for leakages (see Section 8.1).

Two identical '1/4 in B.S.P.T.' port, diaphragm type, fail safe precision regulators (Norgren) were used to accurately maintain the measured inlet pressure of the gas streams before they entered the distribution network. The spring range of the regulators was 100-520 kN m^{-2} (1-60 psig), matching the range of the pressure gauges. On exit from the sequential unit the flowrate of each stream was held constant by a Brook's, '3/8 in B.S.P' port, brass body, diaphragm type flow regulator (Brooks Instruments Ltd., Stockport, Cheshire), the flowrate

Figure 3.12 Silica Gel Air Driers

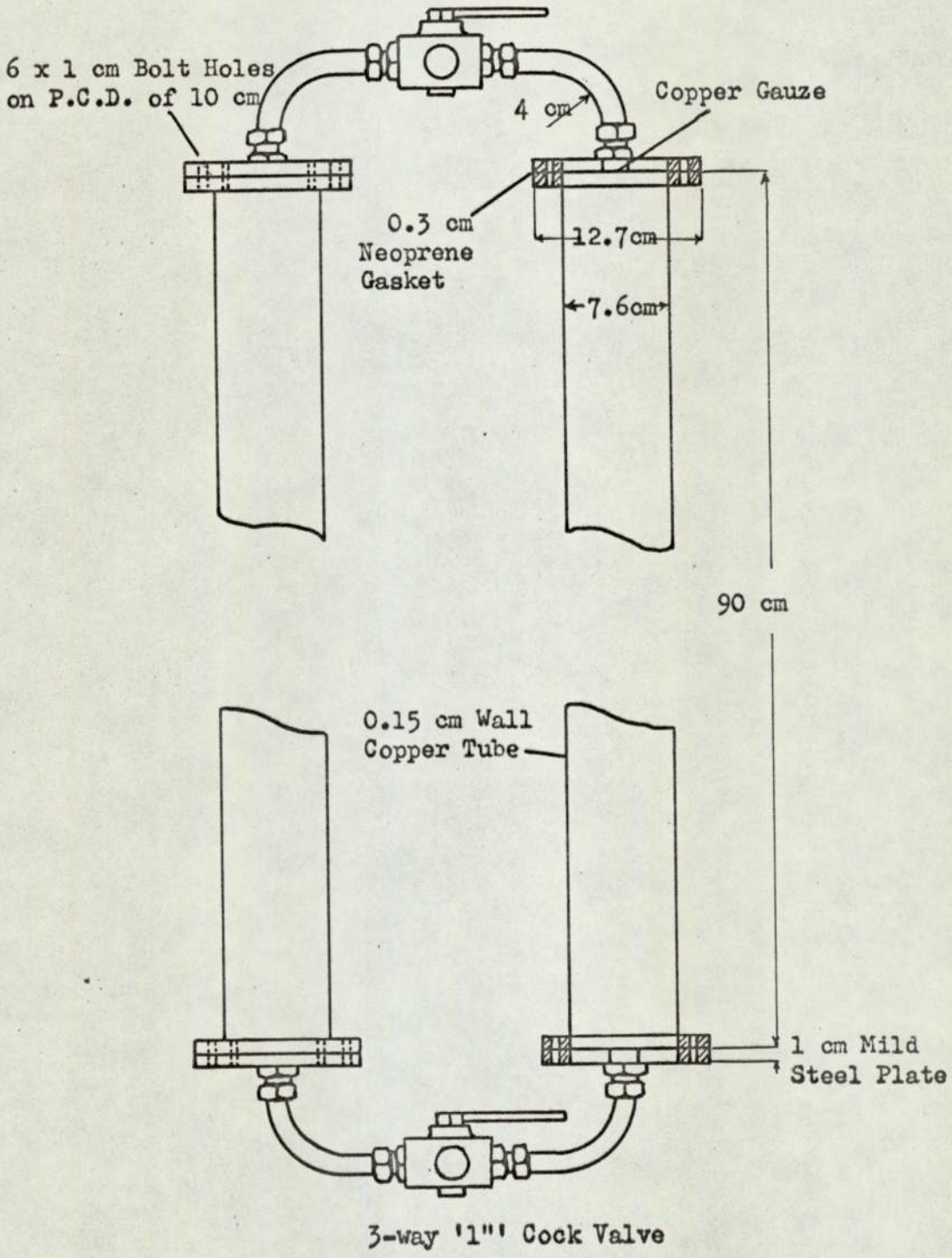

Note: Scale is $^{2}/_{5}$th full size

being registered on an 18 K and 14 K Rotameter for the purge and carrier gas streams respectively. Control therefore gave a set inlet pressure and set outlet flowrate, any column to column variation being registered by the outlet 100-310 kN m^{-2} (0-30 psig) pressure gauges. The control proved adequate for rapid dampening of the surge resultant from sequencing.

It was not possible to construct a refrigerated product recovery system within the capital budget for this research project. The standard nut and septum sampling point was therefore placed in the outlet lines, upstream of the flow regulators, to permit chromatographic analysis of these streams.

The rotameters and pressure gauges were calibrated, the former against a standard gas meter, the latter against a dead weight pressure tester. The calibration curves are given in Appendix 1.

3.3.3 Solute Mixture Feed

Ideally the feed should enter the columns in the vapour phase. However, problems of possible condensation in the feed distribution network led to acceptance of a liquid feed.

The feed pump selected was of the reciprocating, positive displacement type (F.A. Hughes Ltd., Epsom, Surrey). A micrometer adjustment permitted variation of the stroke length of the P.T.F.E. plunger, and hence throughput. A calibration curve is given in Appendix 1.

Experience showed that the pump tended to 'stick' after start-up if the plunger was not lubricated. A mannitol-based grease successfully overcame this problem. The non-return valves in the pump head consisted of two seated stainless steel ball-bearings. A simple filter consisting

of a 15 cm long copper tube packed with glass wool was, therefore, placed between the feed reservoir and the pump head to remove any particulate solid.

The main feed reservoir was a 10 dm^3 glass aspirator fitted with an outlet cock-tap. The line from aspirator ran to a three-way glass tap. A 100 cm^3 burette was connected to the adjacent tap inlet arm, permitting the feedrate to be checked during an experimental run. The tap outlet was connected to the pump, through the simple filter. Placing the reservoir above the pump provided a positive head on the suction side. A connection from the pump outlet to the tap on the base of the feed distributor completed the liquid feed system. The volume of the feed distributor helped to dampen the reciprocating action of the pump.

3.3.4 Monitoring of the Solute Level in the Product Streams

A continuous visual display of the total solute level in the exiting gas streams was incorporated so that the progress of an experimental run could be followed. Two katharometers in conjunction with a dual channel 'Servoscribe' potentiometric recorder (Smiths Industries, Wembley Pk, Middlesex) were used.

The reference side of the respective katharometer blocks were fed by a flow regulated bleed stream from the dried and filtered inlet air lines (Fig 3.11 - flow regulators purchased from Platon Control Ltd.,). As the product streams were already flow regulated, the two reference bleed streams required only throttling by a fine needle valve or capillary tubing.

For the carrier product stream (Product 1) a katharometer block an

power supply purchased as part of a standard Pye 104 analytical chromatograph was used. The two katharometer filaments were of tungsten. Consequently the 'bridge' current was always kept at its lowest value of 80 m A to limit oxidation of the filaments in the presence of air. The recommended gas throughput of 0.83 cm^3 s^{-1} was also used throughout the experimental work (162).

Gow-Mac (Shannon Airport Ltd.,) supplied the katharometer used to monitor the Product 2 stream. This had four, gold sheathed, tungsten filaments for improved oxidation resistance. The associated Wheatstone bridge circuitry was constructed in the department by Mr. Lea (Fig 3.13) from a diagram given by Gow-Mac (163). Setting the bridge at 24 V and 100 m A was found to give adequate sensitivity. A comparatively large throughput of approximately 12.5 cm^3 s^{-1} was recommended.

The katharometer traces give no indication of the composition of the exit streams. The individual components must first be resolved on an analytical chromatographic column. Thus, for quantitative analysis of the product streams and for determination of the concentration profile in the operating unit, a Perkin Elmer F11 gas chromatograph in conjunction with a Kent Chromalog 1 integrator was used.

Two additional control features were added to the basic chromatograph. An accurate pressure regulator of range 140-280 kN m^{-2} was installed on the hydrogen line between the coarse cylinder head regulator and the flame ionisation detector (Elliot Process Instru. Ltd., Birmingham). In the nitrogen line a fine needle flow regulator and rotameter were installed (Brooks Instru. Ltd., Stockport). Accurate

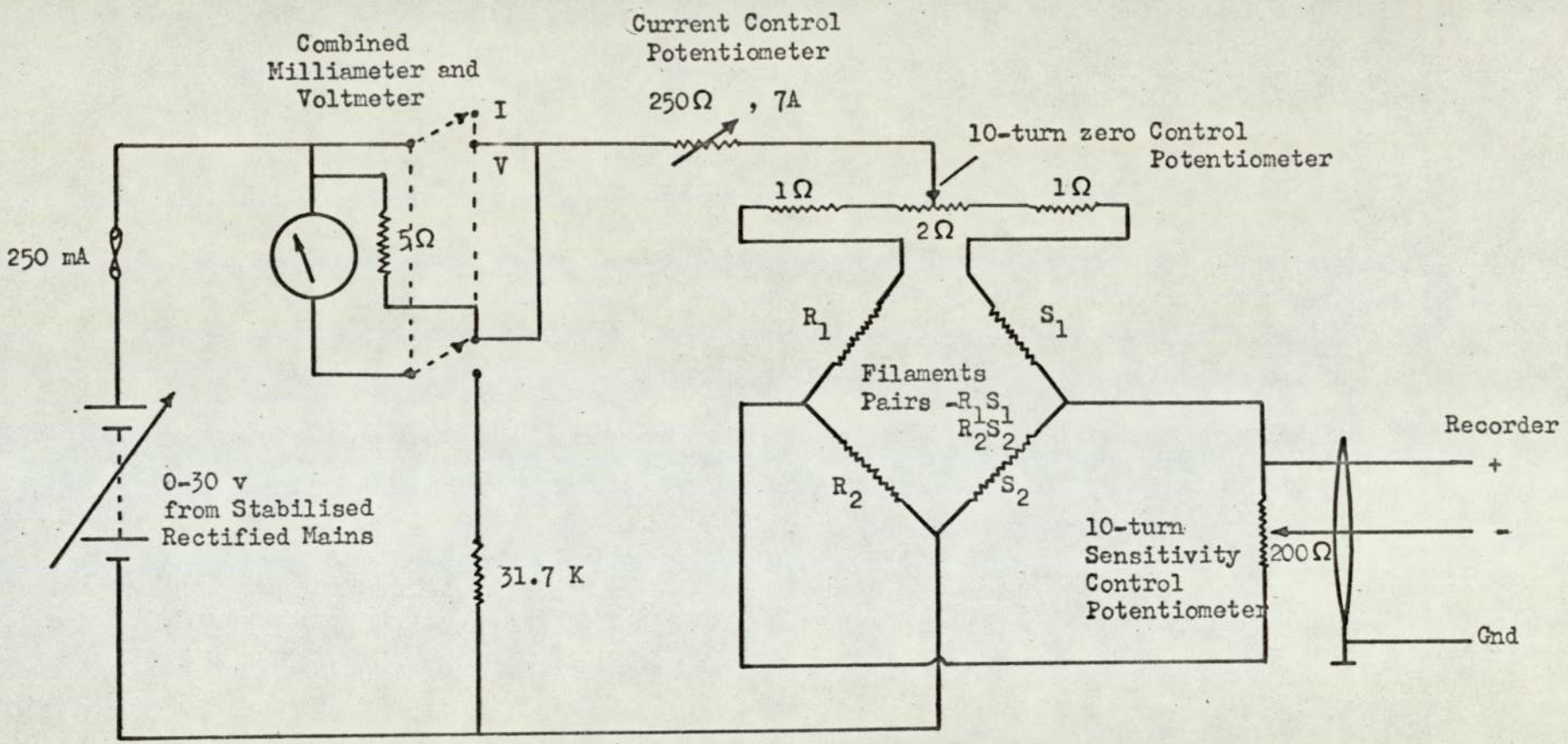

Figure 3.13 Power Supply and Bridge Circuit Control for Katharometer

control of the oxygen supply is not necessary. Hence the cylinder head regulator was adequate.

Iron/constantan thermocouples were positioned in the injection heating block and oven of the chromatograph. A standard circuit incorporating an ice/water reference junction enabled these two temperatures to be accurately recorded.

3.3.5 Safety

The quantity of chemical handled, the pressure of operation and the extensive electrical wiring led to the following safety precautions.

A pressure relief valve was present in the mains air surge tank. This was set to lift at approximately 700 kN m^{-2}, some 100 kN m^{-2} below the stated safe working pressure for the vessel. In addition, a gas tap at the base of the tank provided means of quick pressure relief. The thickness of all metal tube and plate wall under pressure was greatly in excess of that required by British Standards 1500 and 2871.

A solenoid valve, of the type used for the inlet/outlet gas ports, was placed in line after the surge tank. During a run this was permanently energised, de-energisation providing instant isolation of the rig from the mains air.

The inlet air rotameter, operating under a gas pressure of the order of 500 kN m^{-3}, was enclosed in a 1.2 cm thick perspex box. The solute rich product lines were combined after the rotameters and led to a large extractor fan near the roof of the laboratory. The feed reservoir was sealed from the laboratory atmosphere by a rubber bung. A tube passing through this bung was connected into the line running to the extractor fan.

A removeable perspex cover was made for the terminals and connecting blocks at the rear of the timer unit.

Finally all mains operated devices, the solenoid valve in the mains air line, the feed pump, the timer unit and the katharometers, were fed power through a direct, on line, A.C. contacter-starter (M.E.M. Auto Memota, Birmingham). The switch, with separate stop and start push buttons, was fused and incorporated a relay system to prevent restart when power was restored after failure. Thus triggering or pressing the stop button froze the system until the switch was manually reset. All electrical devices were earthed.

Safety considerations also played a substantial part in the selection of chemicals for processing by the sequential separation unit.

CHAPTER 4

Selection of a Chemical System for Study

The chemical systems available for study on the constructed sequential chromatographic separation unit were limited by three factors; the use of air as carrier gas, the lack of heating facilities and the materials of construction. These restrictions led to members of the halocarbon group of chemicals which generally satisfy the criteria of high volatility and non-inflammability.

Such members of the group as 1.1.1. - trichloro-ethane, 1,1,2 - trichloro - 1,2,2, - trifluoro-ethane and dichloromethane satisfied further selection restrictions. All three are liquid at ambient conditions, have a comparatively low toxicity and are available in bulk in reasonable purity from I.C.I. Ltd. 1.1.1. trichloro-ethane is sold under the trade name of 'Genklene' P while that for 1,1,2 - trichloro - 1,2,2 - trifluoro-ethane is 'Arklone' P. The 'P' in the respective names denotes that no stabilisers have been added, their general use being industrial and domestic cleaning.

Private communications with I.C.I. Ltd., gave details of the maximum levels of the impurities in the 'as sold' products. For all three chemicals the total impurity concentration did not exceed 1%, an acceptable figure for a chemical produced in bulk. Relevant physical properties are given in Table 4.1.

The selection of a solvent phase was made from consideration of the partition coefficients chromatographically determined on four recommended phases (167). Experimental procedure is given in Section 6.2 while the results are tabulated in Table 4.2. The method of calculation of partition coefficients is also given in Section 6.2.

Table 4.1 Relevant Physical Properties of 'Arklone' P, 'Genklene' P and Dichloromethane

Chemical Name	Trade Name	ρ_i	Boiling Point	Freezing Point	Vapour pressure at 20°C	M_i	Toxicity [c]
		g cm^{-3}	°C	°C	kN m^{-2}		
1,1,2 - trichloro - 1,2,2 - trifluoroethane	'Arklone' P	1.57 [a]	47.6 [a]	-35 [a]	35.9 [a]	187.4 [a]	T L V 1000 ppm
1,1,1 - trichloroethane	'Genklene' P	1.34 [c]	74.1 [b]	-32.5 [c]	13.3 [b]	133.4 [b]	Narcotic in high concentrations T L V 350 ppm
Dichloromethane (Methylene Chloride)		1.34 [b]	40.1 [b]	-96.7 [b]	47.9 [b]	84.9 [b]	Dangerous to eyes Narcotic powers Decomposes to phosgene gas T L V 500 ppm

References:

a) 164
b) 165
c) 166

Table 4.2 Comparison of Four Solvent Phases for the Separation of the Proposed Halocarbons

a) Column Details

Solvent phase	Column Dimensions	Solid Support (500 - 355 μm)	Total weight of packing	Loading	L
	m x mm		g	%	g cm^{-3}
D.N.P.	1.98 x 4.8	Chromosorb P	9.1	25	0.98
S.F 200/50	2.50 x 4.8	Chromosorb P	11.2	25	0.97
S.F 200/5	2.44 x 4.8	Chromosorb P	11.7	25	0.91
D.2 E.H.S	1.98 x 4.8	Chromosorb P	9.3	25	0.91

b) Chromatographic Measurements

	Solute	T_c	T_a	P_{in}	P_o (= P_a)	F	t_R	K	Separation Factor
		°C	°C	kN m^{-2}	kN m^{-2}	cm s^{-1}	s		
D. N. P.	CH_4	25	22	222.6	97.8	0.96	25		
	D.C.M.	"	"	"	"	"	1125	260	$\frac{D.C.M.}{A.P}$ = 2.44
	A.P	"	"	"	"	"	476	107	$\frac{G.P}{A.P}$ = 5.04
	G.P	"	"	"	"	"	2315	540	
S. F. 200/50	CH_4	25	24	161.9	101.9	0.88	25		
	D.C.M.	"	"			"	458	101	$\frac{A.P}{D.C.M.}$ = 1.16
	A.P	"	"	"	"	"	529	117	$\frac{G.P}{A.P}$ = 2.88
	G.P	"	"	"	"	"	1494	338	
S. F. 200/5	CH_4	25	22	306.2	98.3	1.00	34		
	D.C.M.	"	"	"	"	"	700	93	$\frac{A.P}{D.C.M.}$ = 1.26
	A.P	"	"	"	"	"	870	121	$\frac{G.P}{A.P}$ = 2.62
	G.P	"	"	"	"	"	2260	308	
D. 2 E. H. S.	CH_4	25	14	173.1	96.7	0.88	22		
	D.C.M.	"	"	"	"	"	1326	318	$\frac{D.C.M.}{A.P}$ = 2.51
	A.P	"	"	"	"	"	542	127	$\frac{G.P}{A.P}$ = 4.85
	G.P	"	"	"	"	"	2558	616	

Legend: Solutes

CH_4 - Methane
D.C.M. - Dichloromethane
A.P - 'Arklone' P
G.P - 'Genklene' P

Solvents

D.N.P. - Dinonyl Phthalate
S.F 200/50 - Silicone Fluid
S.F 200/5 - Silicone Fluid
D.2 E.H.S. - Di-(2-Ethyl Hexyl Sebacate)

Silicone fluid DC 200/50 (Dow Corning Ltd.) was chosen for three reasons:

(i) Together with silicone fluid DC 200/5 it gave comparatively low values for the respective partition coefficents. Hence, the analysis time at given analytical chromatographic settings will be less, and the general range of gas flowrates required will be lower, when operating the sequential unit at a given sequencing rate (see Section 6.1).

(ii) It provides two synthetic binary mixtures for study, the pair 'Arklone' P/'Genklene' P being comparatively easy to separate (Separation Factor = 2.88 @ 25°C) while dichloromethane/'Arklone' P is difficult (Separation Factor = 1.16 @ 25°C). Comparing the two silicone fluids, DC 200/5 appeared to give a greater 'stickiness' of the coated support at a high solvent phase loading as witnessed by the high pressure drop across the packed analytical column.

(iii) It is inexpensive and readily available in bulk.

The present studies were restricted to an artificial equivolume mixture of 'Arklone' P and 'Genklene' P which was considered to be an adequate system for the initial investigation of the operating characteristics of a novel unit.

90% of all chromatographic supports are prepared from filter aids mined from deposits of marine diatomites by the Johns-Manville Corporation (89). Table 4.3 compares the properties of the four commonest supports used, trade names Chromosorb P, W, G and A. The desirable properties for large-scale applications are a high packed density and solvent capacity (giving a high level of solvent in the packed

column), a large surface area, mechanical strength and low surface adsorptivity. Chromosorb A, specially developed for preparative work, exhibits all of these properties. However, Chromosorb P is by far the cheapest support available and therefore finds general favour.

Basic chromatographic theory suggests that as the particle size is decreased, column efficiency in terms of N.T.P. will increase. This efficiency increase is gained at the expense of a greatly increased flow resistance. For preparative-scale work the several researchers who have studied the effect of both mesh size and mesh range (41, 47, 54, 105) have generally concluded that the actual particle size is of little importance to column efficiency when large samples are used. However, a narrow particle size range is desired to limit the effect of size segregation on the uniformity of the solute bands.

As a compromise between cost and efficiency 500 - 355 μm (30 - 44 B.S. 410 mesh) Chromosorb P was selected. The supplier was Jones Chromatography and Co., Monmouthshire.

Table 4.3 Chromosorb Support Properties (89)

Chromosorb	P	W	G	A
Alternative Names	Sil-O-Cel Firebrick	Celite		
Colour	Pink	White	Oyster White	Pink
p H	6.5	8.5	8.5	7.1
Free Fall Density ($g\ cm^{-3}$)	0.38	0.18	0.47	0.40
Packed Density ($g\ cm^{-3}$)	0.47	0.24	0.58	0.48
Surface Area ($m^2\ g^{-1}$)	4.0	1.0	0.5	2.7
Surface Area ($m^2\ cm^{-3}$)	1.9	0.3	0.3	1.3
Crushability	hard	friable	hard	hard
Solvent capacity	high	low	low	high
Adsorptivity	high	low	low	medium
Relative Cost (untreated)	1.0	1.2	1.7	1.7

CHAPTER 5

Comparison of Individual Packed Column Chacteristics

5.1 The 'Packing'

A hand sieve analysis was performed on the Chromosorb P as delivered in accordance with the procedure laid down in British Standard 410. From Table 5.1 it can be seen that only half of the sample was in the specified size range of 500 - 355 μm. As a narrow particle size distribution was desired the entire purchased supply was machine sieved in 100 gm batches through 200 mm B.S. 410 metric sieves. The final analysis is also given in Table 5.1.

After sieving, the support was repeatedly washed in water to remove fine dust. This precaution was taken as the particles of dust may have been blown onto either the solenoid valve or flow regulator seatings with consequent malfunctioning of these devices. After washing, the support was spread on trays and thoroughly dried in a large oven.

As the solute feed to the sequential unit is continuous, it was decided to employ the highest solvent loading with which the support could be coated without losing its 'dry' handling properties. A high loading would also reduce the possibility of deleterious solute adsorption on the active sites of the support surface. The latter normally requires that 'acid washing' or 'silanization' of the support be performed. Experimental tests revealed that a solvent loading of 25% of the total coated weight was close to the maximum permissable.

Approximately 200 gm of Chromosorb P were placed in the specially fluted 3 dm^3 flask of a rotary evaporator. The proportional weight (one-third) of silicone fluid DC 200/50, dissolved in dichloromethane, was then added. While the dichloromethane was slowly evaporated under vacuum and slight heating, the flask was rotated. The fluting of the flask

Table 5.1 Sieve Analysis of a 50 g Sample of Chromosorb P

Nominal Apperture size	Mesh Nos. (approx.)	As supplied		After Machine Sieving	
		Weight on sieve	%	Weight on sieve	%
μm		g		g	
600	25	0.03	0.06	0.01	0.02
500	30	4.96	9.95	0.87	1.74
355	44	24.08	48.26	45.04	90.42
300	52	9.33	18.70	1.59	3.20
252	60	9.08	18.20	0.61	1.22
252		2.24	4.83	1.69	3.40
	Total	49.89	100.00	49.81	100.00

improved mixing and minimised 'sticking' of the solid support to the wall of the flask, therefore assisting the attainment of an even coating of the silicone fluid. The coated packing was finally placed in a fume cupboard to allow the remainder of the dichloromethane to evaporate.

Following the conclusions of Hupe et al (45) from their studies of the solute front profiles occurring in a 10 cm-diameter column, the column packing procedure was as follows.

Successive additions of weighed quantities of approximately 50 gm of the coated support were made. Between each addition, the column wall was vigorously beaten around the circumference while a heavy 30° metal cone, concave to the packing, was rested on the packing surface. The diameter of the 3.0 kg cone was 7.3 cm. Its purpose was to ensure a relatively higher packed density at the column wall and hence assist the formation of an even cross-sectional flow profile.

On reaching the column mid-point, the feed cross-distributor was connected in position by a pair of tongs. Packing then continued until each column was apparently full, at which point the top retaining gauge and cone were bolted into position.

The entire unit was then subjected to both static and flowing air pressure for leak testing. In addition, trial separation runs were performed. Observation of column pressure drops and of the individual outlet concentration levels, as monitored by the purged product (Product 2) katharometer revealed the need to improve column equality.

Inspection of column packing levels showed that further settling had occurred. The columns were repacked, being repeatedly subjected to pressure until the level of packing remained constant. Finally the

total weight in each column was made nearly equivalent (Table 5.2). The average packed density (based on uncoated support) was 0.45×10^{3} kg m^{-3} which is in excellent agreement with that reported in Table 4.2.

A comparison of the batch chromatographic efficiency (expressed as H.E.T.P.) of the individual columns was then performed before commencing the study of the unit operating in the separation mode.

Table 5.2 Weight of Coated Solid Support in each Column

Assigned Column Number	Initial Packing	Final Packing
	kg	kg
1	1.585	1.635
2	1.584	1.650
3	1.589	1.650
4	1.573	1.635
5	1.572	1.650
6	1.587	1.650
7	1.574	1.635
8	1.589	1.650
9	1.596	1.650
10	1.604	1.635
11	1.572	1.650
12	1.599	1.650
Total	19.024	19.740

Total weight of solvent phase (25% loading) = 4.935 kg

Total volume of solvent phase (ρ_L = 0.97 g cm^{-3}) = 5.09 dm^3

Average volume of solvent phase per column = 417 cm^3

Note: 1) Column numbers correspond to the position of the isolated bed on 'timer'.

2) Columns 1, 4, 7, 10 are those with additional sample points.

5.2 Theoretical Basis For Comparison

The conventional column performance term in chromatography, height equivalent to a theoretical plate, essentially relates the width of the eluted peak and column length. However, the size and shape of this peak is not solely determined by the chromatographic process occurring within the column. Several contributing extra-column factors can be pinpointed; the size and method of sample injection, the 'dead' volume of the column inlet and outlet lines and the response of the peak detection system.

The contribution made by these factors may be non-Gaussian in form. For example, a liquid sample injected directly into the inflowing carrier gas requires time to evaporate. Coupled with slow mixing and diffusion effects, the resultant injection profile will be exponential in shape. Unless such extra-column factors are minimised, calculating H.E.T.P. by only considering the eluted peak, in addition to assuming that peak to be Gaussian (Equ. 2.7 and 2.11), will introduce large errors.

Following the work of Reilley et al (168), Sternberg (169) employed Laplace Transforms to calculate the shape of the output peak for any shape of input function modified both by a Gaussian operator (the chromatographic column) and additional spreading effects resulting from the column fittings and detector. This work emphasised that the second moment, or variance, of the finally recorded non-Gaussian peak could be obtained by summing the individual variances of all the contributing factors. That is

$$(\sigma_t)^2_{r.o.} = (\sigma_t)^2_{injection} + (\sigma_t)^2_{column} + (\sigma_t)^2_{fittings} + (\sigma_t)^2_{detector} \qquad 5.1$$

where $(\sigma_t)^2$ equals the time-based second moment or variance.

Giddings (170) has shown that the additive property of this statistical quantity extends to non-ideal columns which in themselves can lead to skewed peaks. In such a case the overall column variance, $(\sigma_t^2)_{column}$, would represent the summation of band broadening contributions from such factors as adsorption onto the surface of the solid support and 'dead' volume within the column as well as the mass transfer process.

Thus, for a practical large-scale chromatographic system, H.E.T.P. should be determined from an accurate knowledge of $(\sigma_t)^2_{column}$. Considering Equ. 5.1, this implies that both the injected and eluted profiles should be recorded 'on-column' by a common detection system. Subtraction of the time-based variances calculated from the respective profiles cancels the contribution from extra-column factors. Also, subtraction of the respective peak retention times gives the retention time solely attributable to the column.

The value of H.E.T.P. is given by

$$H = \frac{l \cdot \left[(\sigma_t)^2_{r.o.} - (\sigma_t)^2_{r.i.}\right]}{\left[(t_{r.o.c.} + \bar{t}_{r.o.}) - (t_{r.i.c.} + \bar{t}_{r.i.})\right]^2} \qquad 5.2$$

where : l = column length

$(\sigma_t)^2$ = time-based 2nd moment or variance

$\bar{t}_{r.o.}, \bar{t}_{r.i.}$ = peak mean or 1st moment in time units for the recorded outlet and inlet profiles respectively

$t_{r.o.c.}, t_{r.i.c}$ = time from injection to commencement of recording of the outlet and injection profiles respectively.

5.3 Experimental Procedure

Fig 5.1 diagramatically represents the arrangement for the comparison experiments. Each column was isolated in turn and a constant inlet gas pressure of 231.5 kN m^{-2} applied. The pressure measuring device consisted of a syringe needle connected by a flexible nylon tube to a mercury manometer. Tapping for all accurate pressure readings was a simple matter of inserting the needle, through the septum cap, into the appropriate sample point. The outlet volumetric flowrate was set constant by the purge gas outlet flow regulator in conjunction with a gas meter. Any variation in column flow resistance resulted in a variation in the outlet pressure, which was recorded. Whilst this did not ensure a constant gas velocity through the column it was a more realistic comparison in terms of subsequent sequential operation of the unit.

A 1.0 cm^3 sample of 'Arklone' P was injected, upstream of the purge gas inlet distributor, directly into the gas stream flowing into the column. The profile was monitored by the katharometer in conjunction with the pen recorder, a flow regulated sample stream being bled from the inlet cone sample point through a syringe needle. The reference arm of the block was fed, through a needle valve, from the precision inlet pressure regulator. An equal flowrate of 13.7 cm^3 s^{-1} was set for the two bleedstreams by timing the rise of a bubble in a 100 cm^3 soap bubble meter.

Switching the katharometer sample stream to the column outlet cone enabled monitoring of the elution profile. The flowrate for the comparison study was, therefore, selected as 610 cm^3 s^{-1} at ambient conditions, which permitted complete recording of both traces for a

common injection. Attenuation of the katharometer bridge circuit output and the range of the recorder pen response were set to give a near full scale peak height.

Positioning of the injection point well upstream of the column inlet introduces a large additional 'dead' volume into the injection profile. However, it was found that, if the injection point was brought closer to the inlet sample point, poor reproducibility resulted. This was attributed to the flow regulator in the sample offtake line not responding quickly enough to representatively sample the fast moving peak. The presence of the regulator was necessary to maintain a constant flow through the katharometer when sampling both the inlet and outlet column flow streams which are at significantly different pressures.

The inter-packing void volume for each column was determined from a measurement of the difference in the time taken for the peak of an in-line injected sample of hydrogen to pass two sample points in the column wall. A 10-second sweep stopwatch was used for the measurement. It was reasonably assumed that the hydrogen was not retained on the solvent phase. The pressure at the respective sample points was measured by the manometer.

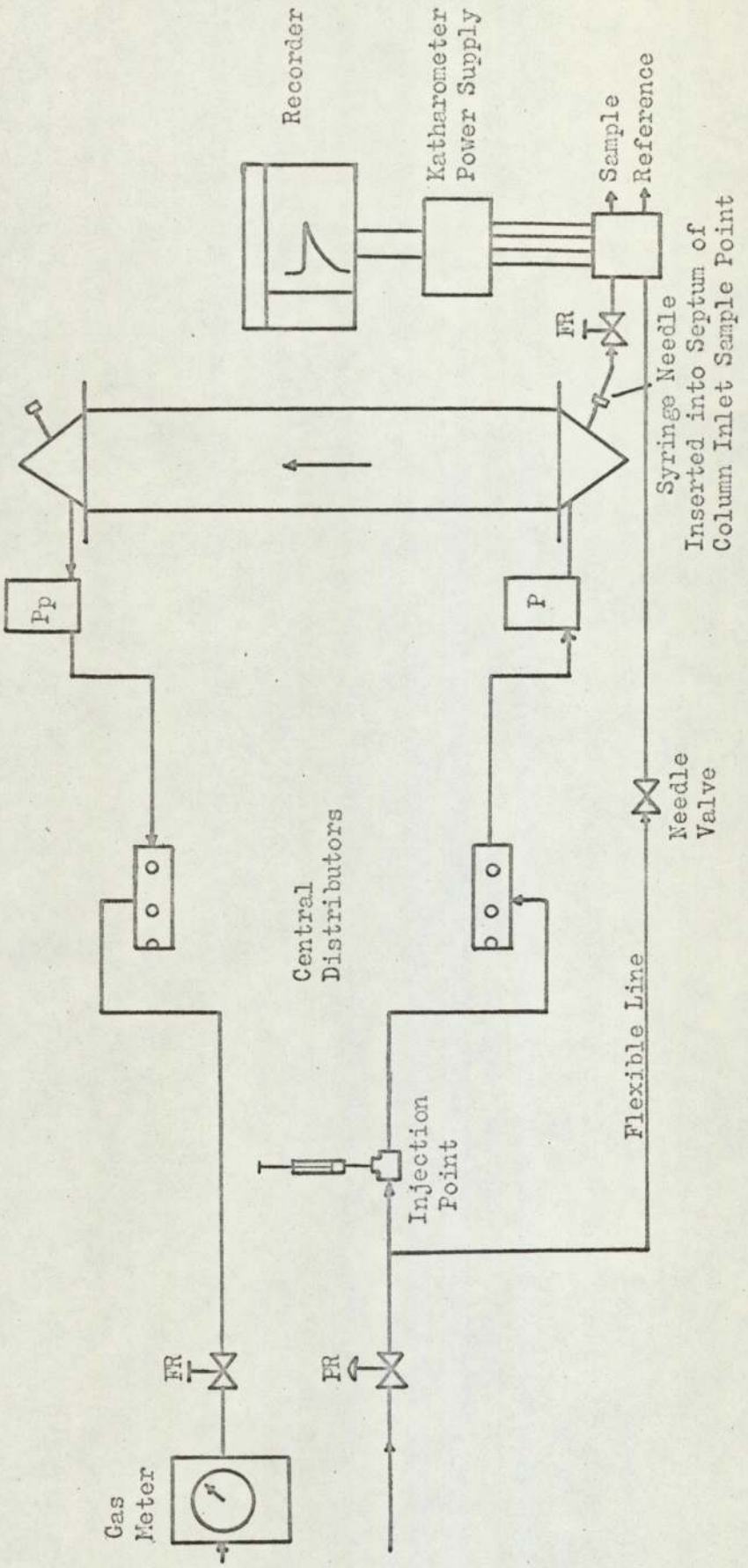

Figure 5.1 Line Diagram to show Arrangement for Single Column Measurements

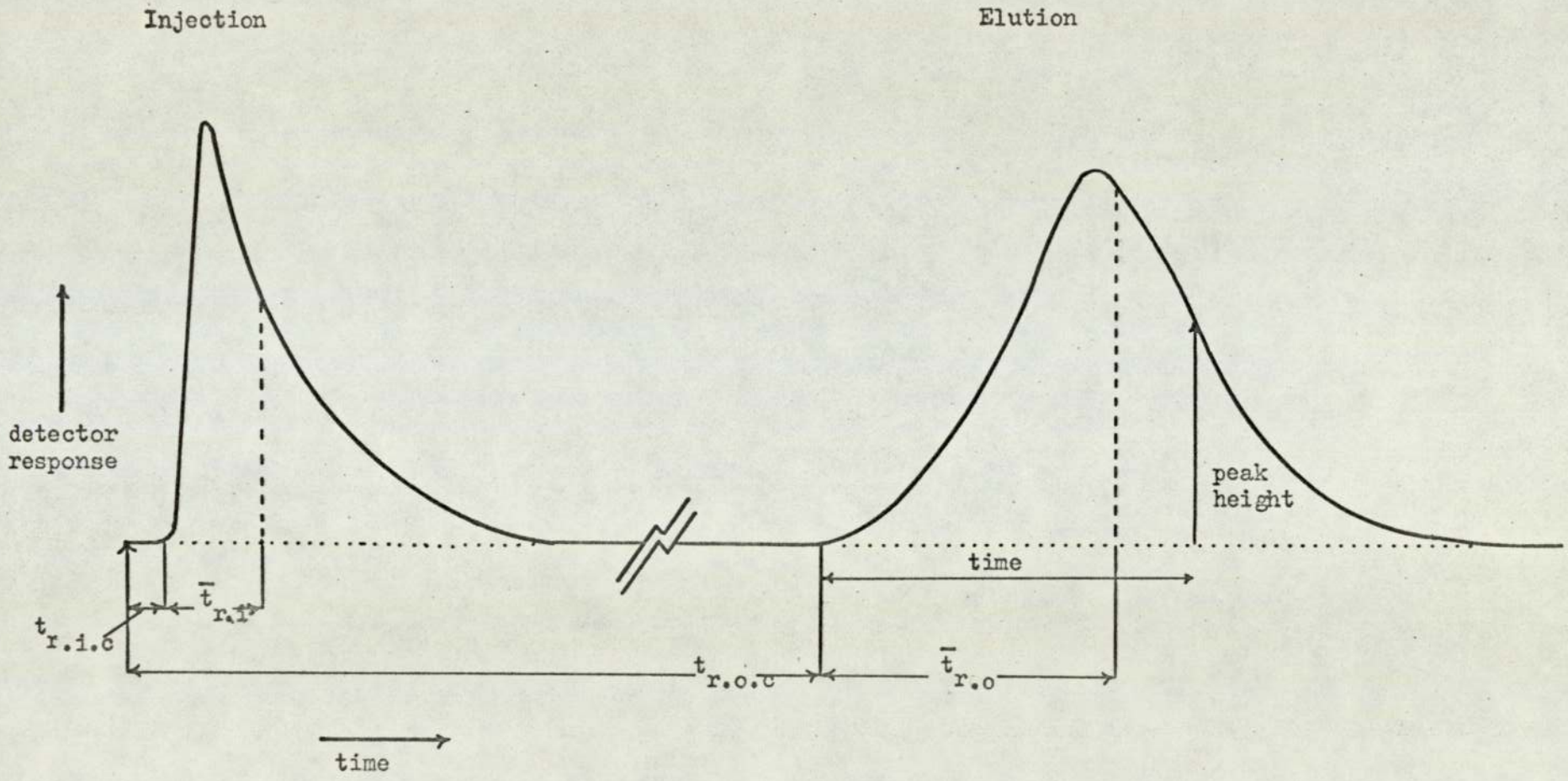

Figure 5.2 Example of Recorded Profiles Obtained for a 1.0 cm^3 Injection of 'Arklone' P into a single column

5.4 Computation of Results

The forms of the recorded traces obtained for the inlet injection and elution profiles are given in Fig 5.2. For each profile, values of the peak height at equal time increments were read from the calibrated recorder chart. The time increment was chosen to give at least thirty values of peak height, this being the minimum for statistical significance (171). $t_{r.i.c.}$ and $t_{r.o.c.}$ were also noted for each peak. The data for each pair of profiles were then processed by a simple computer program, written in BASIC language (172). A flow chart of the calculations is given as Fig 5.3 while the full listing is to be found in Appendix 2.

The program calculated the mean, variance, skew and kurtosis of the injection and elution profiles respectively. Peak retention time was then calculated by the addition of the computed mean ($\bar{t}_{r.i.}$,$\bar{t}_{r.o.}$) to the time to peak commencement ($t_{r.i.c.}$,$t_{r.o.c.}$). Both these profiles include a common contribution from extra-column factors and thus the retention time and variance solely attributable to the column were obtained by subtraction (Equ. 5.2). Finally the program calculated N.T.P. and hence H.E.T.P.

The form of the print-out is given in Fig 5.4. BASIC is an interactive high-level language; i.e. data can be input from a 'teletype' keyboard during the running of the program. A request for input is denoted by an exclamation mark. The results for each column are summarised in Table 5.3.

A simple BASIC language program was also written to calculate the column voidage and interparticle velocity. Fig 5.5 shows a flow chart for the calculation, the listing being given in Appendix 2, while the results have been included in Table 5.4.

Figure 5.3 Flowchart of the Computation of the Mean, Standard Deviation, Skew, Kurtosis, N.T.P. and H.E.T.P. from the Recorded Single Column Injection and Outlet Profiles.

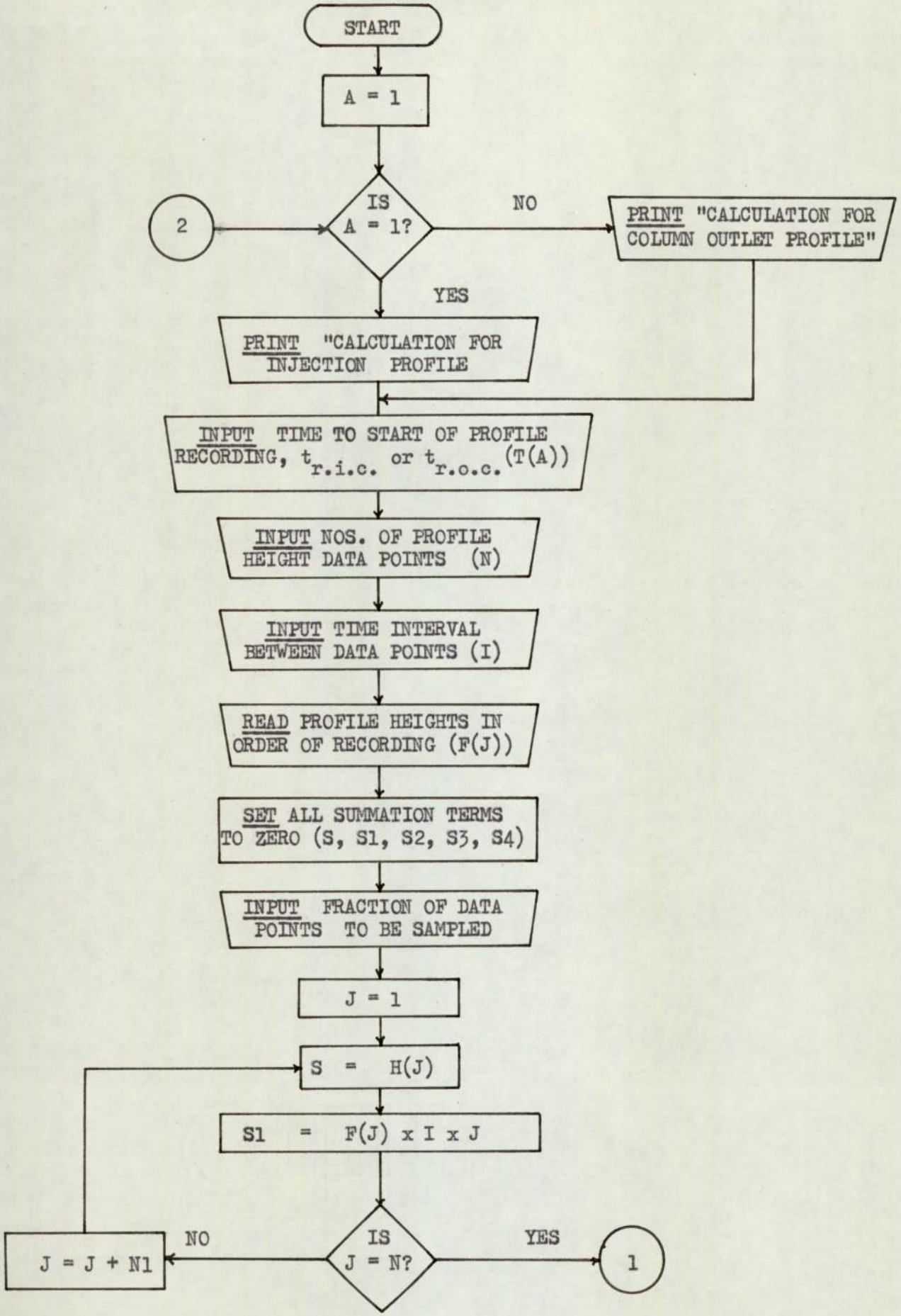

Figure 5.3 (Cont'd.)

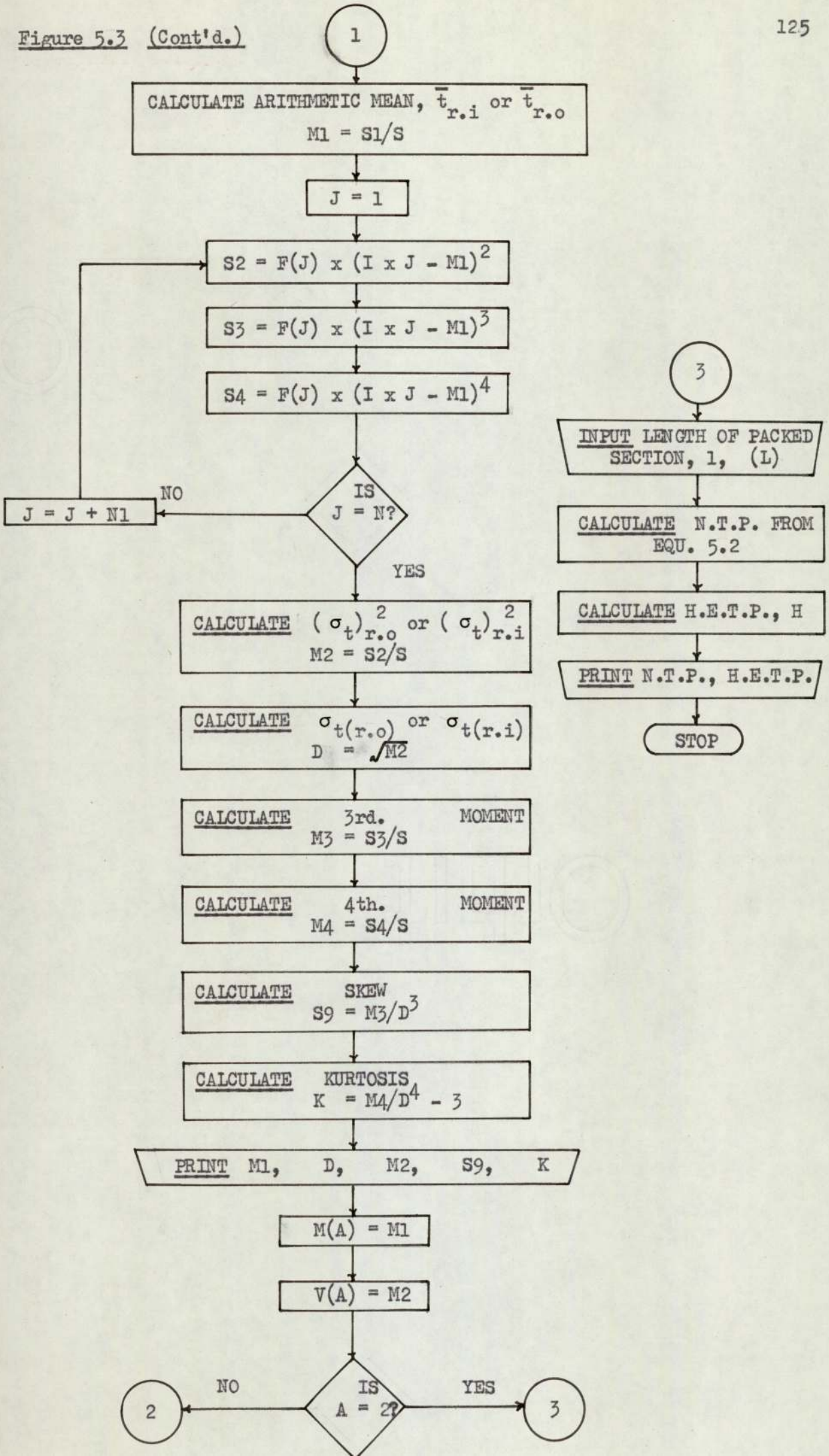

FIGURE 5.4 EXAMPLE PRINT-OUT OF SINGLE COLUMN H.E.T.P. COMPUTATION

```
PROGRAM TO CALCULATE MEAN, STANDARD DEVIATION, SKEW,
KURTOSIS,N.T.P. AND H.E.T.P.
CALC. FOR INJECTION PROFILE
===========================
INPUT TIME TO START OF PROFILE OUTPUT(SECS.)
!5.5
NOS. OF DATA POINTS STORED =
!43
TIME INTERVAL BETWEEN DATA POINTS STORED (SECS.)
!2.5
INPUT FRACTION OF DATA POINTS TO BE SAMPLED
ALL=1,HALF=2,THIRD=3 ETC.
!1
ARITHMETIC MEAN =                19.7071
STANDARD DEVIATION =             14.6981
VARIANCE =       216.034
SKEW=              1.7511
KURTOSIS =         4.0984
CALC FOR COLUMN OUTLET PROFILE
==============================
INPUT TIME TO START OF PROFILE OUTPUT(SECS.)
!161
NOS. OF DATA POINTS STORED =
!34
TIME INTERVAL BETWEEN DATA POINTS STORED (SECS.)
!5
INPUT FRACTION OF DATA POINTS TO BE SAMPLED
ALL=1,HALF=2,THIRD=3 ETC.
!1
ARITHMETIC MEAN =                58.0852
STANDARD DEVIATION =             23.0654
VARIANCE =       532.015
SKEW=               .749193
KURTOSIS =          .905323


NOW CALCULATION FOR N.T.P. AND H. E. T. P.
==========================================
INPUT LENGTH OF PACKED SECTION IN CMS
!61
N.T.P.=          113.959
H.E.T.P.=           .512782  CMS

430 EXIT
?
```

Table 5.3 Summary of the Results of the H.E.T.P. Computation for a Single Column

Assigned Column Nos.	Injection Profile					Outlet Profile					N	H
	$t_{r.i.c.}$	$\bar{t}_{r.i.}$	$(\sigma_t)^2_{r.i.}$	skew	kurtosis	$t_{r.o.c.}$	$\bar{t}_{r.o.}$	$(\sigma_t)^2_{r.o.}$	skew	kurtosis		
	s	s				s	s					mm
1	3.0	23.5	283.1	1.63	3.26	185.0	62.7	674.8	0.57	0.32	125	4.9
2	2.5	22.0	193.6	1.58	3.19	177.0	77.8	917.5	0.60	0.09	73	8.4
3	3.0	21.1	246.7	1.75	4.04	167.0	62.2	907.8	1.55	4.41	64	9.5
4	3.5	21.7	216.0	1.65	3.51	161.0	58.1	532.0	0.68	0.73	119	5.1
5	3.0	20.5	221.0	1.60	3.25	170.0	58.4	714.5	1.14	2.38	85	7.2
6	4.0	19.5	209.8	1.70	3.67	162.0	62.3	675.3	0.83	0.93	87	7.0
7	3.0	19.4	201.3	1.74	3.92	153.0	62.0	639.5	1.00	2.16	85	7.2
8	5.0	19.2	204.9	1.69	3.67	160.0	59.5	570.8	0.69	0.62	104	5.9
9	4.5	20.3	206.9	1.44	2.41	182.0	76.7	1123.8	0.56	0.11	60	10.0
10	5.0	19.0	196.5	1.64	3.33	170.0	60.7	519.3	0.67	0.69	132	4.6
11	3.0	20.9	212.8	1.56	2.91	177.0	65.5	904.2	0.82	0.82	69	8.8
12	5.5	19.4	212.0	1.71	3.84	173.0	78.1	1017.0	0.71	0.55	64	9.5

Figure 5.5 Flowchart of Program used to Compute Interparticle Volume, Volume of Packing and Mean Carrier Gas Velocity for Comparison of Individual Column Physical Properties.

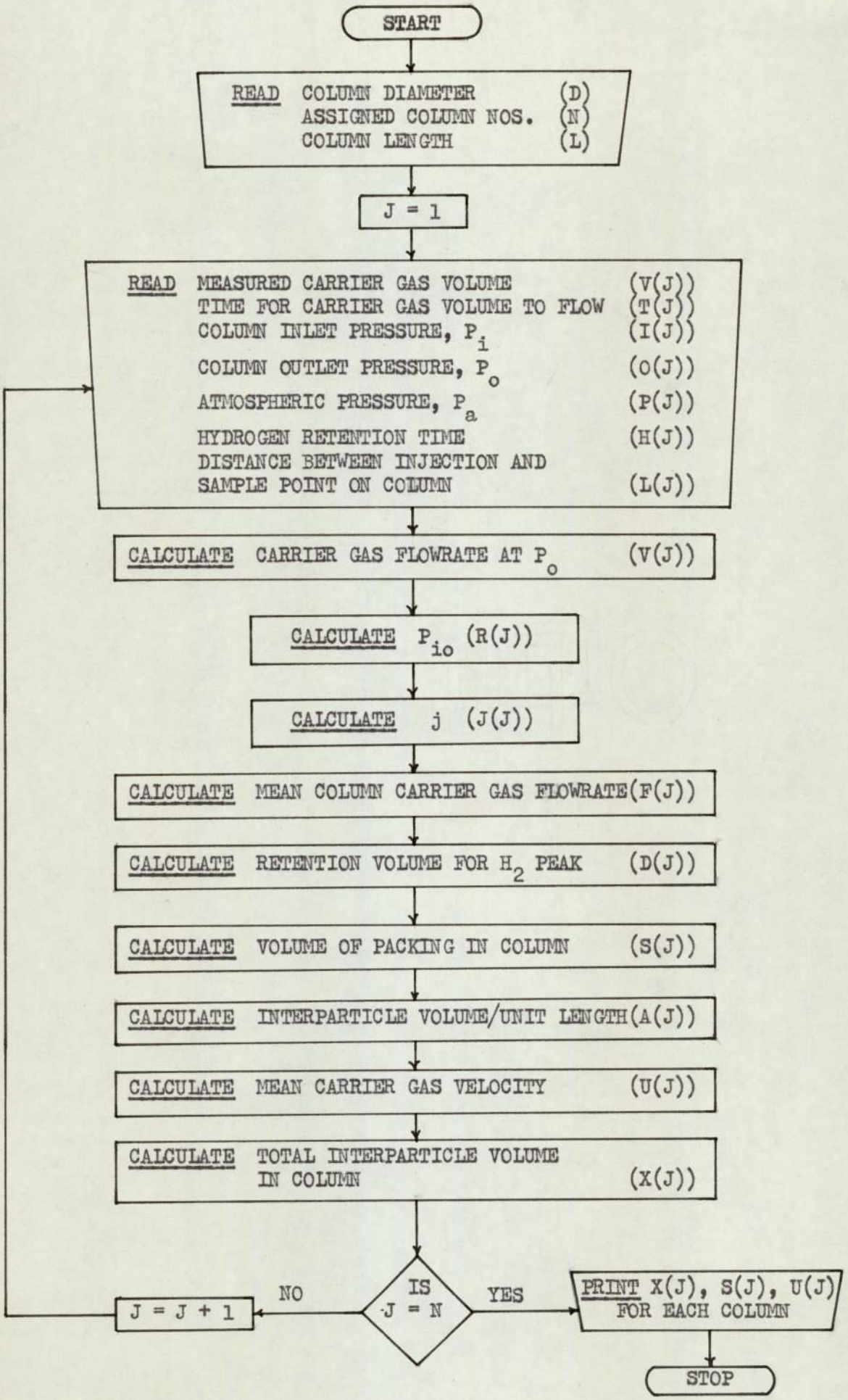

Table 5.4 Comparison of Individual Column Physical Properties

Column inlet pressure = 232.6 kN m^{-2}

Volumetric carrier gas flowrate = 610 cm^3 s^{-1} (@ 101.3 kN m^{-2} and 20°C)

Assigned Column Number	Pressure drop across the column	Weight of packing	Interparticle Volume	Volume of packing	$\bar{u}$	H
	kN m^{-2}	g	cm^3	cm^3	cm s^{-1}	mm
1	6.7	1635	1915	867	8.6	4.9
2	6.9	1650	2007	774	8.2	8.4
3	5.9	1650	1977	804	8.4	9.5
4	6.1	1635	1820	962	9.1	5.1
5	6.7	1650	1861	921	8.9	7.2
6	7.3	1650	1893	890	8.8	7.0
7	7.6	1635	1862	920	8.9	7.2
8	6.7	1650	1896	886	8.8	5.9
9	6.9	1650	2017	765	8.2	10.0
10	7.1	1635	1826	955	8.9	4.6
11	8.5	1650	2014	767	8.3	8.8
12	6.5	1650	1900	881	8.7	9.5
Average	6.9	1645	1917	849	8.7	7.4

5.5 Discussion

Both the injection and elution profiles have long 'tails' as a consequence of several contributing factors, namely:

(i) The experimentally necessary large 'dead' volume between the injection point and the column packing.

(ii) The experimentally necessary presence of a flow regulator in the peak sampling line.

(iii) The injection of a large liquid sample without any addition of heating to assist 'instantaneous' vaporization.

While the experimental technique attempts to nullify the effect of i and ii on the determined value of H.E.T.P., its accuracy is limited by the katharometer and potentiometric recorder. The values of peak mean and variance are very sensitive to the length of the 'tail' and thus care was necessary to ensure that no base line drift or offset occurred during the experimental work. The injection and recording procedure was repeated until the respective peak heights and the time taken for the trace to return to the base line were reproduced to within 2%. This gave a reproducibility for the calculated value of H.E.T.P. of within 5%.

Skew and kurtosis are a measure of the shape of the elution profiles. Consideration of the calculated values show that the technique, despite accuracy limitations, is superior for large-scale systems to the classical graphical method of determining H.E.T.P. The latter assumes the peak to be Gaussian in shape for which the value of skew is one and kurtosis three.

The response of the katharometer and recorder, with respect to speed, was also important to the accuracy of the voidage determination.

The hydrogen peak, being unretained on the silicone fluid solvent, passed the respective sample points very quickly. As the differential time of passing the sample points was only of the order of four seconds, a significant lag in response, if not cancelled out, would introduce a large error. The injected hydrogen sample size, katharometer bridge settings and recorder scale setting were consequently selected to give a peak height of approximately one-tenth of full scale deflection for both sample points. All injections were repeated to give a result reproducible to within $\pm$ 0.1 s, suggesting an accuracy in the calculated voidage of about $\pm$ 5%.

The accuracy of all the above work could be improved by using two matched katharometers of small internal volumes, replacing the flow regulators by capillary tube to restrict sample bleed to an equal value and using a very sensitive recorder with a response time of 0.1 s to full scale deflection.

From the results in Tables 5.3 and 5.4, the variation from column to column appears prohibitive to successful operation of the unit in the separating mode. However, eleven columns are linked to form the main separating section. Thus in sequencing through the cycle the variation in the total number of 'plates' in the separating section at any time is considerably reduced. Further, as the unit is to be operated at high solute concentration it is to be expected that with the consequent further increase in plate height the column to column variation would diminish. Experimental observations substantiated both these points (see Section 8.2.2).

The computed values of the plate heights are high when compared with the 1.2 mm reported for a 7.6 cm (3 in) diameter column by Albrecht and Verzele (99). This is in part attributable to the short length of column over which the measurements were made, coupled with a severe tailing contribution resulting from the substantial 'dead' volume of the unpacked cones. It should also be stressed that the comparison is somewhat erroneous as no attempt was made in this work to minimise the H.E.T.P. values by careful selection of optimum flowrate and sample size.

In conclusion, the experimental comparison of the individual column characteristics emphasised the importance of the packing technique in large-scale chromatography. High H.E.T.P. values coupled with column to column variation, although the effect of the latter is minimised in operation, represents a limitation on the separating potential of this unit with difficult separations. As the system 'Arklone' P/'Genklene' P has a high separation factor, it was considered that the separation studies could be commenced without the need for further repacking. However, it is envisaged that future development work on the sequential system would incorporate the improved column design and packing techniques, reviewed in Section 2.3.3, which have resulted from research in the 'batch' field.

CHAPTER 6

The Partition Coefficient

6.1 The Significance of the Partition Coefficient in the Selection of Column Operating Conditions

6.1.1 A Simplistic Model

Separation in chromatography is dependent on the fact that solutes have differing affinities for the solvent phase. As was shown in Section 2.2, a measure of that affinity is given by the partition coefficient, K. It is therefore to be expected that the respective 'K' values provide the basis for the selection of the relative rates of movement of the gas and liquid phases in counter-current chromatographic systems.

The separation of a binary mixture on an ideal, mechanically continuous, moving-port unit with a separate purging section is illustrated in Fig 6.1. Component i, as the less strongly absorbed component, is to be removed in the carrier gas stream G. Component ii is to be held preferentially on the liquid phase. Through the continuous rotation of the ports, the column section containing componentii will eventually become isolated for purging by gas stream S. Defining phase movement relative to the port positions it can be seen that the liquid phase moves at an apparent rate, L, counter-current to the gas phase. S, G and L are volumetric flowrates. For the purpose of the present discussion S and G are considered to be constant across the column, that is the pressure drop is assumed negligible and the temperature constant.

A material balance on component i at the feed point gives

$$f_i = Gc_i + Lq_i \qquad 6.1$$

where f_i is the feedrate of component i to the column, c_i denotes the

Figure 6.1 Continuous Moving Port Unit

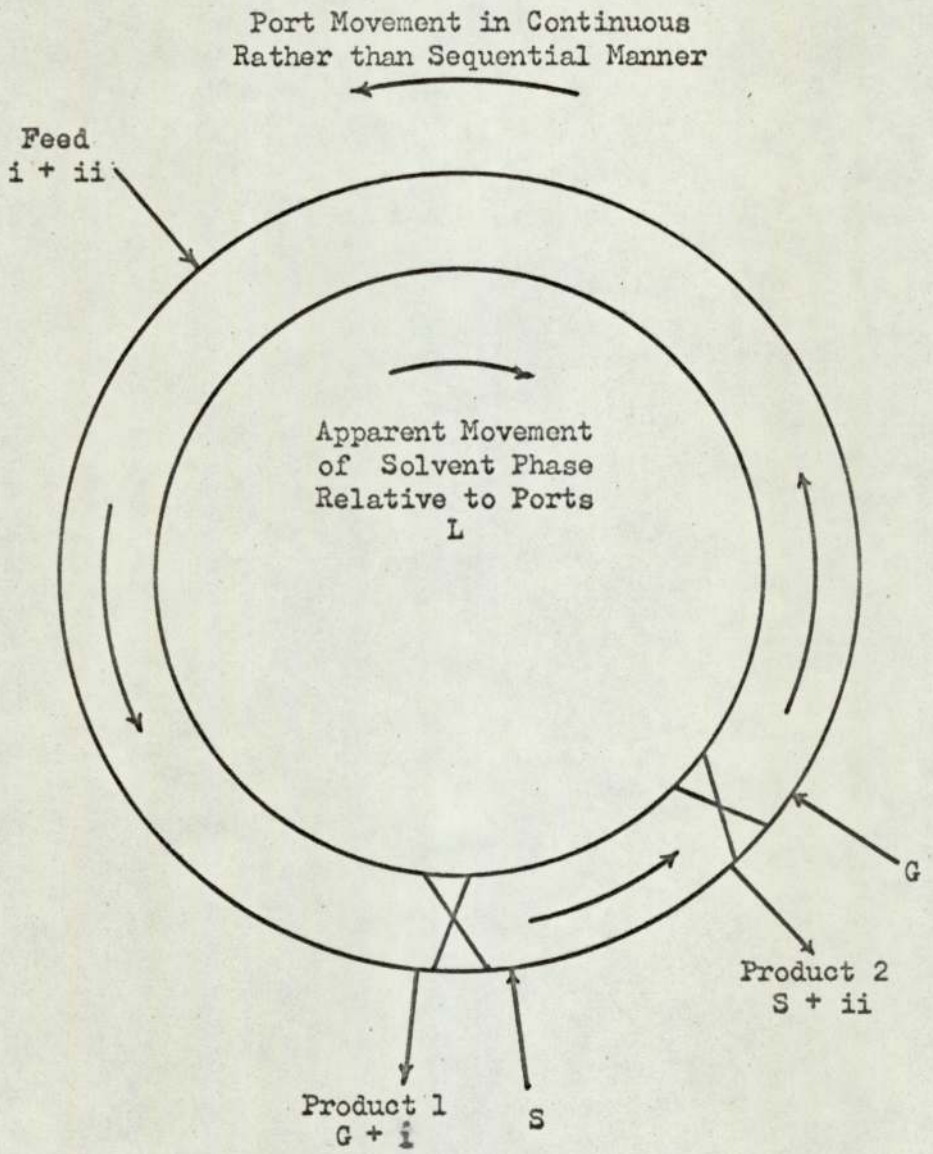

concentration of component i in the gas phase, and q_i the concentration of i in the liquid phase.

The condition for preferential movement of component i in the gas phase is that

$$Gc_i > Lq_i \qquad 6.2$$

i.e. $$\frac{G}{L} > \frac{q_i}{c_i} \qquad 6.3$$

or $$\frac{G}{L} > K_i \qquad 6.4$$

Similarly for component ii to travel preferentially with the solvent phase

$$\frac{G}{L} < K_{ii} \qquad 6.5$$

Thus the two components will have opposing resultant velocities if the ratio of the volumetric gas to apparent liquid flow lies within the range specified by the respective partition coefficients,

$$K_i < {}^{G}/_{L} < K_{ii} \qquad 6.6$$

The same logic suggests that component ii will be purged from the isolated section if

$$\frac{S}{L} > K_{ii} \qquad 6.7$$

6.1.2 The Practical Case

Equations 6.6 and 6.7 provide a basis for the selection of column operating flow conditions for an ideal counter-current system. A discussion of their practical application to the unit under study now follows. Four factors must be considered; (i) column length, (ii) the sequential nature of operation, (iii) pressure drop and (iv) finite solute concentrations.

6.1.2.1 The Effect of a Finite Column Length

Column length is of prime importance in determining whether a successful separation will result when operating the unit at specific flow conditions. As the $^{G}/_{L}$ ratio selected approaches either the upper or lower level of the range for separation, the tendency of the solutes to move in opposing directions is reduced. The separation becomes increasingly difficult until, at the 'K' value limits, an infinite number of equilibration stages are required (a situation analogous to the 'pinch' point in distillation). Thus, for a finite column length, the range of $^{G}/_{L}$ values for a successful separation is narrower than that specified by the respective partition coefficient;

$$\text{i.e. } (K_i + \delta_i) < {}^{G}/_{L} < (K_{ii} - \delta_{ii}) \qquad 6.8$$

where δ is a function of the number of theoretical plates, and therefore column characteristics, as well as the criteria for a 'successful' separation.

Barker and Lloyd (10, 11, 21) have experimentally observed a narrowing of the $^{G}/_{L}$ range for separation when studying the systems benzene/cyclohexane and methylcyclohexane/cyclohexane on a moving-bed column. As the effect of a finite column length was not investigated in isolation from other column parameters, no attempt was made to obtain a specific value for δ.

6.1.2.2 The Effect of the Sequential Mode of Operation

Within a sequencing interval, the unit is operating as a co-current 'frontal-elution' system. The counter-current movement of the liquid phase relative to the gas phase is imposed by the discontinuous stepping of

the port functions around the twelve linked columns. Intuitively this system of operation must further reduce the selectable range for the G/L' ratio.

$$(K_i + \delta_i + s_i) < G/L' < (K_{ii} - \delta_{ii} - s_{ii}) \qquad 6.9$$

where : L' = the apparent volumetric liquid phase flowrate

$$= \frac{\text{total volume of liquid phase in column}}{\text{cycle time.}}$$

s = the reduction in the limits of G/L' attributable to the sequencing action.

s will be a function of the degree of discontinuity in terms of the length of the column sections and sequencing interval as well as the criteria for successful separation and column characteristics.

Discontinuity is of particular importance to the section of column isolated for purging. Within the sequencing interval all solute must be removed as Product 2 if contamination of Product 1 is not to occur. However, equation 6.7 refers to the mean solute molecule migration rate. To overcome diffusion and tailing effects, S must be increased beyond the theoretical value calculated from equation 6.7.

6.1.2.3 The Effect of Pressure Drop Across the Column

For the simplistic model the pressure drop across the column was assumed to be negligible, enabling S and G to be considered constant. In practise, the small particle sizes used in chromatography present a considerable resistance to flow. The consequent pressure drop results in a continual change in the volumetric gas flowrate. At the column inlet G is at a minimum. As the pressure falls G increases to a maximum value at the column outlet.

The implication of this factor is best illustrated by considering the two ends of the separating section. At the point of carrier gas inlet the relatively lower volumetric flowrate means that the rate of migration of solute molecules in the direction of gas flow is reduced. If conditions are such that both solutes appear close to this point in the column, then the rate at which they separate will be decreased. With increasing concentration the eventual result will be contamination of Product 2 (component ii) with component i.

Approaching the Product 1 exit the opposite effect will occur. The migration rate of solute molecules will be increased as the pressure falls. Component ii molecules appearing in this section of the column will be accelerated, forming a long leading edge which will eventually extend to contaminate Product 1 (component i).

A further restriction should therefore be imposed on the limits of G/L' to ensure a successful separation.

$$(K_i + \delta_i + s_i) < \frac{G_{min}}{L'} < \frac{G_{max}}{L'} < (K_{ii} - \delta_{ii} - s_{ii}) \quad 6.10$$

where G_{min}, G_{max} are the respective volumetric flowrates at the separating section inlet and outlet.

The central inequality is important. If the flow conditions imposed by the $(K + \delta + s)$ terms are such that $\frac{G_{max}}{L'} - \frac{G_{min}}{L'}$ is negative, then complete separation is theoretically impossible.

6.1.2.4 The Effect of Finite Solute Concentration

In Section 2.3.2 the direct significance of two phenomena, the form of the absorption isotherm and the 'sorption' effect, to the value of the

partition coefficient at finite solute concentrations was emphasised.

For a non-linear absorption isotherm the point value of the partition coefficient, $^{q}/_{c}$, changes with solute concentration. With increasing concentration K decreases for a type I (Langmuir) isotherm while for a type II (anti-Langmuir) isotherm K increases. A standard point is given by the value at infinite dilution, K^{∞},

$$K = K^{\infty} + \Delta K \qquad 6.11$$

where ΔK is either the positive or negative deviation from K^{∞} with increasing solute concentration, under isothermal conditions.

The sorption effect always results in a migration rate for the solute molecules which is higher than that specified solely by the ratio of the liquid and gas phase solute concentrations. To allow for the contributions of the solute molecules in the gas phase to the carrier gas flowrate an 'apparent' partition coefficient, K', must be defined which is less than the true thermodynamic value.

$$K = K' + \Delta K' \qquad 6.12$$

where $\Delta K'$ equals the positive correction to the apparent partition coefficient attributable to the sorption effect. $\Delta K'$ can be calculated, for a specific value of solute concentration, from equation 2.26.

$$\Delta K' = K.j.y. \qquad 6.13$$

where j is the compressibility factor and y the mole fraction of solute in the gas phase.

A further complication results from a solute concentration dependent phenomena termed by Higgins and Smith (49) as 'enthalpic overloading'.

The heat of solution of solutes from the gas phase is high. Consequently positive and negative deviations from the mean column temperature accompany absorption and desorption of the solute species. Under adiabatic conditions, temperature would have the same distribution along the column as the solute concentration, the temperature rise or fall being controlled by the heat capacity of the column. In practise, these temperature excursions will be modified by the degree of heat redistribution resulting from conduction through the packing and column wall. As the thermal conductivity of the solid support is low, localised regions of comparatively high temperature fluctuation are to be expected near the centre of a large diameter column.

The experimental work of several researchers confirm the significance of this effect (45, 100, 178 - 180). For example, Hupe et al (45) observed a cross-column temperature variation of up to 7.5°C when injecting 6 cm^3 of n-hexane onto a 980 mm long by 100 mm diameter column packed with 20% polypropylene glycol on silica gel (0.2 - 0.3 mm). The mean column temperature was 60°C.

Axial and radial temperature gradients will have the following effects on a separation.

(i) The leading edge of the solute band will tend to be at a comparatively high temperature giving an increased solute migration rate. Conversely, the migration of a solute molecule in the tail of the solute band will be retarded. A further correction to the isothermal partition coefficient should be introduced.

$$K = K'' + \Delta K'' \qquad 6.14$$

where ΔK equals the positive or negative correction to the apparent partition coefficient, K'', attributable to the enthalpic overloading effect. Theoretical expressions for this very complex term have been given by Scott (178) and Higgins and Smith (49).

(ii) Radial temperature gradients will lead to a non-uniform cross-column solute migration profile. The experimental profiles recorded by Hupe et al (45) follow the expected pattern, the centre of the band being advanced relative to the column wall (see Section 2.3.1). This represents a further contribution to the theoretical plate height for large diameter columns. An increased column length is therefore required to effect a separation.

Introducing finite concentration effects on the partition coefficient into equation 6.10 gives:

$$(K_i^{\infty} + \Delta K_i - \Delta K_i' - \Delta K_i'' + \delta_i + s_i) < \frac{G_{min}}{L'} < \frac{G_{max}}{L'}$$

$$< (K_{ii}^{\infty} + \Delta K_{ii} - \Delta K_{ii}' - \Delta K_{ii}'' - \delta_{ii} - s_{ii}) \qquad 6.15$$

For the purge section

$$\frac{S_{min}}{L'} > (K_{ii}^{\infty} + \Delta K_{ii} - \Delta K_{ii}' - \Delta K_{ii}'' + \delta_{ii} + s_{ii}) \qquad 6.16$$

These inequalities give a qualitative indication of the factors which must be considered when selecting column flow settings. However, they cannot be used for accurately predicting the operating limits for a successful separation. Extensive experimental and theoretical work is required.

To elucidate the complex interaction of parameters affecting the performance of the sequential unit purely from experimental data would be extremely difficult, if not impossible. For example, the effect of a finite column length is intimately related to column characteristics, sequencing rate and pressure drop. Also, the concentration of the solutes varies along the length of the column giving a variation in the ΔK, $\Delta K'$ and $\Delta K''$ terms.

A theoretical model is required to enable study of the individual factors in isolation. Operating data would serve both to observe actual performance and to provide basic information with which to test the validity of this model.

Hence equations 6.15 and 6.16 have helped to define the path for the research on the sequential unit. Experimental separation runs are reported in Chapter 8 while a computer simulation is described in Chapter 9. As a preliminary to this work the partition coefficients of the solutes 'Arklone' P and 'Genklene' P were determined both at infinite dilution and as a function of solute concentration. K values for dichloromethane were also obtained, the solute pair dichloromethane/'Arklone' P providing a more difficult system for separation which may be studied in a future research project.

6.2 Determination of the Partition Coefficient

6.2.1 At Infinite Dilution

Equation 2.3 relates the partition coefficient to the elution chromatogram.

$$K = \frac{V_R^o - V_G}{V_L} \qquad 2.3$$

where: V_R^o = corrected retention volume

$$= F. \frac{T_c}{T_a} . \frac{P_o}{P_a} . j . t_R$$

V_G = corrected gas 'hold-up' in the column and associated fittings

$$= j V_m$$

V_L = volume of stationary phase.

As discussed in Section 2.2, the accurate application of this equation, without further modification, is subject to the following restrictions:

(i) The value of the partitiion coefficient must be independent of the level of solute concentration.

(ii) The concentration of the solute in the gas phase must be such that no significant contribution is made to the retention volume (i.e. the 'sorption' effect and 'enthalpic overloading' effects are negligible).

(iii) The gas phase must obey the ideal gas laws, allowing the use of the James and Martin compressibility factor, j.

(iv) No adsorption of the solute onto the surface of the solid support should occur.

The thermodynamic concept of 'infinite dilution' satisfies restrictions (i) and (ii) for all solutes. For elution chromatography at the analytical level, the very small sample sizes used permits the solute concentration within the column to be considered to approximate to this 'ideal' concept. Carrying out the measurements of retention time at near ambient pressures on a column pre-treated to saturate active sites overcomes restrictions (iii) and (iv).

In selecting a suitable chemical system for study, partition coefficients at infinite dilution for 'Arklone' P, 'Genklene' P and dichloromethane were measured on a series of four solvent phases. The experimental procedure was as follows.

2.5 m of 4.8 mm o.d. stainless steel tube was tightly packed with a measured weight of coated solid support. A solvent phase loading of 25% of the total weight on 500 - 355 μm Chromosorb 'P' was used throughout. The coiled column was then connected to the injection head of the Perkin-Elmer chromatograph and the oven temperature raised to 180°C. Three 0.01 cm^3 injections of dimethyl chloro-silane were introduced into the columns to be slowly eluted by the flowing nitrogen stream.

Following this pre-treatment the oven temperature was reduced to 25°C. A soap-bubble meter was used to set the nitrogen flowrate to approximately 0.9 $cm^3\ s^{-1}$ before finally connecting the column to the flame ionisation detector head. The inlet pressure to the column was measured by a mercury manometer. A syringe needle attached to one leg of the manometer permitted sampling of this pressure directly at the sample injection point. Ambient pressure was assumed for the column outlet.

A series of 0.1 mm^3 injections of the respective solutes were introduced and the retention time recorded on a 10-second sweep stopwatch. Reproducibility was better than 1%.

As the flame-ionisation detector does not give an 'air' peak, measurement of the column gas hold-up, V_m, poses a problem. Of the several methods proposed (173 - 176), the most direct was selected. This assumes the retention of methane on the solvent phase to be negligible. Preliminary tests had shown that the standardised value of V_m, calculated from a methane peak, was essentially independent of column temperature. Further, the retention times for the three solutes was generally in excess of 500 s at 25°C while that for methane was approximately 25 s. Any possible error in V_m would, therefore, introduce only a very small error in the partition coefficient.

An example of the calculation of K^{∞} from the experimental data is given as Fig 6.2. A comparative summary of the data used for selection of silicone fluid DC 200/50 as the solvent phase has previously been recorded in Chapter 4.

For the silicone fluid phase, the partition coefficents were determined over the temperature range 20 - 100°C. A plot of log K_i^{∞} versus the reciprocal of absolute temperature gave a straight line (Fig 6.3) in keeping with thermodynamic theory (181). A computed 'least squares' fit to the data gave:

For dichloromethane, $\log_{10} K^{\infty}_{DCM} = 1311.2/\ T\ (K) - 2.3909$

For 'Arklone' P, $\log_{10} K^{\infty}_{AP} = 1363.3/\ T\ (K) - 2.4993$

For 'Genklene' P, $\log_{10} K^{\infty}_{GP} = 1528.3/\ T\ (K) - 2.5976$

The correlation coefficient was in excess of 0.997 for all three solutes.

Fig 6.2 An Example of the Evaluation of the Partition Coefficient at Near Infinite Dilution

Description of Column - 2.5 m of 4.8 mm o.d. stainless steel packed with 11.186 g of 500 - 355 μm Chromosorb 'P' coated with 25% (of total weight) silicone fluid D.C. 200/50

Weight of solvent phase in column (w_L)	2.797 g
Density of solvent phase (ρ_L)	0.97 g cm^{-3}
Column temperature (T_c)	25.0°C = 298.2 K
Ambient temperature (T_a)	24.0°C = 297.2 K
Column inlet pressure (P_{in})	161.9 kN m^{-2}
Column outlet pressure, atmospheric ($P_o = P_a$)	101.9 kN m^{-2}
Flowrate of carrier gas at T_a and P_o (F)	0.880 cm^3 s^{-1}
$j = \frac{3}{2}\left(\frac{(P_{io})^2 - 1}{(P_{io})^3 - 1}\right)$	0.759
Retention time for 'Arklone' P (t_R)	529.3 s
Retention time for methane (t_m)	24.7 s

$$K^{\infty} = \frac{F \cdot \left(\frac{T_c}{T_a}\right) \cdot \left(\frac{P_o}{P_a}\right) \cdot j \cdot (t_R - t_m)}{w_L/\rho_L}$$

$$= 117$$

Figure 6.3 Plot of log K^{∞} versus $^{1}/T$ (K) for Solutes 'Genklene' P, 'Arklone' P and Dichloromethane on the Phase Silicone Fluid DC 200/50

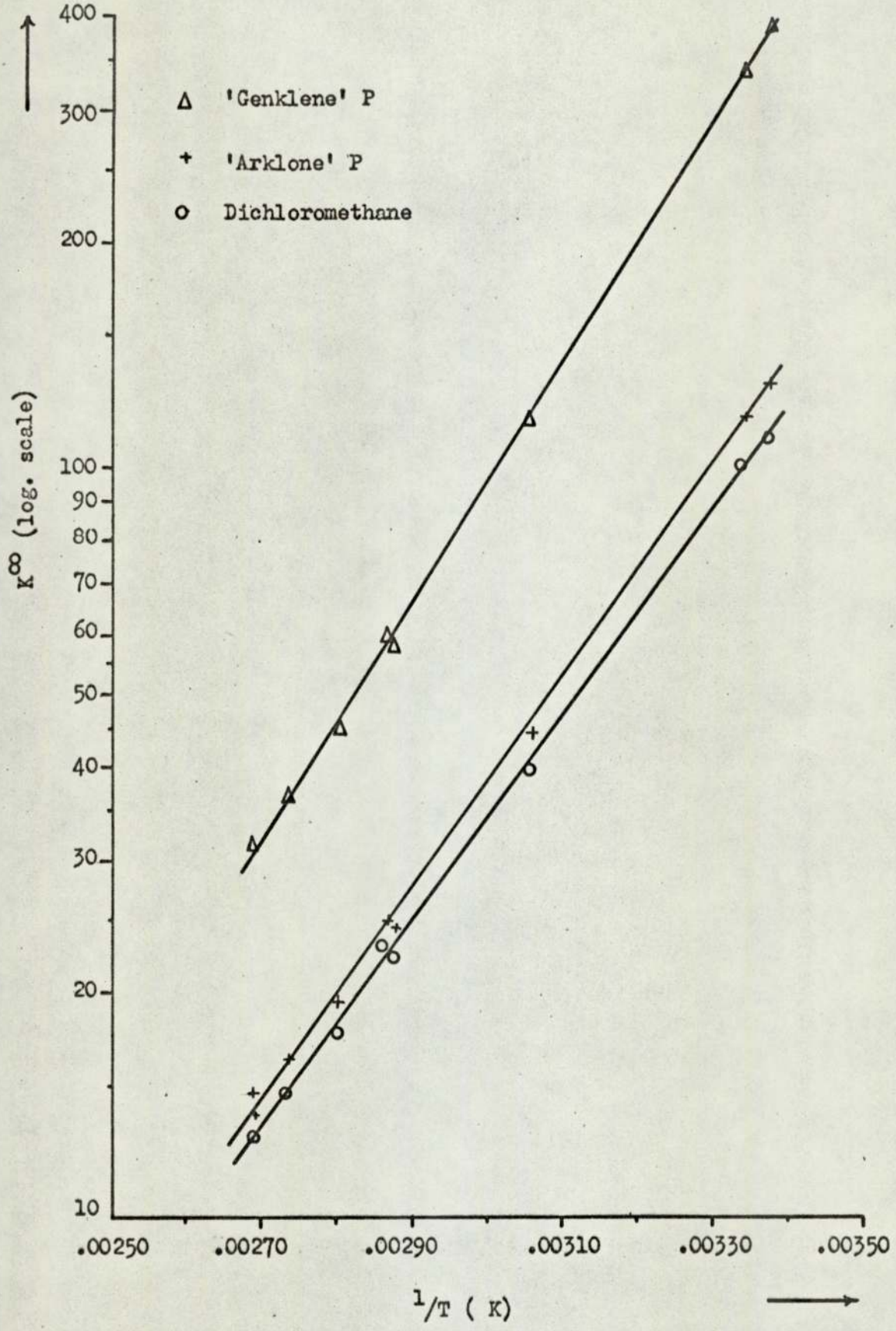

It should be noted that the relationship between K^{∞} and $^{1}/T$ is only exact for the limited temperature range within which no variation in the solvent phase volume occurs. The strength of the fit of the experimental data suggests that the inherent assumption of a negligible volume change was reasonable over the range 20 - 100°C.

6.2.2 At Finite Concentrations

A full expression for the partition coefficient at any solute concentration may be given as

$$K_i = \frac{q_i}{c_i} = \frac{\frac{m_i(L)}{v(L)}}{\frac{m_i(G)}{v(G)}} \qquad 6.17$$

where: $m_{i(L)}$, $m_{i(G)}$ = mass of solute in the liquid solvent phase and gas phase respectively

$v_{(L)}$, $v_{(G)}$ = unit volume of the respective liquid and gas phases.

Now, the mole fraction of in the liquid phase can be written for a single solute as:

$$x_i = \frac{\frac{m_i(L)}{M_i}}{\frac{m_i(L)}{M_i} + \frac{m_L}{M_L}} \qquad 6.18$$

where: m_L = mass of solvent phase per unit volume

M_i, M_L = molecular weight of the solute and solvent respectively.

For a gas obeying the ideal gas laws, the mole fraction, y_i, can be written:

$$y_i = \frac{\frac{m_{i(G)}}{M_i}}{\frac{P.v_{(G)}}{R_g.T}} \qquad 6.19$$

where: P = total pressure

R_g = gas constant

T = absolute temperature

Substituting for $m_{i(L)}$ and $m_{i(G)}$ in equation 6.17 gives

$$K_i = \frac{x_i \cdot R_g \cdot T \cdot \left(\frac{m_{i(L)}}{M_i} + \frac{m_L}{M_L} \right)}{y_i \cdot P \cdot v_{(L)}} \qquad 6.20$$

From Raoult's law for an ideal gas phase

$$\frac{x_i}{y_i.P} = \frac{1}{\gamma_{i(L)}.P_i^o} \qquad 6.21$$

where: $\gamma_{i(L)}$ = activity component for component i

P_i^o = saturated vapour pressure of component i.

Therefore

$$K_i = \frac{R_g \cdot T \cdot \left(\frac{m_{i(L)}}{M_i} + \frac{m_L}{M_L} \right)}{\gamma_{i(L)} \cdot P_i^o \cdot v_{(L)}} \qquad 6.22$$

Equation 6.22 relates the partition coefficient to the moles of a single solute in the liquid phase both explicitly ($\frac{m_{i(L)}}{M_i}$) and implicitly through the concentration dependent activity coefficient. To calculate K_i a correlation between $\gamma_{i(L)}$ and x_i must be known.

Sunal (58) has measured the value of the partition coefficient at a series of finite concentrations for dichloromethane (temperature range 25 - 40°C), 'Arklone' P (temperature range 25 - 40°C) and 'Genklene' P (temperature range 35 - 74°C) on the phase silicone fluid DC 200/50. The experimental values were corrected for the 'sorption' effect. No correction was necessary for enthalpic overloading as the work was performed on a narrow bore column. Activity coefficients calculated from the true K values (i.e. $K^{\infty} + \Delta K$) were correlated with solute mole fraction in the liquid phase through an equation of the Flory-Huggins type.

$$\gamma_{i(L)} = \frac{\tau_i}{\tau_i \cdot x_i + x_L} \exp\left[\frac{x_L \cdot (1 - \tau_i)}{\tau_i \cdot x_i + x_L} + \psi_i \left(\frac{x_L}{\tau_i x_i + x_L}\right)^2\right] \qquad 6.23$$

where: x_L = mole fraction of solvent in the liquid phase.

= $1 - x_i$

τ_i = fitted experimental constant

= 0.008101 for dichloromethane

= 0.0159839 for 'Arklone' P

= 0.0085363 for 'Genklene' P

ψ_i = fitted experimental constant

= 0.9547 for dichloromethane

= 0.437641 for 'Arklone' P

= 0.930414 for 'Genklene' P

For a value of x_i above approximately 0.2 the root mean square deviation from the correlation, for the three solutes, was generally less

than 1%. At this concentration level $\gamma_{i(L)}$ exhibited only a very weak dependence on temperature over the range considered. In fact, the deviation of $\gamma_{i(L)}$ from the correlation with changing column temperature could be included in the above quoted figure for 'Arklone' P and 'Genklene' P. However, as the solute mole fraction was reduced towards infinite dilution the correlation became less satisfactory, the predicted values of $\gamma_{i(L)}$ being lower than those experimentally observed. Further, at infinite dilution, thermodynamic theory gives the relationship

$$\log \gamma_{i(L)} = f\left(\frac{1}{T}\right)$$

for a limited temperature range.

The conclusion to be drawn from Sunal's work is that, at low solute concentrations, a plot of the activity coefficient against solute concentration for a series of temperatures gives a family of curves. The curves converge to the single Flory-Huggins correlation at a value of x_i approximately equal to 0.2 for the chemical systems and temperature range studied. Partition coefficients calculated from values of $\gamma_{i(L)}$ predicted by equation 6.23 will be slightly high at low solute concentrations in the liquid phase.

Fig 6.4 shows the flowchart of a simple BASIC language program which was used to obtain the relationship between the gas phase concentration of solute and the partition coefficient at one degree temperature intervals within the range 19 - 24 ^{o}C. The full program listing is given in Appendix 2.

For each solute $\gamma_{i(L)}$ was calculated for a series of values of x_i in

the range 0 - 0.95. The error introduced by applying equation 6.23 below $x_i = 0.2$ was assumed to be negligible. Substitution of $\gamma_{i(L)}$ into a rearrangement of equation 6.22 gave K_i

$$K_i = \frac{R_g \cdot T}{\gamma_{i(L)} \cdot P_i^o} \cdot \left(\frac{\rho_L}{M_L \cdot x_L} \right) \qquad 6.24$$

where: x_L = the mole fraction of solvent in the liquid phase

$= 1 - x_i$

ρ_L = density of the liquid solvent

$= 0.97 \text{ g cm}^{-3}$

The value of M_L, the average molecular weight of the polymeric liquid solvent, was given by Dow Corning as 7100 g mole^{-1} (182). Values for the saturated vapour pressure were read from Fig 6.5. The source of the data points used to locate the position of the straight line relating $\log_{10} P_i^o$ and $1/T$ (K) was Perry (165).

c_i was finally calculated from

$$c_i = \frac{x_i \cdot \rho_L \cdot M_i}{K_i \cdot x_L \cdot M_L} \qquad 6.25$$

The computed results are presented graphically as Fig 6.6.

A test of the accuracy of the computed partition coefficients at low solute concentrations was given by a comparison of the experimental and computed values of K_i^∞ (Table 6.1). For 'Arklone' P and 'Genklene' P the agreement was satisfactory, the discrepancy between the two values being less than 1% and 2% respectively. A less satisfactory agreement was obtained for dichloromethane. The major source of this error probably lay

in the fitted constants used in the Flory-Huggins equation. It was for the dichloromethane/silicone oil system that Sunals' results exhibited the largest statistical deviation between experimental and predicted values of the activity coefficient.

The assumption of an ideal gas phase in the derivation of equation 6.22 introduces only a very small error provided the column pressure is reasonably close to atmospheric pressure and the gas phase solute concentration is low (59, 61). For the highest concentration level studied by Sunal (0.6×10^{-3} g cm^{-3}) the error was estimated to be about 0.5% (58). However, partition coefficients for 'Arklone' P and dichloromethane have been calculated at concentrations in excess of this value. (Fig 6.6 (a),(b)). K values for these solutes at the upper concentration levels must be subject to an increased error.

Error may also result from extrapolating the correlation for the activity coefficients beyond the experimental temperature range..

Figure 6.4 Flowchart for the Computation of K_i versus C_i at a Series of Temperatures.

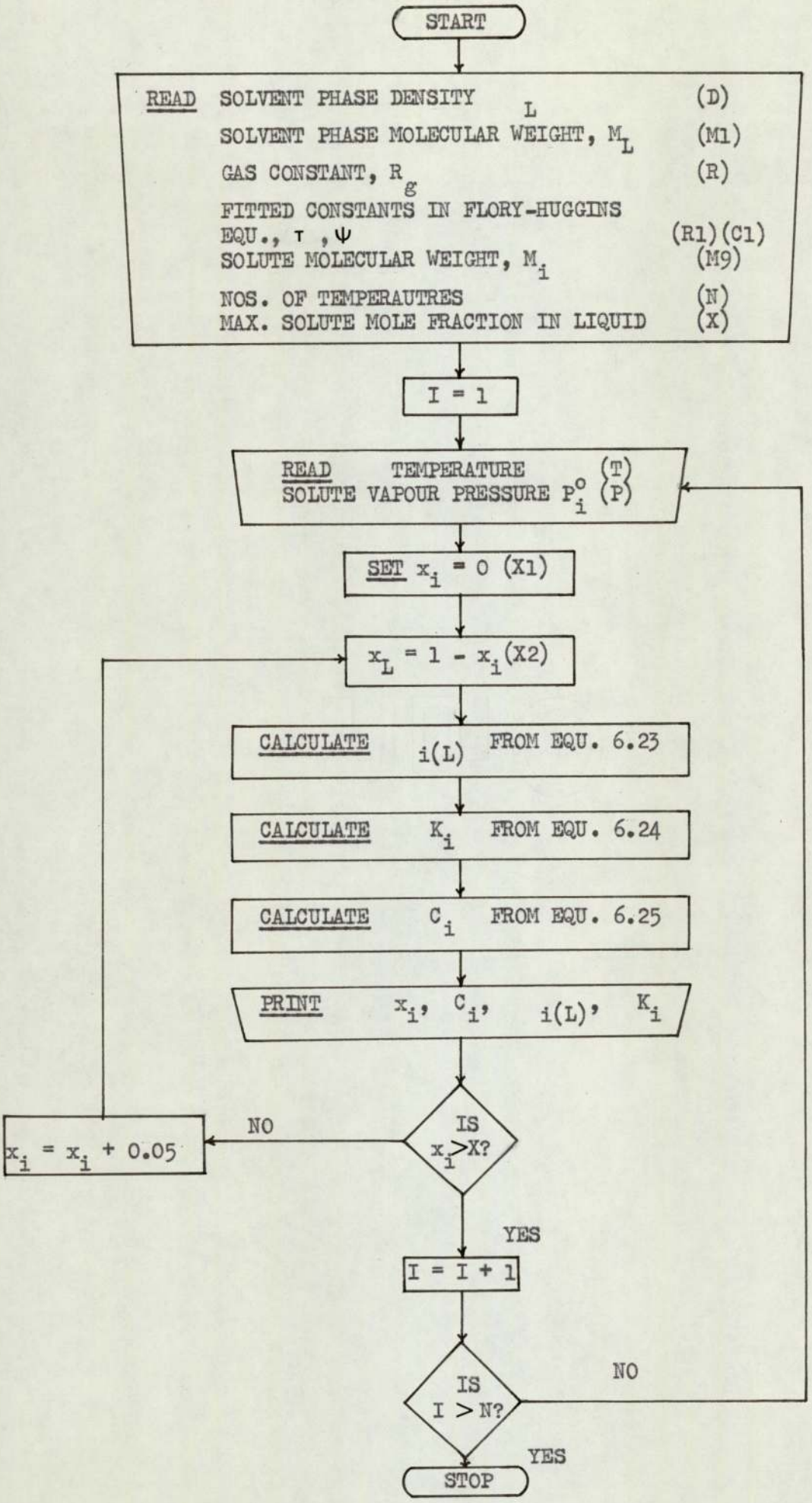

Figure 6.5 Plot of $\log_{10} P_i^o$ versus $^1/T$ (K) for 'Genklene' P 'Arklone' P and Dichloromethane

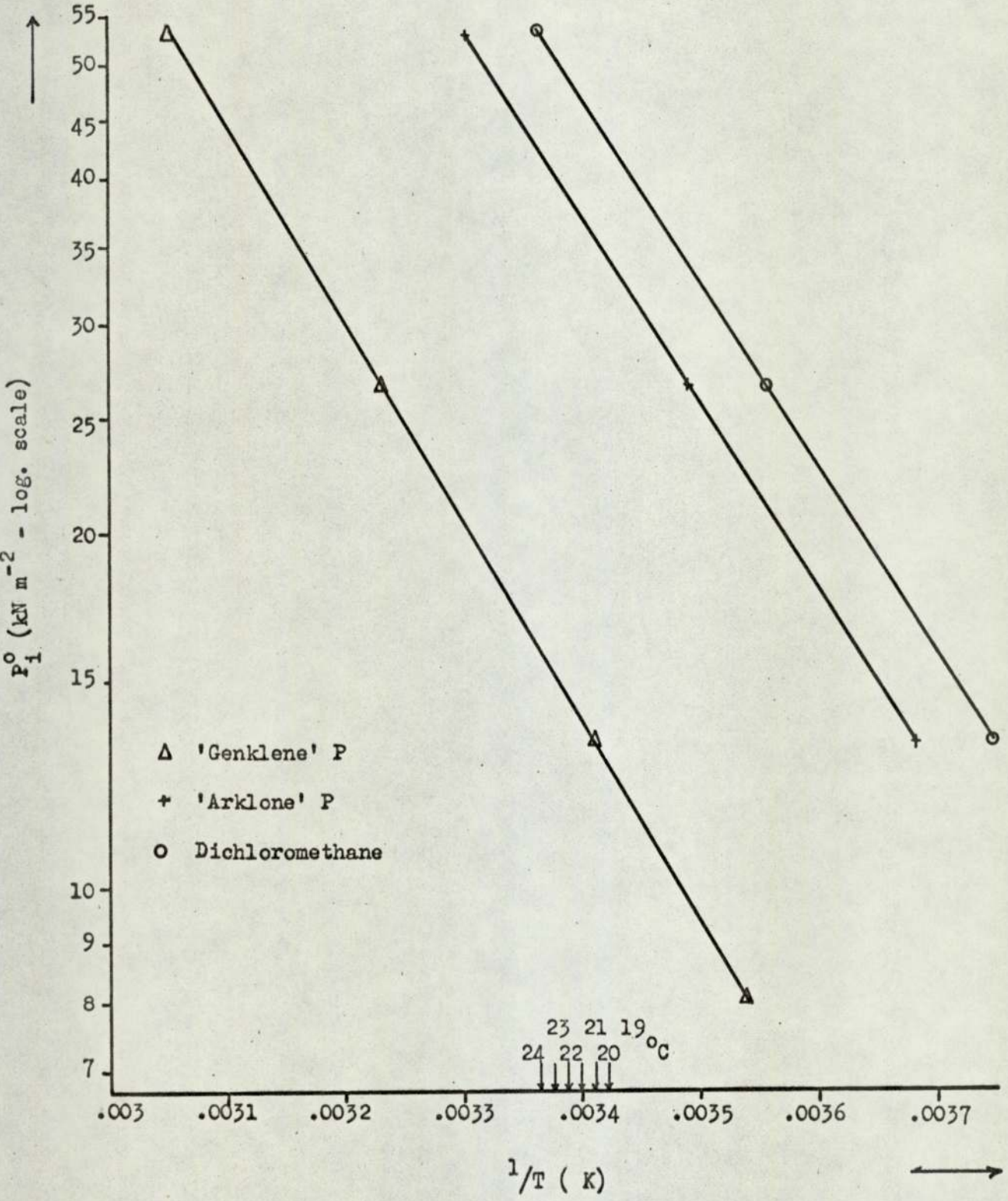

Figure 6.6 Plot of Partition Coefficient (K_i) versus Gas Phase Solute Concentration (σ_i) with Temperature as Third Parameter

a) For Dichloromethane

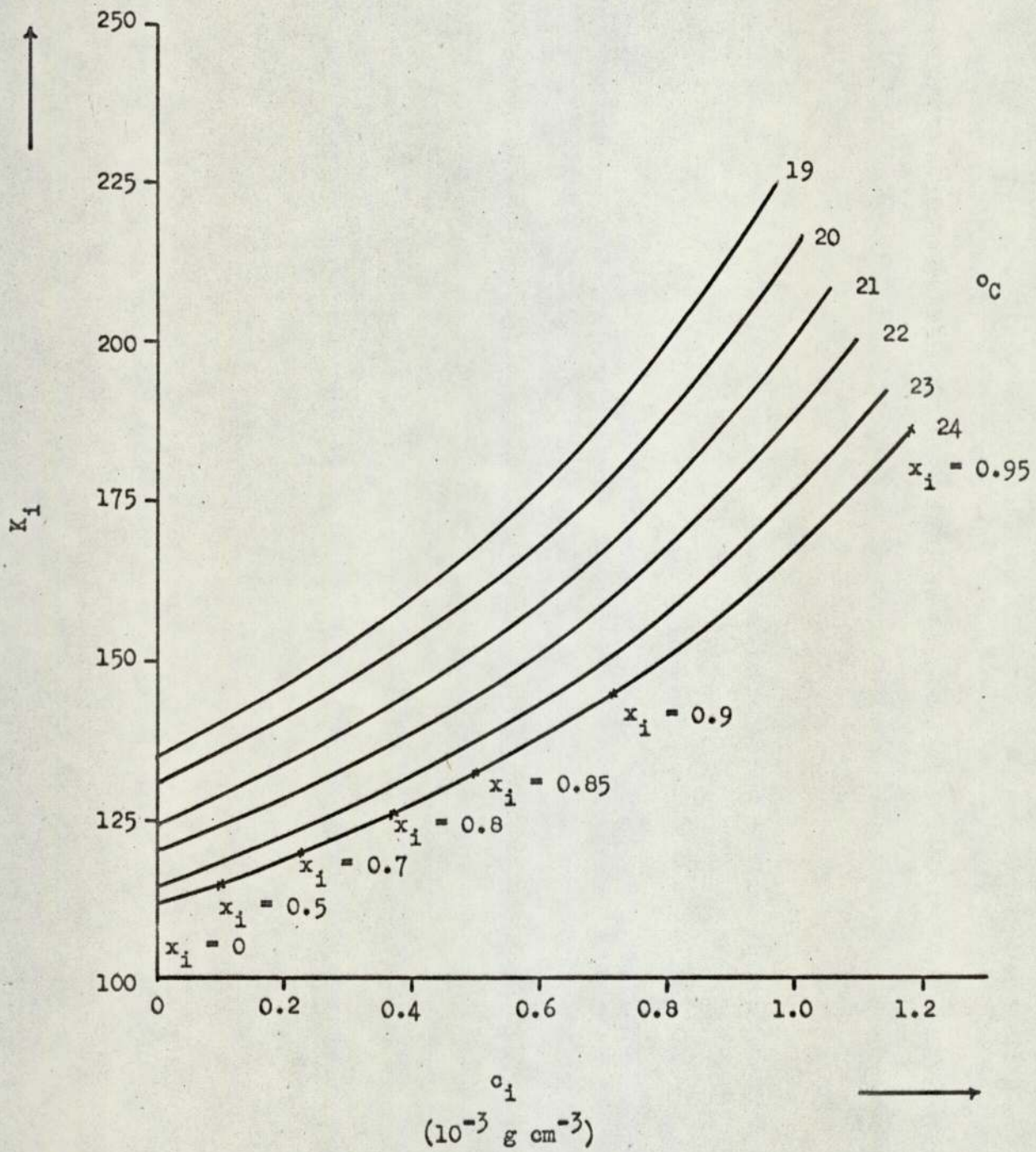

Figure 6.6 (Cont'd.)

b) For 'Arklone' P

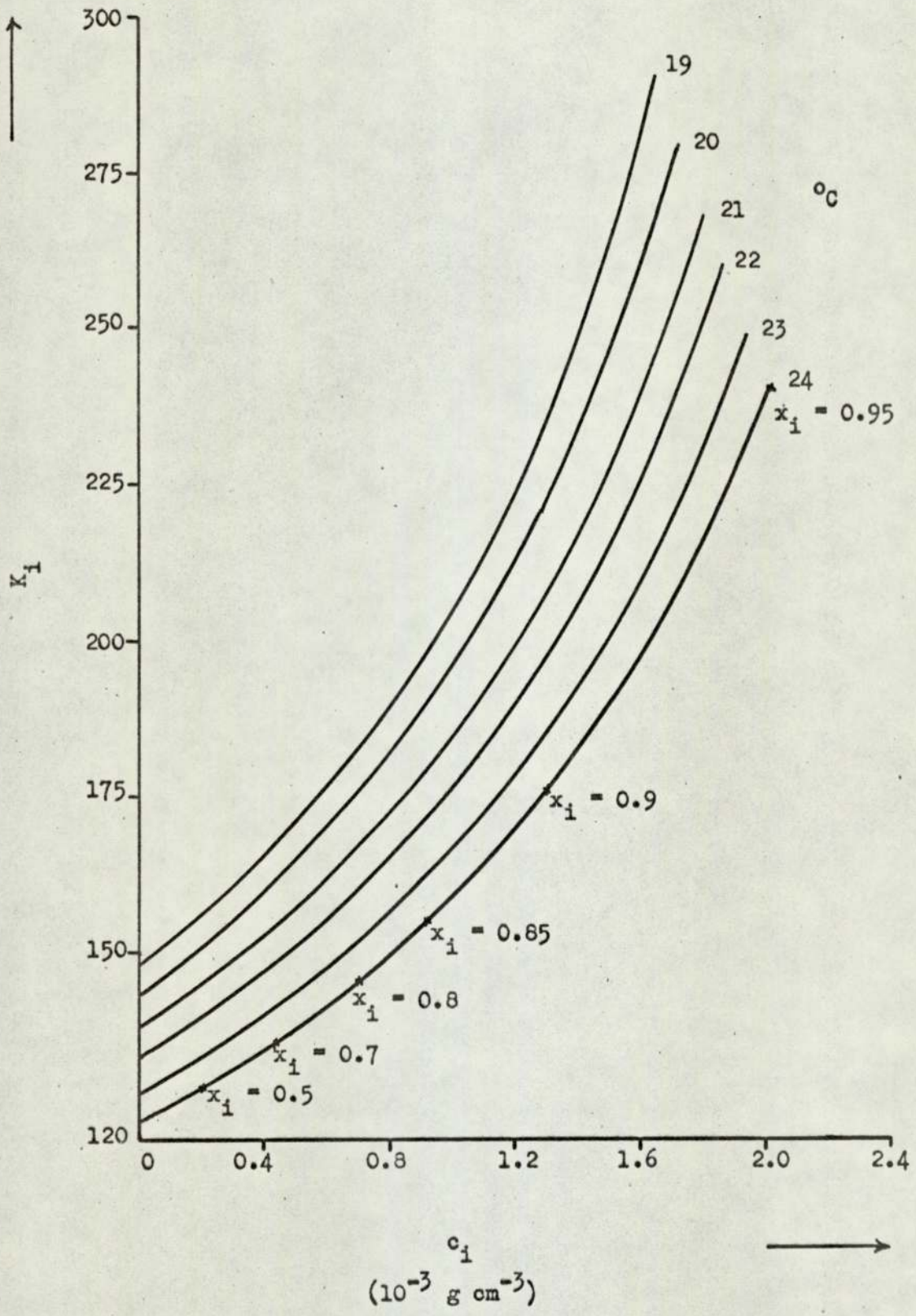

Figure 6.6 (Cont'd.)

c) For 'Genklene' P

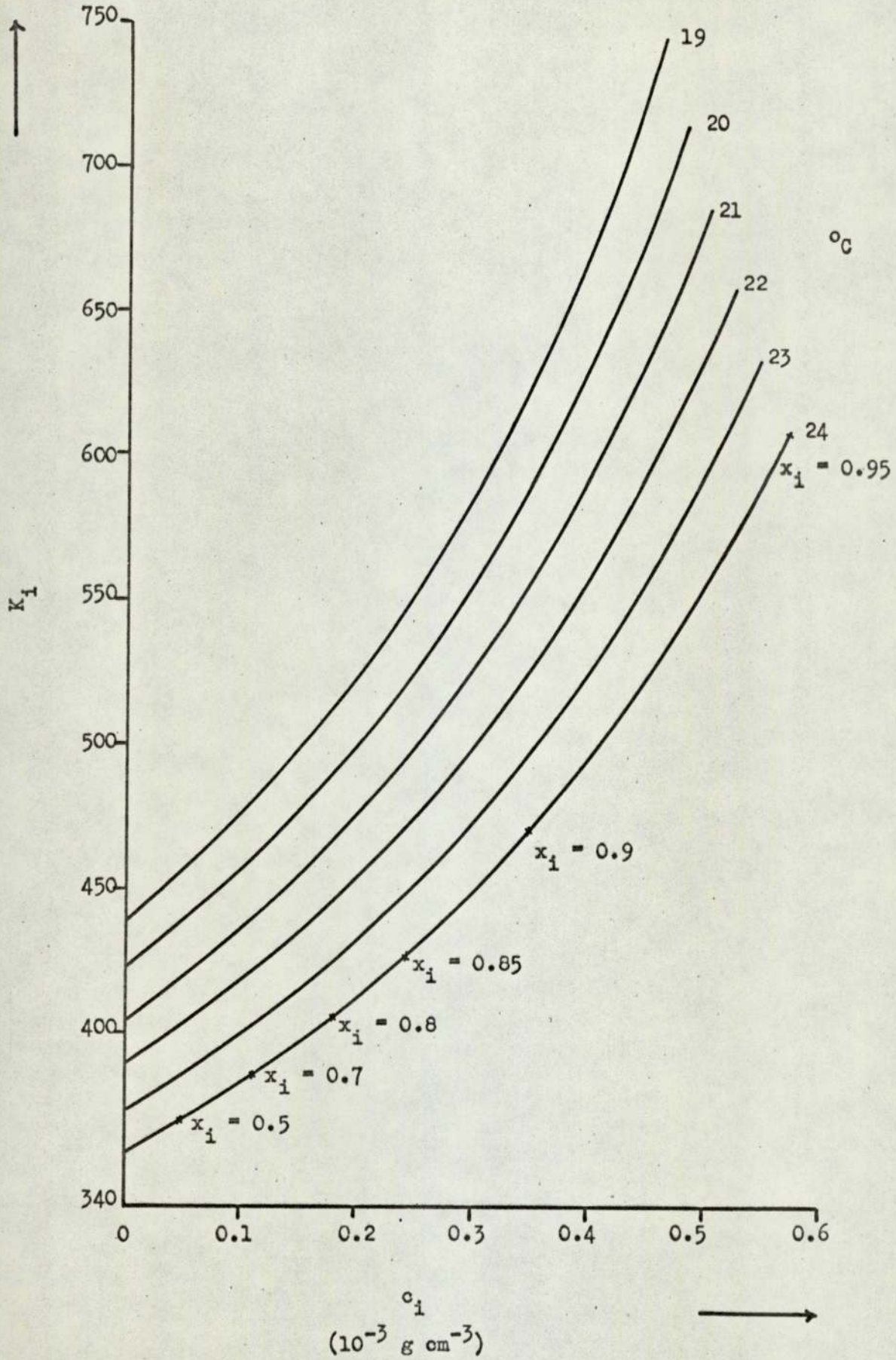

Table 6.1 Comparison of Computed and Experimental Values of K_i^{∞}

Temperature (°C)	Dichloromethane		'Arklone' P		'Genklene' P	
	Comp.	Explt. *	Comp.	Exptl. *	Comp.	Exptl. *
19	135	125	148	147	438	431
20	131	120	143	141	421	411
21	125	116	137	136	404	394
22	120	112	132	131	388	379
23	115	108	127	126	373	366
24	112	105	123	122	358	350

* calculated from fitted straight line relationships between K_i^{∞} and $1/T$

CHAPTER 7

Calibration of the Analytical Chromatographic Detector

Of the several types of analytical chromatographic peak detection systems currently available, the flame ionisation detector (F.I.D.) is to be recommended for quantitative analysis. The response versus eluted component concentration curve for this type of detector has a comparatively long linear range. The recorded area of the elution peak falling within this range is, therefore, directly proportional to the mass of solute injected onto the column.

However, the level of response of an F.I.D. is a function of several variables, namely; design, temperature, hydrogen flowrate, nitrogen flowrate and chemical species. Above a certain level oxygen flowrate has little effect. Hence the detector of the analytical chromatograph was calibrated under specific operating conditions in preparation for analysis during the proposed separation runs.

7.1 Experimental Procedure

Before optimising the hydrogen and oxygen flowrates to the F.I.D., experimentation was required to select the column packing and operating conditions.

There were two conflicting criteria for the analysis. A fast analysis enabled more than one sample to be injected within a sequencing interval of the separation unit. However, for an accurate 'trace analysis', the two peaks for 'Arklone' P and 'Genklene' P had to be sufficiently far apart on elution to permit the peak area for the minor component to be ascertained without contamination from the leading or trailing edge of the major component. The final compromise choice was a 3.04 m, 0.3 cm o.d. annealed stainless steel tube packed with 2.24 gm of 250 - 177 μm particle size (B.S. mesh 60 - 80) 'Universal B' support coated with 10% by weight silicone oil, DC 200/50. Universal B (supplied by Jones Chromatography Ltd., Newport) was chosen as the solid support for its comparatively inert surface properties (183). Treatment, in situ, with D.M.C.S. further reduced 'tailing'. A column temperature of 60° C and nitrogen flowrate of 0.254 $cm^3 s^{-1}$ (corrected to mean column pressure and 0°C) gave a satisfactory complete analysis in approximately 140-seconds with a test mixture of 0.1% 'Genklene' P in 'Arklone' P.

Following the analytical chromatograph instruction manual (184), the oxygen pressure to the flame, as read on the cylinder head regulator, was set at the maximum value consistent with an acceptably stable baseline. This was found to be 275 $kN\ m^{-2}$, giving a large excess delivery of oxygen to the flame.

Finally the hydrogen flowrate was adjusted to give maximum response. A series of constant volume gas injections of fixed concentration were analysed at different hydrogen pressure settings. The resultant peak heights and areas are recorded in Table 7.1. The optimum hydrogen pressure setting of 260 kN m^{-2} was chosen. Once set, the operating conditions for the analytical chromatograph were held constant for all subsequent quantitative analysis.

Gas samples of known composition were prepared for the detector calibration in the simple equipment shown in Fig 7.1. The total volume of the three-necked flask, including the sockets and the line connecting the flask to the manometer, was measured by determining the weight of deaerated water which occupied that space. The carefully cleaned flask was sealed, all joints being greased and held tightly in position by spring clips. Known weights of both 'Arklone' P and 'Genklene' P were then injected into the flask by a previously calibrated 100 mm^3 syringe fitted with a reproducibility adaptor. The samples vaporized causing a small increase in the pressure.

A 1.0 cm^3 'Pressure-Lok' syringe (supplied by Jones Chromatography Ltd., Newport) was used to sample known volumes of gas from the sealed flask. The syringe volume was again calibrated against deaerated water, using grooved 9.6 mm brass rods for reproducibility. (Plate 5). The rods, cut to measured lengths, fitted onto the plunger stem, maintaining a fixed distance between the thumb button and rear lock nut of the barrel. Hence the 'Teflon' plunger was set at a reproducible position in the precision bore glass barrel. The fixed hypodermic needle of the syringe was fitted with

a gas-lock valve ensuring that the gas sample was maintained at the sampling pressure up till the point of injection.

For each injected sample the attenuation of the 'ionisation amplifier' was adjusted to give maximum on-scale peak height. The attenuation, peak height and peak area, as measured by the Kent Chromalog Integrator, were recorded together with the sample volume and pressure in the flask. Each injection of a specific volume was repeated four times. The data are recorded in Appendix 3.

Table 7.1 Flame Ionisation Detector Response as a Function of Hydrogen Cylinder Head Pressure

Description of Column - 3.04 m of 0.3cm o.d. stainless steel tube packed with 2.24 g of 250 - 177 μm 'Universal B' support coated with 10% by weight Silicone oil DC 200/50. D.C.M.S. treated in situ.

Column Operating Conditions - Temperature 59.5°C
Nitrogen flowrate 0.633 cm^3 s^{-1} @ 102 kN m^{-2} and 25°C
Inlet Pressure 310 kN m^{-2}

Oxygen Cylinder Head Pressure - 275 kN m^{-2}

Gas Sample Size - 0.4 cm^3

Concentration of 'Arklone' P in sample - 0.124×10^{-3} g cm^{-3}

Hydrogen cylinder head pressure kN m^{-2}	Peak height adjusted to sensitivity of 1×10^2	Peak area adjusted to sensitivity of 1×10^2
206	7810	11700
241	8740	12400
254	9160	13100
260	9240	13300
275	8800	12400
310	8450	12000
344	8210	11700

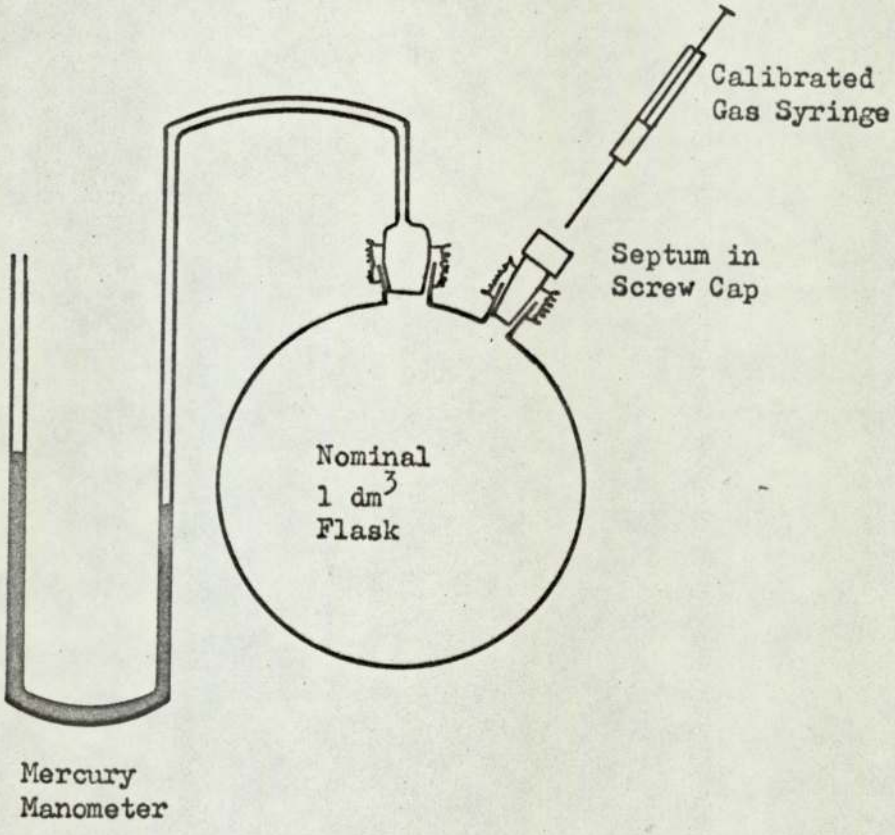

Figure 7.1 Apparatus for Preparing Gas Samples for Calibration of F.I.D.

PLATE 7.1


made in USA
PRESSURE-LOK
0
0.1
0.2
0.3
0.4
0.5
0.6
0.7
0.8
0.9
1.0 CC

7.2 Correlation of Results

The respective weights of the two components in each injection were calculated as shown in Appendix 3. Peak heights and areas were brought to a common base of amplifier attenuation of 1×10^2; e.g. an area or peak height measured at an attenuation of 1×10^4 would be multiplied by a factor of 100. This assumed that the range setting switch for attenuation was linear.

Peak height was then plotted against peak area. (Fig 7.2). The graph gave the expected straight line passing through the origin, the correlation falling off slightly at the higher values as the limit of the linear response was approached. It was therefore decided that the volume of the sample taken from the sequential unit, for quantitative analysis during a separation run, would be chosen to ensure that the response fell within the range covered by these graphs.

The graph of peak area versus weight of sample gave a very good straight line. (Fig 7.3). Using a standard computer library routine the two parameters were correlated by the method of least squares. The slope of the respective straight lines were calculated to be:

'Arklone' P : Weight injected = Peak Area x 0.34338×10^{-8}gm

'Genklene' P : Weight injected = Peak Area x 0.2167×10^{-8}gm

The correlation coefficient for both curves was in excess of 0.999 showing the strength of the 'fit'.

The 'count' rate of the integrator was very slow by more recent standards (185) giving a peak area at 'print out' within a limited range of 0 - 300 integrator units. In addition the response of the detector was found to vary slightly with time. Thus, despite regular recalibration, the accuracy can only be quoted as being generally better than $\pm$ 2% from observations of reproducibility.

Figure 7.2 Plot of Peak Area Versus Peak Height from F.I.D. Response to 'Arklone' P and 'Genklene' P

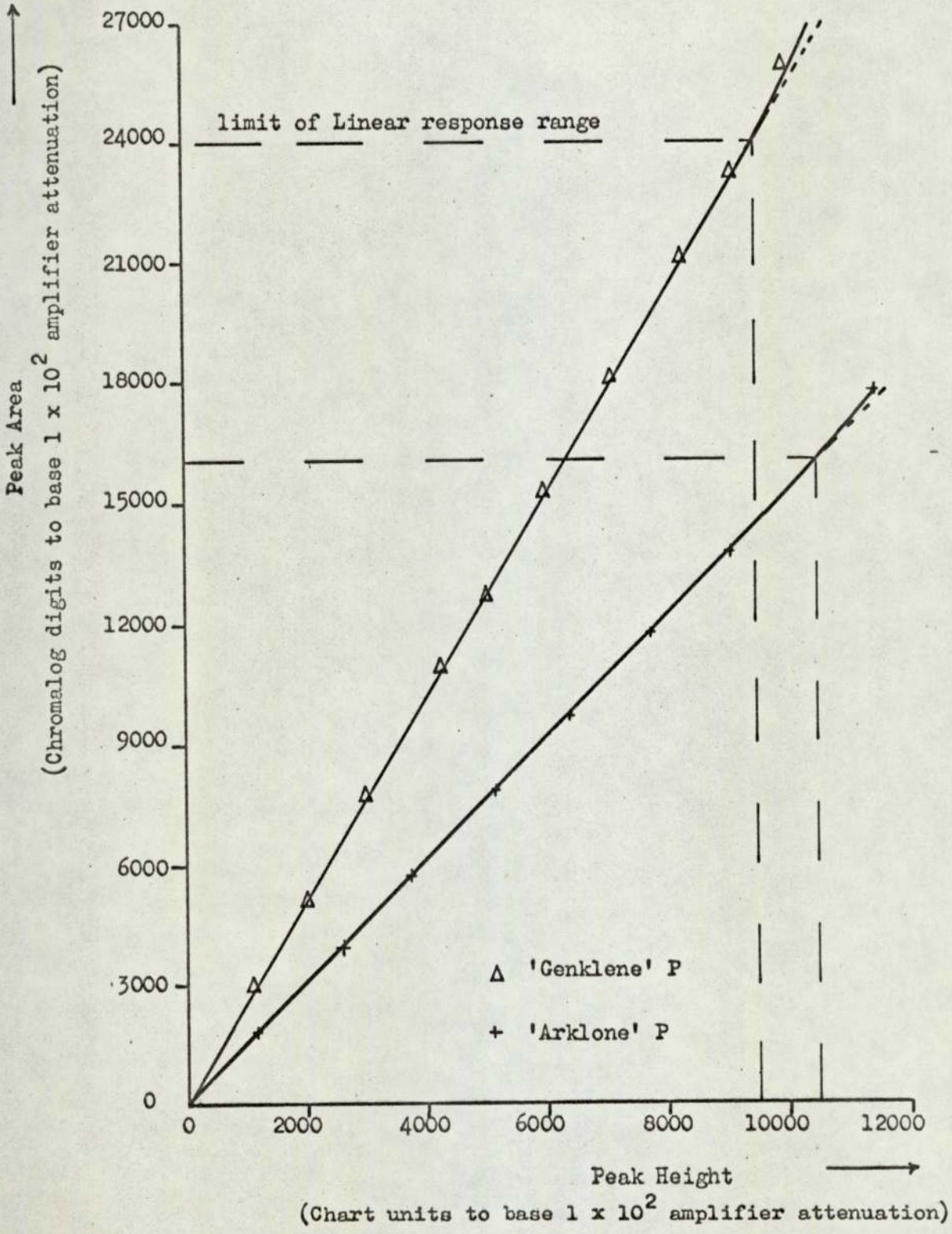

Figure 7.3 Plot of Area Versus Weight of Solute Injected from F.I.D. Response to 'Arklone' P and 'Genklene' P

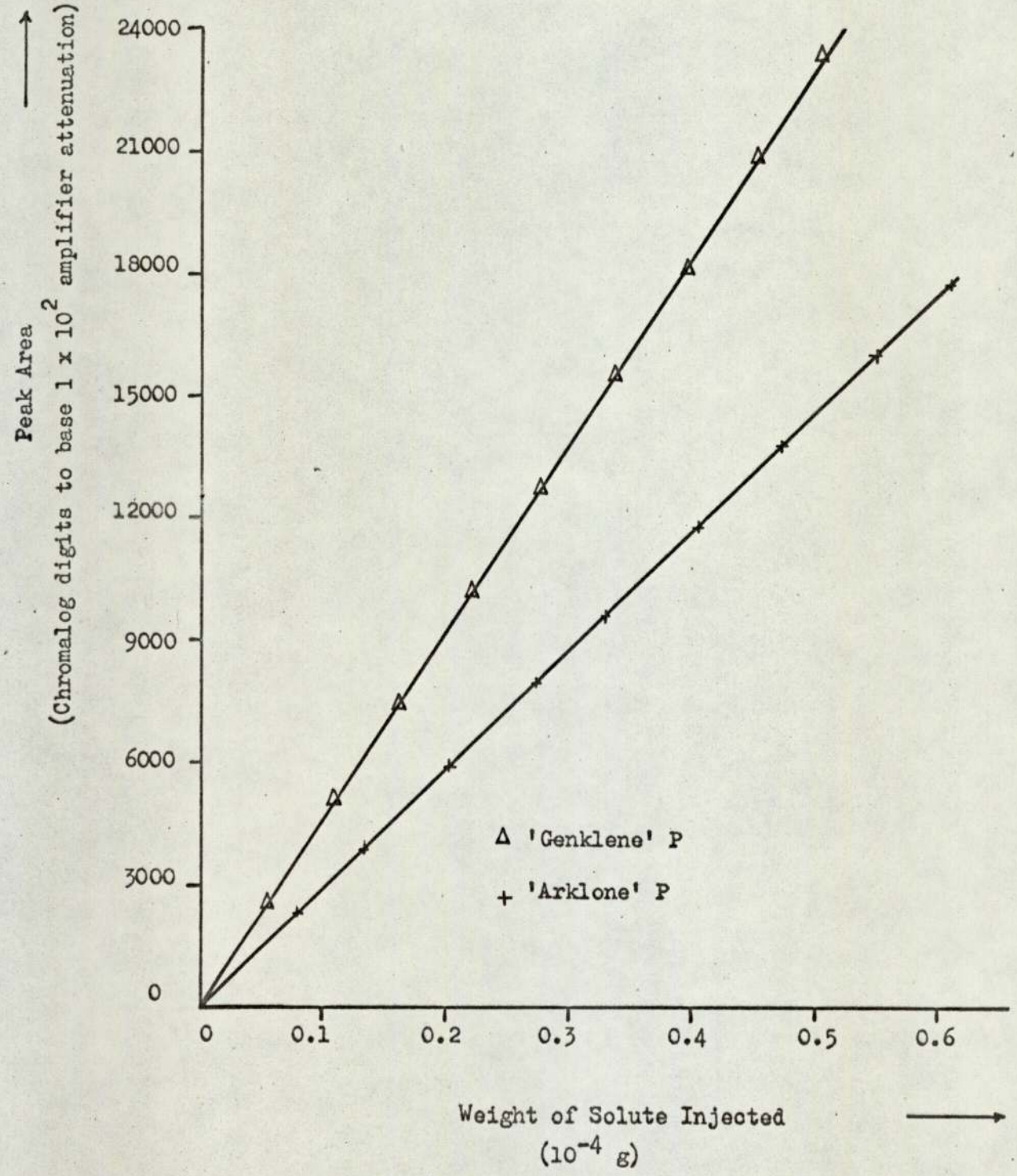

CHAPTER 8

Operation of the Sequential Unit in the Separating Mode

Three objectives were defined for the separation studies:

(i) To investigate the practical viability of the sequential chromatographic process as a separation technique and to establish the mechanical reliability of the design.

(ii) To observe the significance of the factors affecting the separation, as discussed in Section 6.1.

(iii) To provide data for testing the computer model of the unit, reported in Chapter 9.

A systematic study of all the separating process variables would require a very extensive experimental program. The time factor restricted this program to twenty-four experimental runs. Attention was focussed on the solute mixture feedrate, carrier gas rate and sequencing rate.

Throughout the runs performed the feedstock was maintained as an equivolume mixture of 'Arklone' P and 'Genklene' P. The feed inlet was always centrally positioned within the main separating section of eleven columns. Although the purge gas rate was varied to meet the requirement of each run, it was not specifically studied to determine the optimum setting; i.e. the minimum flowrate to ensure complete purging of the isolated bed.

This chapter can be conveniently subdivided into four sections. The first describes experimental procedure and analysis common to all runs. For the second, experimental runs detailing the effect of feedrate on separating performance are discussed. Consideration is then given to the effect of varying the gas to 'apparent' liquid ratio. The chapter is completed by a concluding discussion.

8.1 Experimental Procedure and Analysis

8.1.1 'Start-up'

A formal 'start-up' procedure was established as follows:

(i) A general check and servicing of the various functions of the unit was performed. The taps on the feed system were lightly greased as was the plunger of the reciprocating pump. The packed driers were recharged with regenerated silica gel. Septa were replaced as necessary.

After opening the mains inlet air valve and energising the gas solenoids, two pressure tests for leaks were effected. Initially the timer/sequencing unit was frozen and the carrier and purge gas outlet flow regulators fully closed. Registration of an air flow on the total inlet gas rotameter and/or a discrepancy between the inlet and outlet pressure gauge readings indicated a leak from the system. Small leaks were traced by the use of soap solution.

For the second test the inlet carrier gas pressure regulator was also fully closed. Thus gas pressure was only applied to the isolated column. Any build-up of pressure in the carrier section or in the sealed feed distribution system now indicated a leakage across the seating of a closed solenoid valve. Location of the exact valve was assisted by manually 'skipping' the isolated column round the cycle, depressuring the carrier section between each sequencing step, and observing the effect on the leak rate.

Appropriate action was taken to eliminate any leaks, highlighted by the above procedures, before continuing.

(ii) As a practical guide to the selection of gas and apparent liquid flowrates without a detailed knowledge of the terms in equations 6.15 and 6.16, the approximate inequalities

$$K_{AP}^{\infty} < \frac{G_{m.c.}}{L'} < K_{GP}^{\infty} \qquad 8.1$$

$$\frac{S_{m.c.}}{L'} < K_{GP}^{\infty} \qquad 8.2$$

were used. The subscript m.c. shows that the gas flowrates have been corrected to mean column pressure by the James and Martin compressibility factor.

$$\frac{G_{m.c.}}{L'} = \frac{G_a \times \frac{P_a}{P_o} \times j}{\frac{\text{total volume of solvent in columns}}{\text{time for 1 cycle.}}} \qquad 8.3$$

Having selected a value for L', the sequencing rate (I_s = to one-twelth of the cycle time) was calculated. The variable and pre-set resistance of the clock circuit were then adjusted according to the calibration chart in Appendix 1. An accurate stopwatch was used to check the length of a sequencing interval.

Setting a specific mean column gas flowrate by adjustment of the inlet pressure and outlet flowrate requires a trial and error procedure. To limit this a family of calibration curves was experimentally determined which related both $G_{m.c.}$ and $S_{m.c.}$ to the rotameter height setting for a range of column inlet pressures. (Appendix 1).

Three factors restricted the range of pressure and flow settings available for selection:

(i) The available air pressure after passing through the cleaning, drying and preliminary control stages.

(ii) The need for a pressure drop of at least 50 kN m^{-2} across the outlet flow regulators for effective control.

(iii) A differential pressure in excess of approximately 170 kN m^{-2} could not exist between the carrier gas inlet and purge gas inlet lines or contamination of the product streams, by leakage across their respective solenoid valve systems, may have occurred.

Approximate settings for the purge and carrier gas flowrates, as read from the graphs, were made. A more accurate setting followed the measurement of the respective inlet and outlet column pressures actually on the column. A hypodermic needle was attached to a pressure gauge for this purpose.

(iii) A soap bubble meter was used to adjust the reference and sample bleed streams to the katharometers. The function of the katharometers was to monitor the levels of product concentration in the respective gas exit lines. For Product 1 (carrier gas exit) the bleed flowrates were matched at approximately 0.83 cm^3 s^{-1} while for Product 2 a common flowrate of 12.5 cm^3 s^{-1} was used for the sample and reference streams. These values were recommended by the manufacturers (162, 163).

Switching on the two bridge circuits, the bridge current for Product 1 was adjusted to 80 mA, 100 mA being set for Product 2. Comparatively low bridge current settings were used in view of the use of air as the gas phase

and the high solute concentrations being monitored. The attenuation of the output signals to the two-pen recorder and the associated recorder span were set, from experience, to maintain the maximum pen height below half full-scale deflection. The baseline of the two channels were set at opposite sides of the chart, the direction of pen movement in response to a positive signal also being set in opposition. A clear, independent trace of both product concentration levels was, therefore, recorded.

(iv) The feed pump was started with the feedrate initially being set by reference to the calibration chart (Appendix 1). Fine adjustment of the micrometer setting was made after timing the discharge rate from the side-arm burette.

Pumping of the solute mixture continued to fill the feed distribution network. Air was completely displaced from each line via the open vertical arm of the tee-connection immediately preceding the closed feed solenoid valve. When liquid issued from the 'tee', it was firmly capped with a nut and septum. The highest open point in the feed system was the top of the central distributor. Hence, this was the last point to be sealed.

(v) A pressure gauge was used to observe the pressure in the feed network. As pressure increased with continued pumping the last step in the start-up procedure was hastily performed. The common negative lead for the twelve feed solenoid valves was connected to a socket at the rear of the timer/sequencing unit. Twelve separate live lead connections were then made between the feed valves and the single energised socket terminal rail. The final jack plug was inserted, into the terminal energised at that time, when the monitored liquid feed pressure was approximately equal to the

mid-pressure of the carrier section. This precaution was taken to avoid surging from, or 'blow-back' into, the feed distribution network. The time and point of start-up was noted on the recorder chart.

Two further sets of data were recorded as the run progressed. The column outlet pressure readings changed slightly from the initial values as the concentration of the solutes in the gas phase increased. Therefore, on-column inlet and outlet pressures and the respective rotameter heights were remeasured as the unit sequenced through a complete cycle. Fig 8.1 serves as an example of the recorded data together with the corresponding calculation of the gas to 'apparent' liquid ratio.

At this stage the calibration of the F.I.D. was checked against five differing volume samples of known composition. If necessary, the relationship between peak area and sample mass was recomputed.

8.1.2 Column to Column Concentration Profile Analysis

Being semi-continuous in operation a true steady state was not achieved by the sequential unit. However, a stable state was eventually reached whereby, although the column to column profile changes with time during a sequencing interval, the dynamic profile is reproduced from one interval to another.

The approach to this 'pseudo-steady' state condition was observed on the katharometer traces. From the example given in Fig 8.2 it can be seen that the shape and height of the exiting product concentration level became reasonably consistent. As expected, the fluctuation was greater for the single column exit trace (Product 2) than for the multiple column (Product 1). It should also be noted that, once established, the minor column to column

Fig 8.1 Example of the Data Recorded After Commencement of an Experimental Run and the Subsequent Calculation of $G_{mc/L'}$

Run Title			Time Commenced	T_a	P_a	Measured I_S	Measured Feedrate
Nominal Feedrate	Nominal $G_{mc/L'}$	Nominal I_S					
$cm^3\ hr^{-1}$		S		°C	$kN\ m^{-2}$	S	$cm^3\ hr^{-1}$
300	275	300	08:25	23	101	299	300

Assigned Number of Isolated Column	Main Separating Section			Isolated Section		
	P_{in}	P_o	Rotameter Height	P_{in}	P_o	Rotameter Height
	$kN\ m^{-2}$	$kN\ m^{-2}$	cm	$kN\ m^{-2}$	$kN\ m^{-2}$	cm
1	408	172	21.5	260	228	18.2
2	408	172	21.4	258	228	18.2
3	407	171	21.5	259	228	18.2
4	408	172	21.5	257	229	18.3
5	408	171	21.5	258	228	18.3
6	407	172	21.5	257	227	18.2
7	407	172	21.5	258	227	18.2
8	408	172	21.5	256	229	18.3
9	408	172	21.5	260	228	18.3
10	407	172	21.5	256	226	18.2
11	407	174	21.7	259	224	18.0
12	406	171	21.5	256	228	18.2
Average	407	172	21.5	258	227	18.2
Corresponding values from calibration charts	407	171	G_a 1198 $cm^3\ s^{-1}$	256	226	S_a 2112 $cm^3\ s^{-1}$

Fig 8.1 Cont'd.

Calculation of $G_{m.c}$

$$j = \frac{3}{2} \frac{(P_{io})^2 - 1}{(P_{io})^3 - 1}$$

$$= \frac{3}{2} \frac{\left(\frac{407}{171}\right)^2 - 1}{\left(\frac{407}{171}\right)^3 - 1}$$

$$= 0.545$$

$$G_{m.c} = G_a \times j \times \frac{P_a}{P_o}$$

$$= 1198 \times 0.545 \times \frac{101}{171}$$

$$= \underline{383 \text{ cm}^3 \text{ s}^{-1}}$$

Calculation of L'

Total volume of solvent phase in unit (Table 5.2) = 5090 cm^3

$$L' = \frac{5090}{12.I_S}$$

$$= \frac{5090}{12 \times 299}$$

$$= 1.42 \text{ cm}^3 \text{ s}^{-1}$$

$$\frac{G_{m.c}}{L'} = \frac{383}{1.42}$$

$$= \underline{272}$$

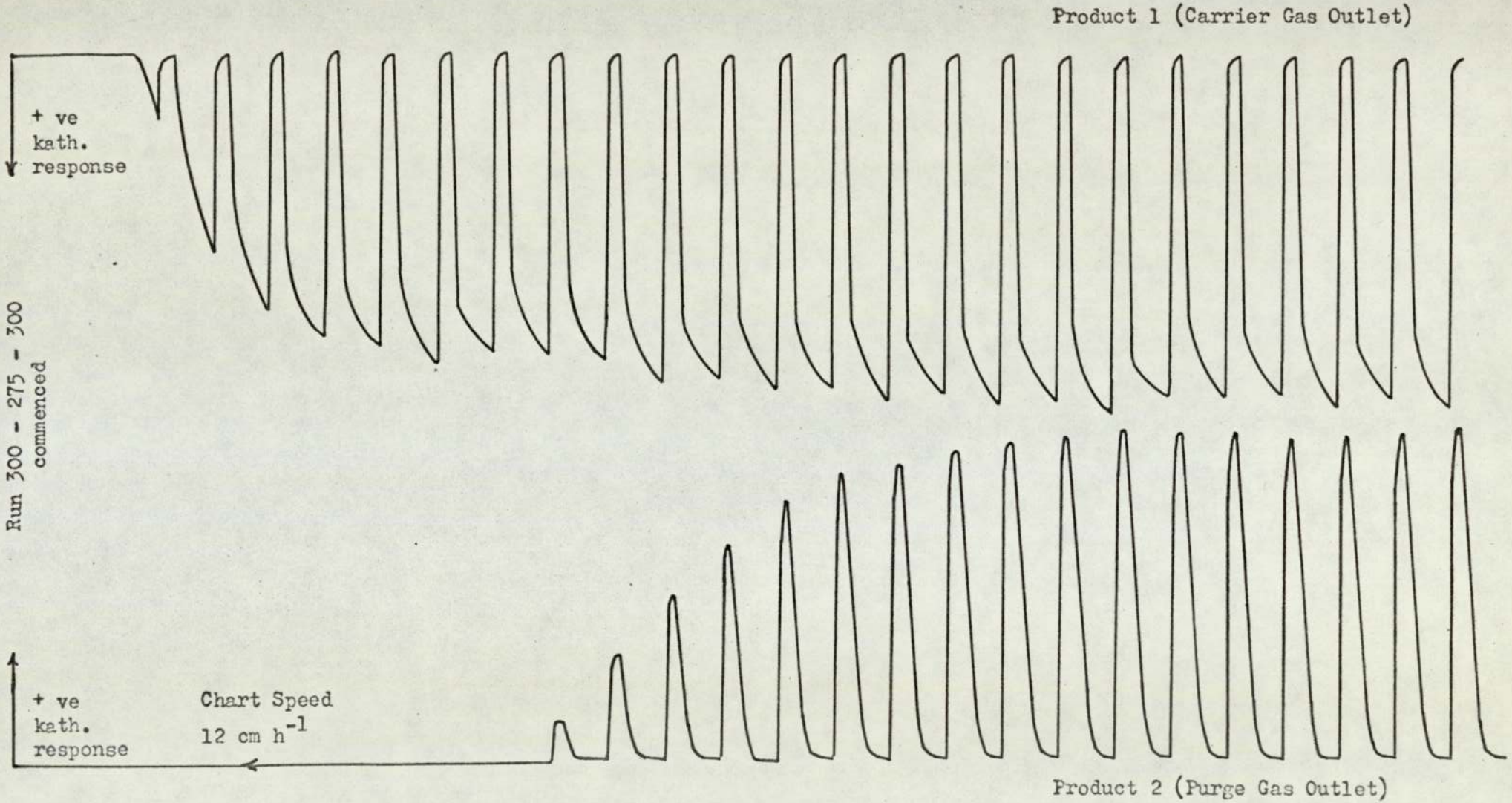

Figure 8.2 An Example of the Recorded Traces of Solute Concentration in the Respective Product Streams

variation was reproduced from one cycle to another.

The symmetry of the sequential unit permitted determination of the on-column concentration profile once the pseudo-steady state condition was achieved. For a complete cycle, a sample was taken from a fixed point in the twelve column arrangement at a set time after each sequencing of the port functions. Suitably plotted, the resultant profile was equivalent to sampling all twelve columns at a single instant.

Throughout this experimental work, all samples were taken from a point 15 cm from the exit of the same column, designated column 2. Using the calibrated 'Pressure-Lok' syringe in conjunction with the grooved spacer rods, at least two accurate volume gas samples at column pressure were quantitatively analysed per sequencing interval. The pressure at the point of sampling was also recorded by a pressure gauge with attached hypodermic needle.

Sampling was continued for at least two cycles, the relative position of column 2 in the cycle being denoted by reference to the position of the isolated column. From the analysis results for the first cycle any necessary adjustments were made to either the volume taken or the amplifier attenuation for a specific sample. The criteria to be met were that the sample volume should be such as to give a response within the linear range of the detector, and the amplifier attenuation be selected to maximise the recorded peak area. Comparison of the results from the two cycles confirmed the achievement of a pseudo-steady state.

Samples were also taken from the product outlet lines to determine their purity. Product 2 was sampled soon after sequencing had occurred

while the Product 1 sample was taken close to the end of a sequencing interval. These points in the sequencing interval correspond to the maximum level of solute concentration in the respective streams. An example of the recorded data is given in Table 8.1a.

A simple BASIC language program was used to compute the concentration of 'Arklone' P and 'Genklene' P in each sample injection (flowchart - Fig 8.3, listing - Appendix 2).

The peak areas, in equivalent chromalog units, were adjusted to the base of amplifier attenuation used for the flame ionisation detector curves; i.e. 1 x 10^2 (Fig 7.4). Hence, the previously computed slope of these curves could be directly applied for the conversion of peak area to solute mass.

Two values of concentration were calculated:

(i) 'On-column', the solute mass being divided by the 'as-sampled' sample volume.

(ii) 'Standardised', the solute mass being divided by the sample volume corrected to atmospheric pressure.

Table 8.1b records the results of the computation for the data given in Table 8.1a.

The sample point, although in a fixed position relative to the column wall, changes its position relative to the input and output functions as the unit sequences round the closed cycle. As the advancing concentration profile is reproduced from one sequencing interval to the next, this profile can be obtained by plotting concentration against the distance of the sample point from the carrier outlet (Product 1) position at a set time after the sequencing action has occurred. For the purpose of plotting the profile the

Table 8.1 Determination of the Column Concentration Profile Around the Sequential Unit

Table 8.1a Recorded Concentration Profile Analysis Data for Run 300 - 275 - 300

(Sampling from point 15 cm from outlet of column 2)

Assigned Number of Isolated Column	Time after sequencing	Calibrated sample volume	Pressure at sample point	Amplifier Attenuation		Recorded Peak Height		Recorded Peak Area	
				AP	GP	AP	GP	AP	GP
	s	cm^3	$kN\ m^{-2}$			chart units		Integrator units	
1	100	0.103	406	1×10^2	50×10^2	4	76	6	189
1	250	0.103	406	1×10^2	50×10^2	2	83	3	209
2	100	0.205	239	1×10^2	10×10^2	3	61	4	148
2	250	0.522	239	1×10^2	1×10^2	4	80	6	212
3	100	0.103	172	50×10^2	1×10^2	49	7	68	18
3	250	0.103	179	50×10^2	1×10^2	59	4	82	10
4	100	0.103	203	50×10^2	1×10^2	61	6	84	15
4	250	0.103	231	50×10^2	1×10^2	65	8	89	20
5	100	0.103	228	50×10^2	1×10^2	67	9	92	22
5	250	0.103	233	50×10^2	1×10^2	70	8	96	22
6	100	0.103	255	50×10^2	1×10^2	83	8	116	21
6	250	0.103	256	50×10^2	1×10^2	86	9	120	21

Table 8.1a Cont'd.

Assigned Number of Isolated Column	Time after sequencing	Calibrated sample volume	Pressure at sample point	Amplifier Attenuation		Recorded Peak Height		Recorded Peak Area	
				AP	GP	AP	GP	AP	GP
	s	cm^3	$kN\ m^{-2}$			chart units		Integrator units	
7	100	0.103	281	50×10^2	1×10^2	88	9	122	21
7	250	0.103	281	50×10^2	1×10^2	96	9	133	22
8	100	0.103	305	1×10^4	20×10^2	69	69	94	163
8	250	0.103	307	1×10^4	50×10^2	71	53	97	123
9	100	0.103	323	1×10^4	50×10^2	59	66	80	155
9	250	0.103	322	5×10^2	1×10^4	44	45	61	106
10	100	0.103	336	1×10^2	1×10^4	41	56	57	135
10	250	0.103	336	1×10^2	1×10^4	24	61	34	144
11	100	0.103	366	1×10^2	50×10^2	21	89	34	221
11	250	0.103	366	1×10^2	50×10^2	21	79	29	194
12	100	0.103	385	1×10^2	50×10^2	16	86	31	222
12	250	0.103	385	1×10^2	50×10^2	10	83	17	211
Product 1	290	0.103	170	50×10^2	1×10^2	49	5	73	11
Product 2	20	0.103	214	1×10^2	50×10^2	4	61	5	160

Table 8.1b Results of the Computation of the Concentration Profile for Run 300 - 275 - 300

(Concentration $< 0.1 \times 10^{-6}$ g cm^{-3} calculated to first significant figure)

Distance of Sample Point From Carrier Gas Outlet	Time after sequencing	Sampled volume corrected to P_{std}	Adjusted Peak Area		Calculated Weight Injected		Concentration at Column Pressure		Standardised Concentration	
			AP	GP	AP	GP	AP	GP	AP	GP
cm	s	cm^3	Base 1 x 10^2		10^{-4} x g	10^{-4} x g	10^{-3} x g cm^{-3}	10^{-3} x g cm^{-3}	10^{-3} x g cm^{-3}	10^{-3} x g cm^{-3}
625	100	0.413	6	9950	0.0002	0.216	0.0002	0.209	0.00005	0.052
625	250	0.413	3	10450	0.0001	0.227	0.0001	0.220	0.00002	0.055
686	100	0.484	4	1480	0.0001	0.032	0.0001	0.016	0.00002	0.055
686	250	1.230	6	212	0.0002	0.005	0.00004	0.0009	0.00002	0.0004
15	100	0.175	3400	18	0.117	0.0004	0.113	0.0004	0.067	0.0002
15	250	0.183	4100	10	0.141	0.0002	0.137	0.0002	0.077	0.0001
76	100	0.207	4200	15	0.144	0.0003	0.140	0.0003	0.070	0.0002
76	250	0.210	4450	20	0.153	0.0004	0.149	0.0004	0.073	0.0002
137	100	0.232	4600	22	0.158	0.0005	0.154	0.0005	0.068	0.0002
137	250	0.237	4800	22	0.165	0.0005	0.160	0.0005	0.070	0.0002
198	100	0.259	5800	21	0.199	0.0005	0.194	0.0004	0.077	0.0002
198	250	0.261	6000	21	0.206	0.0005	0.200	0.0004	0.079	0.0002

Table 8.1b Cont'd.

Distance of Sample Point From Carrier Gas Outlet	Time after sequencing	Sampled volume corrected to P_{std}	Adjusted Peak Area		Calculated Weight Injected		Concentration at Column Pressure		Standardised Concentration	
			AP	GP	AP	GP	AP	GP	AP	GP
cm	s	cm^3	Base 1 x 10^2		10^{-4} x g	10^{-4} x g	10^{-3} x g cm^{-3}	10^{-3} x g cm^{-3}	10^{-3} x g cm^{-3}	10^{-3} x g cm^{-3}
259	100	0.286	6100	21	0.210	0.0005	0.204	0.0004	0.073	0.0002
259	250	0.286	6650	22	0.229	0.0005	0.222	0.0005	0.080	0.0002
320	100	0.311	9400	3260	0.323	0.071	0.314	0.069	0.104	0.023
320	250	0.313	9700	6150	0.333	0.135	0.324	0.129	0.107	0.043
381	100	0.329	8000	7750	0.275	0.168	0.267	0.163	0.083	0.051
381	250	0.329	305	10600	0.011	0.230	0.010	0.223	0.003	0.070
442	100	0.343	57	13500	0.002	0.293	0.002	0.284	0.0006	0.085
442	250	0.343	34	14400	0.001	0.312	0.001	0.303	0.0003	0.091
503	100	0.373	34	11050	0.001	0.240	0.001	0.232	0.0003	0.064
503	250	0.371	29	9700	0.001	0.210	0.001	0.204	0.0003	0.057
564	100	0.392	31	11100	0.0008	0.241	0.0008	0.234	0.0002	0.061
564	250	0.392	17	10550	0.0006	0.229	0.0006	0.222	0.0002	0.058
Product 1	290	0.173	3650	11	0.125	0.0002	Purity > 99.8			
Product 2	20	0.218	5	8000	0.0001	0.173	Purity > 99.9			

Figure 8.3 Flowchart of the Computation of the Solute Concentration Profiles within the Sequential Unit.

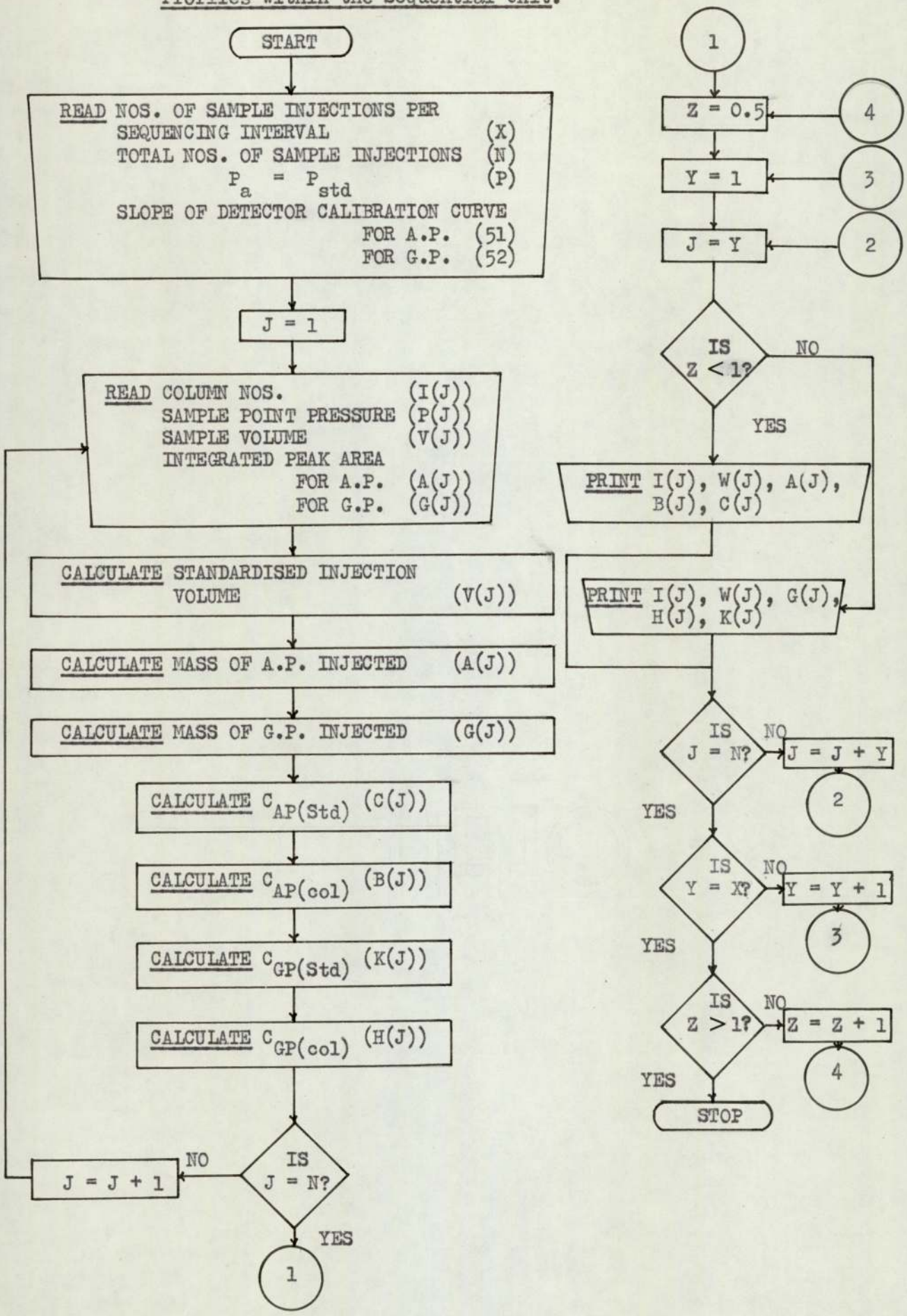

Figure 8.4 Concentration Profile Around Sequential Unit for Run 300 - 275 - 300

a) On-Column Concentration

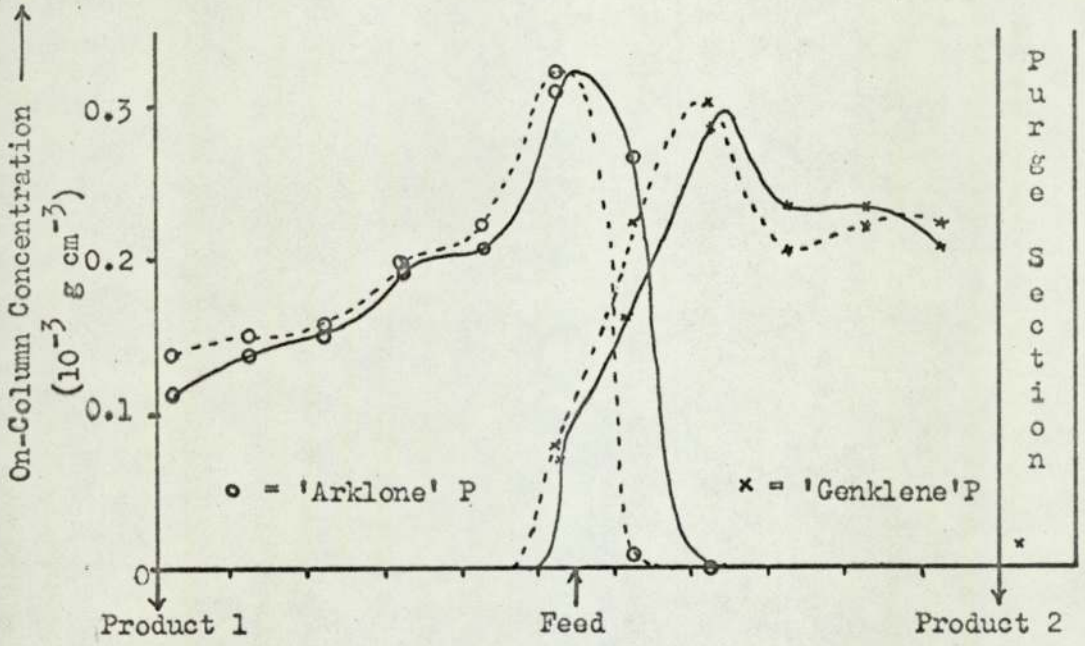

b) Standardised Concentration

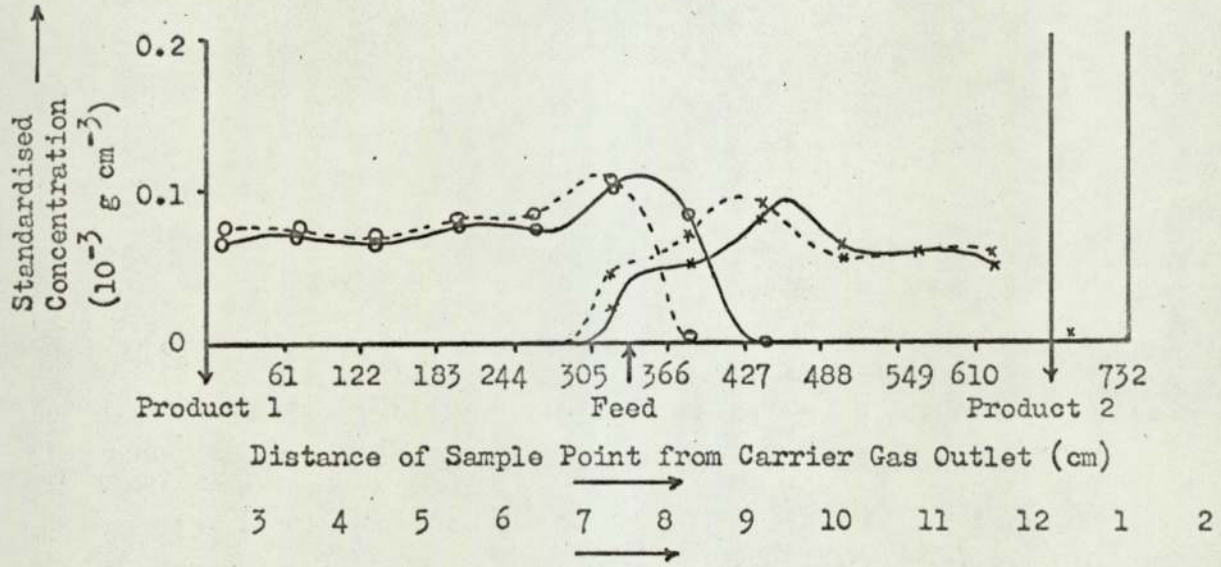

Notes: i) Sampling 15 cm from exit of Column 2

ii) Concentrations less than 0.1×10^{-6} g cm^{-3} not shown

iii) —— 100 s after sequencing, ---- 250 s after sequencing

column to column transfer lines were ignored; i.e. each column length was equivalent to the packed length of 61 cm. Fig 8.4 shows the forms of profile obtained when plotting the data given in Table 8.1b.

Gas phase solute concentration expressed at a standard pressure differs from mole fraction by a constant factor.

From equation 6.17

$$c_{i(std)} = \frac{m_i}{v_{(G)(std)}} = y_i \cdot \frac{M_i}{R_g T} \cdot P_{std} \qquad 8.4$$

where: $c_{i(std)}$ = standardised concentration of solute in the gas phase; i.e. concentration at atmospheric pressure

y_i = solute mole fraction in the gas phase.

$v_{(G)} = v_{(G)} \times \frac{P_{col}}{P_{std}}$

A concentration profile in terms of mole fraction would, therefore, change only the scale of the abscissa axis. However, standardised concentration was selected as the basis for comparison of experimental runs rather than mole fraction to maintain consistency with other chromatographic terms, particularly the partition coefficient.

8.1.3 Measurement of H.E.T.P.

Within a sequencing interval a solute front is 'carried' through the final bed in the main separating section to elute as Product 1. Therefore, the katharometer trace is equivalent to the 'break-through' of the leading edge of a frontal elution system in conventional chromatography. Similarly the trace recorded for Product 2 is akin to the tailing edge in such a system. Fig 8.5 shows the form of the respective traces, recorded at a

Figure 8.5 Form of Product Katharometer Traces

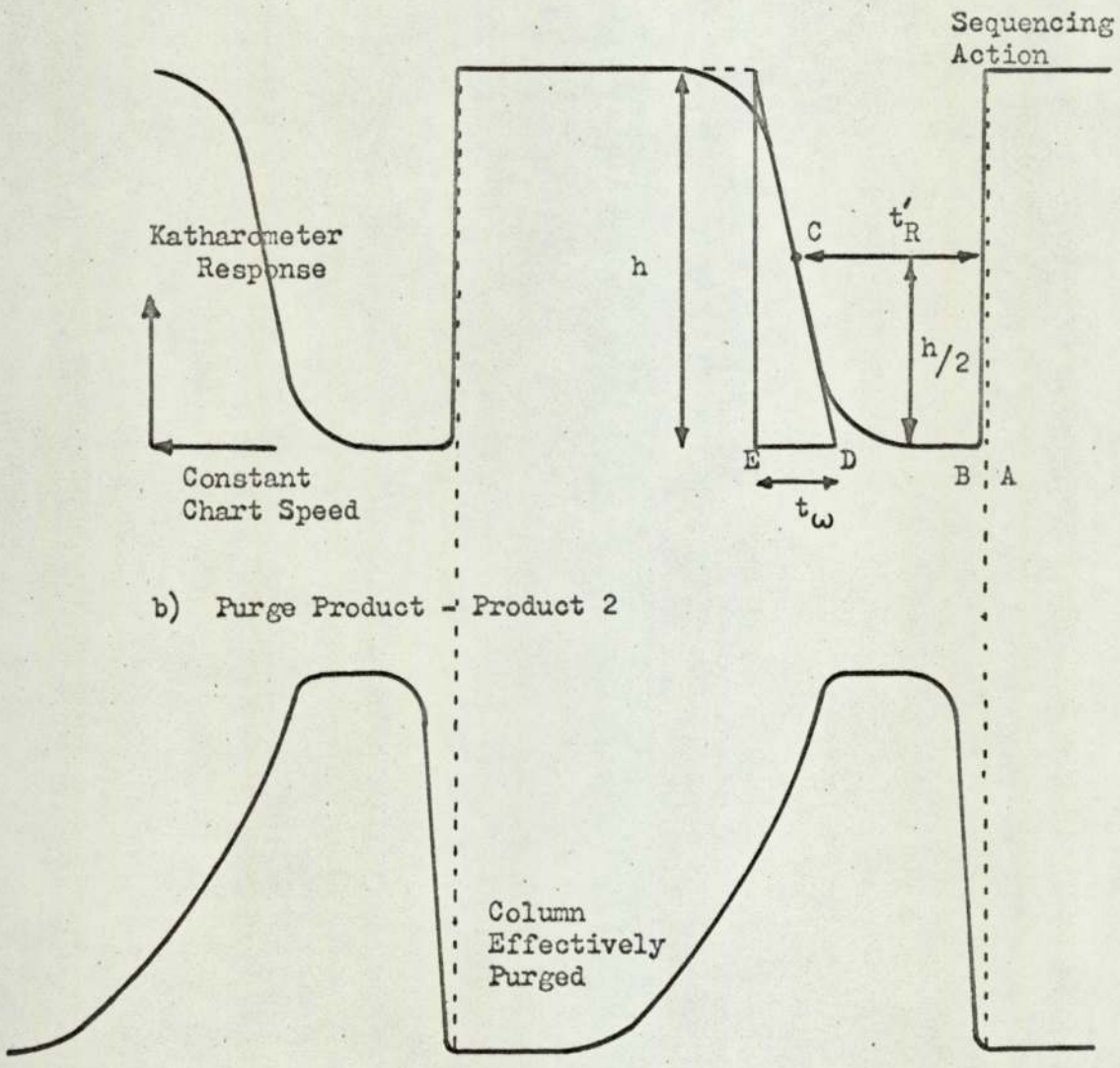

greater chart speed than shown in Fig 8.3.

An estimate of H.E.T.P. was made from the enlarged Product 1 traces once pseudo-steady state was achieved. The graphical technique used was that proposed by Reilley et al (168).

Following Gluekauf (28) these workers analysed the response of a series of ideal equilibrium stages, or theoretical plates, to a step change in inlet solute concentration and found the resultant column outlet trace could be related to the number of plates by

$$N.T.P. = 2\pi \frac{V_R'}{\omega^2} \qquad 8.5$$

where: V_R' = the net retention volume

= the corrected volume of gas having flowed from the commencement of the step impulse to the emergence of the front to half-height.

ω = the volume of the eluted solute front

= the volume between the intersections of the tangent to the curve's inflection point with the axis and plateau line.

Comparing equation 8.1 with the analogous equation for single pulse injection elution chromatography (equation 2.8) gives a value for the standard deviation of $2\pi\omega$. Assuming a constant value for the flowrate, irrespective of the 'sorption' effect, equation 8.1 can be expressed in time units, and hence recorder chart distances (Fig 8.5), as

$$N.T.P. = 2\pi \left(\frac{t_R'}{t_\omega} \right)^2 \qquad 8.6$$

where: $t_R' = t_R - t_m$

t_R = the time from the commencement of the step impulse (in our case, sequencing) to the emergence of the front to half-height (A C in Fig 8.5).

t_m = the contribution to t_R attributable to the non-absorptive lags in the system; i.e. the sum of the extra-column and on-column 'dead volume'.

In practice, t_R was determined by measuring the distance from the peak front half-height to a perpendicular drawn through point where the trace returned to the base line after sequencing (C B). t_ω was determined by measuring the distance D E shown in Fig 8.5. The value of H.E.T.P. was then calculated, for each column, by dividing the individual column length of 61 cm by the value of N.T.P.

8.1.4 Estimation of Experimental Errors

Before presenting and discussing the results obtained from the separation studies, they must first be put into perspective by an estimation of their accuracy.

Having carefully calibrated all the rotameters and pressure gauges, it is to be expected that the individual measurements made by these instruments were accurate. However, in order to estimate the mean carrier and purge gas flowrates, average values were taken from those recorded as the unit sequenced round the cycle.

For the main separating section two sources of fluctuation can be pinpointed; the variation in flow resistance from the differing configuration of 11 packed beds and the changing solute concentration at the column outlet. As the carrier gas flowrate and inlet pressure were

accurately controlled at a constant value, the fluctuation occurred in the measured outlet column pressure. An extreme fluctuation of $\pm$ 5 kN m^{-2} in the value of carrier gas outlet pressure would introduce a possible error into $G_{m.c.}$ of $\pm$ 2%. It should be noted that all readings for the separating section were taken towards the end of the sequencing interval when Product 1 concentration was at a maximum. The recorded values of $G_{m.c.}$, therefore, inherently include an approximate correction for the 'sorption' effect.

The fluctuation in the outlet pressure from the isolated purge section was generally less than that observed for the main section. Consequently the extreme error in $S_{m.c.}$ is expected to be less than 2%.

As the sequencing rate was accurately measured by a 10-second sweep stopwatch, and the packing weight and solvent loading were also accurately determined, the possible error in the calculated value of the apparent liquid rate can be considered negligible.

In Chapter 7 the error in the calibration of the flame ionisation detector was quoted as being generally less than $\pm$ 2%, inclusive of a contribution from the sample volume. For the accuracy of the standardised column to column concentration profile three other factors must be considered; the pressure, the time of sampling and the assumed symmetry of the operating performance of the unit.

The calibrated pressure gauge used to determine the sample point pressure can be assumed to have given a value correct to within $\pm$ 1%. The possible error in the standardised concentration of the withdrawn sample, therefore, becomes $\pm$ 3%.

Having used the accurate stopwatch to time sample withdrawal, the error in the recorded time is expected to be small. However, to quantify the effect of any such error on the concentration profile is not realistic as it is a function of the shape of the curve. If the concentration was changing rapidly at the time of sampling then a significant error could have occurred. Consideration of Fig 8.6a, in which the point values of standardised concentration determined for two successive cycles are plotted, shows the reproducibility to be satisfactory.

The assumption of perfectly matched columns, which forms the basis of the concentration profile analysis technique, is idealistic. As a test of this assumption an experimental run was performed in which two complete profiles were obtained from sample points at opposite sides of the unit. Samples were taken, at the same time after sequencing, from columns of assigned numbers 2 and 8 during two successive cycles. Fig 8.6b shows that, despite the known individual column variation in efficiency, very similar point concentration values were obtained.

This latter reproducibility test was performed at column operating conditions and a solute mixture throughput which represented an easy separation. It was to be expected that when the unit was operated at conditions close to the limits of its separating power then the column to column variation would have greater effect. For this reason sampling was restricted to a single point in column 2 to give a reasonable basis for comparison of the experimental runs.

Of all the experimental measurements, the determination of H.E.T.P. was the most inaccurate. The development of equation 8.1 was based on the

Figure 8.6 Experimental Test of the Reproducibility of the Concentration Profiles

a) Run 300 - 275 - 300, Comparison of Profiles Obtained from Two Successive Sequencing Cycles

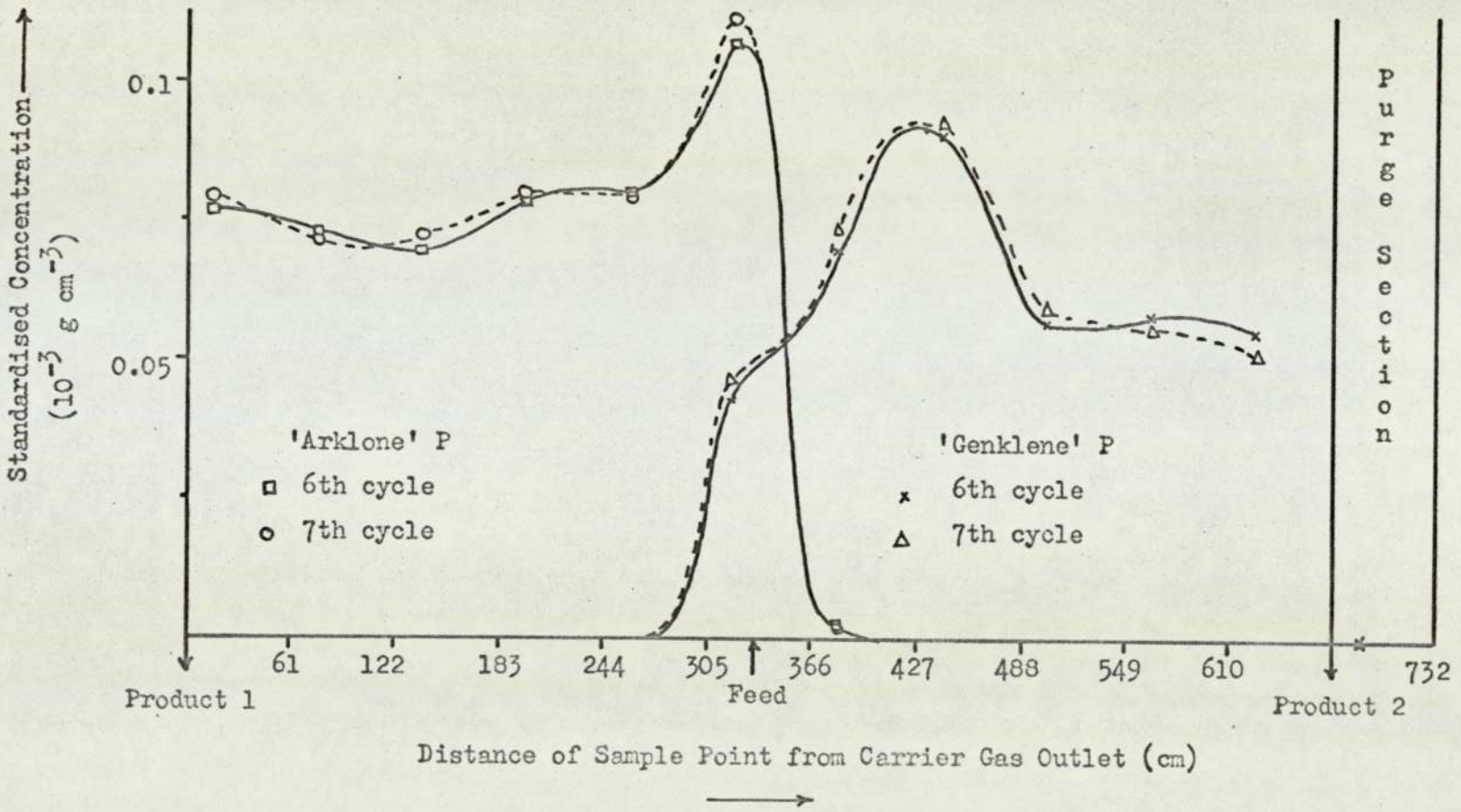

Note: Samples taken from Column 2, 250 s after sequencing action

Figure 8.6 (Cont'd.)

b) Run 300 - 275 - 300, Comparison of Profiles Obtained During Two Successive Cycles from Differing Sample Points

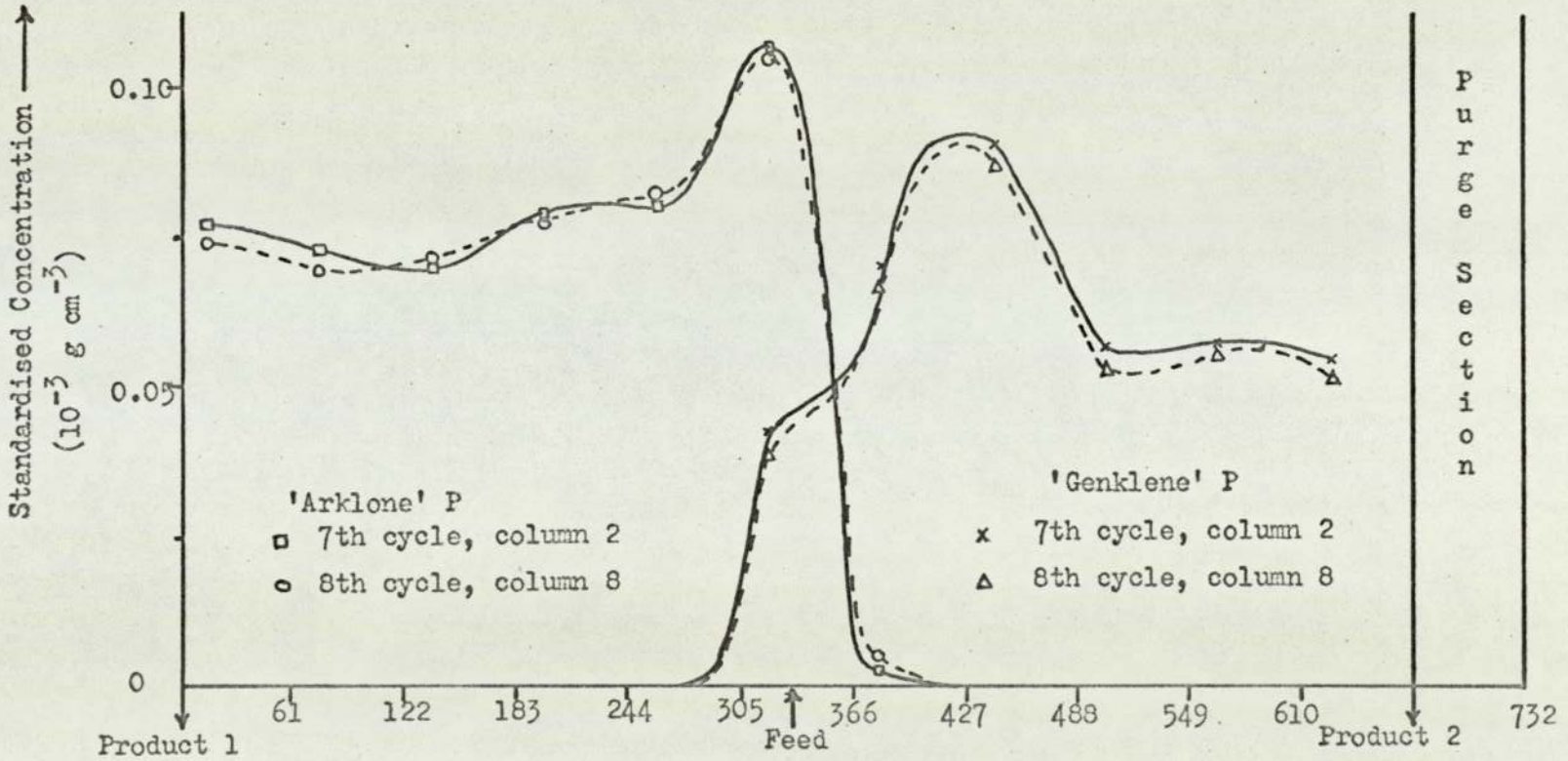

assumption of 'linear-ideal' chromatography. Thus any consideration of the effect of a finite solute concentration on the shape of the front has been ignored.

Considering the actual graphical measurements made, constructing a tangent to the inflection point of the frontal curve is an obvious error source. For a chart speed of 0.5 mm s^{-1}, a front width of, say, 30 s would well have been subject to an incorrect measurement of $\pm$ 2 s. Combining this with a 1 s error in the equivalent 80 s corrected retention time measurement gives a total possible error of approximately $\pm$ 16% in the calculated value of N.T.P. Although an extreme case has been considered the recorded values can be taken only as an estimate of the magnitude of H.E.T.P.

8.2 The Study of Feedrate

8.2.1 Experimental Results

Summaries of the experimental operating conditions and results together with the standardised concentration profiles for the fourteen runs performed are given as Figs 8.7 to 8.10 inclusive*. A complete record of the concentration profile analysis, including both the calculated on-column and standardised concentration values, is to be found in Appendix 4.

Each run is denoted by a combination of three significant variables; the nominal solute mixture feedrate, the nominal ratio of the mean column gas flowrate to apparent liquid phase flowrate ($G_{m.c.}/L'$), and the nominal sequencing rate, I_S.

Throughout these runs the calculated value of $\frac{G_{m.c.}}{L'}$ was maintained within 275 ± 5. This range of values lay approximately midway between the limits defined by the respective partition coefficients of 'Arklone' P ('A' P) and 'Genklene' P ('G' P) at infinite dilution. In keeping with the $\frac{G_{m.c.}}{L'}$ ratio, as the length of the sequencing interval was increased from 300 to 600 s in 100 s steps, $G_{m.c.}$ was proportionately reduced. For each value of $G_{m.c.}$ and L' the feedrate of the equivolume mixture was increased, at 100 $cm^3\ hr^{-1}$ intervals, to a value at which Product 2 purity was lost. It should be emphasised that 'purities' are quoted strictly as a chromatographically measured ratio of the two components, 'Arklone' P and 'Genklene' P.

The mean column purge gas rate, $S_{m.c.}$ was set such that $\frac{S_{m.c.}}{L'}$ was substantially in excess of the partition coefficient at infinite dilution of 'Genklene' P. For several runs, on analysis, the selected value was

*Note: Presented at end of subsection, p 203.

found to be inadequate resulting in a reduction in the purity of Product 1.

The summary of results given for each figure includes values of the respective partition coefficients, $K^{\infty} + \Delta K$, at the maximum recorded on-column solute concentrations. These were read from Figs 6.6b and 6.6c. From the average outlet gas flowrates and inlet and outlet pressures for both the separating and purge sections, $\frac{G_{min}}{L'}$, $\frac{G_{max}}{L'}$ and $\frac{S_{min}}{L'}$ have been calculated.

The individual column values of H.E.T.P. for four runs at constant $G_{m.c.}$ and L' settings are presented for comparison in Table 8.2. Only the average values have been included in the results summaries.

With respect to the standardised concentration profiles, two points should be noted:

(i) All gas samples were taken from a fixed point which was 15 cm from the outlet of assigned column number 2.

(ii) Standardised concentrations which were less than 0.5×10^{-6} g cm^{-3} have not been plotted.

8.2.2 Discussion

For the duration of a sequencing interval the main separating section was equivalent in operation to a conventional frontal elution chromatographic system. Hence, plotting the standardised concentration profiles for at least two sampling times within that interval allowed the progress of the respective components through the columns to be followed.

Under the influence of the flowing carrier gas both components moved towards the Product 1 exit. In keeping with the partition coefficients the rate of advancement of 'Arklone' P was greater than for 'Genklene' P,

Table 8.2.

Comparison of H.E.T.P.'s graphically determined from Product 1 output traces at four feedrates.

Product 1 exiting from column	H.E.T.P. (mm)			
	Run 300 - 275 - 400 Feedrate 300 $cm^3 hr^{-1}$	Run 400 - 275 - 400 Feedrate 400 $cm^3 hr^{-1}$	Run 500 - 275 - 400 Feedrate 500 $cm^3 hr^{-1}$	Run 600 - 275 - 400 Feedrate 600 $cm^3 hr^{-1}$
1	8.4	9.8	10.9	14.2
2	10.9	10.9	11.7	12.4
3	13.7	13.8	16.9	17.9
4	10.2	11.9	13.6	15.3
5	9.1	10.9	11.1	16.5
6	11.1	11.3	11.3	13.0
7	9.4	10.9	11.7	13.3
8	9.4	9.4	10.0	12.4
9	12.0	12.4	13.6	14.9
10	10.2	11.5	12.0	12.4
11	12.0	14.2	15.3	16.5
12	11.5	11.3	12.2	13.0
Average	10.7	11.5	12.5	14.3

the latter being preferentially retained on the solvent phase. This fact also explains why an equivolume mixture of two chemicals of similar density should give gas phase concentrations of substantially different levels.

As the first sampling time after sequencing was never less than 100-seconds it was only for the longer sequencing intervals, nominally 500-seconds and 600-seconds, with their correspondingly lower values of $G_{m.c.}$, that the leading edge of the 'Arklone' P profile was observed in the freshly purged column (Figs 8.9 and 8.10). For the other sequencing intervals, 300-seconds and 400-seconds, the front had already broken through this column, to be recorded by the katharometer as Product 1, before the first sample was withdrawn.

Considering the purge section, an indication of the concentration level of the respective components within this column on isolation was given by the levels in the preceding column for the sampling time closest to the end of a sequencing interval. The success of the purging could be gauged from the concentration of solute(s) remaining within the isolated column at the same time.

A successful separation was defined as one giving high 'purity' (measured component ratio greater than 997:3) for both products, 'Arklone' P as Product 1 and 'Genklene' P as Product 2. In terms of the concentration profiles this demanded that 'Genklene' P should not at any time markedly appear in equivalent column 3 (0 - 61 cm from carrier gas outlet) while 'Arklone' P should not remain in equivalent column 1 (610 - 671 cm) when sequencing occurred.

Throughout these experimental runs the recorded profile for 'Genklene' P

did not extend beyond equivalent column 7 (244 - 305 cm from carrier gas outlet). While the purity of Product 1 was sometimes marred, particularly at the higher solute feedrates, by the incomplete purging of the isolated column, the level of 'Genklene' P was always less than 1%. Therefore, the assumption of a single component front of 'Arklone' P breaking through equivalent column 3 for the H.E.T.P. determination was fully acceptable.

An example of a series of individual column measurements of H.E.T.P. was given in Table 8.2. It can be seen that the relative column to column variation observed for a single 1.0 cm^3 injection (Table 5.3) was considerably reduced when operating the unit in the separating mode. As expected the level of solute concentration plus interaction with other columns was exerting a smoothing influence on the measured values.

Considering the average H.E.T.P. values for all twelve columns in the unit reported in the result summaries (Figs 8.7 to 8.10) two clear trends were indicated:

(i) a gradual increase in the average value of plate height as the solute concentration in the solvent increases with increased throughput. This observation is consistent with the reported effects of concentration on the spreading of the solute band.

(ii) a diminishing of the plate height as the carrier gas flowrate was decreased to maintain the $\frac{G_{m.c.}}{L'}$ ratio constant at the longer sequencing intervals.

A conflict therefore arises when considering this measure of mass transfer efficiency. The lower gas flowrates, while given a velocity closer to the optimum value for minimum H.E.T.P. (see Fig 2.2), result in a higher

solute concentration for a given throughput. As successively higher throughputs were successfully separated at increasing gas flowrates, the effect of concentration on the form of the concentration profiles appeared to be the most important factor for the system under study.

The five standardised concentration profiles from the separation runs carried out at a sequencing interval of 400-seconds clearly show this concentration effect (Figs 8.8a - 8.8e). Feeding solute at a rate of 200 and 300 cm^3 hr^{-1} the comparatively easy separation was largely achieved within a distance of two columns. The remaining length of the separating section served to marginally improve the purity of both products. For 300 cm^3 hr^{-1}, the purge gas rate being set sufficiently high, product purities were in excess of 99.9%. The maximum concentration of 'Genklene' P occurred close to the feed point.

As the feedrate increased, the profiles for both solutes tended toward the isolated column. This observation is consistent with the type II (anti-Langmuir) absorption isotherms; i.e. the preference of the solutes for the solvent phase increases with increasing concentration.

At 500 cm^3 hr^{-1}, the 'Arklone' P profile extended into the fourth column following the feed point (549 - 610 cm from the carrier gas outlet). The maximum 'Genklene' P concentration also occurred in that column. While the purity of Product 1 was still measured in excess of 99.9% 'Arklone' P, Product 2 was now, at best, 99.8% 'Genklene' P.

Increasing the feedrate by a further 100 cm^3 hr^{-1} resulted in a severe reduction in the purity of the purged product, the 'Arklone' P profile covering the entire length of the separating section. The maximum feedrate

in accordance with a successful separation has been exceeded for the operating conditions employed.

It is perhaps more correct to state that the maximum concentration of 'Arklone' P for a successful separation has been exceeded. Comparison with the series of runs performed at a sequencing interval of 300-seconds shows that the reduction of 'Arklone' P concentration gained by the use of an increased carrier gas flowrate enabled resolution of 700 cm^3 hr^{-1} of the solute mixture feed (Figs 8.7a to 8.7d). However, at the slower sequencing rates of 500 and 600-seconds the maximum throughput for a successful separation was reduced below 500 and 400 cm^3 hr^{-1} respectively (Figs 8.9a to 8.9c and 8.10a, 8.10b). Insufficient mains air supply pressure was available to determine the maximum throughput at a shorter sequencing interval than 300-seconds.

Inspection of all the column to column profiles suggests that a limiting standardised 'Arklone' P gas phase concentration of the order of 0.3×10^{-3} g cm^{-3} existed, beyond which successful separation of the feed mixture was unlikely to be achieved with this particular setting for $\frac{G_{m.c.}}{L'}$ Appendix 5 shows that the calculated partial pressure of 'Arklone' P at the highest recorded standardised concentration (from Run 500 - 275 - 500) was considerably lower than the saturated vapour pressure at ambient temperature. Hence, it can be stated, that saturation of the gas phase by this solute did not occur during any experimental run.

Contamination of Product 2 occurred when the 'Arklone' P concentration profile stretched the entire length of the separating section. The summary of results given for each figure shows that the simplified inequality

$$K_{AP} \left(= K_{AP}^{\infty} + \Delta K_{AP} \right) < \frac{G_{min}}{L'} \quad , \qquad 8.7$$

which should ensure preferential movement of 'Arklone' P in the direction of carrier gas flow towards the Product 1 outlet, was satisfied even for unsuccessful runs. Similarly, for the purge section, the criteria

$$\frac{S_{min}}{L'} < K_{GP} \qquad 8.8$$

was met when incomplete regeneration of the isolated column gave contamination of Product 1.

Thus, despite deliberately erring on the conservative side by recording K_{AP} and K_{GP} at the maximum on-column concentration, these two inequalities do not, by themselves, dictate whether successful separation of the solutes will be achieved.

The partition coefficient is specifically related to the migration rate of the mean solute molecule. As solute concentration is increased the spread of the solute band around the mean increases giving a wide variation in the velocity of individual molecules in the direction of gas flow. This variation results from the combined effects of the form of the absorption isotherm, the 'sorption effect' and 'enthalpic overloading'. Resolution of the two solute species becomes more difficult, the length of column required to effect the separation consequently increasing. At the limit all available separation length is being used. Increasing the solute concentration levels beyond this value will, for the operating flowrates used in this series of runs, result in contamination of Product 2 even though equation 8.7 is satisfied. Similarly for the isolated section of fixed length, 'tailing' will result in the need for considerably higher purge gas rates than predicted by equation 8.8.

Fig 8.7. The Study of Feedrate - Sequencing Rate = 300 s

Summary of Experimental Settings

Run Title	T_a	K^{∞}		P_a	Solute mixture Feedrate	I_S	L'	Separating Section				Purge Section			
		'A'P	'G'P					G_a (ave.)	P_{in} (ave.)	P_{out} (ave.)	$G_{m.c.}$ / $\overline{L'}$	S_a (ave.)	P_{in} (ave.)	P_{out} (ave.)	$S_{m.c.}$ / $\overline{L'}$
	°C			kN m^{-2}	cm^3 hr^{-1}	s	cm^3 s^{-1}	cm^3 s^{-1}	kN m^{-2}	kN m^{-2}		cm^3 s^{-1}	kN m^{-2}	kN m^{-2}	
300 - 275 - 300	23	126	366	101	300	299	1.42	1198	407	171	272	2112	256	226	616
500 - 275 - 300	23	126	366	102	488	298	1.42	1197	408	182	277	2133	257	227	629
600 - 275 - 300	21	136	394	101	600	300	1.41	1193	407	178	278	2502	253	214	765
700 - 275 - 300	21	136	394	100	698	299	1.42	1198	404	169	280	2975	269	224	856

Summary of Results

Run Title	$K^{\infty} + \Delta K$ (max.)		Separating Section		Purge Section	H.E.T.P. (ave.)	Concentration Profile Analysis				
	'A'P	'G'P	G_{min} / $\overline{L'}$	G_{max} / $\overline{L'}$	S_{min} / $\overline{L'}$		Figure	Time to recorded analysis	Product Purities 1('A'P)	Product Purities 2('G'P)	Comments
						mm		hr	%	%	
300 - 275 - 300	137	476	209	497	586	12.9	8.7a	6.25	>99.8	>99.9	Purging incomplete - contamination of Product 1.
500 - 275 - 300	146	490	210	472	595	13.8	8.7b	7.75	>99.7	>99.7	Purging incomplete - contamination of Product 1.
600 - 275 - 300	169	618	210	477	704	15.7	8.7c	5.75	>99.6	>99.7	Purging incomplete - contamination of Product 1.
700 - 275 - 300	173	700	209	499	795	18.9	8.7d	5.5	>99	>99.8	Purging incomplete - severe contamination of Product 1.

Figure 8.7a Standardised Concentration Profile for Run 300 - 275 - 300

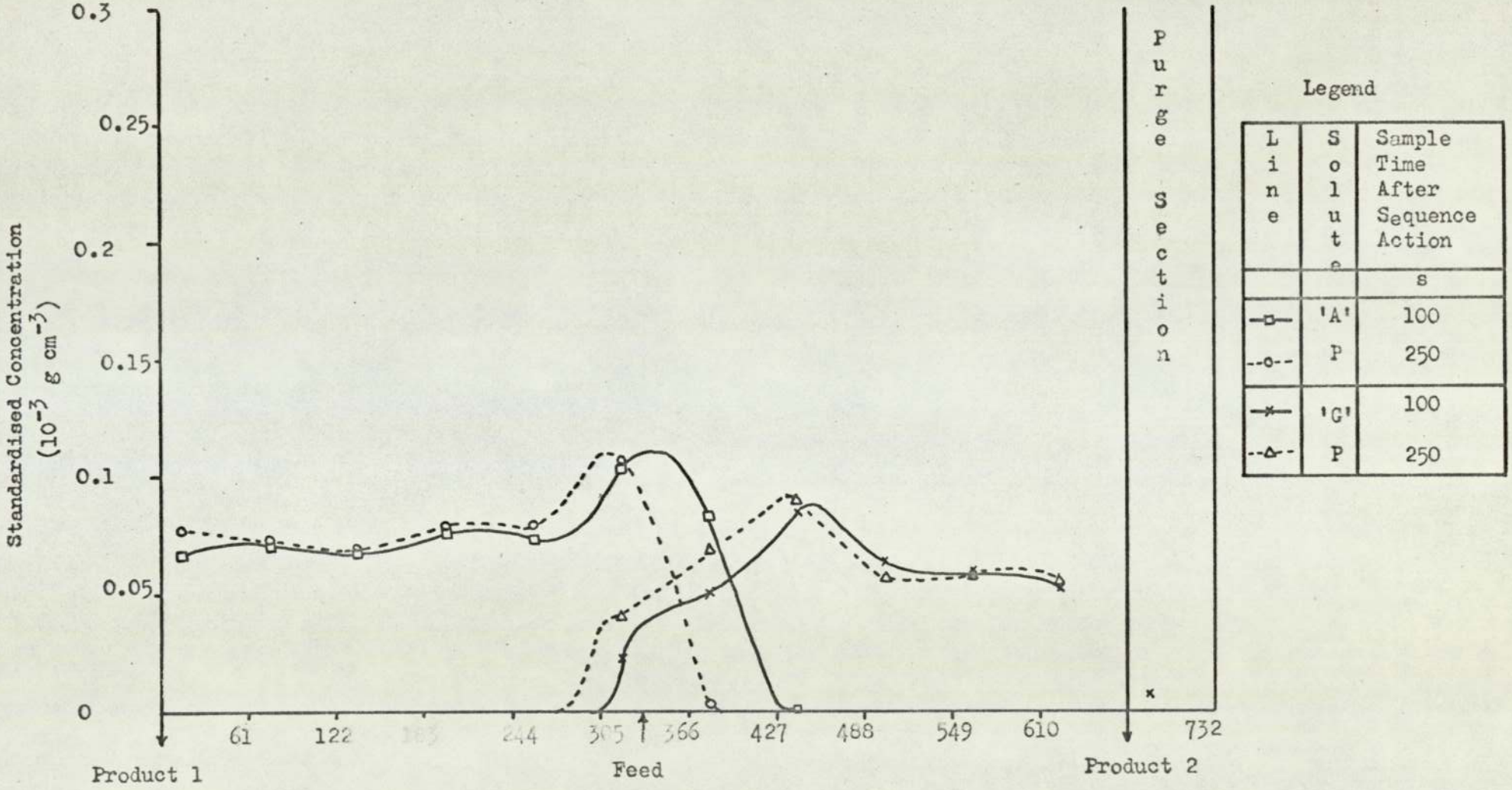

Figure 8.7b Standardised Concentration Profile for Run 500 - 275 - 300

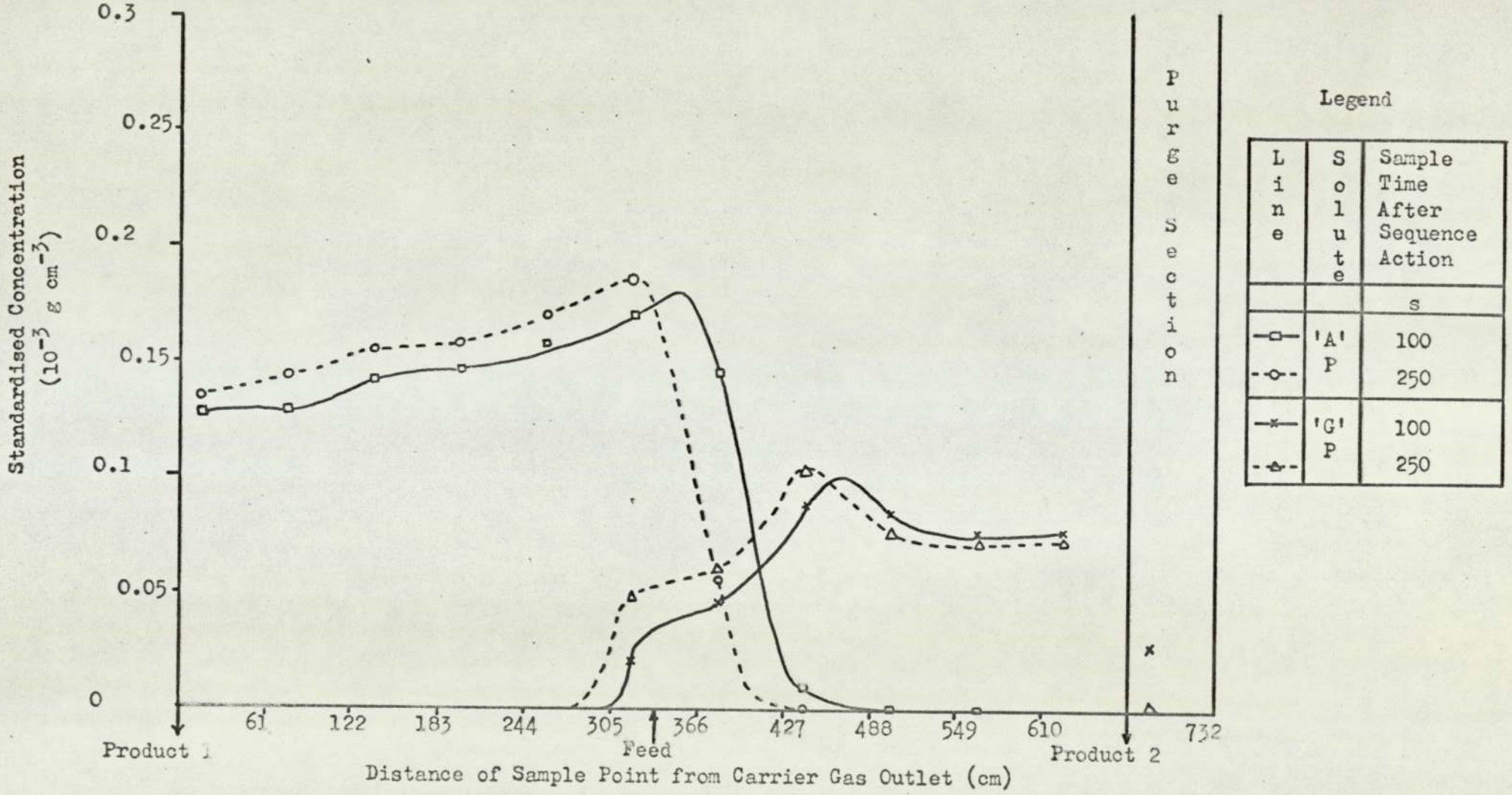

Legend

Line	Solute	Sample Time After Sequence Action
		s
—□—	'A' P	100
- -○- -		250
—×—	'G' P	100
- -△- -		250

Figure 8.7c Standardised Concentration Profile for Run 600 - 275 - 300

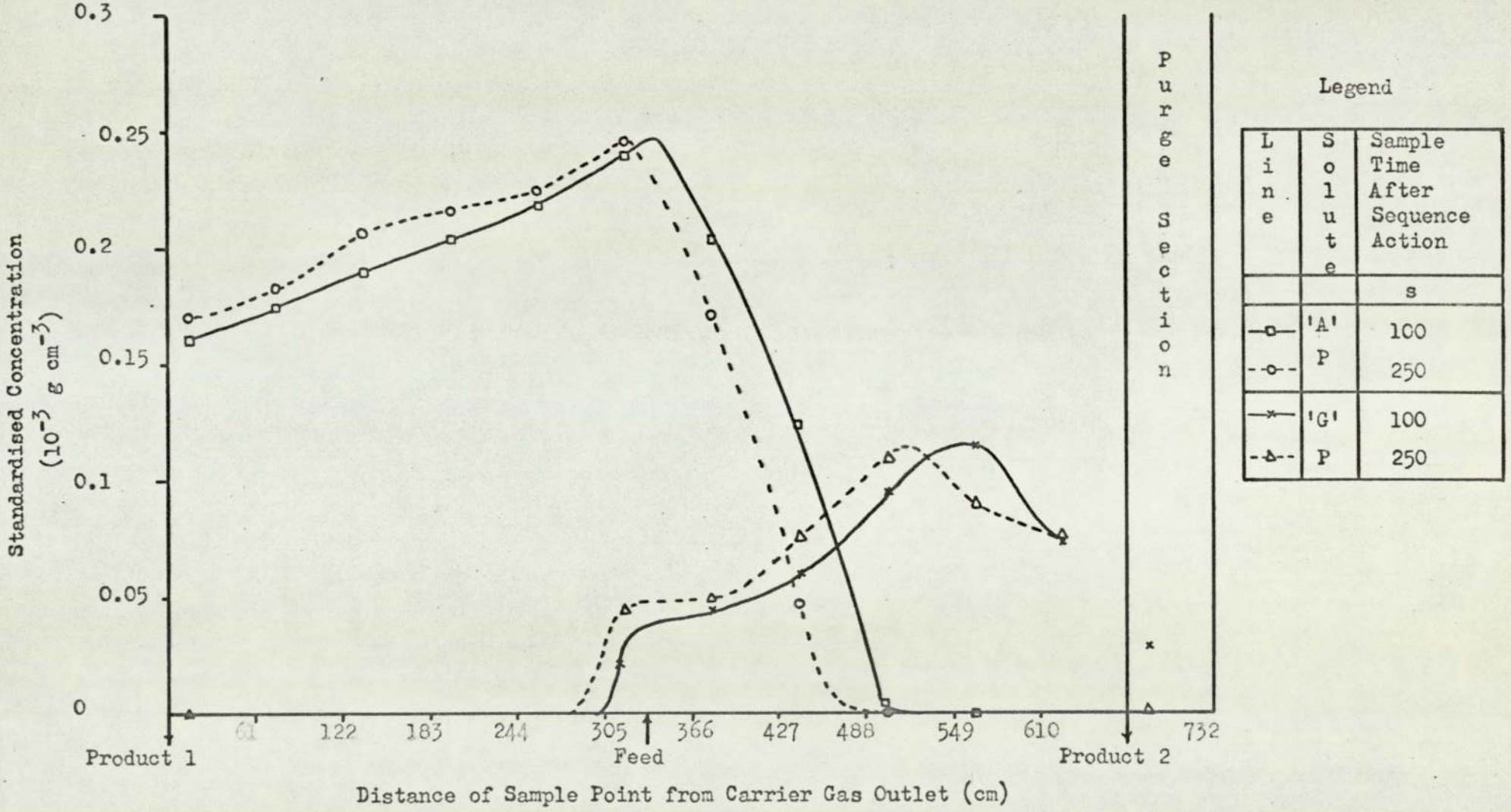

Figure 8.7d Standardised Concentration Profile for Run 700 - 275 - 300

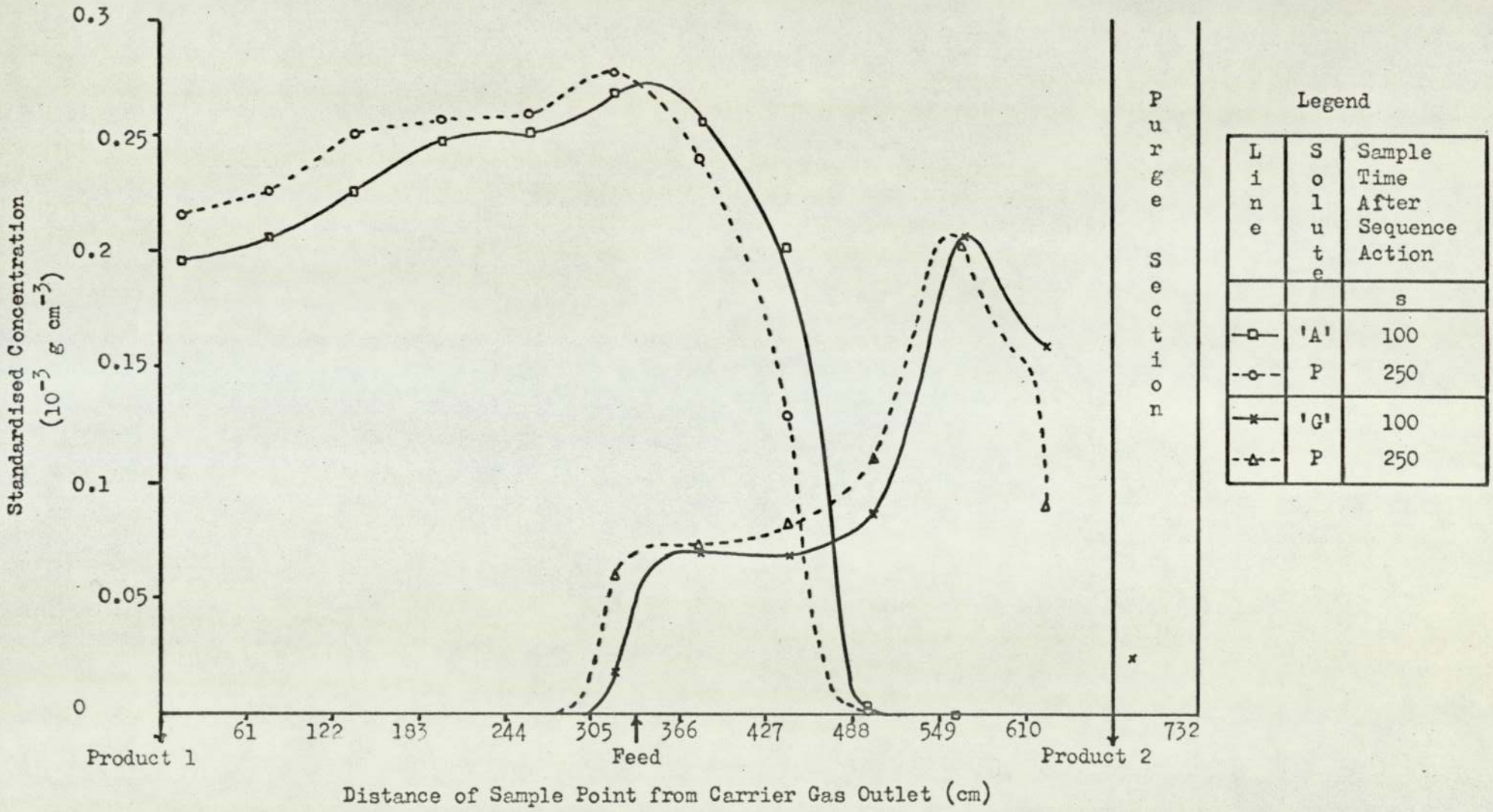

Legend

Line	Solute	Sample Time After Sequence Action
		s
—□—	'A'	100
--○--	P	250
—×—	'G'	100
--△--	P	250

Fig 8.8. The Study of Feedrate - Sequencing Rate = 400 s

Summary of Experimental Settings

Run Title	T_a	K^{∞}		P_a	Solute mixture Feedrate	I_S	L'	Separating Section				Purge Section			
		'A'P	'G'P					G_a (ave.)	P_{in} (ave.)	P_{out} (ave.)	$\frac{G_{m.c.}}{L'}$	S_a (ave.)	P_{in} (ave.)	P_{out} (ave.)	$\frac{S_{m.c.}}{L'}$
	°C			kN m^{-2}	cm^3 hr^{-1}	s	cm^3 s^{-1}	cm^3 s^{-1}	kN m^{-2}	kN m^{-2}		cm^3 s^{-1}	kN m^{-2}	kN m^{-2}	
200 - 275 - 400	23	126	366	101	200	403	1.05	825	369	187	276	1233	227	212	530
300 - 275 - 400	21	136	394	102	304	401	1.06	825	356	193	276	1545	226	200	698
400 - 275 - 400	21	136	394	102	400	404	1.05	825	368	191	280	2110	254	227	855
500 - 275 - 400	21	136	394	102	501	401	1.06	825	368	193	276	2110	254	227	845
600 - 275 - 400	21	136	394	102	600	403	1.05	825	366	188	281	2550	244	203	1080

Summary of Results

Run Title	$K^{\infty} + \Delta K$ (max.)		Separating Section		Purge Section	H.E.T.P. (ave.)	Concentration Profile Analysis				
							Figure	Time to recorded analysis	Product Purities		Comments
	'A'P	'G'P	$\frac{G_{min}}{L'}$	$\frac{G_{max}}{L'}$	$\frac{S_{min}}{L'}$				1('A'P)	2('G'P)	
						mm		hr	%	%	
200 - 275 - 400	142	466	215	425	522	not recorded	8.8a	7.75	99.5	>99.9	Purging incomplete - contamination of Product 1.
300 - 275 - 400	153	516	223	411	658	10.7	8.8b	11.0	>99.9	>99.9	
400 - 275 - 400	159	545	218	420	808	11.5	8.8c	8.66	>99.8	>99.8	
500 - 275 - 400	166	570	216	411	808	12.5	8.8d	6.66	>99.8	>99.8	
600 - 275 - 400	177	516	214	426	1015	14.3	8.8e	7.5	>99.8	-	'A'P profile covers whole separating section.

Figure 8.8a Standardised Concentration Profile for Run 200 - 275 - 400

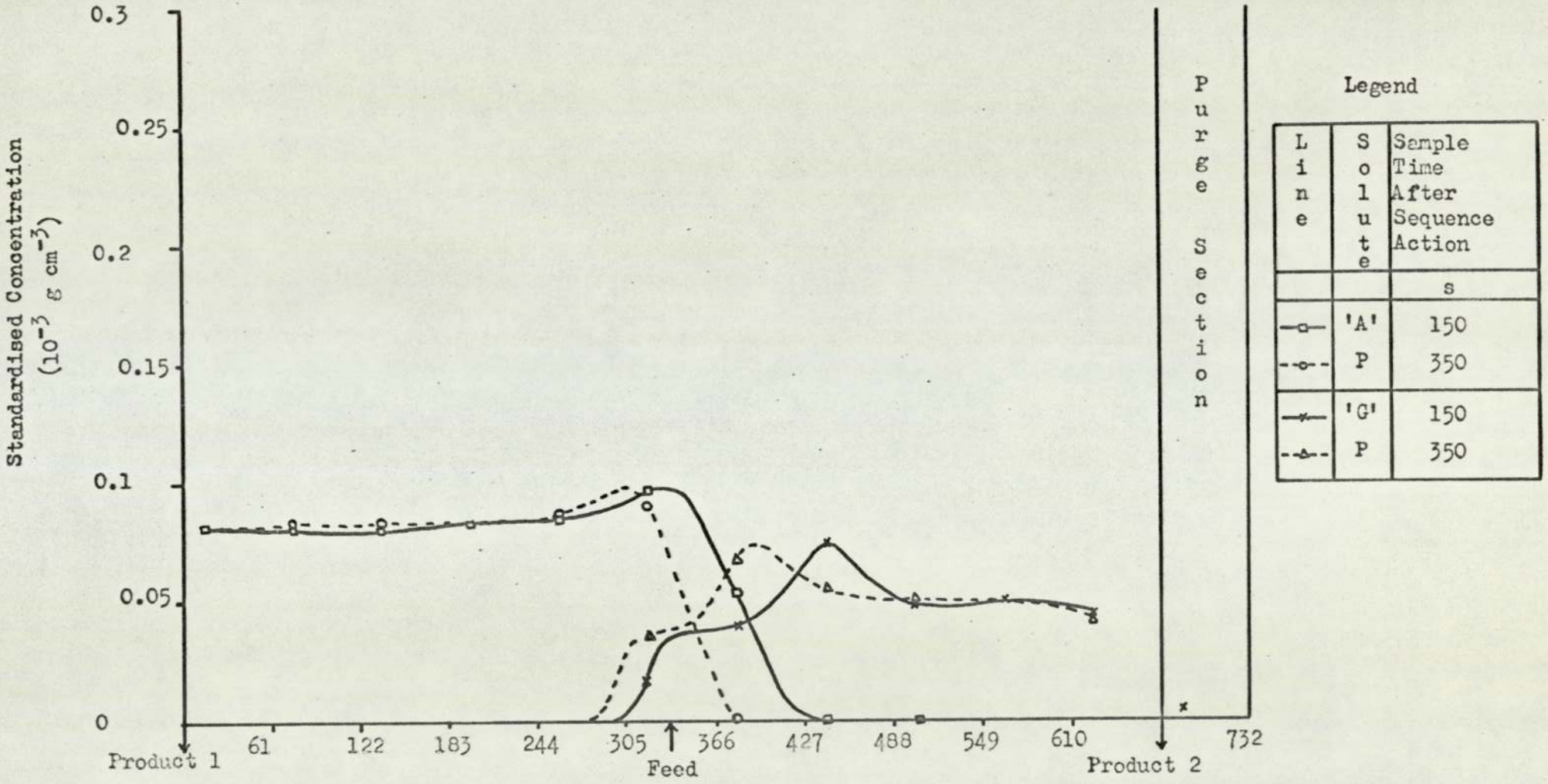

Figure 8.8b Standardised Concentration Profile for Run 300 - 275 - 400

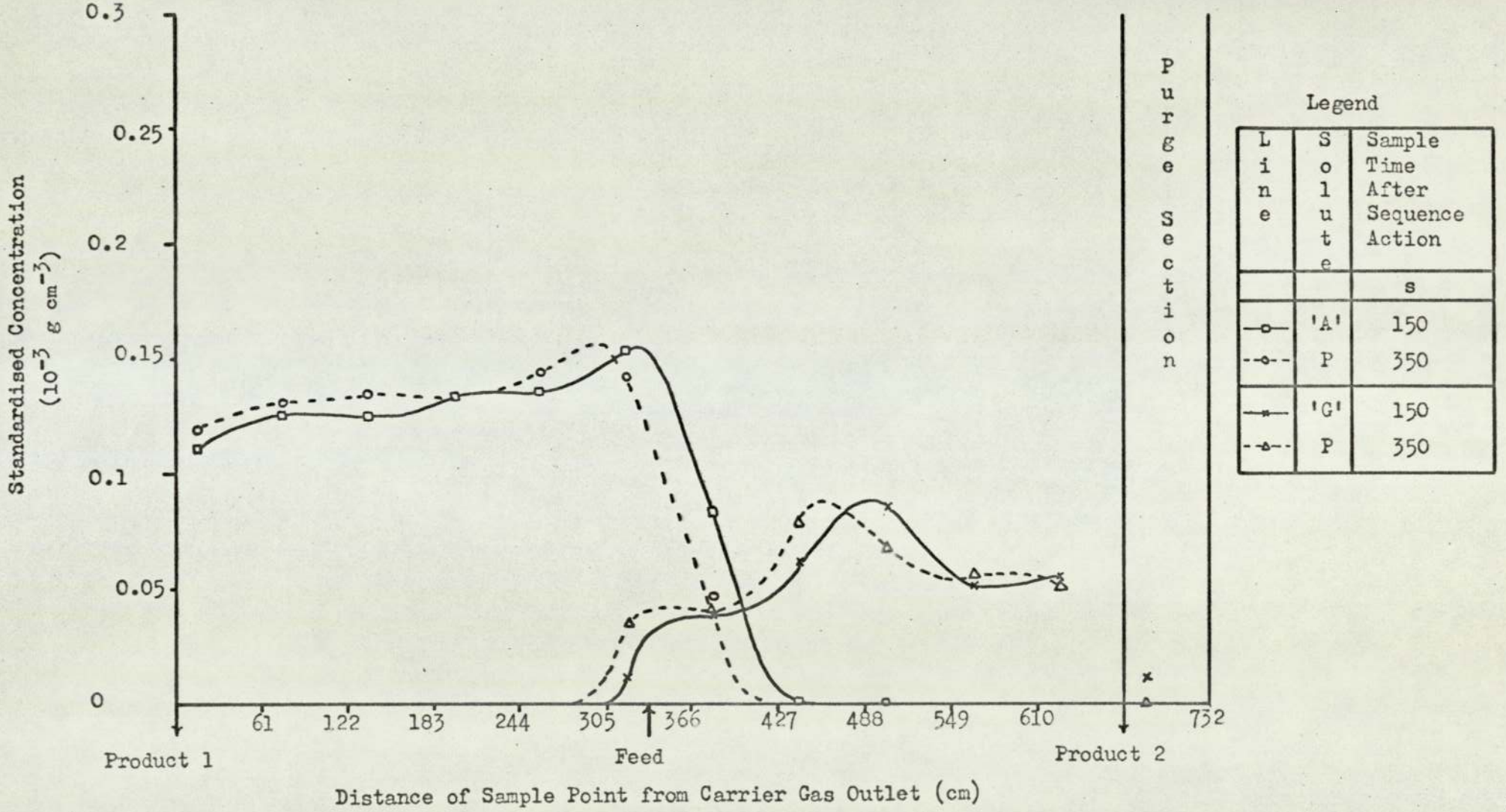

Figure 8.8c Standardised Concentration Profile for Run 400 - 275 - 400

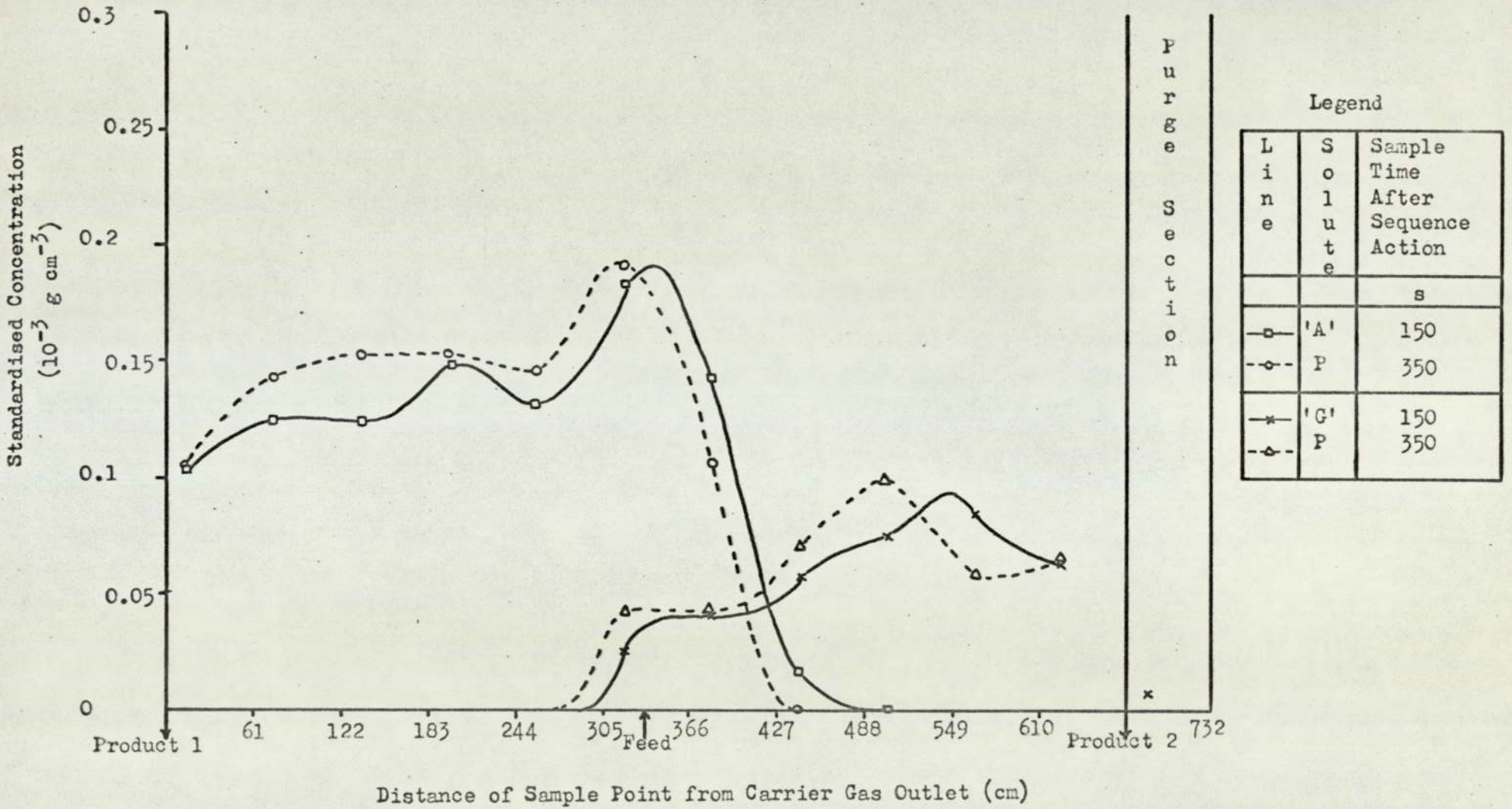

Figure 8.8d. Standardised Concentration Profile for Run 500 - 275 - 400

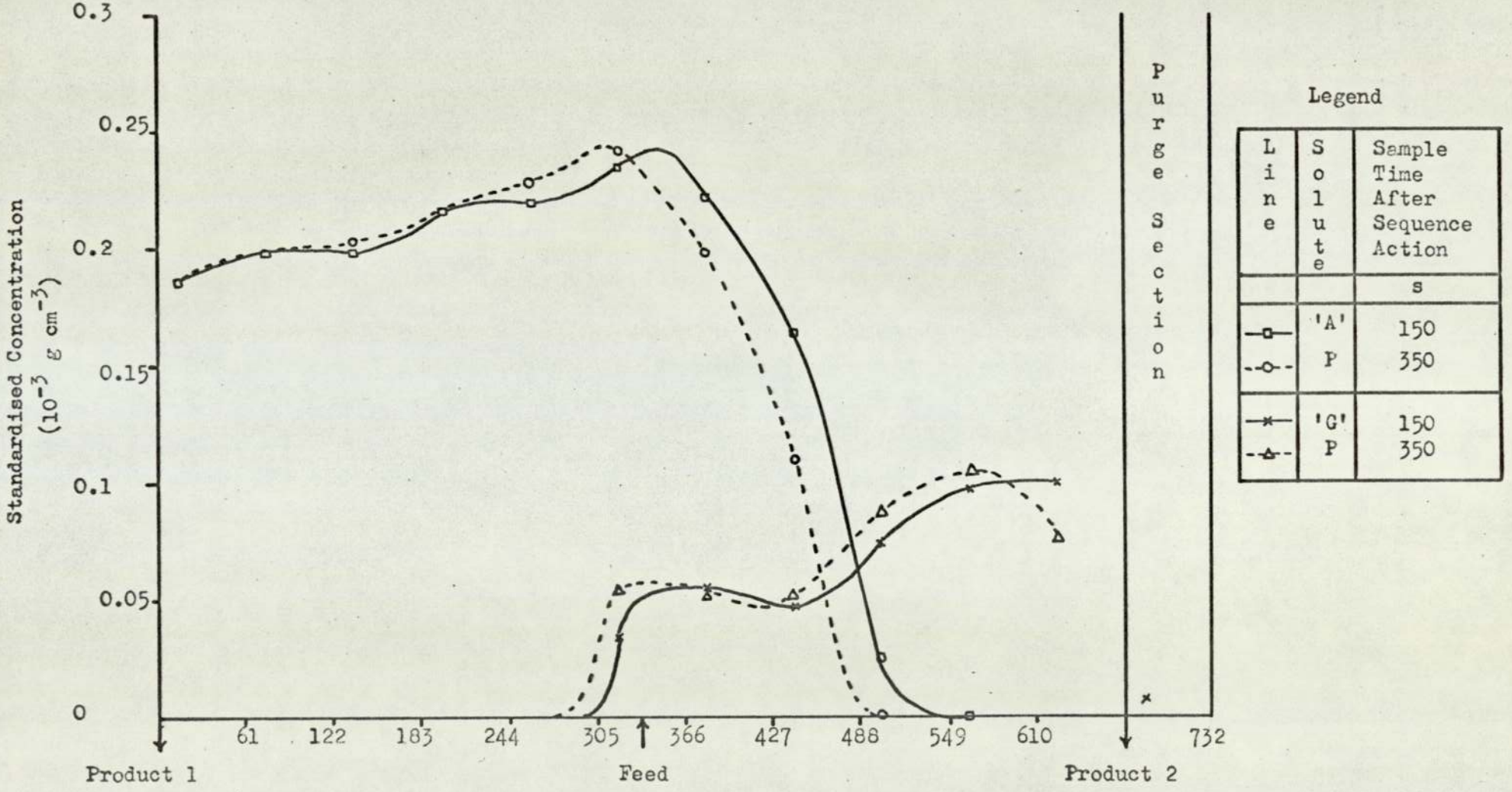

Figure 8.8e Standardised Concentration Profile for Run 600 - 275 - 400

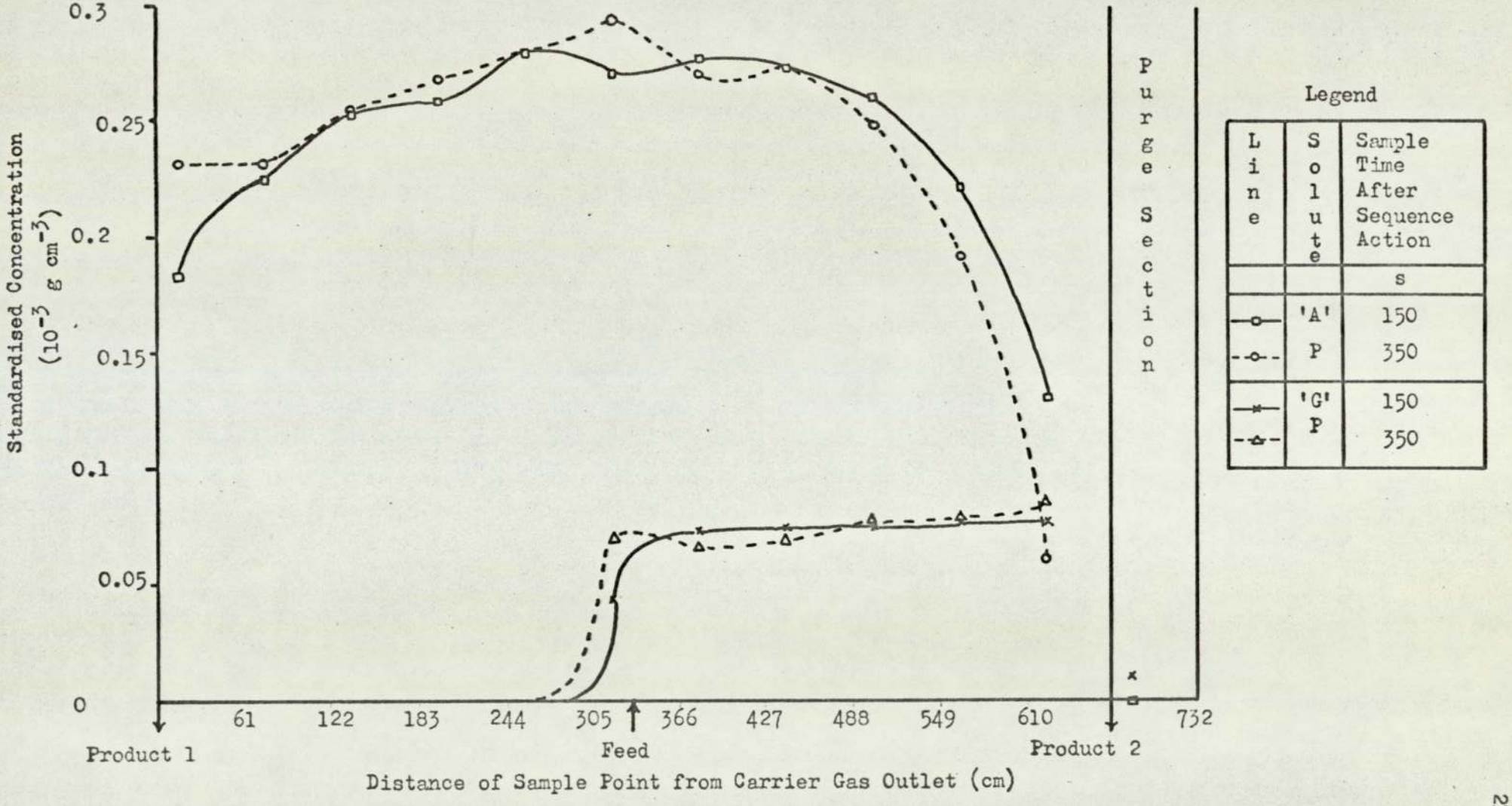

Fig 8.9. The Study of Feedrate - Sequencing Rate = 500 s

Summary of Experimental Settings

Run Title	T_a	K^∞		P_a	Solute mixture Feedrate	I_S	L'	Separating Section				Purge Section			
		'A'P	'G'P					G_a (ave.)	P_{in} (ave.)	P_{out} (ave.)	$G_{m.c.}$ $\overline{L'}$	S_a (ave.)	P_{in} (ave.)	P_{out} (ave.)	$S_{m.c.}$ $\overline{L'}$
	°C			kN m^{-2}	cm^3 hr^{-1}	s	cm^3 s^{-1}	cm^3 s^{-1}	kN m^{-2}	kN m^{-2}		cm^3 s^{-1}	kN m^{-2}	kN m^{-2}	
300 - 275 - 500	23	126	366	101	298	500	0.85	603	330	177	274	1548	220	197	868
400 - 275 - 500	22	131	379	100	400	500	0.85	603	330	179	275	1548	221	196	870
500 - 275 - 500	22	131	379	102	500	500	0.85	615	339	194	273	1867	226	197	1080

Summary of Results

Run Title	$K^\infty + \Delta K$ (max.)		Separating Section		Purge Section	H.E.T.P. (ave.)	Concentration Profile Analysis				
							Figure	Time to recorded analysis	Product Purities		Comments
	'A'P	'G'P	G_{min} $\overline{L'}$	G_{max} $\overline{L'}$	S_{min} $\overline{L'}$				1('A'P)	2('G'P)	
						mm		hr	%	%	
300 - 275 - 500	146	508	217	405	835	8.7	8.9a	6.0	>99.9	>99.7	
400 - 275 - 500	166	690	215	396	824	10.2	8.9b	7.0	99.8	99.6	Purging incomplete - slight contamination of Product 1.
500 - 275 - 500	214	700	218	380	990	11.3	8.9c	7.66	>99.5	-	'A'P just extending into isolated section, purging incomplete.

Figure 8.9a Standardised Concentration Profile for Run 300 - 275 - 500

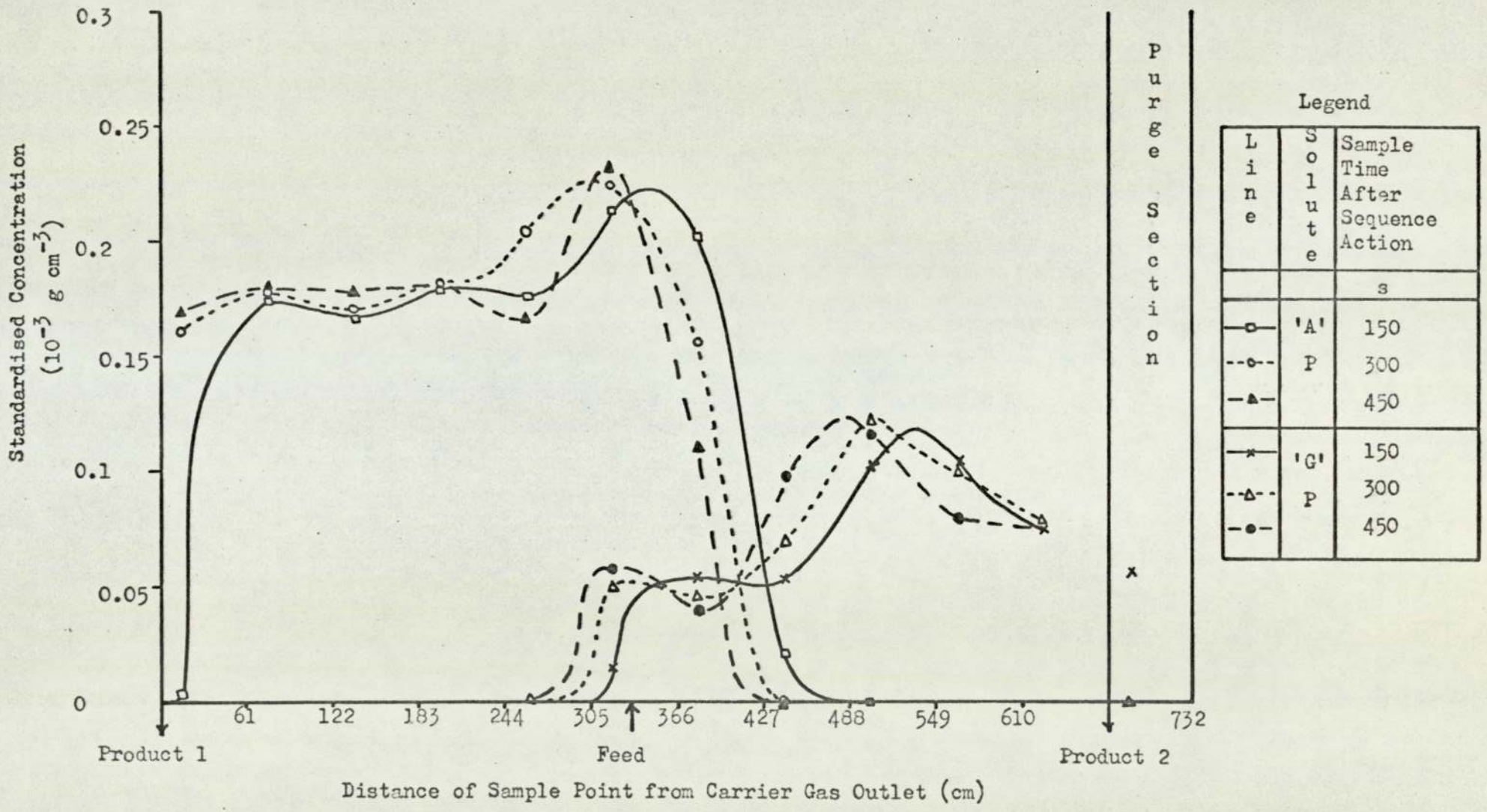

Figure 8.9b Standardised Concentration Profile for Run 400 - 275 - 500

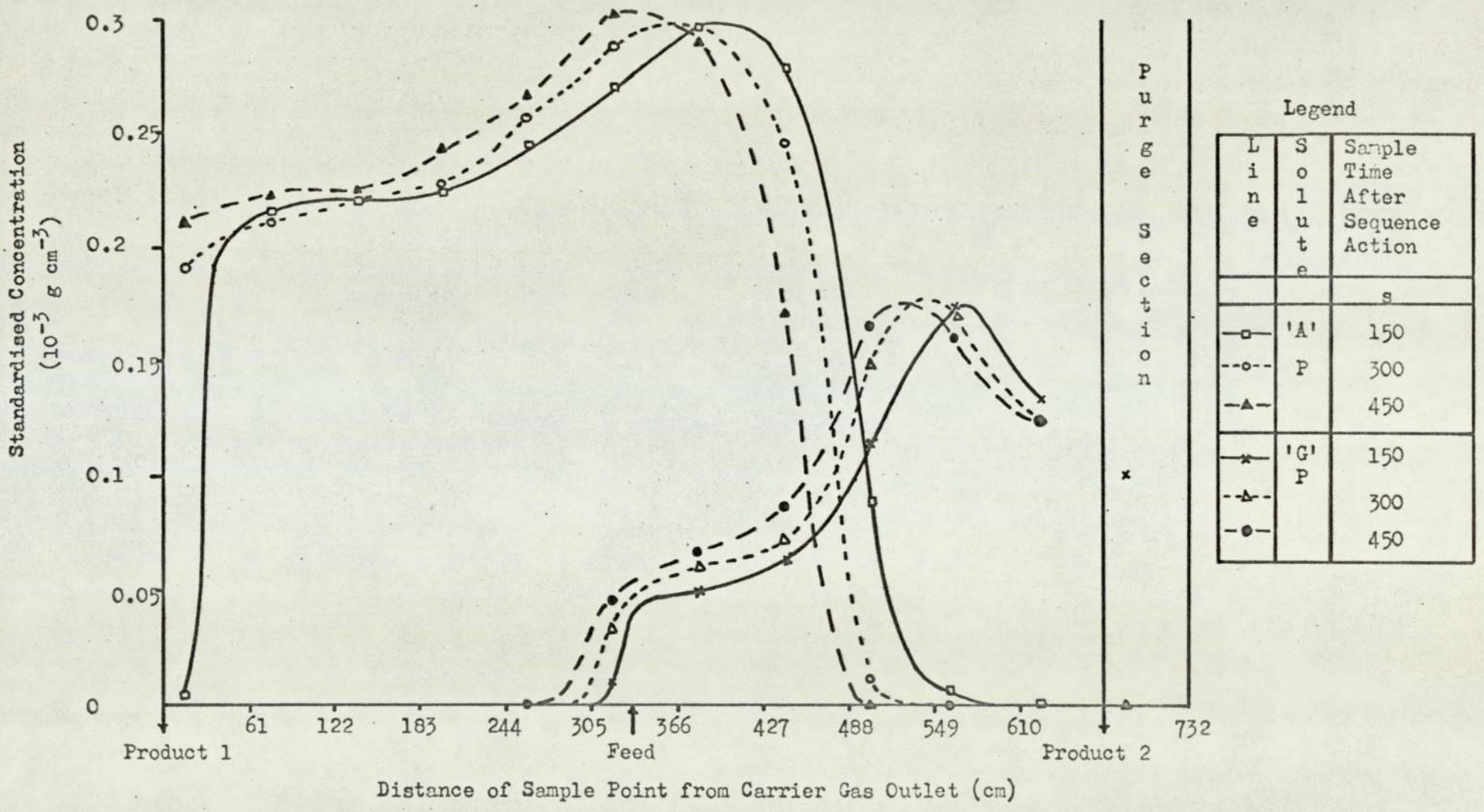

Figure 8.9c Standardised Concentration Profile for Run 500 - 275 - 500

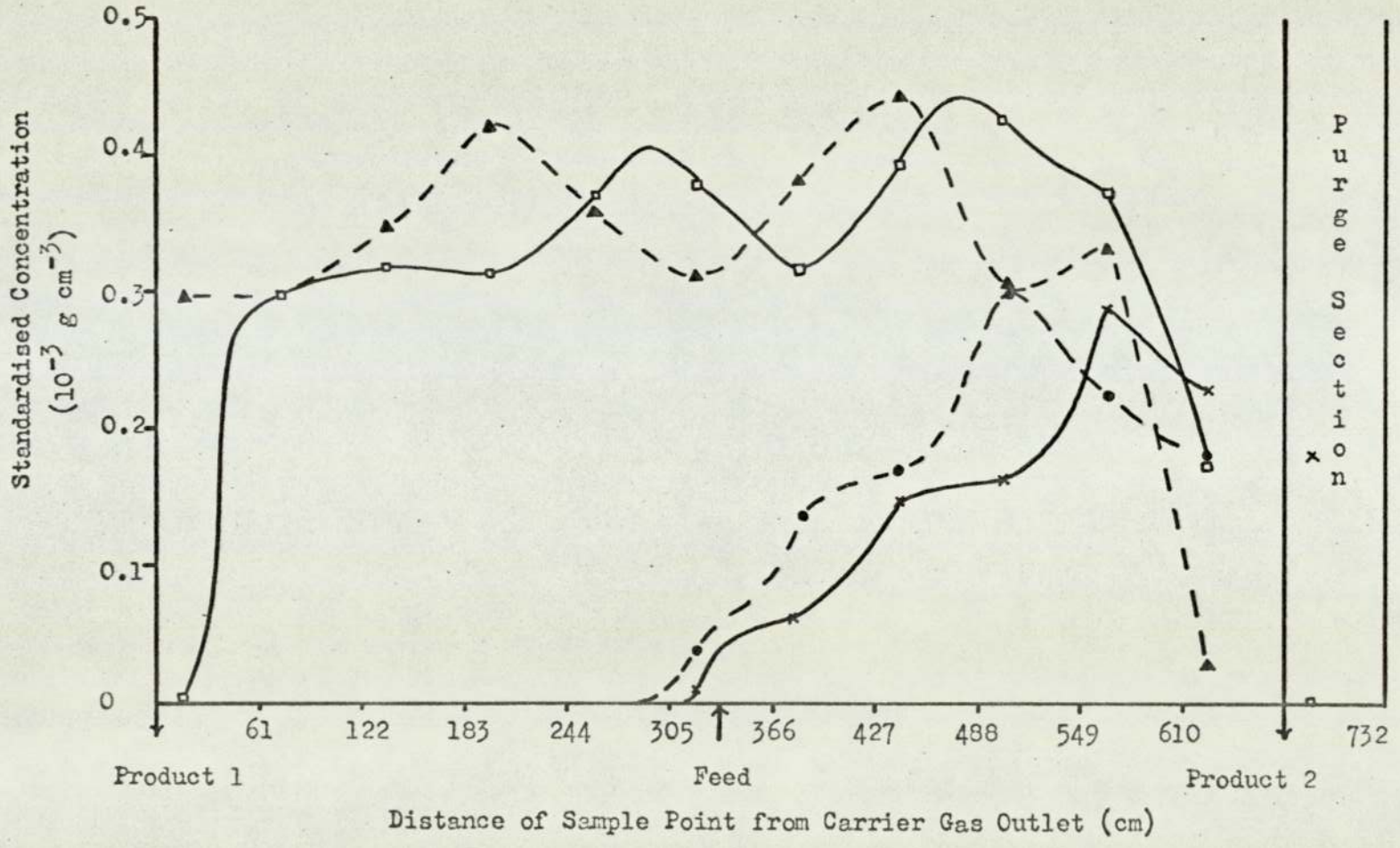

Legend

Line	Solute	Sample Time After Sequence Action
		s
—□—	'A' P	150
—▲—		450
—×—	'G' P	150
—●—		450

Note: Only 2 curves plotted for clarity.

Fig 8.10. The Study of Feedrate - Sequencing Rate = 600 s

Summary of Experimental Settings

Run Title	T_a	K^{∞}		P_a	Solute mixture Feedrate	I_S	L'	Separating Section				Purge Section			
		'A'P	'G'P					G_a (ave.)	P_{in} (ave.)	P_{out} (ave.)	$G_{m.c.}$ $\overline{L'}$	S_a (ave.)	P_{in} (ave.)	P_{out} (ave.)	$S_{m.c.}$ $\overline{L'}$
	°C			kN m^{-2}	cm^3 hr^{-1}	s	cm^3 s^{-1}	cm^3 s^{-1}	kN m^{-2}	kN m^{-2}		cm^3 s^{-1}	kN m^{-2}	kN m^{-2}	
300 - 275 - 600	24	122	350	101	298	595	0.71	533	339	195	276	1242	237	218	785
400 - 275 - 600	20	141	411	101	398	599	0.71	540	339	198	280	2370	239	222	1398

Summary of Results

Run Title	$K^{\infty} + \Delta K$ (max.)		Separating Section		Purge Section	H.E.T.P. (ave.)	Concentration Profile Analysis				
							Figure	Time to recorded analysis	Product Purities		Comments
	'A'P	'G'P	G_{min} $\overline{L'}$	G_{max} $\overline{L'}$	S_{min} $\overline{L'}$				1('A'P)	2('G'P)	
						mm		hr	%	%	
300 - 275 - 600	143	518	224	388	746	7.3	8.10a	5	99.8	>99.9	Slight contamination of Product 1 through incomplete purging.
400 - 275 - 600	188	644	226	386	1410	11.1	8.10b	5.5	>99.8	-	Arklone 'P' profile just covers whole separating section - incomplete purging.

Figure 8.10a Standardised Concentration Profile for Run 300 - 275 - 600

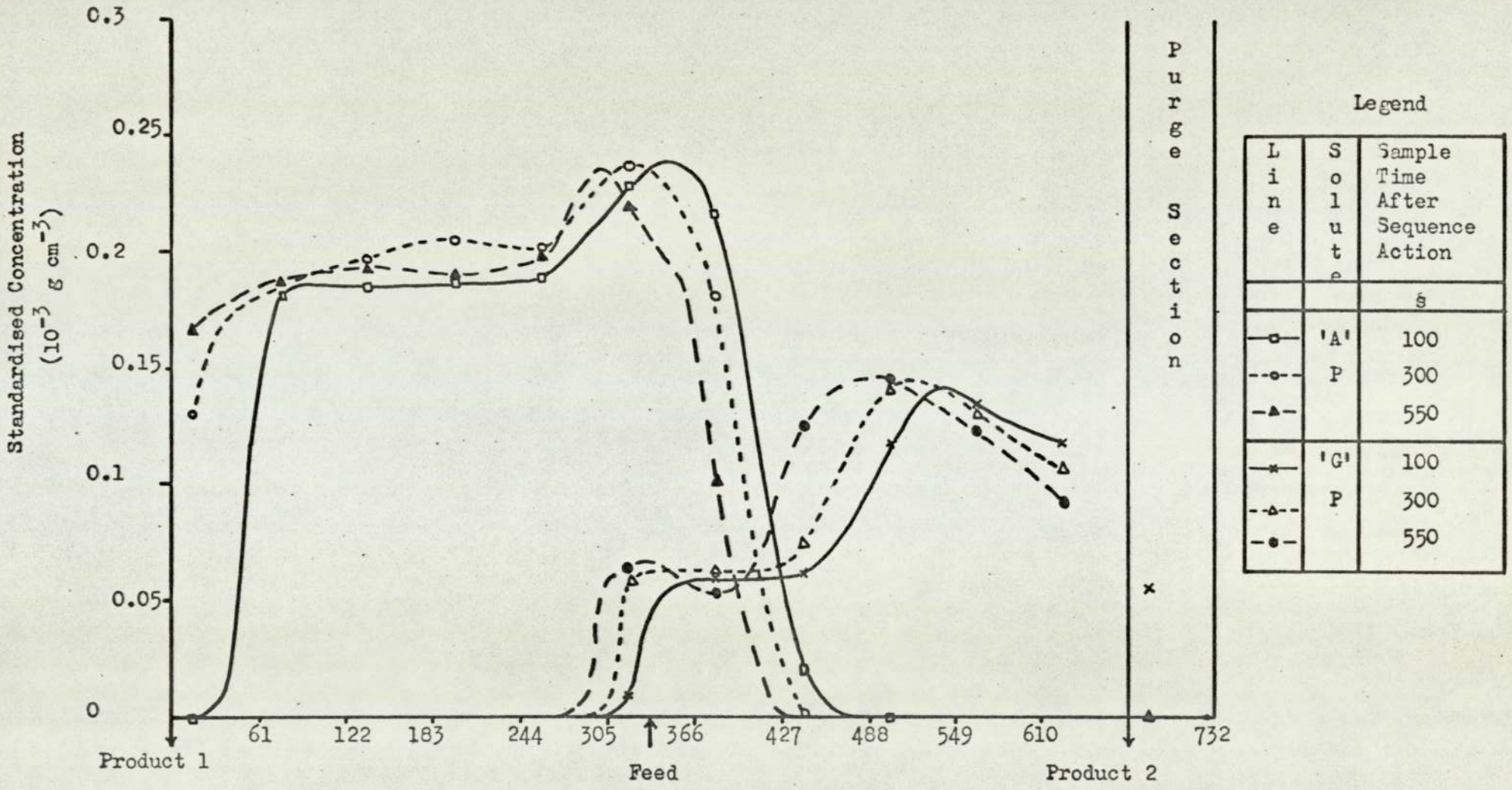

Figure 8.10b Standardised Concentration Profile for Run 400 - 275 - 600

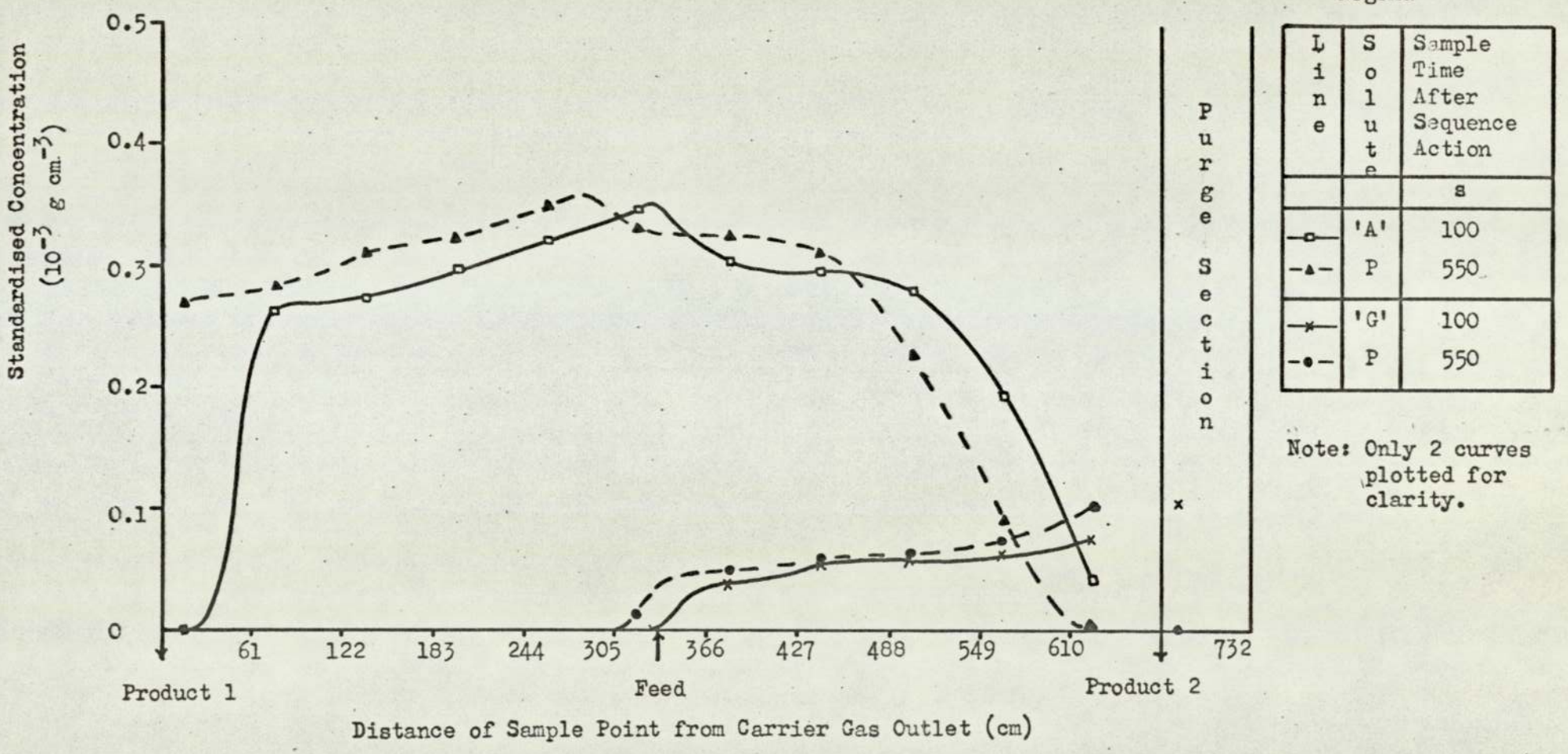

Legend

Line	Solute	Sample Time After Sequence Action
		s
—□—	'A'	100
–▲–	P	550
—×—	'G'	100
–●–	P	550

Note: Only 2 curves plotted for clarity.

8.3 The study of the 'Apparent Gas to Liquid Rate' Ratio

8.3.1 Results

The presentation of the experimental results within this subsection follows the format of the feedrate studies.

A further nine runs were performed which combined with the previously presented results to give the following series:

(i) $\frac{G_{m.c.}}{L'}$ held constant while both $G_{m.c.}$ and L' are proportionately varied. Runs 500 - 275 - 300, 500 - 275 - 400 and 500 - 275 - 500 provide an example of such a series, the value of $\frac{G_{m.c.}}{L'}$ being held within 275 ± 2 as the sequencing rate was increased from 300 to 500-seconds. These results are represented as Fig 8.11 for discussion.

(ii) $\frac{G_{m.c.}}{L'}$ varied by changing both $G_{m.c.}$ and L'. A guideline for the settings was given by the ratio of $G_{m.c.}$ to the length of the sequencing interval, this being 0.73 $cm^3\ s^{-2}$ for all five runs in the series. The feedrate of the binary equivolume solute mixture was 300 $cm^3\ hr^{-1}$. Fig 8.12 records the results.

(iii) Finally $G_{m.c.}$ was held constant within 293 ± 3 $cm^3\ s^{-1}$ while the sequencing interval was increased from 300 to 550-seconds in 50-second steps. A feedrate of 300 $cm^3\ hr^{-1}$ was again used throughout the series (Fig 8.13).

The full details of the concentration profile analyses for the additional nine runs are included in Appendix 4.

8.3.2 Discussion

Comparing the three experimental runs conducted at a constant solute feedrate of 500 $cm^3\ hr^{-1}$ and constant $\frac{G_{m.c.}}{L'}$ ratio re-emphasises the importance of concentration to the successful separation of this chemical system (Fig 8.11). As the sequencing interval was extended from 300 to 500-seconds, with a corresponding reduction in the mean column carrier gas flowrate of 394 $cm^3\ s^{-1}$ to 232 $cm^3\ s^{-1}$, the column concentration of 'Arklone' P and 'Genklene' P more than doubled. In keeping with the absortion isotherm the two components increased their preference for the solvent phase, both component profiles exhibiting an increasing tendency toward the isolated section. For Run 500 - 275 - 500 insufficient column length between the feed point and isolated section was available to effect the separation and Product 2 purity was lost.

Changing the $G_{m.c.}/L'$ ratio by varying both the carrier gas flowrate and the sequencing permitted observation of the concentration profiles from one extreme, loss of purity of Product 2, to the other, Product 1 impure (Fig 8.12).

For run 300 - 155 - 300 the value of $\frac{G_{m.c.}}{L'}$ was greater than K_{AP} but $\frac{G_{min}}{L'}$ was less than K_{AP} at the column concentration. In keeping with the understanding of the separation process, the expected loss of Product 2 purity resulted with the 'Arklone' P profile covering all of the available separating length. Increasing $\frac{G_{m.c.}}{L'}$ to 215 (run 300 - 215 - 300) still gave a Product 2 purity of only 98%. In this case K_{AP} was less than $\frac{G_{min}}{L'}$, the respective numeral values being 157 and 167. Inclusion of factors in addition to the pressure gradient and concentration dependent partition

coefficient in the inequality defining the lower limit for successful separation again appears justified.

With a further increase in the value of $\frac{G_{m.c.}}{L'}$ the two components exhibited a greater preference to move in the direction of the flowing carrier gas stream towards the Product 1 exit port. This resulted in a general reduction in the 'hold-up' of 'Arklone' P, while that for 'Genklene' P increased. The length of separating section achieving the bulk of the separation decreased to a minimum of approximately 150 cm for run 300 - 275 - 400 before beginning to increase once again.

Finally for run 300 - 425 - 500 the 'Genklene' P profile had developed a long leading edge which contaminated the 'Arklone' P exiting as Product 1. K_{GP} was substantially less than $\frac{G_{max}}{L'}$ which must contravene the operating conditions for the upper separation limit (equation 6.15). The result, therefore, follows the expected pattern.

The third series of runs was performed to give further insight into the operating limits of the G/L' ratio for a successful separation. $G_{m.c.}$ was held constant within 293 ± 3 cm^3 s^{-1} to eliminate an additional variable, only the sequencing interval being changed (Fig 8.13).

For separation of the two solutes to occur then, within a sequencing interval, the distance travelled by all 'Arklone' P molecules in the direction of carrier gas flow must be greater than one equivalent column length, while that travelled by 'Genklene' P molecules must be less than this distance of 61 cm. Similarly, for the isolated section, the sequencing interval must be such as to permit all solute molecules to be at least carried a single column length by the flowing purge gas. These

restrictions follow directly from the discontinuous mode of operation.

As the sequencing interval was increased from 300 to 550-seconds the carrier gas flowrate and binary mixture feedrate were such that the series of runs passed through the lower and upper limiting conditions. For run 300 - 205 - 300 the tail of the 'Arklone' P profile contaminated Product 2. Increasing the length of the sequencing interval to 350 s recovered Product 2 purity. The value of the partition coefficient of 'Arklone' P at the maximum recorded column concentration was 162 which, in accordance with equation 6.15, is less than the $\frac{G_{min}}{L'}$ value of 189.

Progressively increasing the sequencing interval increased the 'hold-up' of 'Genklene' P while that for 'Arklone' P was reduced. In particular the maximum 'Genklene' P concentration moved closer to the feed, representing a balance point between the actual on-column gas to liquid rate and 'apparent' partition coefficient.

At a sequencing interval of 500-seconds (run 300 - 340 - 500) the distance travelled by the fastest moving 'Genklene' P molecules per interval was very close to one column length. A long leading edge was developing for the 'Genklene' P profile to give contamination of Product 1. The maximum values of K_{GP} and $\frac{G_{max}}{L'}$ were almost equal, being 520 and 519 respectively.

The final run, run 300 - 370 - 550, resulted in the full development of the leading edge to the 'Genklene' P profile. In this case K_{GP} at the maximum recorded on-column concentration level is greater than $\frac{G_{max}}{L'}$ which should ensure successful separation if only the pressure gradient and non-linear absorption isotherm factors were considered. However, the

general concentration level of 'Genklene' P in the leading edge was considerably lower than the maximum value for the profile. Hence the resultant velocity of 'Genklene' P molecules towards the Product 1 outlet in this low concentration region is greater than for the bulk, the partition coefficient being less. Once formed, a leading edge to the 'Genklene' P profile will tend to be extended, requiring an increasing length of column to effect the separation.

The inclusion of a negative length and sequencing action term in the full inequality defining the upper separation limit appears to be justified by these results (see equation 6.13).

Inspection of all results obtained for experimental runs performed at a binary mixture feedrate of 300 cm^3 hr^{-1} shows that the minimum point value for the gas to apparent liquid rate ratio which gave pure Product 2 was in the region of 170. The maximum point value for pure Product 1 was 520. These values must be considered approximate as the temperature dependence of the partition coefficient is an important variable. Future experimental work should be carried out in a controlled temperature environment. Measurement of the on-column temperature profiles should also be made to gain insight into the magnitude of the enthalpic overloading effect.

Fig 8.11. The Study of the G/L' ratio - Constant $\overline{L'}^{G_{m.c.}}$, vary $G_{m.c.}$ and L'

Summary of Experimental Settings

Run Title	T_a	K^{∞}		P_a	Solute mixture Feedrate	I_S	L'	Separating Section				Purge Section			
		'A'P	'G'P					G_a (ave.)	P_{in} (ave.)	P_{out} (ave.)	$\overline{G_{m.c.}}^{L'}$	S_a (ave.)	P_{in} (ave.)	P_{out} (ave.)	$\overline{S_{m.c.}}^{L'}$
	°C			kN m^{-2}	cm^3 hr^{-1}	s	cm^3 s^{-1}	cm^3 s^{-1}	kN m^{-2}	kN m^{-2}		cm^3 s^{-1}	kN m^{-2}	kN m^{-2}	
500 - 275 - 300	23	126	366	102	488	298	1.42	1197	408	182	277	2133	257	227	629
500 - 275 - 400	21	136	394	102	501	401	1.06	825	368	193	276	2110	254	227	845
500 - 275 - 500	22	131	379	102	500	500	0.85	615	339	194	273	1867	226	197	1080

Summary of Results

Run Title	$K^{\infty} + \Delta K$ (max.)		Separating Section		Purge Section	H.E.T.P. (ave.)	Concentration Profile Analysis				
							Figure	Time to recorded analysis	Product Purities		Comments
	'A'P	'G'P	$\overline{G_{min}}^{L'}$	$\overline{G_{max}}^{L'}$	$\overline{S_{min}}^{L'}$				1('A'P)	2('G'P)	
						mm		hr	%	%	
500 - 275 - 300	146	490	210	472	595	13.8	8.11a	6.25	>99.8	>99.9	Purging incomplete - contamination of Product 1.
500 - 275 - 400	166	370	216	411	808	12.5	8.11b	6.66	>99.8	>99.8	
500 - 275 - 500	214	700	218	380	990	11.3	8.11c	7.66	>99.5	-	'A'P just extending into isolated section, purging incomplete.

Figure 8.11a Standardised Concentration Profile for Run 500 - 275 - 300

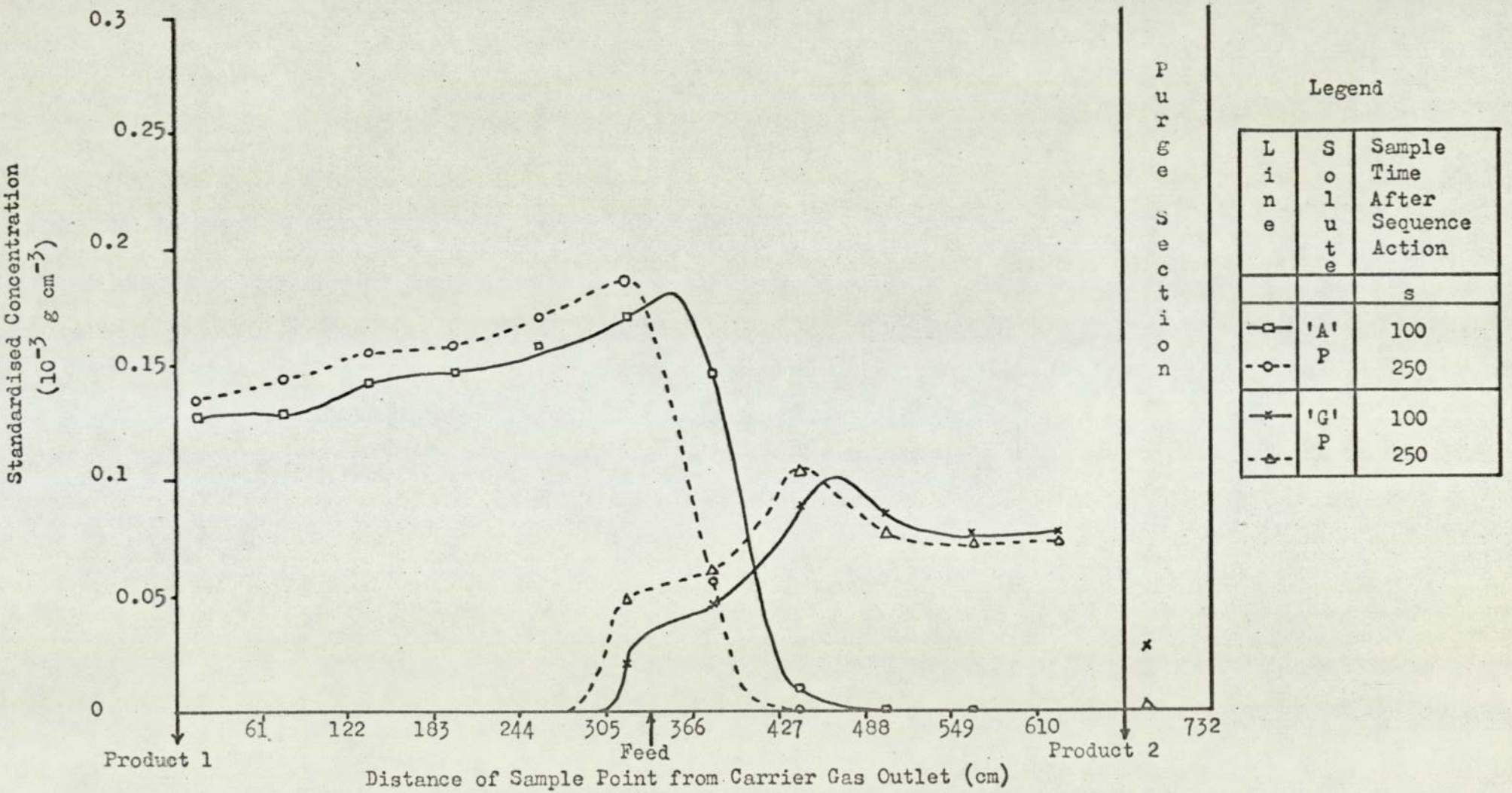

Figure 8.11b Standardised Concentration Profile for Run 500 - 275 - 400

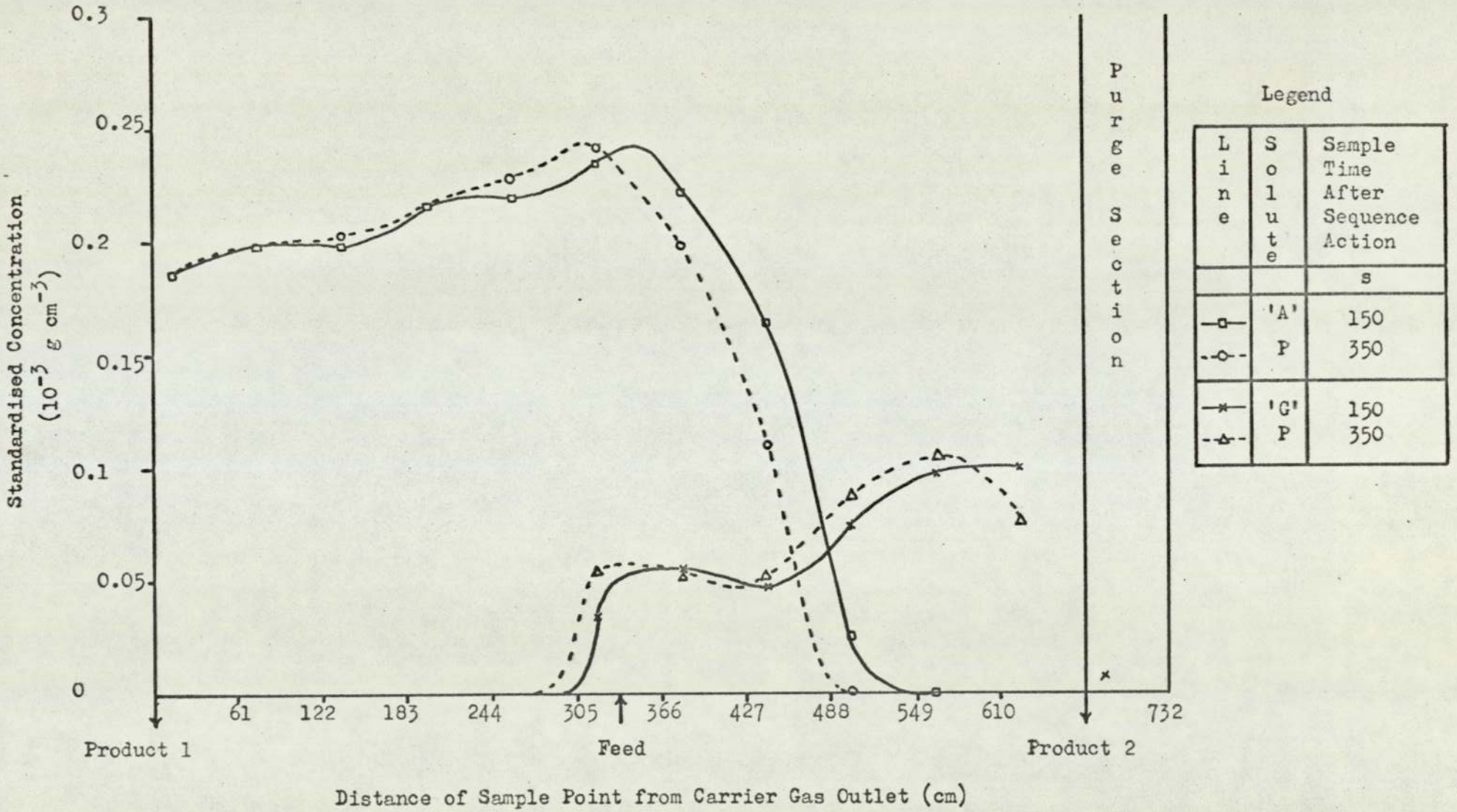

Figure 8.11c Standardised Concentration Profile for Run 500 - 275 - 500

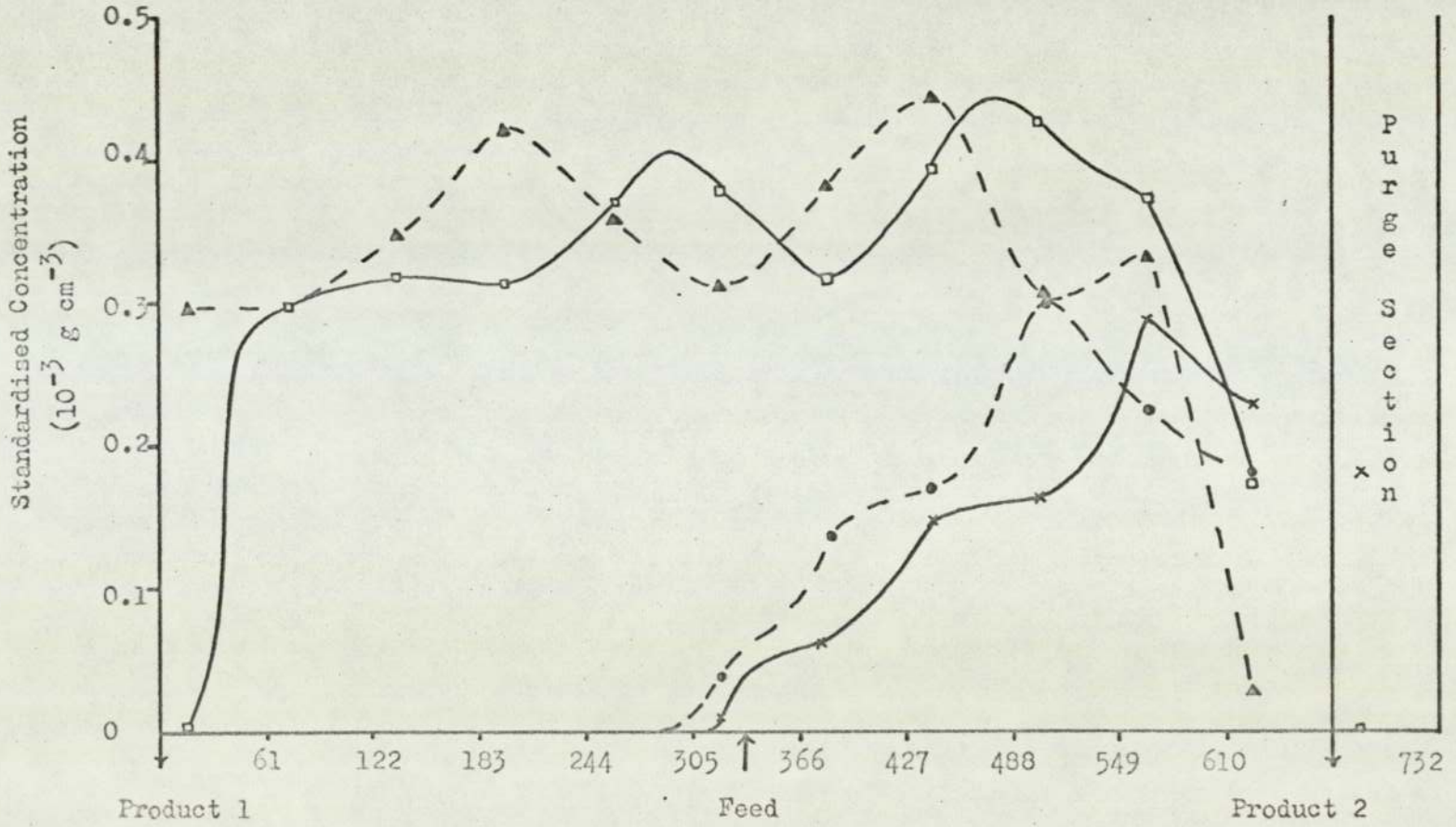

Legend

Line	Solute	Sample Time After Sequence Action
		s
—□—	'A' P	150
—△—		450
—×—	'G' P	150
—•—		450

Note: Only 2 curves plotted for clarity.

Fig 8.12. The Study of the G/L' ratio - vary $G_{m.c.}$ and L'

Summary of Experimental Settings

Run Title	T_a	K^∞		P_a	Solute mixture Feedrate	I_S	L'	Separating Section				Purge Section			
		'A'P	'G'P					G_a (ave.)	P_{in} (ave.)	P_{out} (ave.)	$\frac{G_{m.c.}}{L'}$	S_a (ave.)	P_{in} (ave.)	P_{out} (ave.)	$\frac{S_{m.c.}}{L'}$
	°C			kN m^{-2}	cm^3 hr^{-1}	s	cm^3 s^{-1}	cm^3 s^{-1}	kN m^{-2}	kN m^{-2}		cm^3 s^{-1}	kN m^{-2}	kN m^{-2}	
300 - 155 - 300	22	131	379	101	298	303	1.40	567	333	172	157	2010	212	180	775
300 - 215 - 350	22	131	379	100	300	353	1.20	662	330	164	215	2097	250	223	740
300 - 275 - 400	21	136	394	102	304	401	1.06	825	356	193	276	1545	226	200	698
300 - 345 - 450	21	136	394	98	295	446	0.95	923	350	170	348	1565	220	195	771
300 - 425 - 500	21	136	394	99	298	501	0.85	1083	391	183	427	1547	222	197	861

Summary of Results

Run Title	$K^\infty + \Delta K$ (max.)		Separating Section		Purge Section	H.E.T.P. (ave.)	Concentration Profile Analysis				
							Figure	Time to recorded analysis	Product Purities		Comments
	'A'P	'G'P	$\frac{G_{min}}{L'}$	$\frac{G_{max}}{L'}$	$\frac{S_{min}}{L'}$				1('A'P)	2('G'P)	
						mm		hr	%	%	
300 - 155 - 300	159	444	123	238	685	8.0	8.12a	7.0	> 99.9	-	'A'P profile covers whole column.
300 - 215 - 350	157	462	167	336	698	9.1	8.12b	8.5	> 99.9	> 98	'G'P contaminated by tailing edge of 'A'P profile.
300 - 275 - 400	153	516	223	411	658	10.7	8.12c	11.0	> 99.9	> 99.9	
300 - 345 - 450	151	576	272	505	734	11.5	8.12d	7.0	> 99.7	> 99.8	
300 - 425 - 500	152	596	323	690	811	-	8.12e	8.67	-	> 99.9	'G'P profile has long leading edge to Product 1.

Figure 8.12a Standardised Concentration Profile for Run 300 - 155 - 300

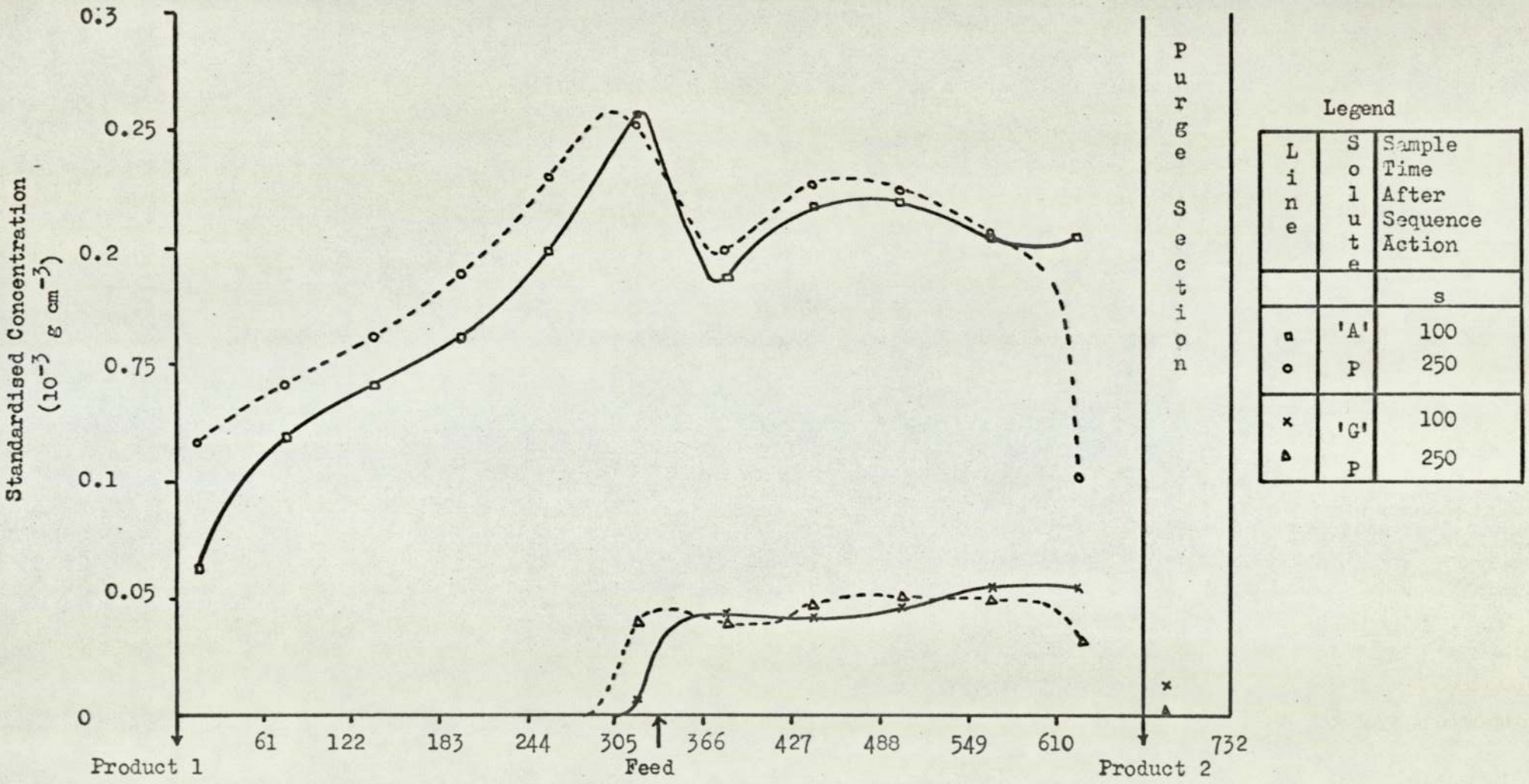

Legend

Line	Solute	Sample Time After Sequence Action
		s
□	'A'	100
o	P	250
×	'G'	100
△	P	250

Figure 8.12b Standardised Concentration Profile for Run 300 - 215 - 350

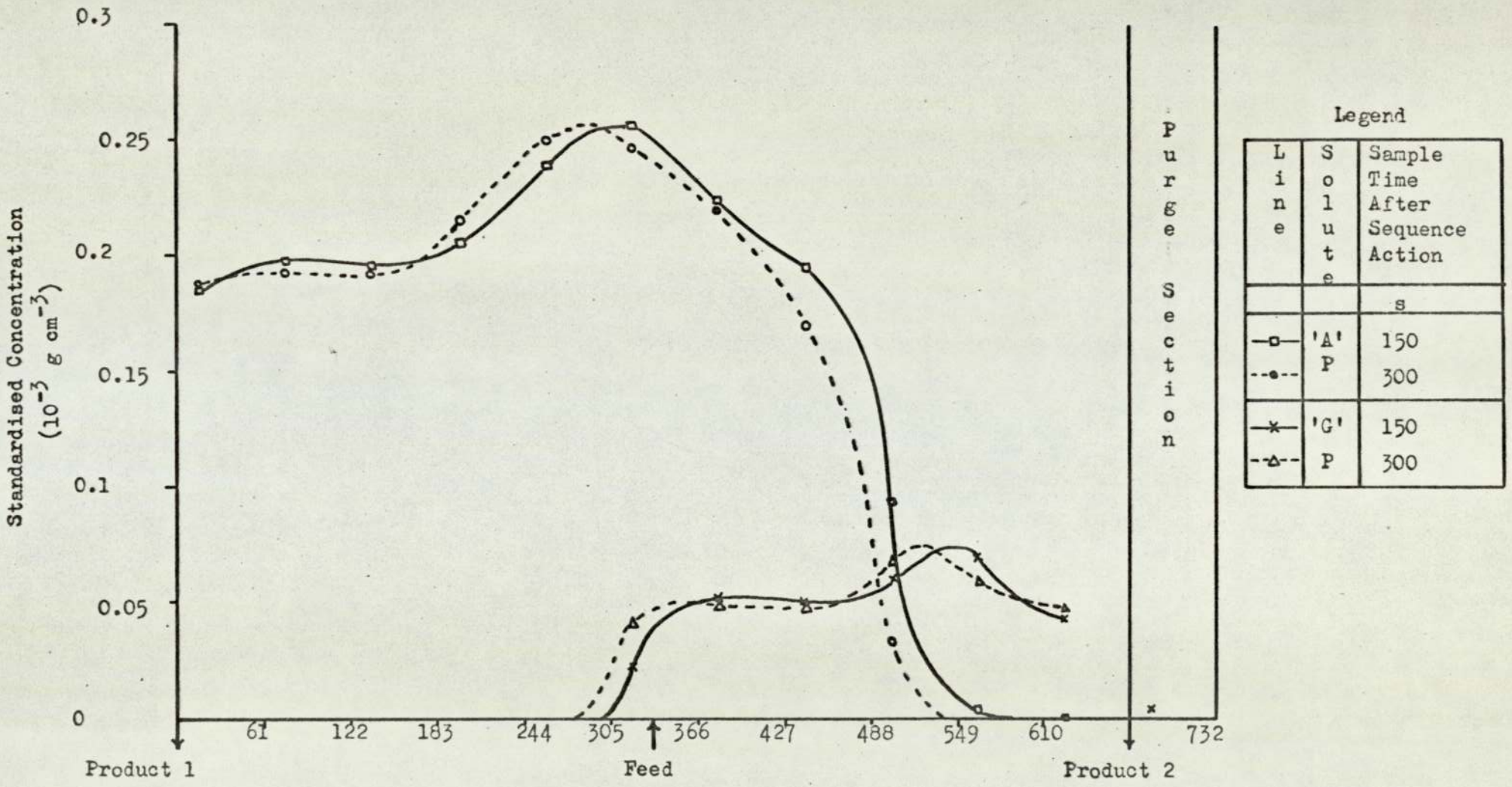

Figure 8.12c Standardised Concentration Profile for Run 300 - 275 - 400

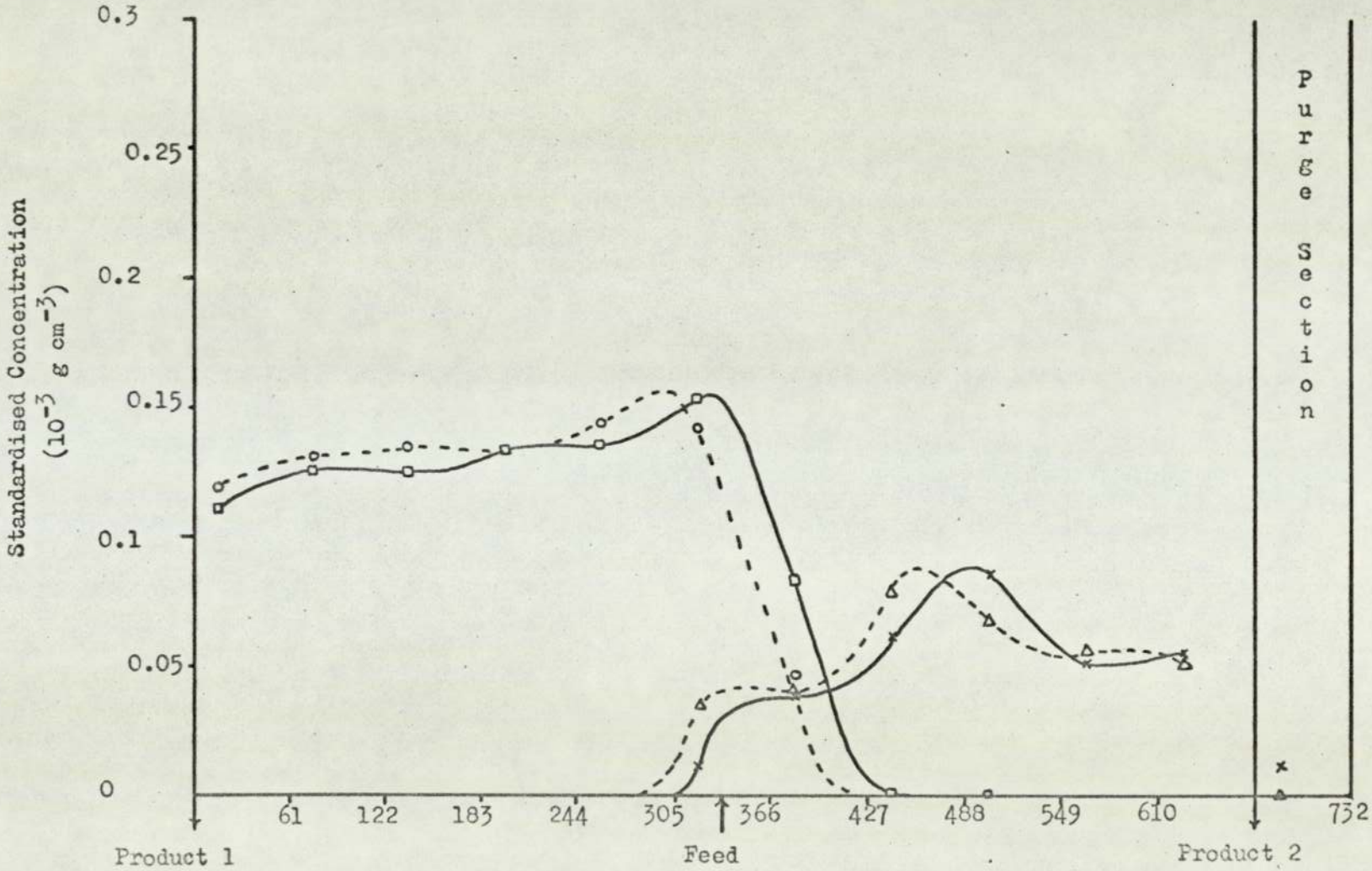

Legend

Line	Solute	Sample Time After Sequence Action
		s
—o—	'A'	150
--o--	P	350
—x—	'G'	150
--△--	P	350

Figure 8.12d Standardised Concentration Profile for Run 300 - 345 - 450

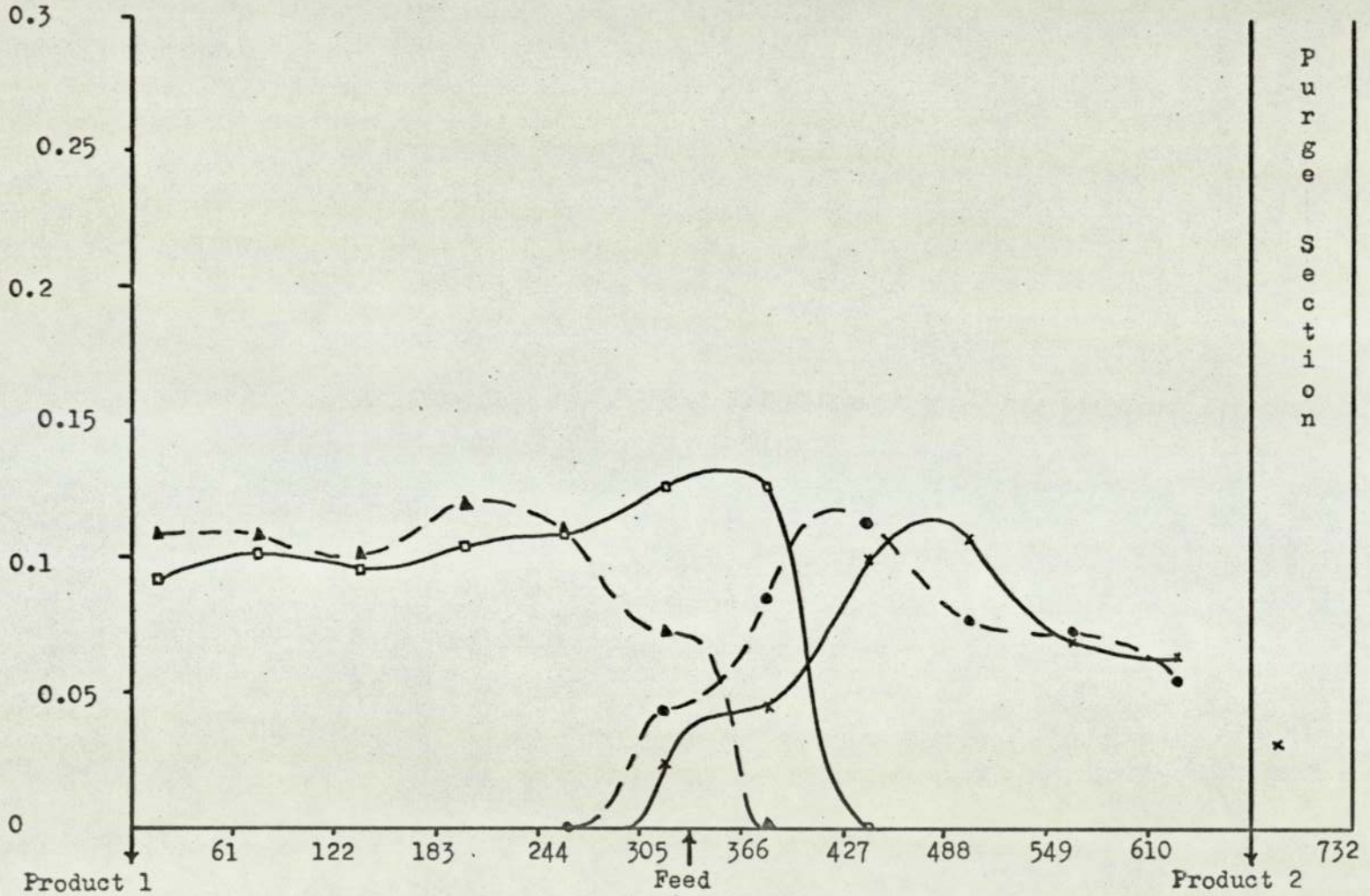

Distance of Sample Point from Carrier Gas Outlet (cm)

Legend

Line	Solute	Sample Time After Sequence Action
		s
—o—	'A' P	100
—▲—		400
—×—	'G' P	100
—●—		400

Note: Only 2 curves plotted for clarity.

Figure 8.12e Standardised Concentration Profile for Run 300 - 425 - 500

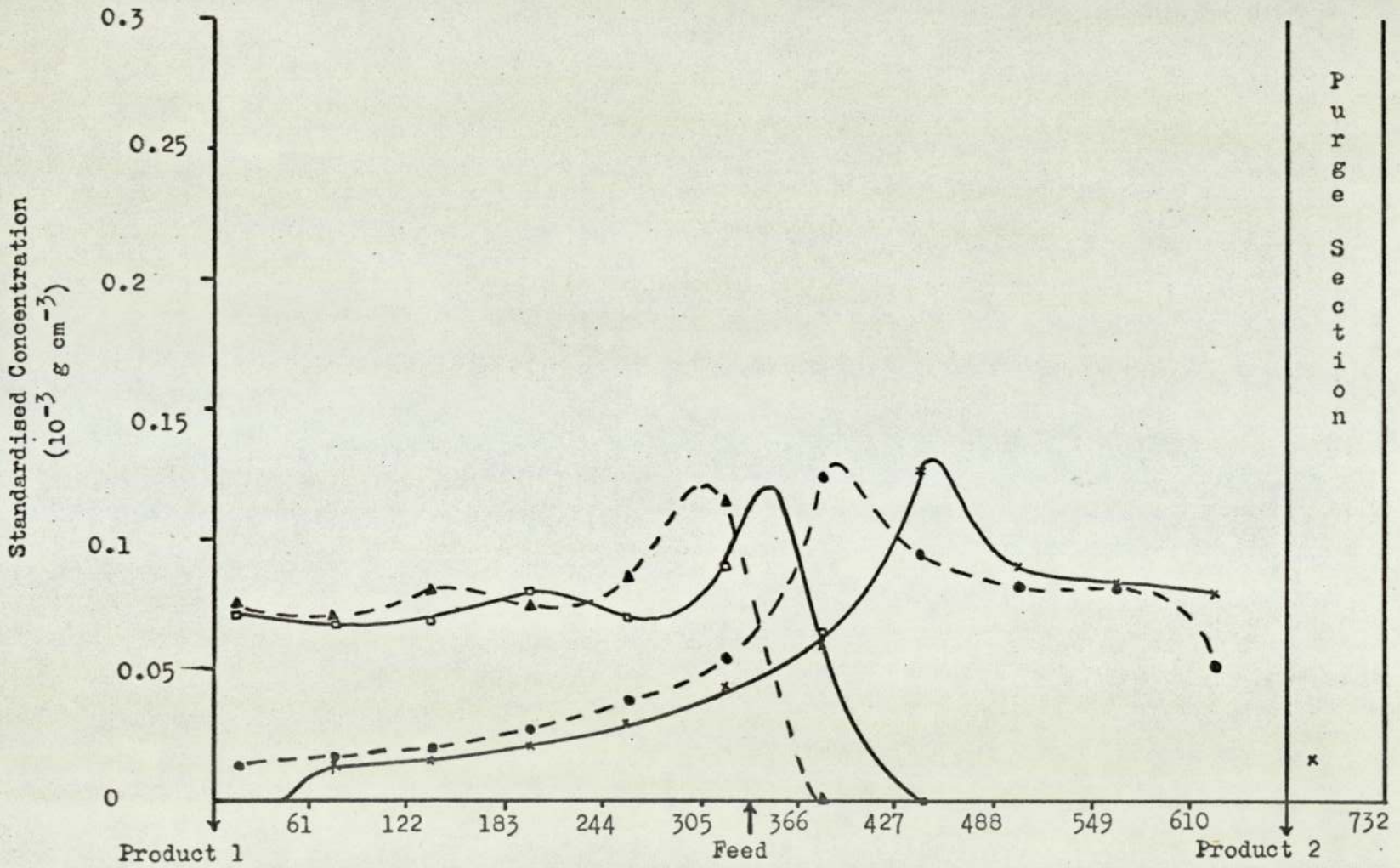

Legend

Line	Solute	Sample Time After Sequence Action
		s
—○—	'A'	150
–▲–	P	450
—×—	'G'	150
–●–	P	450

Note: Only 2 curves plotted for clarity.

Fig 8.13. Study of the G/L' ratio - constant $G_{m.c.}$ vary L'

Summary of Experimental Settings

Run Title	T_a	K^{∞}		P_a	Solute mixture Feedrate	I_S	L'	Separating Section				Purge Section			
		'A'P	'G'P					G_a (ave.)	P_{in} (ave.)	P_{out} (ave.)	$\frac{G_{m.c.}}{L'}$	S_a (ave.)	P_{in} (ave.)	P_{out} (ave.)	$\frac{S_{m.c.}}{L'}$
	°C			kN m^{-2}	cm^3 hr^{-1}	s	cm^3 s^{-1}	cm^3 s^{-1}	kN m^{-2}	kN m^{-2}		cm^3 s^{-1}	kN m^{-2}	kN m^{-2}	
300 - 205 - 300	20	141	411	101	296	301	1.41	825	365	183	208	2083	253	224	625
300 - 240 - 350	20	141	411	101	291	350	1.21	825	365	183	242	2083	253	224	727
300 - 275 - 400	21	136	394	102	304	401	1.06	825	356	193	276	1545	226	200	698
300 - 310 - 450	22	131	379	101	298	445	0.95	830	365	186	310	1540	219	197	781
300 - 340 - 500	20	141	411	99	292	494	0.86	825	363	183	338	1545	222	197	837
300 - 370 - 550	23	126	366	100	296	540	0.79	825	362	184	373	1543	218	195	955

Summary of Results

Run Title	$K^{\infty} + \Delta K$ (max.)		Separating Section		Purge Section	H.E.T.P. (ave.)	Concentration Profile Analysis				
	'A'P	'G'P	$\frac{G_{min}}{L'}$	$\frac{G_{max}}{L'}$	$\frac{S_{min}}{L'}$		Figure	Time to recorded analysis	Product Purities 1('A'P)	Product Purities 2('G'P)	Comments
						mm		hr	%	%	
300 - 205 - 300	170	477	162	323	590	9.9	8.13a	8.0	> 99.8	-	'A'P profile covers entire separating section.
300 - 240 - 350	162	582	189	376	688	10.2	8.13b	8.5	> 99.8	> 99.2	Incomplete purging - slight contamination of Product 1.
300 - 275 - 400	153	516	223	411	658	10.7	8.13c	11.0	> 99.9	> 99.9	
300 - 310 - 450	147	550	242	475	747	10.1	8.13d	6.67	> 99.8	> 99.9	
300 - 340 - 500	164	520	262	519	802	10.9	8.13e	9.0	> 99.7	> 99.9	Slight contamination of Product 1 by trace leading edge of 'G'P.
300 - 370 - 550	140	580	288	568	905	-	8.13f	6.75	> 96.5	> 99.9	Leading edge of 'G'P contaminating Product 1.

Figure 8.13a Standardised Concentration Profile for Run 300 - 205 - 300

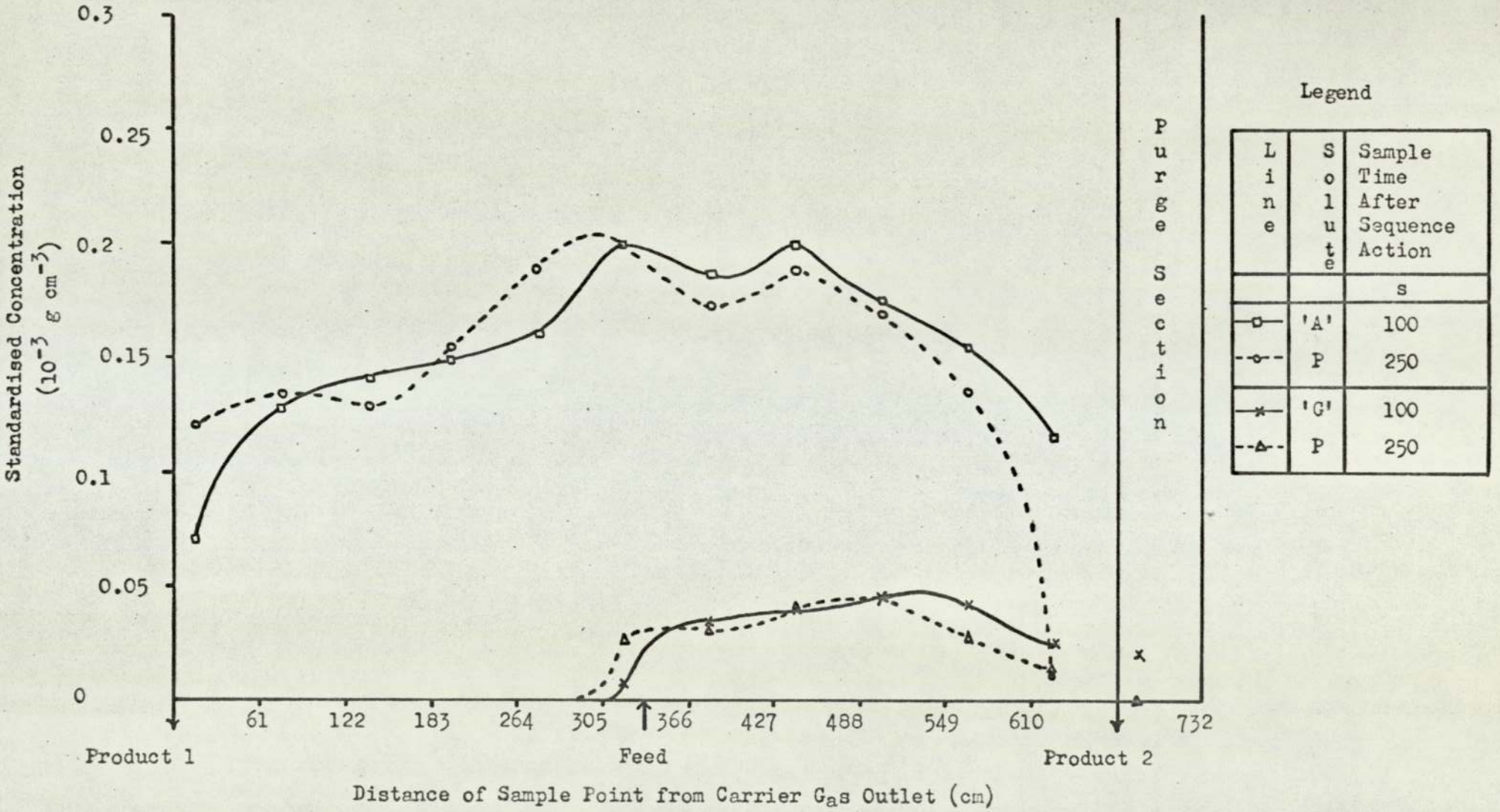

Figure 8.13b Standardised Concentration Profile for Run 300 - 240 - 350

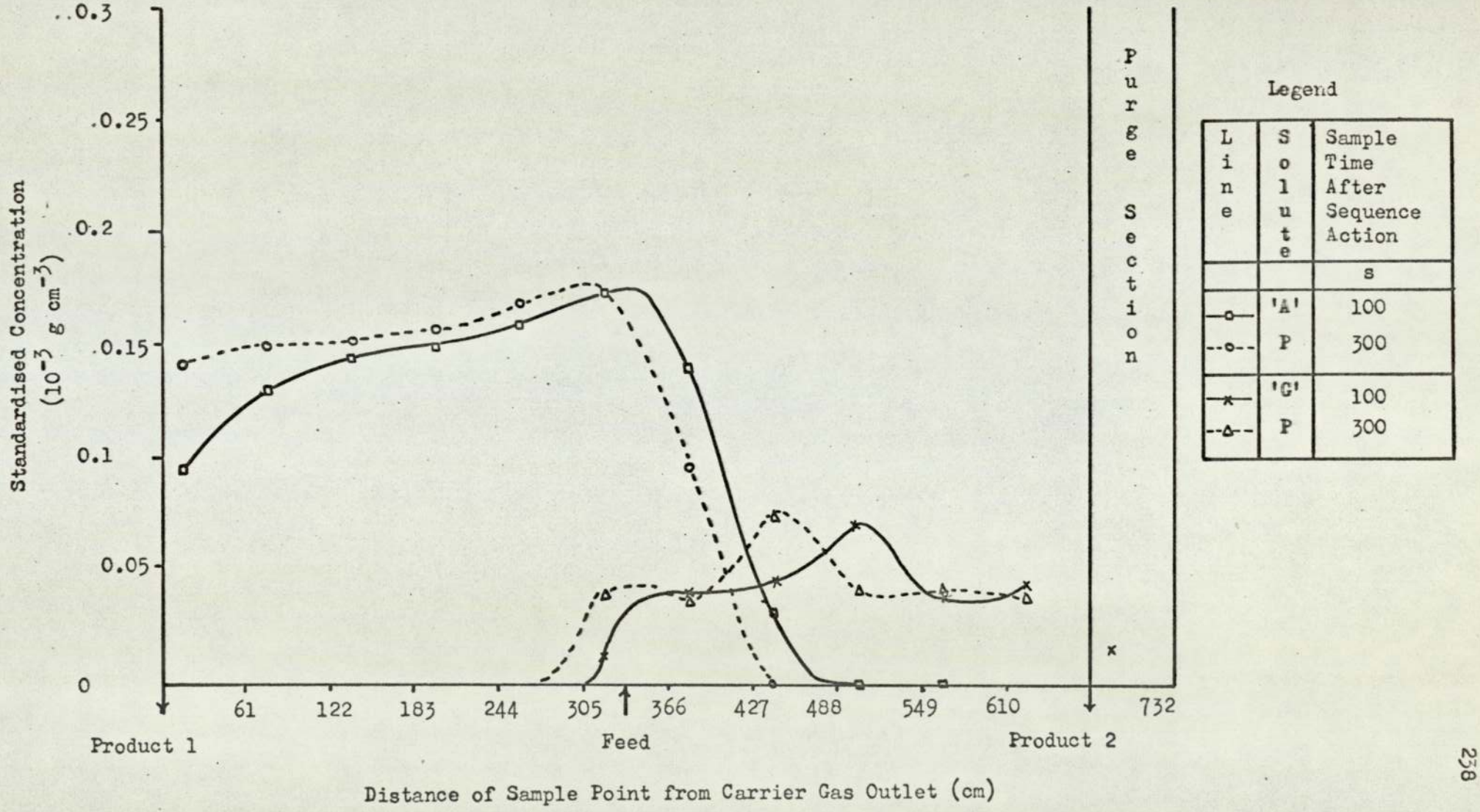

Figure 8.13c Standardised Concentration Profile for Run 300 - 275 - 400

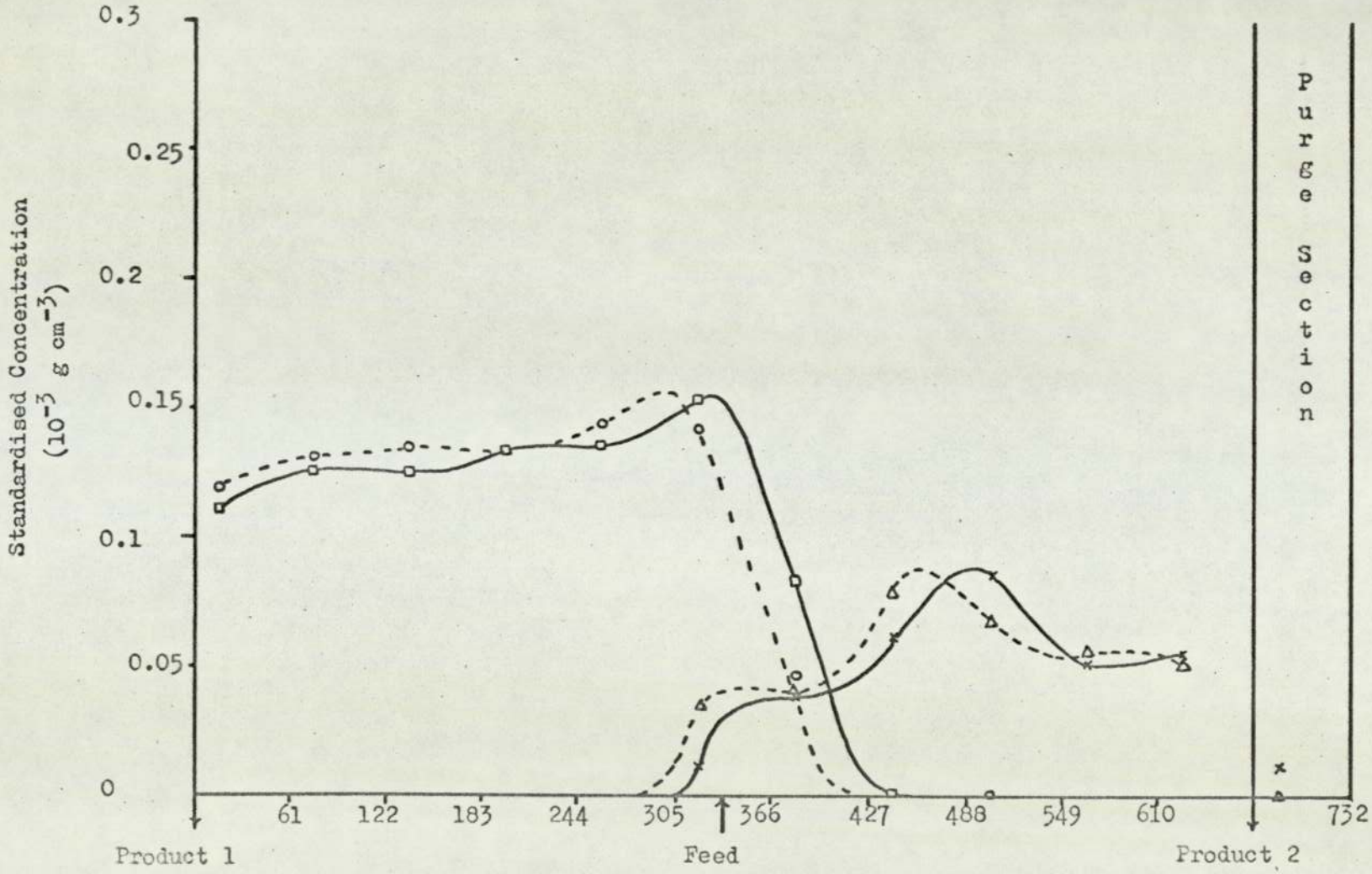

Legend

Line	Solute	Sample Time After Sequence Action
		s
—o—	'A'	150
--o--	P	350
—x—	'G'	150
--Δ--	P	350

Figure 8.13d Standardised Concentration Profile for Run 300 - 310 - 450

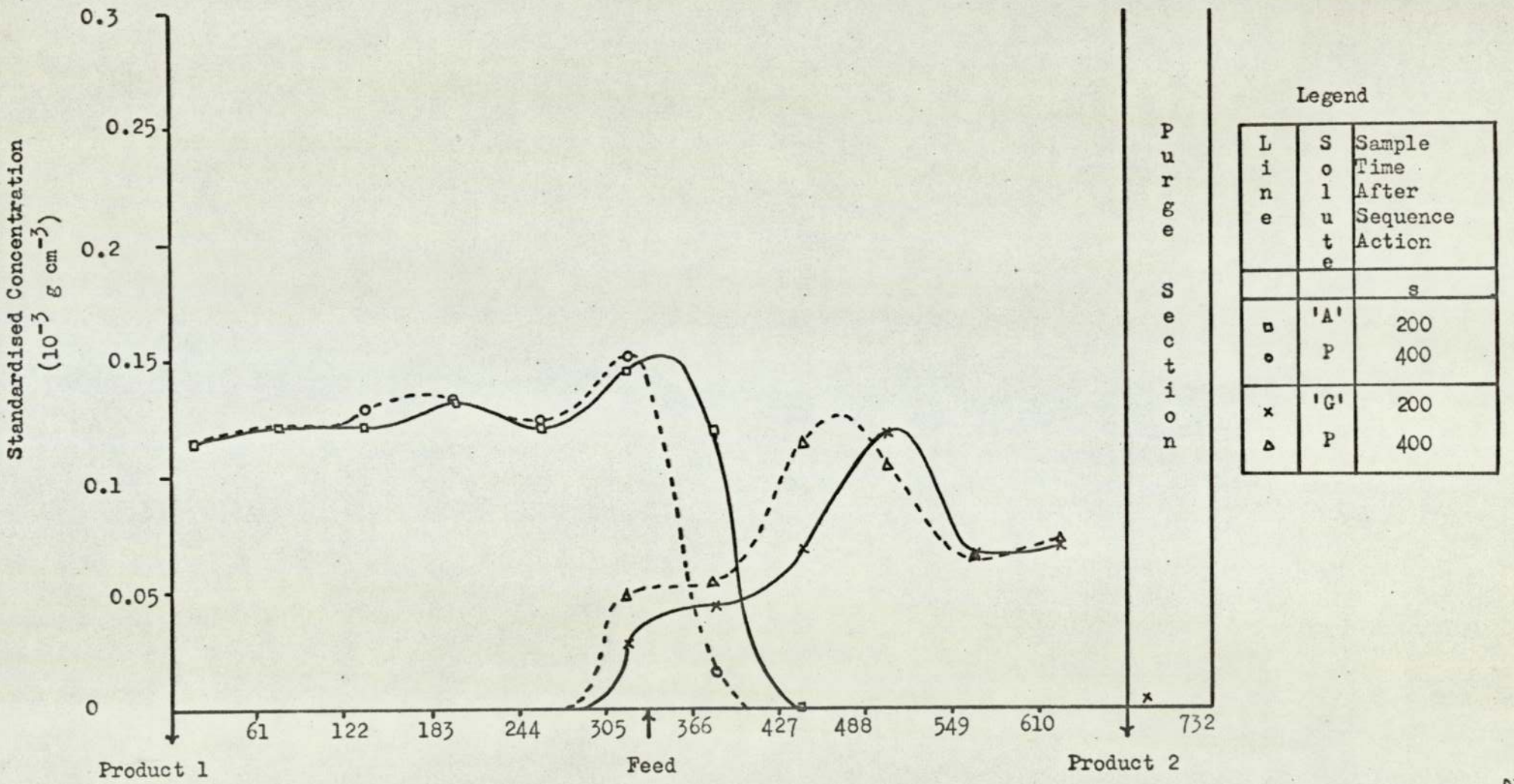

Legend

Line	Solute	Sample Time After Sequence Action
		s
□	'A'	200
○	P	400
×	'G'	200
△	P	400

Figure 8.13e Standardised Concentration Profile for Run 300 - 340 - 500

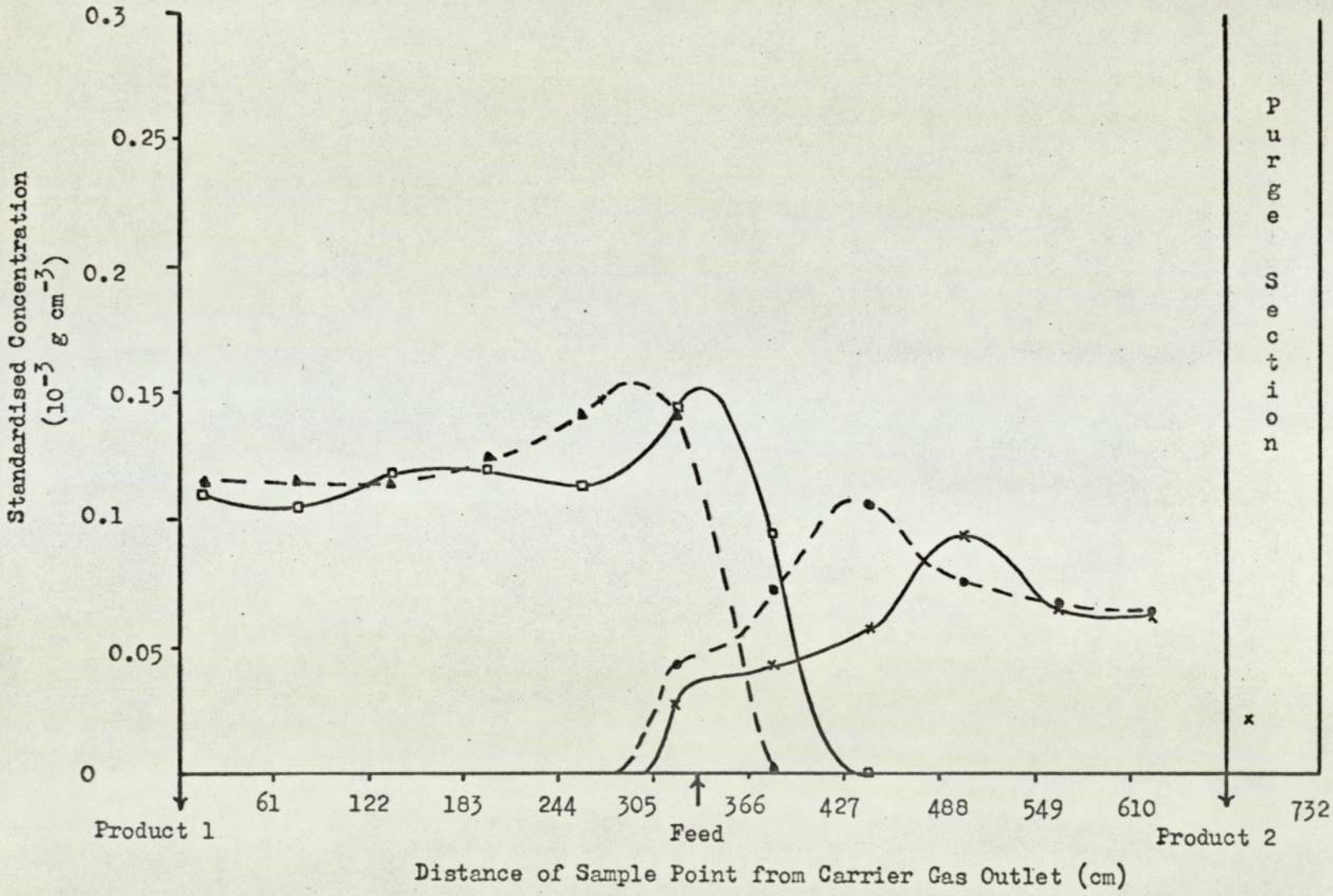

Legend

Line	Solute	Sample Time After Sequence Action
		s
—□—	'A'	150
—▲—	P	450
—×—	'G'	150
—●—	P	450

Note: Only 2 curves plotted for clarity.

Figure 8.13f Standardised Concentration Profile for Run 300 - 370 - 550

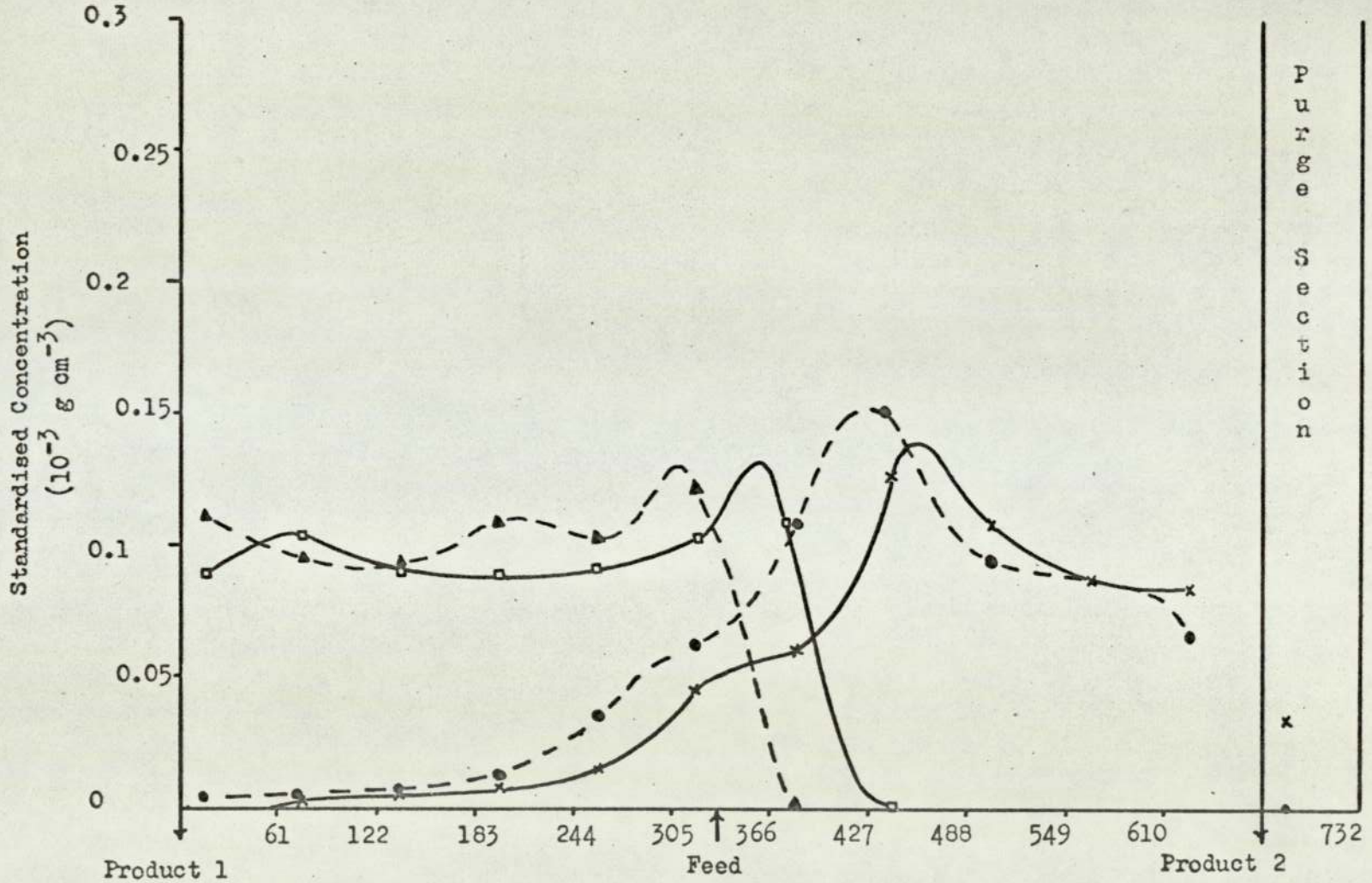

Legend

Line	Solute	Sample Time After Sequence Action
		s
—□—	'A'	100
—▲—	P	500
—×—	'C'	100
—●—	P	500

Note: Only 2 curves plotted for clarity.

8.4 Concluding Discussion of the Separation Studies

Equations 6.15 and 6.16 have served as an adequate guide to the interpretation of the experimental results. Four factors have been identified as restricting the separation power of the sequential unit, namely;

(i) the increase in the respective solute partition coefficients with finite concentrations.

(ii) the additional variation of the solute molecule velocity through the separating section with both solute concentration and the inevitable pressure gradient.

(iii) the finite length of the separation section or, to be exact, the finite number of theoretical plates.

(iv) the semi-continuous nature of operation.

Factors (i) and (ii) appeared to be the most significant for the comparatively easy separation of the binary equivolume mixture 'Arklone' P/'Genklene' P. The maximum throughput achieved which gave two products of purity in excess of 99.7% was 700 cm^3 hr^{-1}.

Considering other chemical systems having similar absorption chacteristics, as the separation difficulty is increased (i.e. separation factor approaches unity), the potential throughput of the unit in its present form will be substantially reduced. From the observed performance four possible changes can be suggested to improve potential capacity.

A larger sized solid support would reduce the pressure drop, for a given flowrate, across the separating section and hence reduce the

variation in the point values of the gas to apparent liquid rate ratio. The associated increase in H.E.T.P. with increased particle size could be counteracted by an improved packing technique or the use of flow homogenisers.

As the effect of pressure on partition coefficients is generally negligible below about 1000 kN m^{-2} the level of column operating pressure could be set at a higher value. The cross-column variation in volumetric gas flowrate would be relatively reduced while the solute capacity of the gas phase would be increased. Care must be taken in selecting the pressure conditions for the present unit to ensure that the restrictions imposed by the solenoid valves are strictly upheld.

As the temperature approaches the boiling point of a component the deviation of the absorption isotherm from linearity is reduced. Increasing the temperature reduces the partition coefficient. Lower values for the gas to apparent liquid rate ratio would be required, in particular lower gas flowrates, in view of the increased mobility of solute molecules. The advantage is that the cross-column pressure drop can be reduced without having to accept an increase in gas phase solute concentration. This must be balanced against a reduction in the value of the separation factor with increasing temperature.

The conclusion drawn by Conder (132) that the optimum temperature in production-scale gas/liquid chromatographic separations is close to the solute boiling points does not agree with the experimental results of Craven (131). He found that a temperature some 40°C below the boiling

points of α- and β- pinene gave maximum throughput on a 10 cm-diameter column.

Experimental study to determine the effect of temperature on separations performed on the sequential unit is required. A maximum ambient temperature of 55°C, dictated by the solenoid valves, is possible. Placing the unit in an oven would overcome a limitation of the experimental results reported here in that ambient temperature could be closely controlled. The on-column temperature profiles should also be recorded to gain insight into the magnitude of the 'enthalpic overloading' effect.

Finally the contamination of Product 1 as a result of incomplete regeneration of the isolated section could be counteracted by isolating two successive columns. The time interval for purging would therefore be twice the sequencing interval. Complete elution of the tail of the more strongly absorbed component could be ensured at lower purge gas flowrates, although this advantage is gained at the expense of the column length in the separating section.

The final choice of operating conditions would, in the industrial situation, be largely determined by economics. The provision of heating facilities and high pressures are obvious contributors to the capital and running costs of the equipment. Also, minimising the column concentration by the use of high carrier and purge gas flowrates must be balanced against the capital and running costs of the product recovery and gas recycle systems.

CHAPTER 9

Computer Simulation of the Sequential Unit

9.1 Introduction

Theoretical models of mass transfer processes are usually based on either the 'transfer unit' or 'equilibrium stage' concepts. Both concepts have been used to analyse counter-current chromatography.

Barker and Lloyd (11, 21) considered the counter-current chromatographic process to be equivalent to a conventional packed absorption tower with a central solute mixture feed point. For the case of straight 'operating' and 'equilibrium' lines they gave the following equation for the number of overall gas phase transfer units over a section of the column lying between the feed point and Product 1 offtake.

$$(N_{OG})_R = \frac{1}{G/(KL - 1)} \ln \left[\frac{E_1/KL - c_a(G/KL - 1)}{E_1/KL - c_b(G/KL - 1)} \right] \qquad 9.1$$

Analysis of a section lying between the feed point and Product 2 offtake gave:

$$(N_{OG})_S = \frac{1}{(1 - G/KL)} \ln \left[\frac{E_2/KL - c_a(1 - G/KL)}{E_2/KL - c_b(1 - G/KL)} \right] \qquad 9.2$$

where:

$(N_{OG})_R$, $(N_{OG})_S$ = the number of overall gas phase transfer units in the 'rectifying' and 'stripping' sections respectively

E_1, E_2 = the mass flowrate of solute leaving in the Product 1 and Product 2 streams respectively

c_a, c_b = the gas phase solute concentration at points a and b within the column, c_b being greater than c_a.

(Note: G and L, the gas and liquid volumetric flowrates and K, the partition coefficient, were defined here on a solute free basis).

Experimental studies on a 2.5 cm-diameter vertical moving-bed column with benzene, cyclohexane and methylcyclohexane as solutes and solvent phase polyoxyethylene 400 diricinoleate showed that the resistance to mass transfer essentially lay in the gas phase. A first order relationship was found between the logarithm of H_{OG} and the solvent phase flowrate, H_{OG} values for the systems and operating conditions studied were of the order of 10 cm (10, 11, 21).

Following the work of Fitch et al (148), Barker and Huntington (15, 16, 21) adapted the theory of stagewise liquid/liquid extraction given by Alders (186) to obtain a relationship between the difficulty of separation, the number of equilibrium stages and product purity. For a solute mixture feed point at the centre of the separating section the derived expression was

$$\log \frac{(G/L)_R}{(G/L)_S} = \log SF + \frac{2}{N_{cc}} \left[\log \left(1 - \frac{(E_i)_1}{\bar{f}_i} \right) + \log \frac{(E_{ii})_1}{\bar{f}_{ii}} \right] \qquad 9.3$$

where: $(G/L)_R$, $(G/L)_S$ = the ratio of gas to liquid phase flowrates in the 'rectifying' and 'stripping' sections respectively

SF = the separation factor $\frac{K_{ii}}{\bar{K}_i}$

N_{cc} = the total number of counter-current theoretical plates (stages) in the column

$(E_i)_1$, $(E_{ii})_1$ = the mass production rate of components i and ii as Product 1

f_i, f_{ii} = the mass feedrate of components i and ii to the column.

Barker and Huntington calculated H.E.T.P. values of approximately 5 cm when separating benzene and cyclohexane on the circular, moving-column unit described in Section 2.4.2.2.

It should be re-emphasised that a theoretical plate height determined from a counter-current stage model is not equivalent to the co-current plate height usually associated with elution chromatography. Rony (187 - 9) gives the relationship between these two plate definitions as

$$N_{cc} = \frac{N}{\sqrt{2\pi}} \frac{(1 + K_i)}{(u_m t / \sigma_l)} \qquad 9.4$$

where: N_{cc} = the number of counter-current theoretical plates or equilibrium stages

N = number of co-current theoretical plates (elution chromatography)

K_i = the partition coefficient for component i

u_m = the molar velocity of the mobile phase

t = time

σ_l = the length based variance of the peak in elution chromatography.

The derivation of equation 9.3 was based on the assumption that infinite dilution conditions prevailed within the column. To enable introduction of a non-linear absorption isotherm into the theoretical treatment of counter-current chromatography, Tiley (190) developed a computer program which performed a stage-to-stage calculation for a

vertical moving-bed column. The column operating conditions, number of equilibrium stages, the position of the feed point and ternary Margules constants were input as data. The calculation was repeated with successive guesses for the liquid phase composition at the feed stage until mismatch between the assumed and calculated values for this composition were eliminated.

Using approximate equilibrium data for such systems as benzene/cyclohexane and dimethoxymethane/dichloromethane on the solvent phase dinonyl phthalate Tiley was able to study the effect of stage number, flow conditions and temperature on the column concentration profiles. Two significant conclusions were drawn:

(i) There exists a limiting feed mixture throughput for a given solvent rate, product purity and number of stages which is dependent on the phase equilibrium characteristics. The experimental results from the sequential unit appear to substantiate this conclusion.

(ii) There is an optimum operating temperature just below the mean boiling points of the feed mixture.

Tiley also suggested that the existence of temperature or pressure gradients within the column could easily be introduced into the computer program.

In a subsequent paper, Pritchard et al (191) improved the predictive accuracy of the program by incorporating the Wilson equation for computing activity coefficients in the ternary liquid phase (two solutes plus solvent).

Sunal (58) developed a computer model of the moving-bed process based on the 'two film theory' of mass transfer. While the partition coefficient, pressure and temperature were assumed constant, the program included consideration of diffusion in the controlling gas phase. A comparison of experimental and predicted concentration profiles for the single solute system cyclohexane/polyoxyethylene 400 diricinoleate led to the conclusion that the effect of axial mixing on separation efficiency was negligible.

The four theoretical treatments of counter-current chromatography described above together with the statistically based model given by Sciance and Crosser (192) all inherently assumed a true steady state process. In the strict sense this assumption is only satisfied by the original continuous moving-bed system. For the sequential unit time must be introduced as an additional variable.

The experimental results emphasised that a realistic model of the sequential unit must also include the deleterious effects of solute concentration and a pressure gradient. Following Tiley, a digital computer program has been developed which, by means of a plate-to-plate computation, simulates operation of the unit in time. A similar approach has been used by Sunal (58) to describe the operation of the compact circular counter-current chromatograph reported in Section 2.4.2.2.

9.2 The Computer Model

9.2.1 Basis

For the duration of a sequencing interval the sequential unit operates as two separate batch columns with:

(i) a continuous feed entering at some point within the main separating section.

(ii) no solute feed being introduced into the initially solute rich purging section.

The essence of the programming approach was to impose the sequencing action onto a simple chromatographic plate model of these two sections.

9.2.2 Mass Balance Over a General 'Theoretical Plate'

A theoretical plate is defined as that volume element in which an equilibration of solute between the gas and liquid phase occurs. This is an empirical quantity and the theory does not deal with the mechanisms which determine its equivalent height. The limitations introduced by the use of a discontinuous plate model for the description of a continuous packed column are well appreciated.

For programming simplicity each of the twelve packed columns forming the unit is considered to consist of an equivalent number of theoretical plates, N. Let $v_{n(G)}$ and $v_{n(L)}$ be the volumes of the respective phases in a general plate, n, while c_n and q_n are the average gas and liquid phase concentrations of a single solute occurring in that plate over a small time increment $(t - \Delta t)$ to t. Let G denote the gas phase volumetric flowrate in the main separating section. The unit is assumed to operate isothermally.

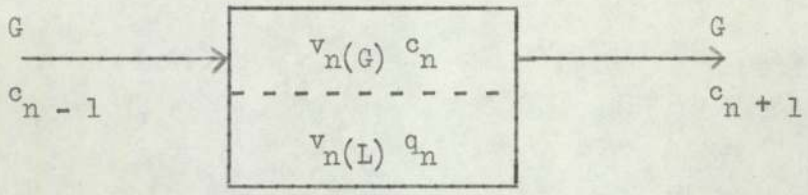

plate n

It is convenient at this stage in the development of the model to also assume that:

(i) the solute volume in the gas phase is negligible in comparison to the carrier gas volume; i.e. G is independent of solute concentration

(ii) no pressure change occurs on a plate; i.e. the values of G and $v_{n(G)}$, being in volumetric units, do not change across the column

(iii) the value of the partition coefficient is independent of solute concentration.

A mass balance over plate n for a small differential time element, d (Δt), within the small time increment (t - Δt) to t yields

$$G.c_{n-1} - G.c_n = v_{n(G)} \cdot \frac{d\,c_n}{d(\Delta t)} + v_{n(L)} \cdot \frac{d\,q_n}{d(\Delta t)} \qquad 9.5$$

Substituting $K.c_n = q_n$ and collecting c_n terms on the right hand side gives

$$G.c_{n-1} = G.c_n + (v_{n(G)} + K.v_{n(L)}) \cdot \frac{d\,c_n}{d(\Delta t)} \qquad 9.6$$

The term $(v_{n(G)} + K.v_{n(L)})$ is known as the 'effective plate volume', v_n (29).

Now, providing Δt is sufficiently small to allow c_{n-1} to be considered constant, integration of equation 9.6 yields

$$c_n = c_{n-1}\left(1 - e^{-\frac{G.\,\Delta t}{v_n}}\right) + c_{n(t-\Delta t)} \cdot e^{-\frac{G.\,\Delta t}{v_n}} \qquad 9.7$$

where: c_{n-1} = the average input gas phase concentration to plate n from the preceding plate in the small time increment $(t - \Delta t)$ to t

$c_{n(t-\Delta t)}$ = the initial condition

= the average gas phase concentration in plate n in the preceding time increment $(t - 2\,\Delta t)$ to $(t - \Delta t)$.

An equivalent equation to 9.7 is obtained for the purge section with G replaced by **S**, the purge gas volumetric flowrate.

Equation 9.7 is applicable to all plates in the unit for all time with the following exceptions:

(i) For the plate which is receiving the solute the feed concentration, c_F, is added to c_{n-1} to give the total input gas phase concentration to that plate.

(ii) For the first plate in either the purge or separating sections there is no input from the previous plate and, therefore, the equation simplifies to only one term as the right hand side.

A more general expression may be given as:

$$c_n = c_{input} \cdot \left(1 - e^{-\frac{G.\ \Delta t}{v_n}}\right) + c_{n(t - \Delta t)}\, e^{-\frac{G.\ \Delta t}{v_n}} \qquad 9.8$$

where: c_{input} = the total average input gas phase concentration to plate n in the small time increment $(t - \Delta t)$ to t

= 0 for the first plates in either the purge or separating sections

= $c_{n-1} + c_F$ for the feed plate

= c_{n-1} for all other plates.

Commencing from time zero, a plate to plate calculation for a single solute over a small time increment can be performed by substituting successive values of c_{input} into the appropriate form of equation 9.8. In the first time increment $c_{n(t - \Delta t)}$ is, of course, zero. The resultant concentration profile can then be updated by repeating the entire calculation for successive time increments, c_n in the first time increment becoming $c_{n(t - \Delta t)}$ in the second and so on.

9.2.3 Imposing the Sequencing Action onto the Plate to Plate Calculation

The close loop nature of the symmetrical unit permits three possible approaches when imposing the sequencing action onto the basic plate to plate calculation.

(i) The twelve linked columns can be considered stationary and the port functions advanced by N plates at the end of a sequencing interval (Fig 9.1a).

Figure 9.1 Diagramatic Representation of the Imposition of the Sequencing Mechanism onto the Plate to Plate Calculation

a) Columns Fixed, Ports Advanced

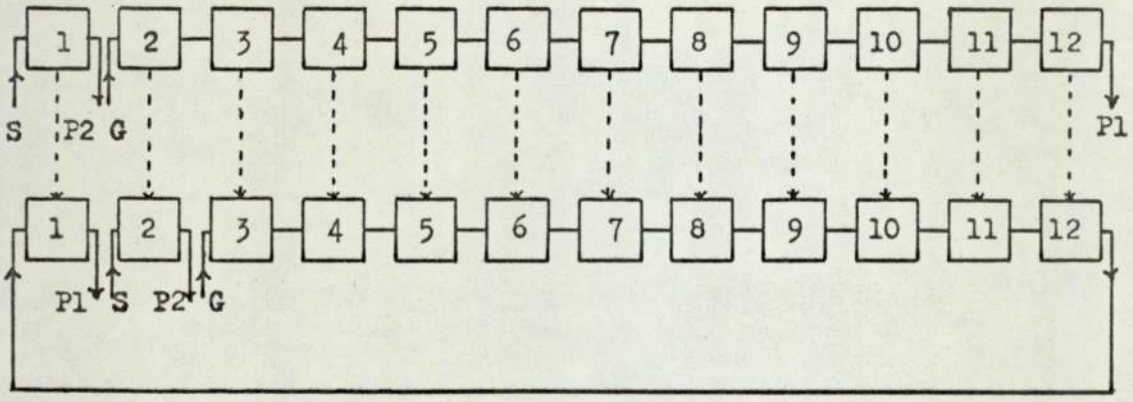

b) Ports Fixed, Columns Stepped Backwards

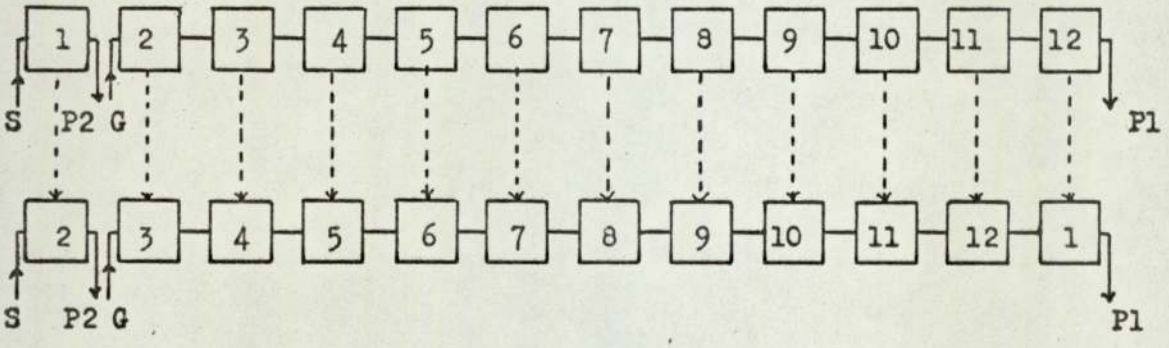

c) Ports and Columns Fixed, Concentration Profile Stepped Backwards

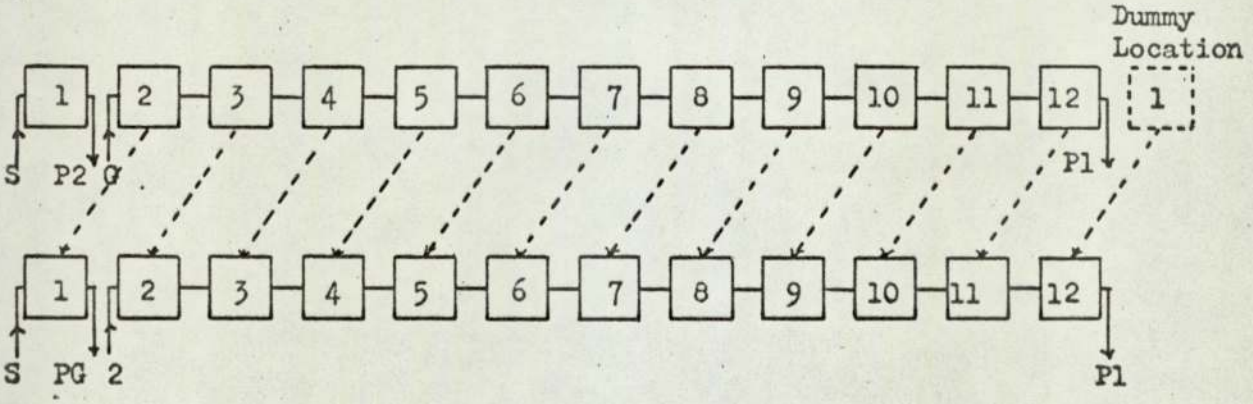

Legend: N = Column containing n plates

↑↓ = Port position

= Transfer of concentration profile

(ii) The port functions can be considered stationary and the columns of N plates stepped backwards by redefining the relative position of the plate number at the end of a sequencing interval (Fig 9.1b).

(iii) Both the columns and the port functions can be considered stationary and the concentration profile stepped backwards by N plates at the end of a sequencing interval.

Although (i) describes the operating system in practise, approach (iii) was found easier to program and was, therefore, adopted.

Numbering the theoretical plates from 1 to 12 N then, for all time:

(i) Plates 1 to N represents the isolated section. Purge gas enters at plate 1 and exits, as Product 2, from plate N. Hence

$$c_{input} = 0 \text{ when } n = 1 \qquad 9.9$$

(ii) Plates N + 1 to 12 N form the main separating section. Carrier gas enters plate N + 1 and exits, as Product 1, from plate 12 N. Hence

$$c_{input} = 0 \text{ when } n = N + 1 \qquad 9.10$$

The gas stream leaving the final plate in a column is taken as the input to the first plate in the subsequent column, save for the above noted exceptions. It has, therefore, been assumed that no change in the gas phase solute concentration occurs when the gas stream passes through the transfer line linking two consecutive columns.

For simplicity, it was also assumed that the solute feed was introduced as vapour onto a single plate in the centre of a column, F_c, lying between columns 2 and 12. Hence

$$c_{input} = c_{n-1} + c_F \text{ for } n = (F_c - 1)\, N + {}^{N}/_{2} + 1 \qquad 9.11$$

Sequencing occurs when the entire plate to plate calculation has been performed for a specified number of small increments. Before the calculation proceeds, the relative position of the solute concentration profile is adjusted by putting

$$c_n = c_{(n - N)} \text{ for } N + 1 \leqslant n \leqslant 12.N \qquad 9.12$$

and

$$c_n = c_{(n + 11.N)} \text{ for } 1 \leqslant n \leqslant N \qquad 9.12$$

The latter equality follows from the fact that, for the practical closed loop system, the isolated column becomes the final column in the main separating section.

Substituting the redefined plate concentrations for $c_{n(t - \Delta t)}$ into equation 9.8 during the first time increment after sequencing effectively imposes the port movement onto the plate to plate calculation.

9.2.4 The Introduction of a Second Solute

The above description of the computer model has considered only one solute to be present in the sequential unit. A second solute is included by duplicating the calculation at each plate with different variable names for the respective solute concentrations ($c_{n(i)}$, $c_{n(ii)}$) and partition coefficients (K_i, K_{ii}). The assumption being made is that the solute concentration profiles are independent.

9.2.5 The Introduction of Solute Concentration Effects

Two solute concentration effects have been introduced into equation 9.8:

(i) For each plate a value is calculated for the gas flowrate

(G_n, S) which includes the contribution made by the presence of both species of solute molecules in the gas phase. For the main separating section

$$G_n = G^o \cdot \left[1 + M_v \cdot \left(\frac{c_{n(i)}}{M_i} + \frac{c_{n(ii)}}{M_{ii}}\right)\right] \qquad 9.14$$

where: G^o = the volumetric flowrate of solute free carrier gas

M_v = the molar volume at the column operating temperature

M_i, M_{ii} = the respective molecular weights for solutes i and ii.

(ii) As a consequence of a non-linear absorption isotherm the relationship between the partition coefficient and gas phase concentration for the solutes 'Arklone' P and 'Genklene' P on the silicone fluid solvent phase was found to be curved (Fig 6.6). A series of tests with a standard 'least squares fit' computer library routine showed the relationship for each solute to be accurately expressed by a third order polynomial. The polynomial constants at each temperature between 19 and 24°C are given in Table 9.1. Therefore, rather than K being considered a constant it is calculated from

$$K_i = a_{i(i)} + a_{1(i)}c_{n(i)} + a_{2(i)}c_{n(i)}^2 + a_{3(i)}c_{n(i)}^3 \qquad 9.15$$

If the above concentration dependent terms were introduced directly into equation 9.8 as a function of c_n then a trial and error computation would be required. To avoid such a time consuming requirement a dummy variable, c_d, is defined which is taken to be the closest known value to

Table 9.1 Constants for the Relationship $K = a_o + a_1 c + a_2 c^2 + a_3 c^3$

a) For 'Arklone' P

Temperature	a_o	a_1	a_2	a_3	Range of c
°C	x 10^3	x 10^5	x 10^7	x 10^{11}	10^{-3} g cm^{-3}
19	0.1477	0.4400	-0.4141	0.1718	0-1.67
20	0.1424	0.4079	-0.3440	0.1482	0-1.73
21	0.1364	0.3731	-0.3073	0.1243	0-1.81
22	0.1321	0.3498	-0.2728	0.1090	0-1.87
23	0.1268	0.3223	-0.2419	0.0926	0-1.95
24	0.1224	0.3000	-0.2168	0.0802	0-2.02

b) For 'Genklene' P

Temperature	a_o	a_1	a_2	a_3	Range of c
°C	x 10^3	x 10^6	x 10^9	x 10^{12}	10^{-3} g cm^{-3}
19	0.4382	0.3587	0.1135	1.143	0-0.47
20	0.4207	0.3212	0.2523	0.5514	0-0.30
21	0.4038	0.3116	0.5322	0.6900	0-0.50
22	0.3878	0.2875	0.0469	0.7398	0-0.53
23	0.3726	0.2653	0.0418	0.6300	0-0.55
24	0.3581	0.2454	0.0337	0.5444	0-0.57

c_n at a particular point in time.

Hence

$$c_d = c_{input} \quad \text{for } n \neq 1 \text{ or } N+1 \qquad 9.16$$

$$c_d = c_{n(t - \Delta t)} \quad \text{for } n = 1 \text{ or } N+1 \qquad 9.17$$

The latter equality is introduced as c_{input} equals zero for the first plate in either the purge or main separating sections.

Equations 9.14 and 9.15 become

$$G_n = G^o \cdot \left[1 + M_v \left(\frac{c_{d(i)}}{\overline{M}_i} + \frac{c_{d(ii)}}{\overline{M}_{ii}} \right) \right] \qquad 9.18$$

$$K_i = a_{o(i)} + a_{1(i)} c_{d(i)} + a_{2(i)} c^2_{d(i)} + a_{3(i)} c^3_{d(i)} \qquad 9.19$$

Analogous expressions are used to calculate S_n and K_{ii}.

9.2.6 The Introduction of a Pressure Gradient

The basic equation for the plate to plate calculation, equation 9.8, was simplified by the assumption that no change in pressure occurred across either the purge or separating sections of the unit. In practise a significant pressure gradient existed. Indeed, it was concluded from the experimental results that the consequent variation in volumetric gas flowrate had a detrimental effect on the separation process. A pressure gradient has therefore been introduced into the simulation.

It is assumed that the pressure drop along each section is directly proportional to the distance from the point of gas entry. Hence the average plate pressure, P_n, can be expressed as a function of plate number

(i) For the purge section ($1 \leqslant n \leqslant N$)

$$P_n = P_{in} - \left(\frac{P_{in} - P_o}{N} \right) \cdot (n - 0.5) \qquad 9.20$$

(ii) For the main separating section $(N + 1 \leqslant n \leqslant 12.N)$

$$P_n = P_i - \left(\frac{P_{in} - P_o}{11.N} \right) \cdot (n - N - 0.5) \qquad 9.21$$

where: P_{in}, P_o = the respective inlet and outlet pressures to the purge and main separating sections.

The point concentration values used to plot the experimental concentration profiles were adjusted to a standard pressure. As it is proposed to compare the experimental and simulated results it was convenient to compute the concentration profiles on the same basis

Equation 9.8 can be written:

$$c_{n(std)} \cdot \frac{P_n}{P_{std}} = c_{input(std)} \cdot \frac{P_n}{P_{std}} \left[1 - e^{\left(\frac{- G_{n(std)} \cdot \frac{P_{std}}{P_n} \cdot \Delta t}{v_{n(std)}} \right)} \right] + c_{n(t - \Delta t)(std)} \cdot \frac{P_n}{P_{std}} \cdot e^{\left(\frac{- G_{n(std)} \cdot \frac{P_{std}}{P_n} \cdot \Delta t}{v_{n(std)}} \right)} \qquad 9.22$$

where: $v_{n(std)} = v_{n(G)(std)} \cdot \frac{P_{std}}{P_n} + K \cdot v_{n(L)}$

K = a third order polynomial in $c_{d(std)} \cdot \frac{P_n}{P_{std}}$

subscript std = the value of the respective terms at a standard pressure.

For the purge section $G_{n(std)}$ is replaced by $S_{n(std)}$. Thus the concentration profiles for solutes i and ii generated by successive plate

to plate calculations based on equation 9.22 includes a correction for the pressure gradients within the sequential unit yet is recorded at a standard pressure.

9.2.7 The Program

A detailed flow chart of the computation is given as Fig 9.2. The listing of the program, written in Fortran IV, is given in Appendix 6. Definitions of variable names and explanatory 'comments' relating the program to the above text are included in the flow chart.

Figure 9.2 Flowchart for the Computer Simulation of the Sequential Unit.

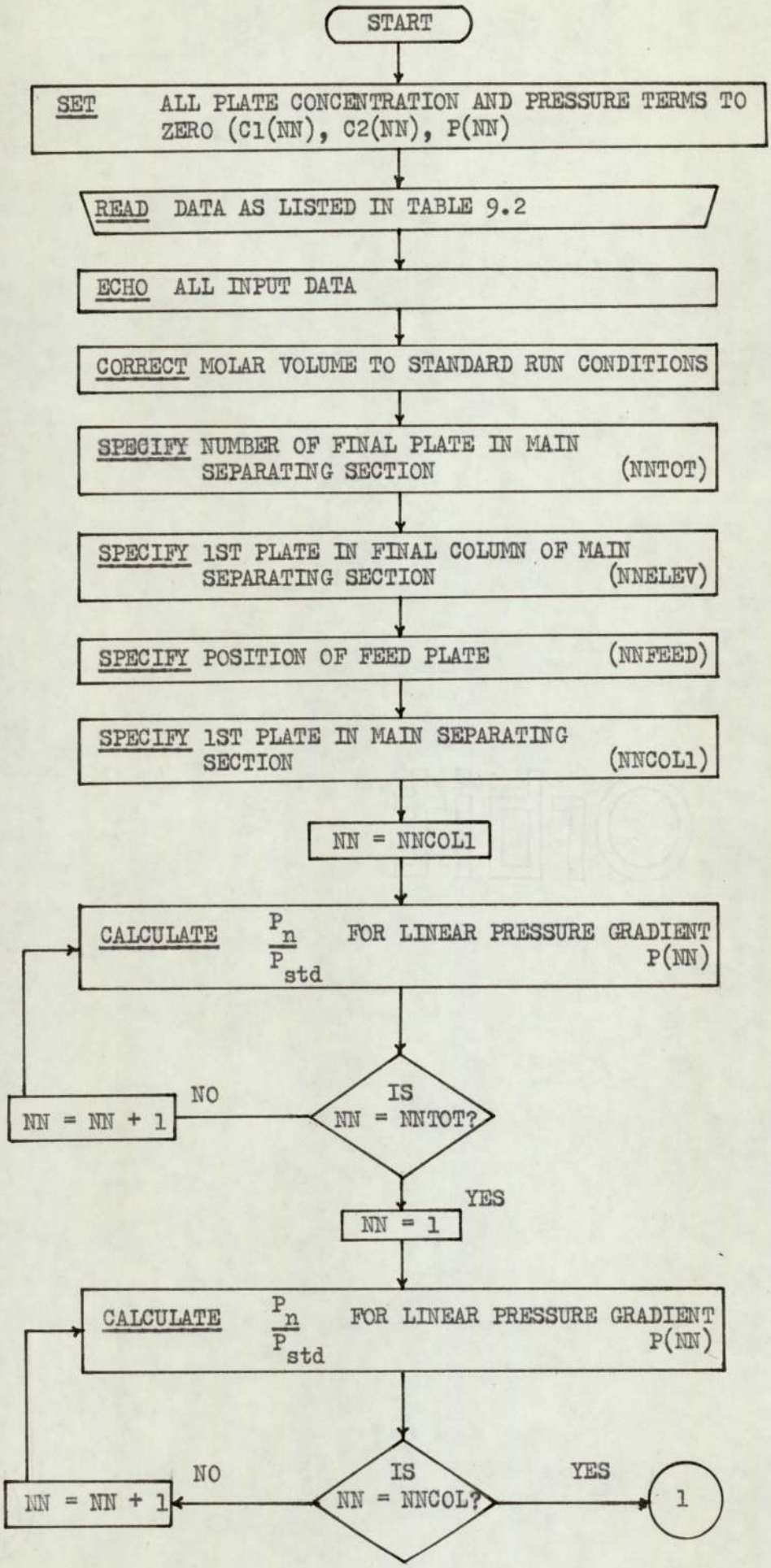

Figure 9.2 (Cont'd.)

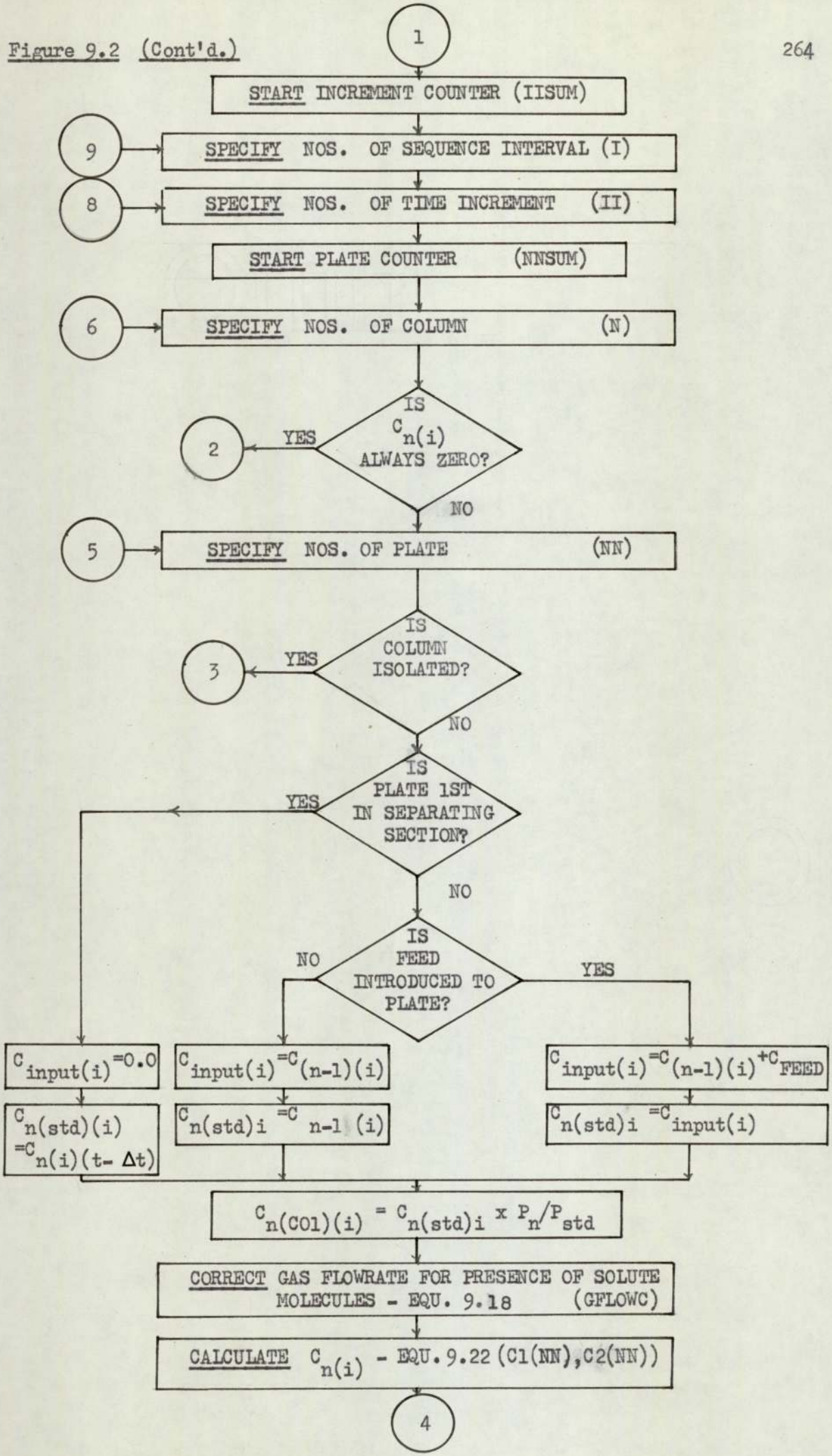

Figure 9.2 (Cont'd.)

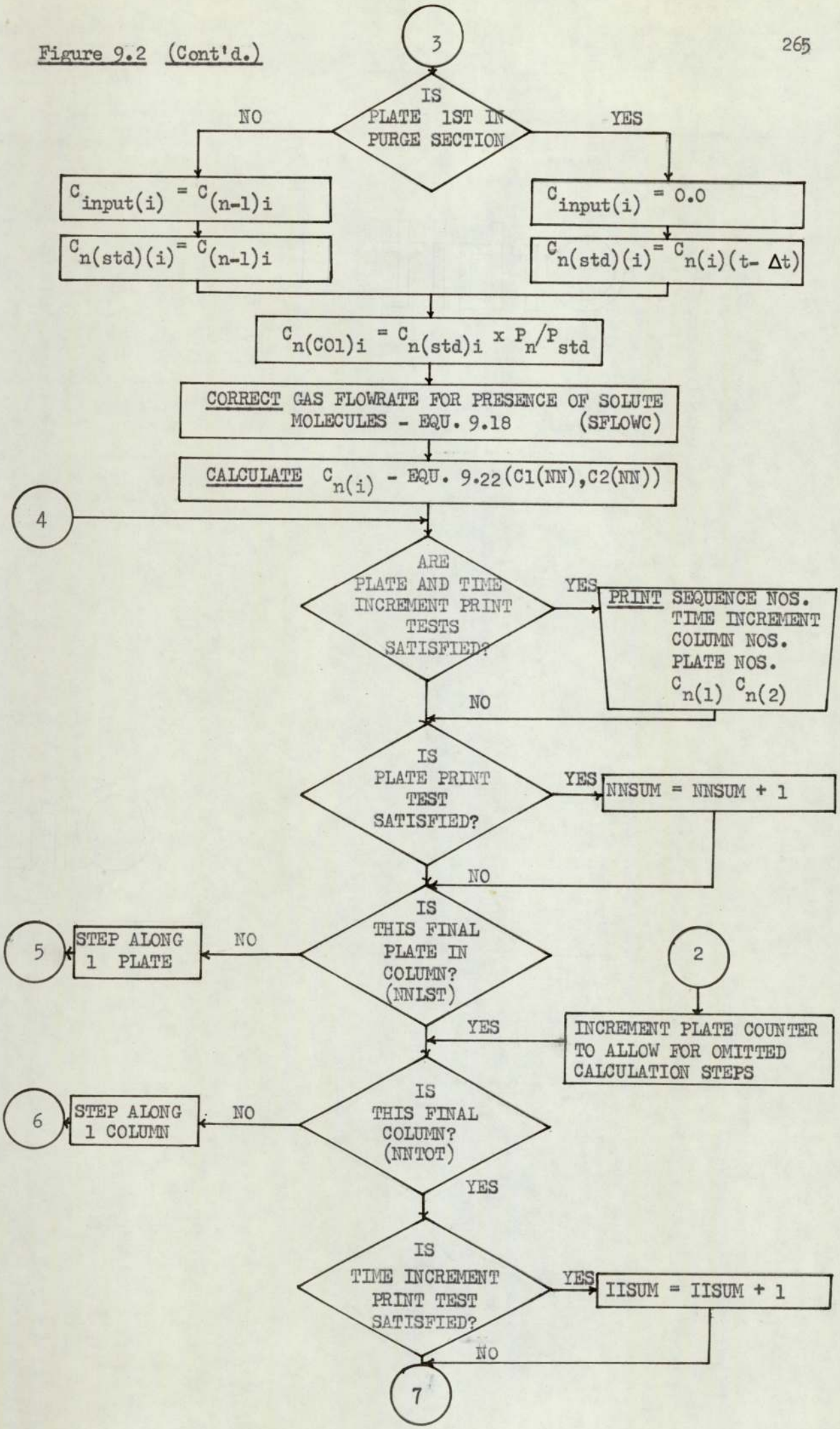

Figure 9.2 (Cont'd.)

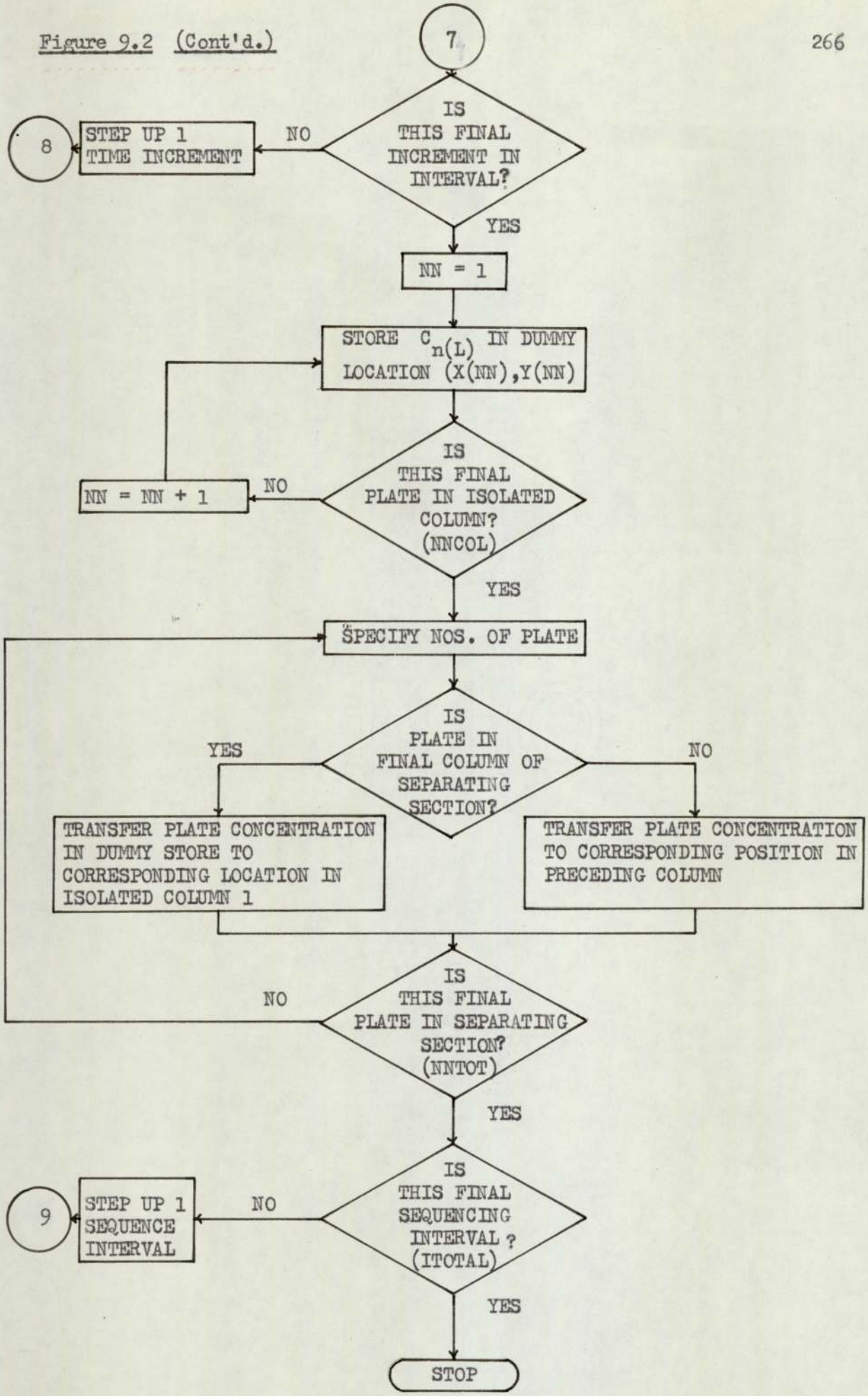

9.3 Results

If the number of theoretical plates per column is defined as 40 and the length of a small time increment defined as 1.0 s then, for a binary feed, 24,000 plate calculations must be performed per 300 s sequencing interval. Consequently, running the program on the departmental Honeywell 316 computer required approximately one hour of computing time to simulate the operation of the sequential unit for one sequencing interval. As a 'pseudo-steady state' condition was not reached by the 'Genklene' P concentration profile until at least sixteen sequences had occurred, the total computation time was generally 16-20 hrper run.

Attention has been focussed on a single experimental run, Run 300 - 275 - 300. The experimental operating conditions and concentration profile are represented for comparison as Fig 9.3.

Eight simulation runs have been performed to date. A summary of the input date for each run is given in Table 9.2.

The pure carrier gas flowrate at standard pressure, G^{o}_{std}, differs slightly from the experimental value as it has been corrected for the concentration of solute, 0.8×10^{-4} g cm^{-3} of 'Arklone' P, in the stream when measured. As the purge gas stream was solute free when the flowrate was measured no correction to S^{o}_{std} was required.

The gas phase volume per plate, $v_{n(G)(std)}$, was calculated by dividing the experimentally measured average dead volume per column (Table 5.4) by the assumed number of theoretical plates per column, N. Similarly, $v_{n(L)}$ was obtained by dividing the average measured volume of solvent phase per column (Table 5.2) by N.

The respective standardised solute feed concentrations were calculated from

$$c_{F(i)(std)} = \text{volumetric feedrate per second} \times \frac{\rho_i}{G^o_{std}}$$

A record of the build-up of the respective solute concentration profiles was obtained from a print-out of the current standardised solute concentrations in both the central and final plates of each column at 100 s intervals.

With Run 1 providing a standard, the effect of independently changing four variables on the computed solute concentration profiles has been studied.

(i) For Runs 1, 2 and 3 the length of a small time increment, Δt, was respectively 1, 2 and 0.5 s.

(ii) For Runs 1, 4 and 5 the number of theoretical plates per column, N, was respectively 40, 30 and 20.

(iii) For Runs 1, 6 and 7 the column temperature was respectively 23, 22 and 20°C.

(iv) For Runs 1 and 8 the combined equivolume solute feedrate was respectively 300 and 600 $cm^3\ hr^{-1}$.

In general only the standardised concentration profiles 100 s after sequencing have been plotted (Figs 9.4a - h). However, for Run 1 (Fig 9.4a) additional profiles at 200 and 300 s are plotted to show the progress with time of the two solutes through the unit. The number of sequencing intervals which had been simulated before a 'pseudo-steady' condition was established by each solute profile is also recorded.

Figure 9.3 Standardised Concentration Profile for Run 300 - 275 - 300

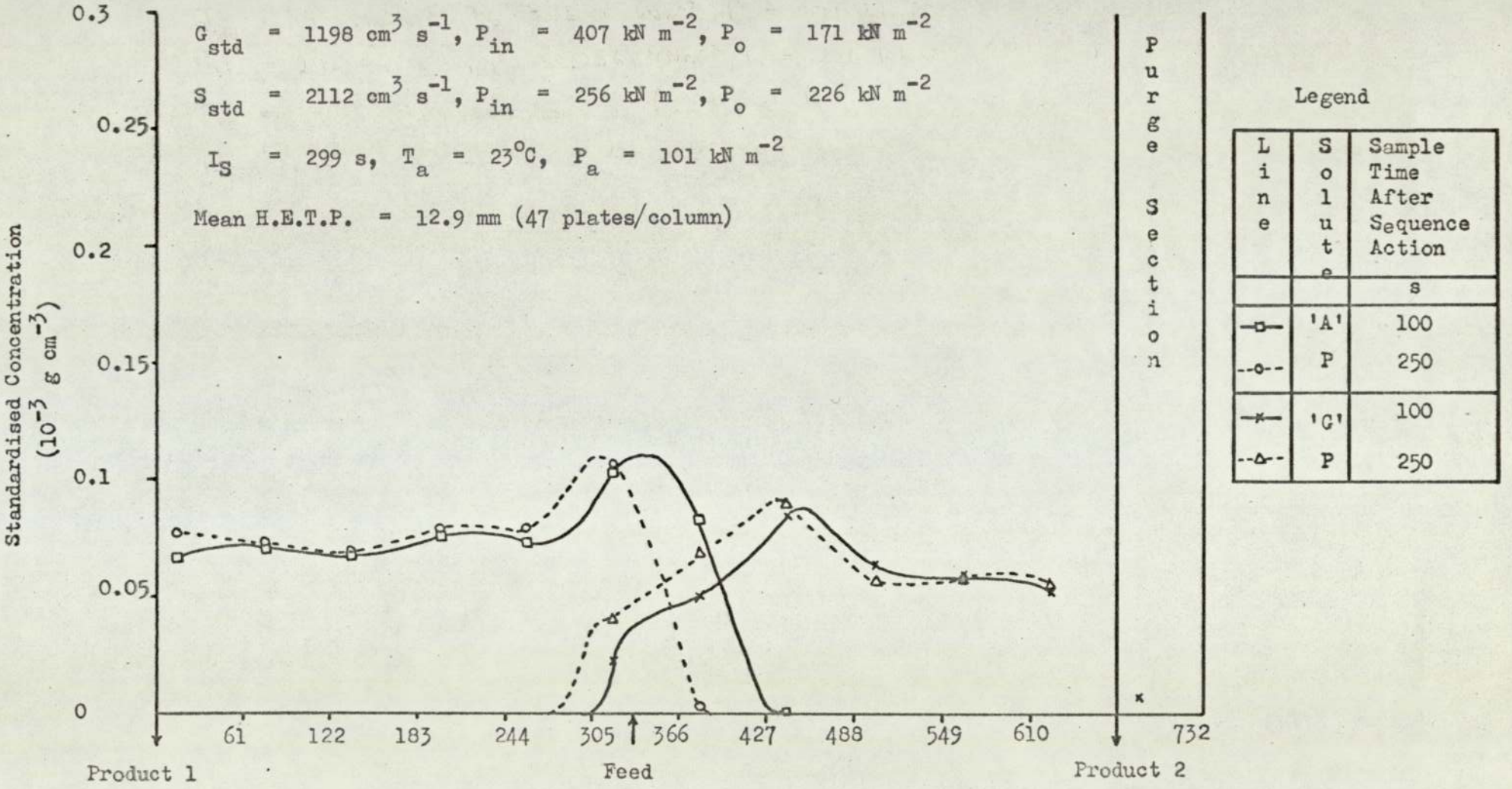

Table 9.2 List of Variables Together with their Values for the Eight Computer Simulation Runs

(Variables changed from Run 1 are underlined)

Variable	Symbol	Units	Program Name	Value							
				Run 1	Run 2	Run 3	Run 4	Run 5	Run 6	Run 7	Run 8
Volumetric flowrate at standard pressure of solute free carrier gas											
i) Main separating section	G^{o}_{std}	$cm^3\ s^{-1}$	GFLOW	1186.0	1186.0	1186.0	1186.0	1186.0	1186.0	1186.0	1186.0
ii) Purge Section	S^{o}_{std}	$cm^3\ s^{-1}$	SFLOW	2112.0	2112.0	2112.0	2112.0	2112.0	2112.0	2112.0	2112.0
Gas volume per plate at standard pressure	$V_{n(G)(std)}$	cm^3	VG	47.9	47.9	47.9	<u>63.9</u>	<u>95.8</u>	47.9	47.9	47.9
Liquid volume per plate	$V_{n(L)}$	cm^3	VL	10.8	10.8	10.8	<u>14.4</u>	<u>21.6</u>	10.8	10.8	10.8
Feed concentrations at standard pressure											
i) Solute i	$C_{F(i)(std)}$	$g\ cm^{-3}$ $(x10^{-4})$	CFEED1	0.5538	0.5538	0.5538	0.5538	0.5538	0.5538	0.5538	<u>1.1076</u>
ii) Solute ii	$C_{F(ii)(std)}$	$g\ cm^{-3}$ $(x10^{-4})$	CFEED2	0.6455	0.6455	0.6455	0.6455	0.6455	0.6455	0.6455	<u>0.9310</u>
Length of small time increment	Δt	s	DT	1.0	<u>2.0</u>	<u>0.5</u>	1.0	1.0	1.0	1.0	1.0

Table 9.2 Cont'd.

Variable	Symbol	Units	Program Name	Value							
				Run 1	Run 2	Run 3	Run 4	Run 5	Run 6	Run 7	Run 8
Number of column into which solute feed is introduced	F_c	-	NFEED	7	7	7	7	7	7	7	7
Number of theoretical plates per column	N	-	NNCOL	40	40	40	30	20	40	40	40
Total number of sequencing intervals in run	-	-	ITOTAL	24	24	24	24	24	24	24	24
Number of small time increments per sequencing interval	-	-	IIDNI	300	150	600	300	300	300	300	300
Number of small time increments per print-out	-	-	IITYPE	100	50	200	100	100	100	100	100
Number of theoretical plates per print-out	-	-	NNTYPE	20	20	20	15	10	20	20	20

Table 9.2 Cont'd.

Variable	Symbol	Units	Program Name	Value							
				Run 1	Run 2	Run 3	Run 4	Run 5	Run 6	Run 7	Run 8
Standard pressure	P_{std}	kN m^{-2}	PAMB	101.0	101.0	101.0	101.0	101.0	101.0	101.0	101.0
Inlet pressure to main separating section	P_{in}	kN m^{-2}	PING	407.0	407.0	407.0	407.0	407.0	407.0	407.0	407.0
Outlet pressure from main separating section	P_o	kN m^{-2}	POUTG	171.0	171.0	171.0	171.0	171.0	171.0	171.0	171.0
Inlet pressure to purge section	P_{in}	kN m^{-2}	PINS	256.0	256.0	256.0	256.0	256.0	256.0	256.0	256.0
Outlet pressure from purge section	P_o	kN m^{-2}	POUTS	226.0	226.0	226.0	226.0	226.0	226.0	226.0	226.0

Table 9.2 Cont'd.

Variable	Symbol	Units	Program Name	Value			
				Run 1	Run 2	Run 3	Run 4
Third order polynomial constants for computation of partition coefficient							
i) Solute i	$a_{0(i)}$	-	A01	0.1268×10^{3}	0.1268×10^{3}	0.1268×10^{3}	0.1268×10^{3}
	$a_{1(i)}$	-	A11	0.3223×10^{5}	0.3223×10^{5}	0.3223×10^{5}	0.3223×10^{5}
	$a_{2(i)}$	-	A21	-0.2419×10^{7}	-0.2419×10^{7}	-0.2419×10^{7}	-0.2419×10^{7}
	$a_{3(i)}$	-	A31	0.926×10^{10}	0.926×10^{10}	0.926×10^{10}	0.296×10^{10}
ii) Solute ii	$a_{0(ii)}$	-	A02	0.3726×10^{3}	0.3726×10^{3}	0.3726×10^{3}	0.3726×10^{3}
	$a_{1(ii)}$	-	A12	0.2653×10^{6}	0.2653×10^{6}	0.2653×10^{6}	0.2653×10^{6}
	$a_{2(ii)}$	-	A22	0.4177×10^{8}	0.4177×10^{8}	0.4177×10^{8}	0.4177×10^{8}
	$a_{3(ii)}$	-	A32	0.630×10^{12}	0.630×10^{12}	0.630×10^{12}	0.630×10^{12}
Molecular weight							
i) Solute i	M_i	-	MWT1	187.4	187.4	187.4	187.4
ii) Solute ii	M_{ii}	-	MWT2	133.4	133.4	133.4	133.4
Molar volume at 273 K and 101.3 kN m^{-2}	M_v	cm^3	MOLVOL	22414.0	22414.0	22414.0	22414.0
Column temperature		^{o}K	TAMB	296.0	296.0	296.0	296.0

Table 9.2 Cont'd.

Variable	Symbol	Units	Program Name	Value			
				Run 5	Run 6	Run 7	Run 8
Third order polynomial constants for computation of partition coefficient							
i) Solute i	$a_{0(i)}$	-	A01	0.1268×10^{3}	0.1321×10^{3}	0.1427×10^{3}	0.1268×10^{3}
	$a_{1(i)}$	-	A11	0.3223×10^{5}	0.3498×10^{5}	0.4079×10^{5}	0.3223×10^{5}
	$a_{2(i)}$	-	A21	-0.2419×10^{7}	-0.2728×10^{7}	-0.344×10^{7}	-0.2419×10^{7}
	$a_{3(i)}$	-	A31	0.926×10^{10}	0.109×10^{10}	0.1482×10^{10}	0.926×10^{10}
ii) Solute ii	$a_{0(ii)}$	-	A02	0.3726×10^{3}	0.3878×10^{3}	0.4207×10^{3}	0.3726×10^{3}
	$a_{1(ii)}$	-	A12	0.2653×10^{6}	0.2875×10^{6}	0.3212×10^{6}	0.2653×10^{6}
	$a_{2(ii)}$	-	A22	0.4177×10^{8}	0.4687×10^{8}	0.2523×10^{8}	0.4177×10^{8}
	$a_{3(ii)}$	-	A32	0.630×10^{12}	0.7398×10^{12}	0.5514×10^{12}	0.630×10^{12}
Molecular weight							
i) Solute i	M_i	-	MWT1	187.4	187.4	187.4	187.4
ii) Solute ii	M_{ii}	-	MWT2	133.4	133.4	133.4	133.4
Molar volume at 273 K and 101.3 kN m^{-2}	M_v	cm^3	MOLVOL	22414.0	22414.0	22414.0	22414.0
Column temperature		^{o}K	TAMB	296.0	295.0	293.0	296.0

Figure 9.4a Computer Simulation of Run 300 - 275 - 300

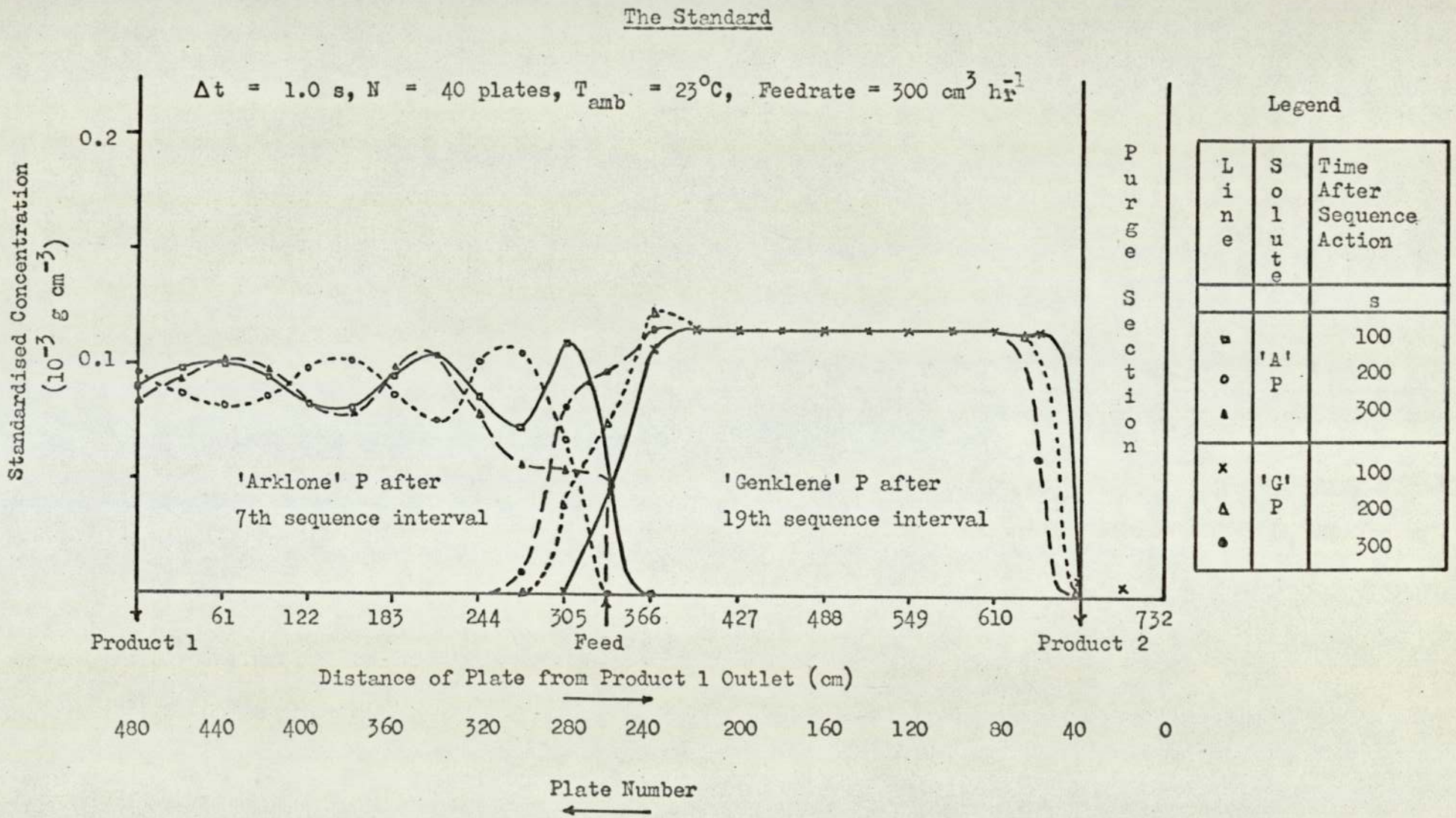

Figure 9.4b Computer Simulation of Run 300 - 275 - 300

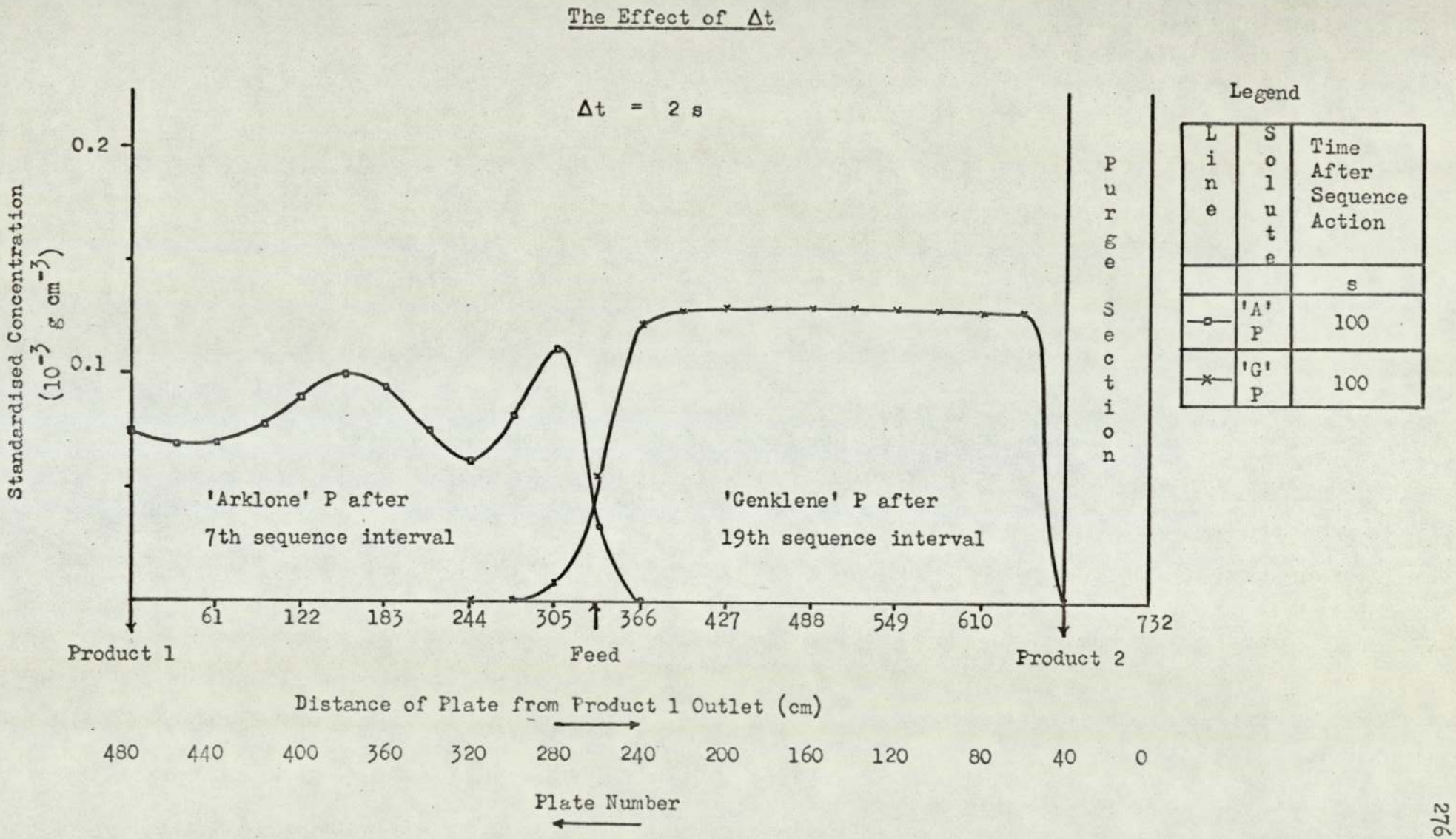

Figure 9.4c Computer Simulation of Run 300 - 275 - 300

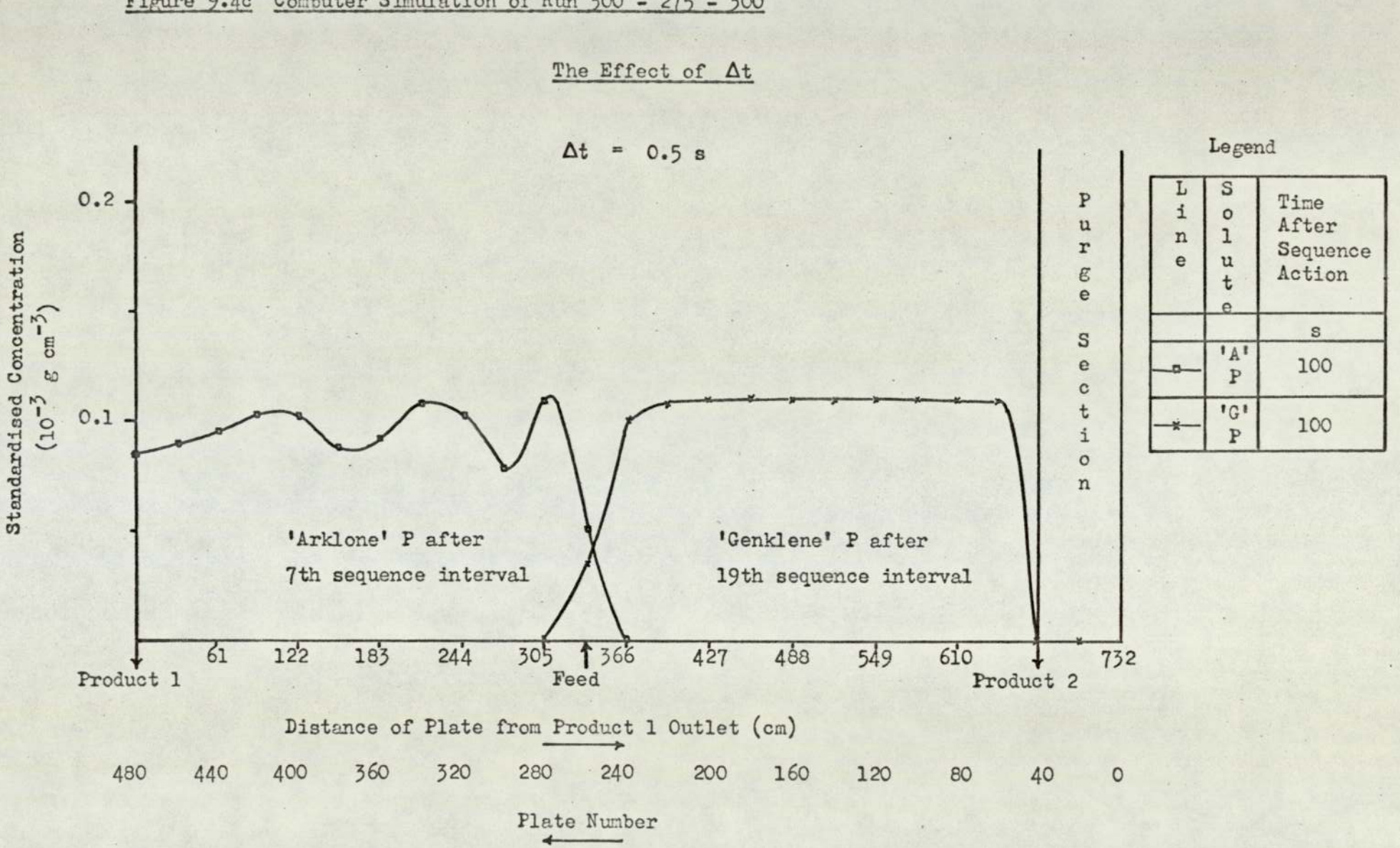

Figure 9.4d Computer Simulation of Run 300 - 275 - 300

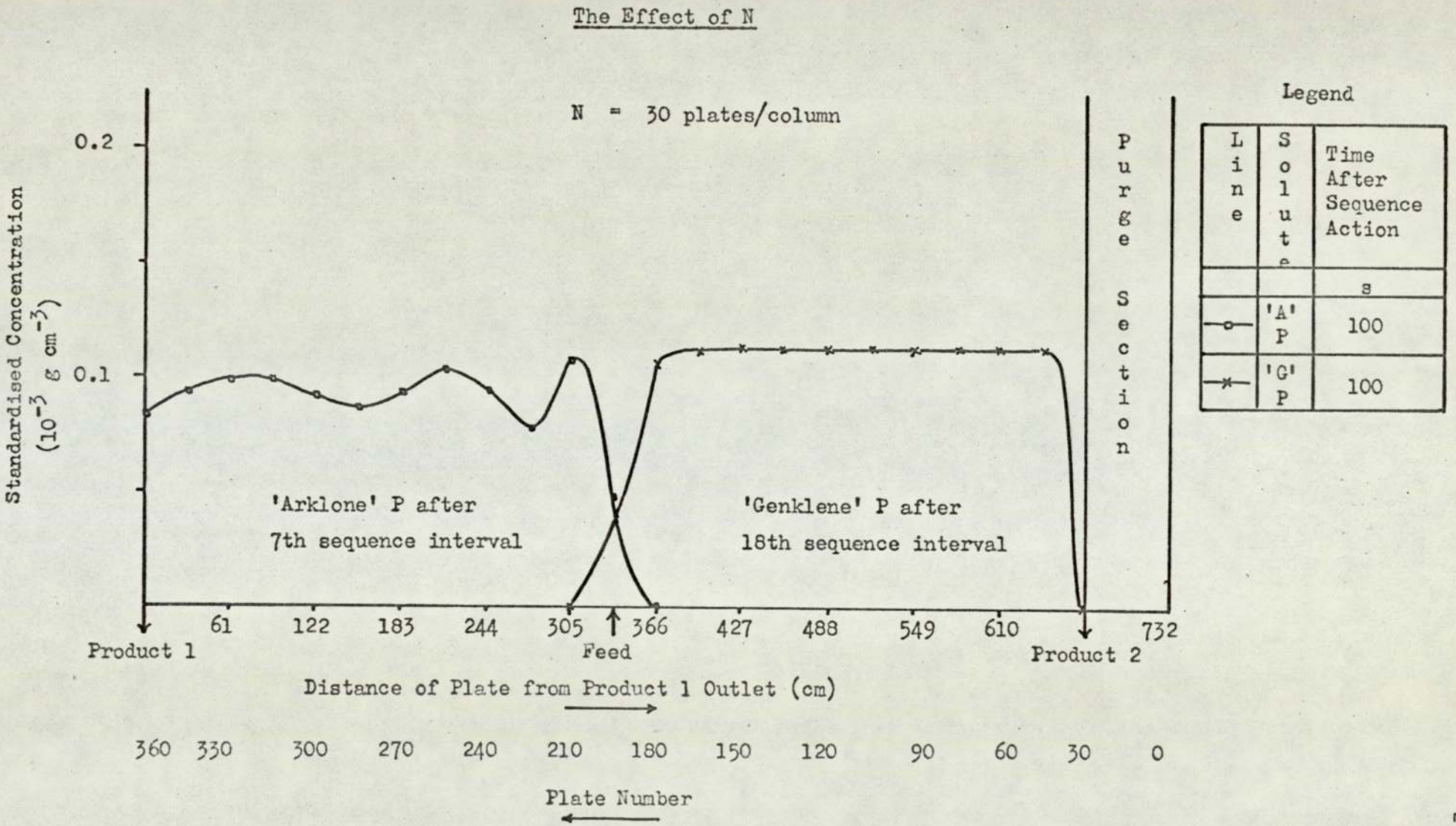

Figure 9.4e Computer Simulation of Run 300 - 275 - 300

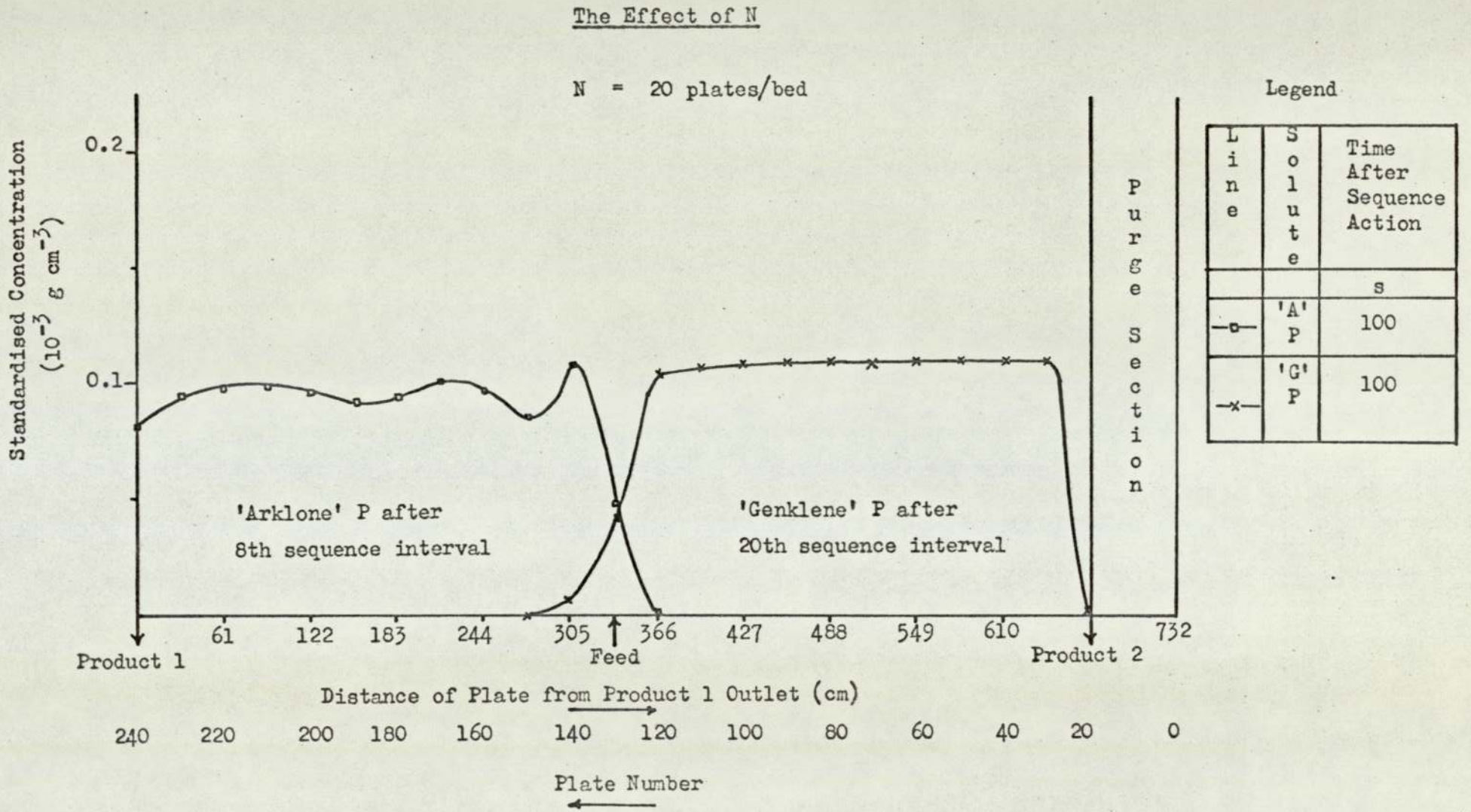

Figure 9.4f Computer Simulation of Run 300 - 275 - 300

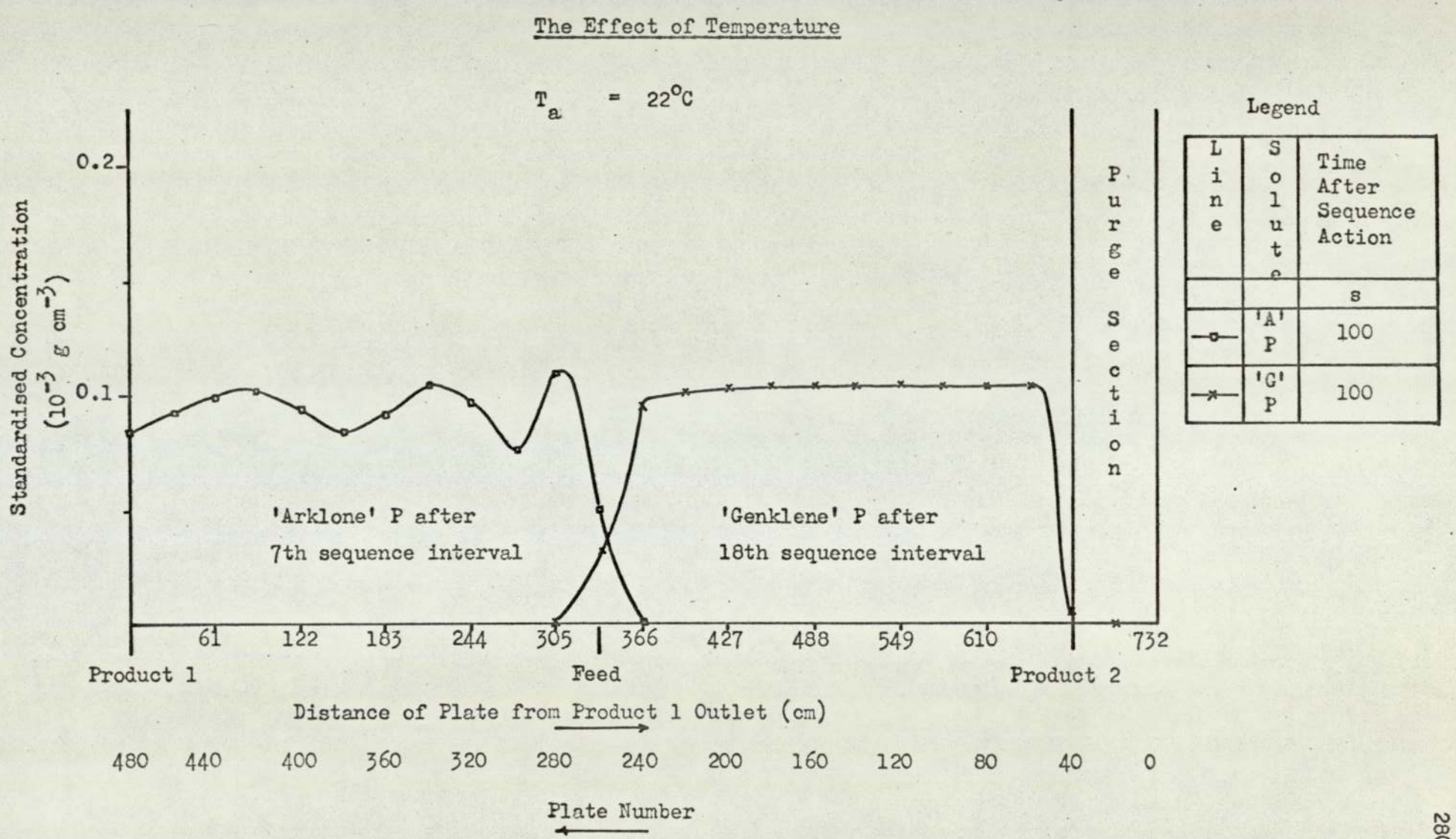

Figure 9.4g Computer Simulation of Run 300 - 275 - 300

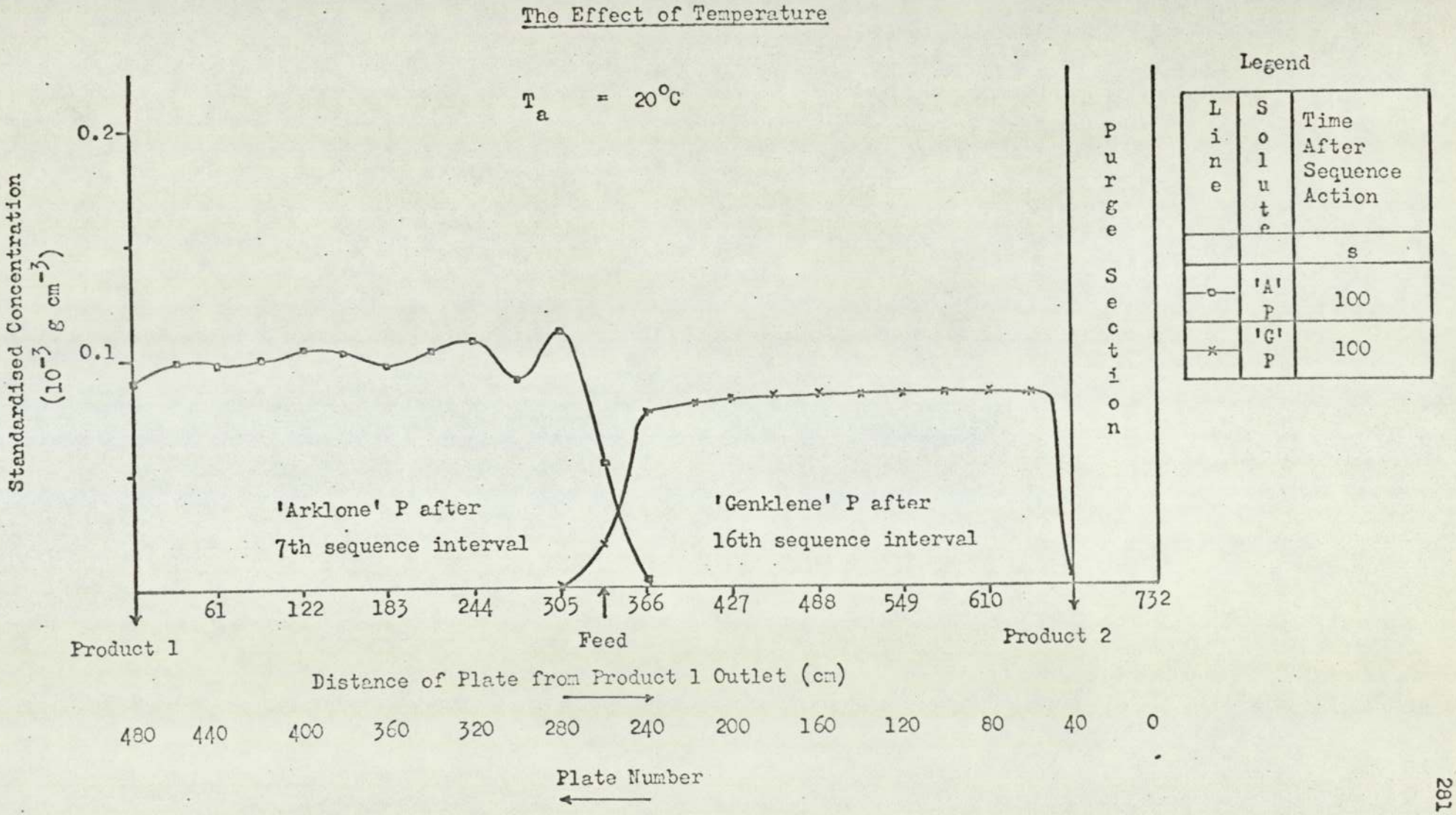

Figure 9.4h Computer Simulation of Run 300 - 275 - 300

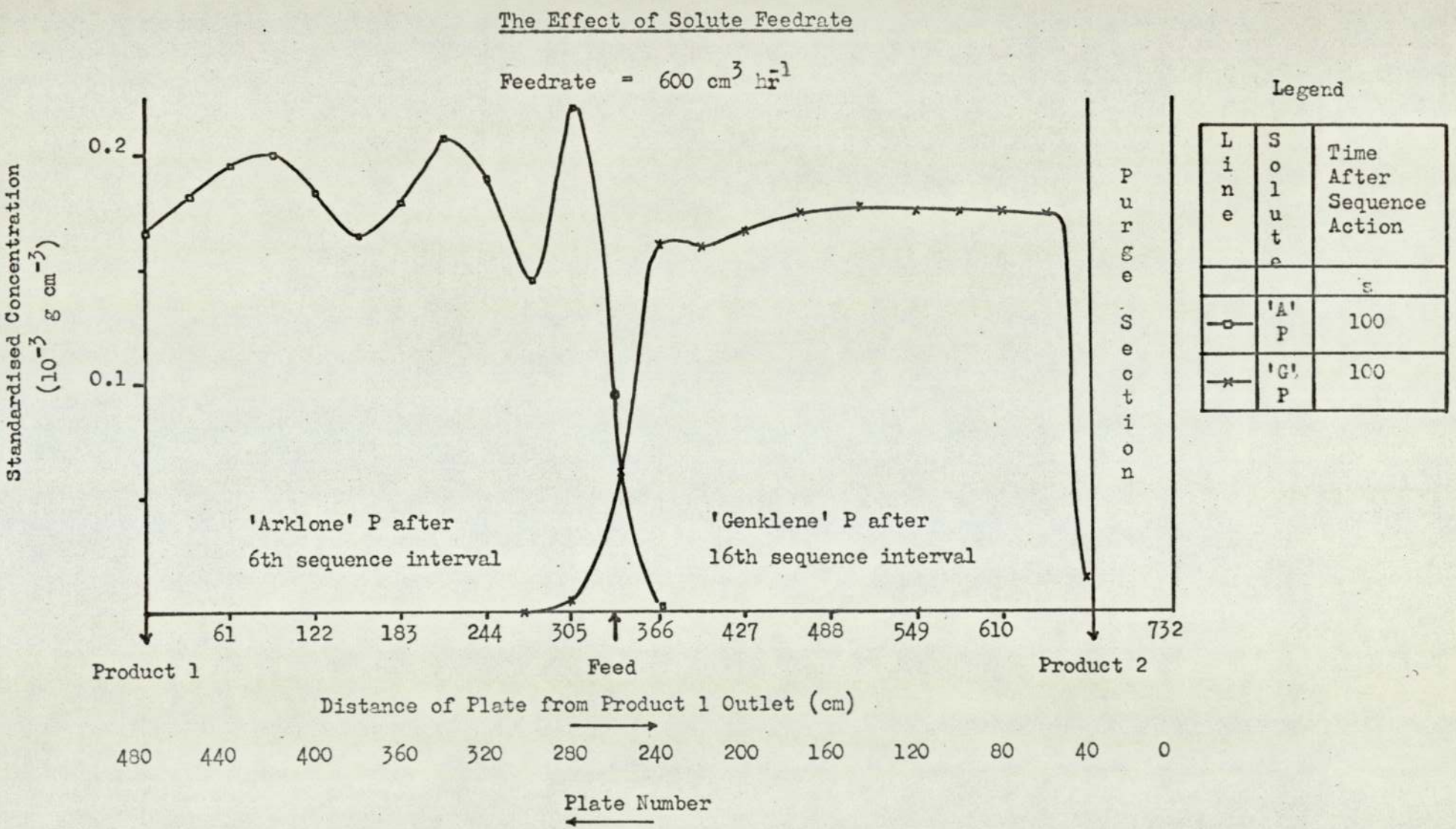

9.4 Discussion of the Results

9.4.1 The Effect of the Length of a Small Time Increment (Δt)

The mathematical development of the basic equation describing the change in gas phase solute concentration across a general plate was simplified by the assumption that, for a small time increment, the input to that plate could be represented by a constant average value. In practise the input solute concentration changes continually with time and the assumption will only be reasonable if Δt is small. However, the total computation time increases in inverse proportion to Δt. A compromise value was sought.

Comparing the solute concentration profiles 100 s after sequencing has occurred for Runs 1 and 2 (Figs 9.4a and b) shows that when Δt was increased from 1 to 2 s then both the plateau concentration for 'Genklene' P and the amplitude of the variation in the 'Arklone' P concentration were significantly increased. When Δt was reduced from 1 to 0.5 s, as in Run 3 (Fig 9.4c), little change in the level and form of the respective concentration profiles was observed. It can be concluded that $\Delta t = 1$ s represents a good compromise between computation time and accuracy.

9.4.2 The Effect of the Number of Theoretical Plates per Column (N)

As the number of theoretical chromatographic plates per column was reduced from 40 to 20, only a marginal change was noted in the concentration profiles (Figs 9.4a, d, e). This response is consistent with the experimental results, from which it was concluded that the number of plates was not a major factor in the successful separation of the system 'Arklone' P/'Genklene' P on the silicone fluid solvent phase. If the

operating conditions were selected closer to either limit for the G/L' ratio or the solute feedrate increased (i.e. the difficulty of separation increased) then the number of plates is expected to play a more important role.

It is interesting to note that the above conclusion is in agreement with that drawn for large scale 'batch' units employing repetitive injection (89, 132, 193).

9.4.3 The Effect of Column Temperature

As the temperature is reduced the value of the solute partition coefficients increase. Consequently the preference of the solutes to move in the direction of carrier gas flow within the sequential unit is decreased giving a greater 'hold-up' of 'Arklone' P, while that for 'Genklene' P falls.

This effect is clearly shown by Figs 9.4a, f and g. A $3^{o}C$ reduction in the assumed isothermal operating conditions results in the plateau of the standardised 'Genklene' P profile being reduced from 0.116 to 0.84 g cm^{-3}. For 'Arklone' P the increase in solute concentration with falling temperature was not so marked, reflecting the lower value of the partition coefficient relative to 'Genklene' P, although a definite decrease in the amplitude of the profile fluctuation was recorded.

The sensitivity of the concentration profiles to temperature is an important observation.

9.4.4 The Effect of Solute Feedrate

For Run 9 the solute feed concentrations were increased to give an equivalent combined volumetric feedrate of 600 cm^3 hr^{-1}. The effect on the

'Arklone' P profile was to approximately double the computed plate concentration values (Figs 9.4a and 9.4h). However, for 'Genklene' P, the concentration level of the plateau in the computed profile only increased by a factor of approximately 1.5 as the solute molecules exhibited an increased tendency to remain in the solvent phase and notionally move with that phase towards the isolated column at an increased rate.

This result shows that, as expected from Fig 6.6, the 'K' value for 'Genklene' P is more sensitive to solute concentration than 'Arklone' P.

9.4.5 The Accuracy of the Simulation

A comparison of the experimental (Fig 9.3) and computed concentration profiles leads to the following two criticisms:

(i) Poor agreement was obtained around the feed zone. In particular the computed profile for 'Genklene' P did not exhibit a distinct 'hump' as recorded experimentally

(ii) The establishment of a 'pseudo-steady' state condition during a simulated run was comparatively rapid.

It can be concluded that the model, despite correction for pressure and concentration effects, represents an idealised picture of the actual process taking place within the sequential unit. A more realistic simulation can be achieved by the removal of the several simplifying assumptions which have been made.

Each column was considered to contain an equivalent number of theoretical plates, N. The experimental measurements of N, reported in Chapters 5 and 8, show this was not the case in practise. However, the

effect of uniformly changing the plate number per column on the computed concentration profiles was marginal. Therefore, the additional computation time incurred is unlikely to warrant an extension of the program to permit N to vary from column to column. It should also be noted that, for an easy separation, the insensitivity of the concentration profiles to N implies that one object for the model cannot be met; i.e. the determination of the number of theoretical plates per column by a comparison of experimental and computed results.

An indication of the pressure gradient which existed across the main separating sections during the experimental run, Run 300 - 275 - 300, is given by plotting the pressure at the time of sampling against the distance of the sample point from the Product 1 outlet (Fig 9.5). While the graph is not a straight line, the error introduced into the model by assuming that P_n decreased in direct proportion to n was quite small. Again, the slight improvement in the simulation which would result from a more accurate definition of the pressure gradient (e.g. as a polynomial in n), together with an allowance for the pressure drop across the transfer lines, would have to be balanced against the corresponding increase in computation time.

A basic assumption to the model was that the column operates isothermally. The literature suggested that, in practise, both longitudinal and radial temperature fluctuations are to be expected across the unit as a result of the 'enthalpic overloading' effect (Section 6.1.2.4). In addition, the heat required to vaporize the liquid solute feed may lead to cooling around the feed point, particularly at high feedrates.

Figure 9.5 Pressure Profile for Run 300 - 275 - 300 100 s after Sequencing

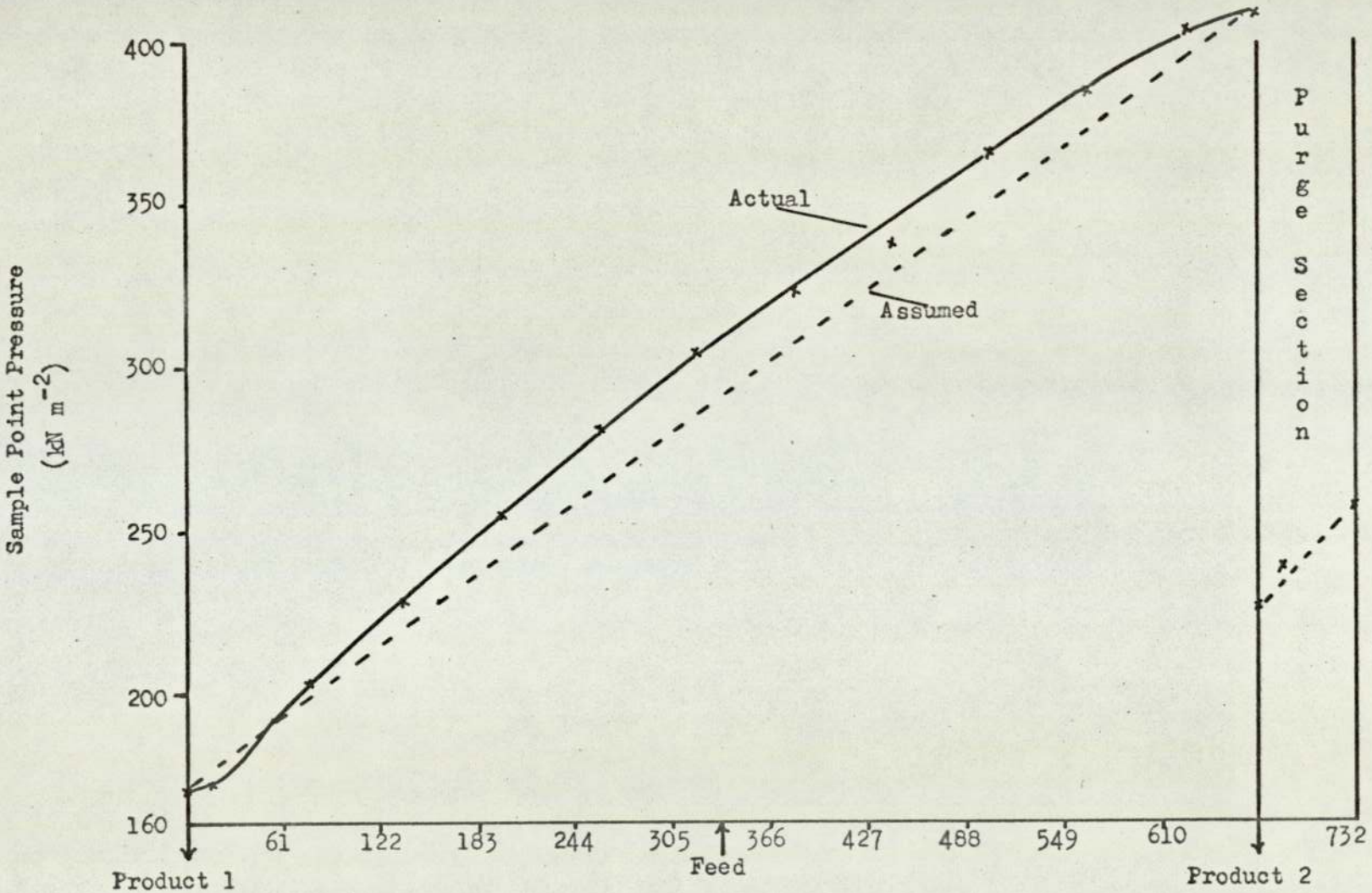

As the concentration profiles have been shown to be sensitive to temperature, the inclusion of an experimentally measured temperature profile in the model would appear to be a necessary improvement. Each plate temperature could be specified in a similar manner to the pressure gradient. The partition coefficients would then be defined in terms of both concentration and absolute temperature.

For the model, the solute feed was assumed to be introduced onto a single plate in the gas phase. The practical difficulty of maintaining the feed vaporized in the distribution network led to the feed being introduced in reality as a liquid. A wide feed zone could, therefore, result from two sources:

(i) Solute not instantly vaporized by the flowing carrier gas stream would tend to spread around the feed point.

(ii) On sequencing, liquid trapped in the internal cross distributor (Fig 3.4) would be relatively transferred to a point one column length behind the true feed point, where it would slowly vaporize.

The inaccuracy of the simulation around the feed point, which was magnified at an increased solute feedrate, suggests that the program be modified to accommodate a wide feed zone by defining several 'feed' plates. The input gas phase solute concentration to each of these plates, $(c_{F(std)} + c_{n-1\,(std)})$, could then be varied according to experimental observations.

A conclusion which can be drawn from the idealised simulated concentration profiles is that an improvement in the separation efficiency

of the sequential unit will be gained by introducing the solute feed as vapour. Additional heating for the feed distribution network could be provided when the unit is placed in an oven, as previously suggested, to study the effect of operation at a controlled temperature close to the solute boiling points.

A final criticism of the model lies in the assumption that the two solute profiles are totally independent of each other. As both solutes are competing for the same solvent phase then, at high solute concentrations, interaction will occur. Sunal (58) has experimentally measured and correlated activity coefficients for the solutes 'Arklone' P and 'Genklene' P, on the silicone fluid phase, in the presence of each other. Although the accuracy of the correlations was less satisfactory than for the pure solute case, some improvement may be gained by using this data for the prediction of the point values of the partition coefficients within the unit.

Summarising, the limited number of simulation runs performed to date have served to evaluate the effect in isolation of three key variables, the number of theoretical plates per column, column temperature and feedrate, on the separation process. Several improvements to the model have been suggested, most significantly the inclusion of a temperature profile and a wide feed zone. However, the extremely long computation time required for a simulated run must represent a limitation on its practical value.

CHAPTER 10

Conclusions and Recommendations for Future Work

1. The principal of counter-current chromatography has been successfully applied at a column diameter of 7.6 cm. The mechanical reliability of the sequential operating scheme, proven by virtually trouble free research operation over a period of two years, has, however, been gained at the expense of product continuity.

Designing the unit in discrete sections satisfies the desire for flexibility. Column dimensions can be varied without increased complexity, while an increase in separating length can be achieved by the addition of further identical sections.

2. 99.7% 'pure' products were obtained for the system 'Arklone' P/ 'Genklene' P on the phase silicone fluid DC 200/50 at equivolume feedrates of up to 700 $cm^3\ hr^{-1}$ despite a significant measured variation in individual column characteristics. Future work with a system of greater separation difficulty may require an improvement in both column efficiency and equality for comparable performance. The literature suggests that this can be achieved by

(i) the use of an improved packing technique; e.g. the shake, turn and pressure method.

(ii) packing the inlet and exit cones of each column with inert glass spheres

(iii) the use of 'baffling' within each column.

3. The experimental concentration profiles confirm that the separating power of the sequential unit is restricted by

(i) the effect of high solute concentrations on the partition coefficients

(ii) the inevitable pressure gradient

(iii) the finite separating length

(iv) the sequencing action,

as postulated in equations 6.15 and 6.16. It was found that successful resolution of 'Arklone' P and 'Genklene' P was unlikely over the range of operating conditions studied if the standardised concentration of 'Arklone' P exceeded 0.3×10^{-3} g cm^{-3}.

Future investigation of methods to improve the capacity of the unit should include:

(i) using a higher carrier gas flowrate, and thus faster sequencing rate, in conjunction with a larger particle size solid support to reduce the pressure gradient

(ii) operating at a temperature closer to the solute boiling points

(iii) isolating two columns for purging to increase the time available for regeneration.

4. To enable the study, in isolation, of the individual factors affecting the performance of the sequential unit a digital computer simulation, based on a simple chromatographic plate model, has been developed. Despite the inclusion of a pressure gradient and concentration dependent partition coefficients in the model, the experimentally recorded concentration profiles are not accurately reproduced. Preliminary studies have, however, shown that for the 'Arklone' P/'Genklene' P/silicone fluid system:

(i) a 'pseudo-steady' state condition is established within two cycles, a fact assumed for the experimental analysis

(ii) the concentration profiles are insensitive to the number of theoretical plates per column as a consequence of the comparative ease of the separation. Hence the simulation could not be used to determine the actual H.E.T.P. values, as was hoped.

(iii) the concentration profiles are very sensitive to temperature emphasising the future need to place the unit in a controlled temperature environment.

(iv) an improvement in performance would be gained by the introduction of the solute feed in the vapour phase.

Several improvements to the existing computer program have been suggested, the most significant being the introduction of an experimentally measured on-column temperature profile and a wider feed zone. Unfortunately, the move towards a more realistic simulation is likely to be accompanied by an increase in the already very long program execution time.

5. Alternative applications for the basic design and operating principle of the sequential unit should be investigated.

(i) The compartmentalised nature of the design permits its modification to a co-current system capable of resolving periodically injected complex mixtures. As each injection progresses through the unit the column(s) containing the trailing component would be isolated in turn for recovery of that component in a purified state (Fig 10.1). The advantage over a conventional 'batch' column is that the solvent phase in each column could be varied in type and loading to suit the separation steps. Flow programming would also be possible.

(ii) Operating in the normal sequential mode, a third component whose solvent affinity lay between that of the other two would tend to be

concentrated on-column. The addition of a third product port system in the main separating section would permit the removal of this component in a higher purity state than initially introduced in the feed.

(iii) A ternary separation would be possible if the unit was divided into two separating sections, each followed by a purge section. Additional port functions would be required as illustrated in Fig 10.2.

(iv) Although designed for gas/liquid chromatography, the process scheme can be generally adapted to solid/fluid contacting systems (160). In particular, ion-exchange and gel permeation offer attractive applications for the future.

Figure 10.1 Illustration of One Mode of Operating the Sequential Unit to Separate a Multicomponent Batch Injection

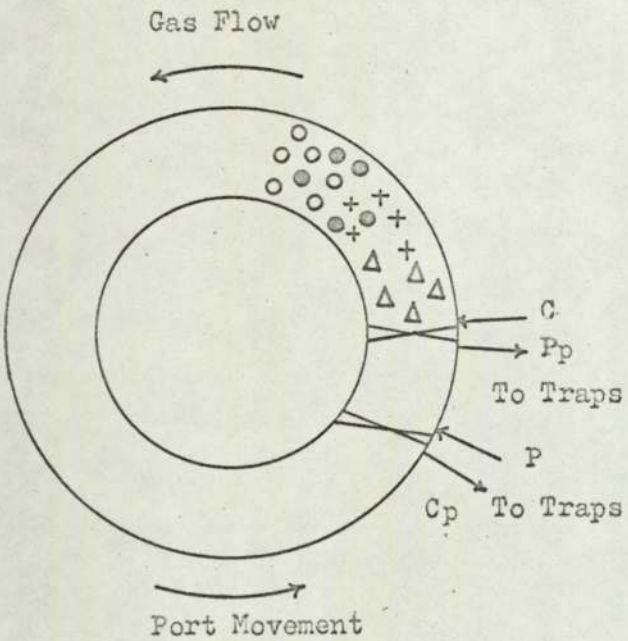

a) Solutes Δ, +, ●, ○ injected into Carrier Gas, C.

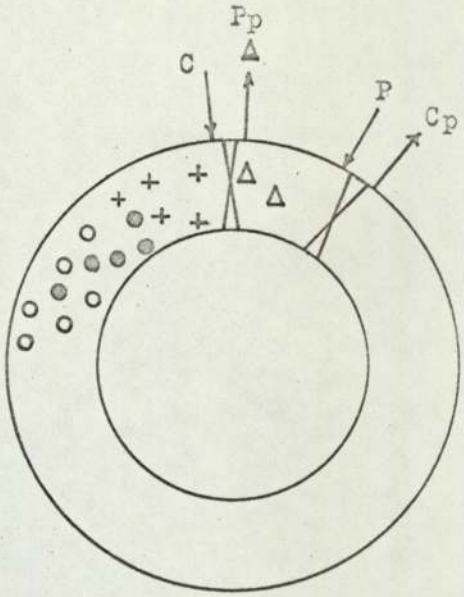

b) Tailing Component, Δ, Recovered From Exit Purge Gas.

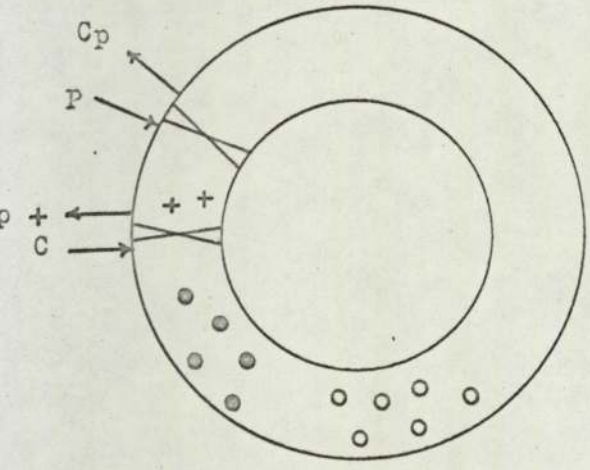

c) Second Slowest Moving Component, +, Recovered.

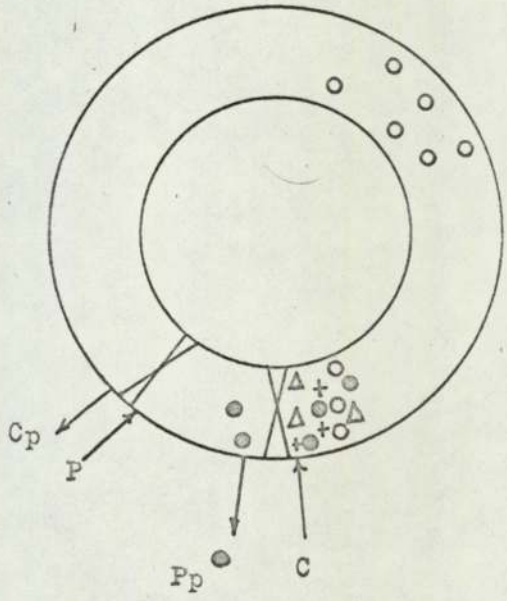

d) Component, ●, Recovered from P at outlet.
Component, ○, Recovered from Exiting C
Fresh Solute Mixture injected into C.

Figure 10.2 Diagram to show Flow Scheme for a Ternary Separation on the Sequential Unit

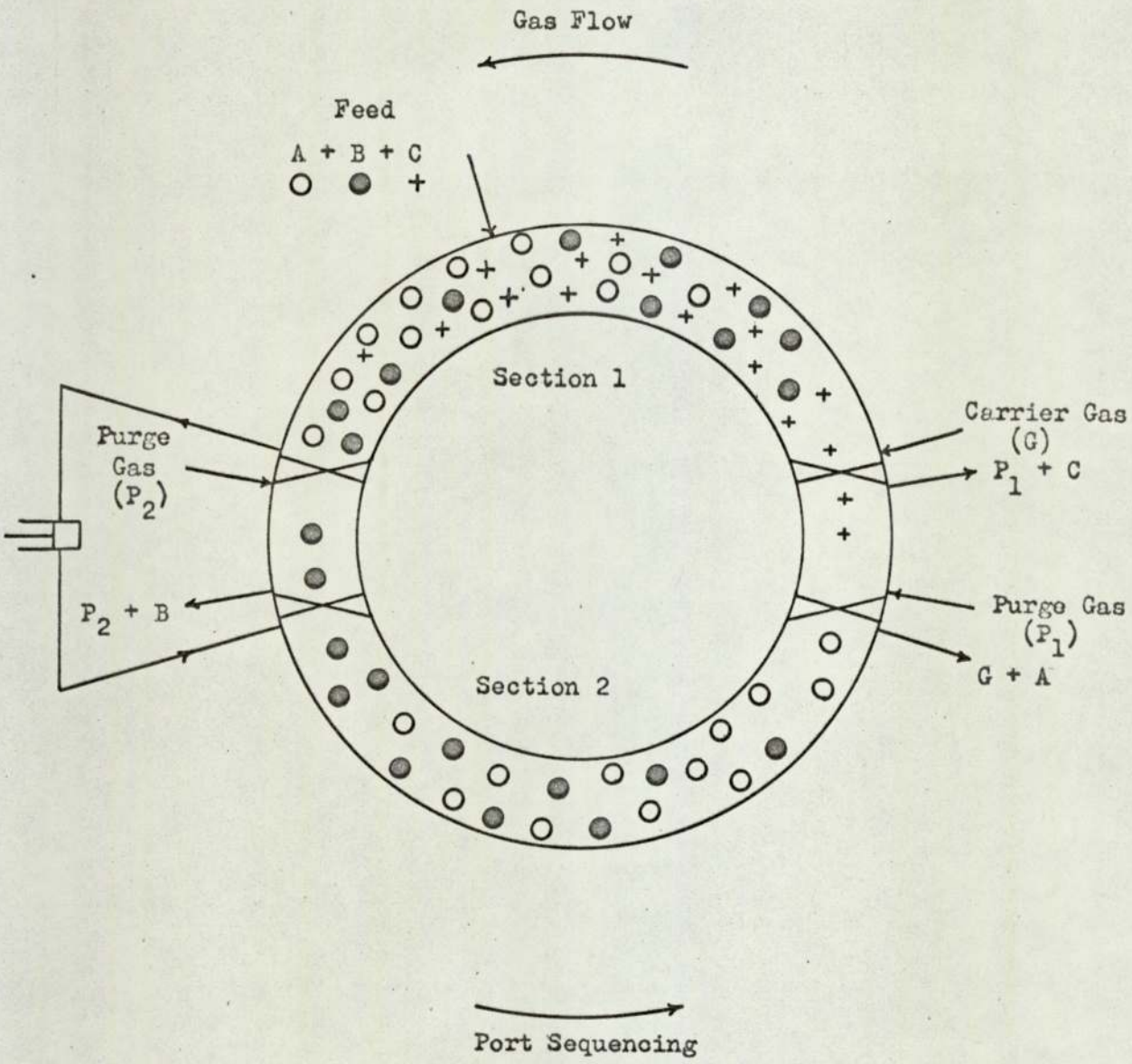

Note: 1) $K_A < K_B < K_C$

2) Velocity of G in Section 1 > Velocity of G in Section 2

NOMENCLATURE

A	Eddy diffusion term in the chromatographic theoretical plate height expression.
a_o, a_1, a_2, a_3	Fitted constants in the third order polynomial relationship between K and c.
B	Longitudinal gas phase diffusion term in the chromatographic theoretical plate height expression.
C	Mass transfer resistance term with respect to the gas phase in the chromatographic theoretical plate height expression.
C_G^o	C with respect to the gas phase corrected to column outlet pressure.
$\overline{C}_G$	C with respect to the gas phase corrected to mean column pressure.
c	Concentration of solute in the gas phase.
c_a, c_b	c at points a and b within a column.
c_d	Dummy c value used in the computer simulation of the sequential unit to evaluate concentration dependent terms: i.e. c_d = closest known value to c_n.
c_F	Gas phase concentration for a single solute in the feed to the sequential unit.
c_{input}	Total average input gas phase concentration of a single solute to plate n.
$c_{n(t - \Delta t)}$	Average gas phase concentration of a single solute in plate n during the time increment $(t - 2\ \Delta t)$ to $(t - \Delta t)$.

D	Molar diffusivity.
D_G^o	Molar diffusivity in the gas corrected to column outlet pressure.
D_r	Effective radial diffusivity.
d_c	Column diameter.
d_f	Effective thickness of a liquid film coating on the solid support.
d_p	Mean particle diameter.
d_{pc}	Ratio of the particle to column diameter.
E	Mass production rate of a single component, i.
E'	E/inlet concentration of i.
E_1, E_2	Mass flowrate of product leaving in the Product 1 and Product 2 streams respectively.
$(E_i)_1$, $(E_{ii})_1$	Mass production rate of components i and ii as Product 1.
F	Carrier gas flowrate at ambient conditions.
F_c	Number of column in the sequential unit, relative to the isolated column, into which solute feed is being introduced.
F_G, F_L	Fractional volume of a chromatographic theoretical plate occupied by the gas and liquid phases respectively.
f	Feedrate of component to the column.
f_L	Fraction of the total weight of column packing which is solvent.

G	Gas phase volumetric flowrate in the main separating section of the sequential unit.
G^o	G on a solute free basis.
G_1, G_2	Dimensionless constants in the general expression for a quadratic velocity profile.
$(G/L)_R$, $(G/L)_S$	The ratio of the gas to liquid phase flowrates in the rectifying and stripping sections respectively.
H	Height equivalent to a (chromatographic) theoretical plate.
H_c	Contribution to H attributable to a non-uniform velocity profile in a large diameter column.
H_{OG}	Height of an overall gas phase transfer unit.
I_S	The length of a sequencing interval.
i, ii	General solutes, component ii being more soluble than i in the solvent phase.
j	Gas phase compressibility factor.
K	Partition coefficient.
K^∞	Partition coefficient at infinite dilution.
K'	Apparent partition coefficient including the sorption effect.
K''	Apparent partition coefficient including the enthalpic overloading effect.
K^*	$\int_0^1 2p \cdot X^*(p) \cdot \phi^*(p)\, dp.$
ΔK	Change in the value of the partition coefficient from the value at infinite dilution with increasing solute concentration.

$\Delta K'$	Correction to the apparent partition coefficient K' for the sorption effect.
$\Delta K''$	Correction to the apparent partition coefficient K'' for the enthalpic overloading effect.
k	Mass distribution coefficient or capacity factor.
L	Liquid solvent volumetric flowrate.
L'	Apparent liquid solvent volumetric flowrate in the sequential unit.
l	Column length.
l_{min}	Minimum column length required for the separation of 2 component peaks by four standard deviations.
M	Molecular weight.
M_v	Molar volume.
m_i	Mass of component i produced at the column outlet per sample injection.
m_L	Mass of solvent per unit volume of the liquid phase.
Δm_i	Mass of component i discarded during fraction cutting.
N	Number of co-current chromatographic theoretical plates within a column.
N_{cc}	Number of counter-current theoretical plates within a column.
$(N_{OG})_R$, $(N_{OG})_S$	Number of overall gas transfer units in the rectifying and stripping sections respectively.
N_{req}	Number of chromatographic theoretical plates required to resolve two components.

n	A general chromatographic theoretical plate.
P	Pressure.
P_a	Ambient pressure.
P_{io}	Ratio of the inlet to outlet column pressures.
P_i^o	Saturated vapour pressure for component i
p	r_x/r_c
p_i	Partial pressure of component i.
Q	Production rate.
Q_{n+1}	Quantity of solute on the $(n+1)^{th}$ plate.
q	Concentration of solute in the liquid phase.
R	Relative solute band migration rate.
R_g	Gas constant.
R_s	Resolution $= \dfrac{t_{Rii} - t_{Ri}}{4\sigma_{ii}}$
r_c	Column radius.
r_x	General point on the lateral axis of the column.
S	Volumetric gas flowrate in the purge section of the sequential unit.
S^o	S on a solute free basis.
S^*	Processing cost.
SF	Separation factor $= \dfrac{K_{ii}}{K_i}$
s	Correction to the operating G/L limits for a successful separation on the sequential unit attributable to the sequencing action.

T	Temperature (absolute).
T_a	Ambient temperature (absolute).
T_c	Column temperature (absolute).
t	Time.
t_b	Width of an eluted peak at the base in time units.
t_d	'Dead' time; i.e. contribution to the retention time made by extracolumn fittings.
t_m	Elution or retention time for an unabsorbed component.
t_R	Elution or retention time for an absorbed component.
t'_R	Adjusted retention time, $t_R - t_m$.
t_ω	Width of the eluted solute front in frontal analysis (time units).
$\bar{t}_{r.o}$, $\bar{t}_{r.i}$	Peak mean or first moment in time units for the recorded inlet and outlet profiles.
$t_{r.o.c}$, $t_{r.i.c}$	Time from injection to the commencement of the recording of the outlet and inlet profiles.
Δt	Small time increment.
u	Carrier gas velocity through a chromatographic column.
$\bar{u}$	Mean carrier gas velocity = $j.u_o$
u_m	Molar velocity of the gas phase.
$u(r)$	Arbitrary velocity profile.
V^o	Carrier gas volume to plate n corrected for gas compressibility.

V_{fG}	Volume of a gas phase injection to the column.
V_G	Volume of the gas phase in a column corrected for gas compressibility = $j.V_m$
V_L	Volume of liquid solvent phase impregnated on the solid support.
V_m	Retention volume for an unabsorbed component (uncorrected).
V_R	Retention volume for an absorbed component (uncorrected).
V'_R	Adjusted or net retention volume = $V_R - V_m$
V^o_R	Corrected retention volume for an absorbed component.
V_{SL}	Volume of injected liquid sample.
v_n	Effective volume of plate n = $v_{n(G)} + Kv_{n(L)}$
$v_{n(G)}$, $v_{n(L)}$	Gas phase volume and liquid phase volume in plate n.
W	Mass feed.
W_{to}	Total chromatogram width per sample at the column outlet inside the column.
w_L	Weight of solvent phase in a column.
x	Mole fraction in the liquid phase.
y	Mole fraction in the gas phase.

General Subscripts.

A.P	'Arklone' P = 1.1.2 trichloro - 1.2.2 trifluoro-ethane.
col	Refers to the value on-column.
D.C.M.	Dichloromethane.
G	Refers to the gas phase.
G.P	'Genklene' P = 1.1.1 trichloro-ethane.
i, ii	Refers to components i and ii.
L	Refers to the liquid phase.
in	Refers to the column inlet.
min, max	Refer to the minimum and maximum values following correction for a pressure gradient.
mc	Refers to the mean column value following correction for a pressure gradient.
n	Refers to the average value in plate n during the time interval $(t - \Delta t)$ to t.
n - 1	Refers to the average value in plate n - 1 during the time interval $(t - \Delta t)$ to t.
o	Refers to the column outlet.
p	Refers to the packing.
std.	Refers to the value at standard pressure.

Greek

α	Separation factor for a given column = $\frac{V_{Rii}}{V_{Ri}}$
γ'	Labyrinth factor.
$\gamma_{i(L)}$	Activity coefficient for component i in the liquid phase.
γ'_r	Radial labyrinth factor.
δ	Correction to the operating G/L' limits for a successful separation on the sequential unit attributable to a finite column length.
ε	Void fraction.
η	Column utilisation = $\frac{\text{moles of product per unit time}}{\text{column volume}}$
λ	Eddy diffusion factor.
λ_r	Eddy diffusion factor in the radial direction.
ν	Kinematic viscosity.
ρ	Density.
ρ_p	Density of coated packing.
σ	Standard deviation.
σ_l	Standard deviation in length units.
σ_t	Standard deviation in time units.
σ_v	Standard deviation in volumetric units.
$(\sigma_t)^2_{r.i}$	Time based variance of the eluted peak recorded at the column inlet.
$(\sigma_t)^2_{r.o}$	Time based variance of the eluted peak recorded at the column outlet.

Greek

τ	Fitted constant in Florry-Huggins equation.
ϕ	Porosity.
$\phi(p)$	$-\int \frac{dp'}{p'} \int_0^{p'} p'' \times \chi^* \quad (p'')\, dp''$
χ	Characteristic of packing interstices.
$\chi^*(p)$	$\frac{u - \bar{u}}{\bar{u}}$
ψ	Fitted constant in Florry-Huggins equation.
ω	Volume of the eluted solute front in frontal analysis.

Dimensionless Groups.

Re_p	Reynolds number for a packed column $= \frac{d_p \cdot u}{\nu_g} \cdot \frac{\varepsilon}{1 - \varepsilon}$
$Sc_{(G)}$	Schmidt number for the gas phase, $\frac{\nu}{D_G}$
$Sc_{(L)}$	Schmidt number for the liquid phase, $\frac{\nu}{D_L}$

REFERENCES

1. M. Tswett, Ber. deut. botan. Ges., 24, 316, 384 (1906)

2. A. J. P. Martin and R. L. M. Synge, Biochem. J. 35, 1358 (1941)

3. A. T. James and A. J. P. Martin, Biochem. J., 50, 679 (1952)

4. D. E. M. Evans and J. C. Tatlow, J. Chem. Soc., 1184 (1955)

5. R. S. Timmins, L. Mir and J. M. Ryan, Chem. Eng., 76, 170 (1969)

6. H. Pichler and H. Schultz , Brenn. Chem., 39, 48 (1958)

7. R. P. W. Scott in discussion of paper by E. P. Atkinson and G. A. P. Tuey, "Gas Chromatography 1958", D. H. Desty, Ed., Butterworths, London, 1958, p270

8. P. E. Barker and D. Critcher, Chem. Eng. Sci., 13, 82 (1960)

9. D. Critcher, Ph. D. Thesis, Univ. of Birmingham, 1963

10. P. E. Barker and D. Lloyd, Symposium on the Less Common Means of Separation 1963, Inst. Chem. Eng., London, 1964, p68

11. D. Lloyd, Ph. D. Thesis, Univ. of Birmingham, 1963

12. P. E. Barker and D. Lloyd, U. S. Patent 3,338,031

13. P. E. Barker and D. H. Huntington, J. Gas Chromatogr., 4, 59 (1966)

14. P. E. Barker and D. H. Huntington, "Gas Chromatography 1966", A. B. Littlewood, Ed., Inst. of Petroleum, 1967, p135

15. D. H. Huntington, Ph. D. Thesis, Univ. of Birmingham, 1967

16. P. E. Barker and D. H. Huntington, Dechema Monograph, 62, 153 (1969)

17. P. E. Barker and Universal Fisher Engineering Co. Ltd., British Patent Applications 33630/65; 43629/65; 5764/68; 44375/68

18. P. E. Barker and S. Al-Madfai, J. Chromatogr. Sci., 7, 425 (1969)

19. P. E. Barker and S. Al-Madfai, Proc. 5th International Symposium on 'Advances in Chromatography, Las Vegas, 1969, Preston Technical Abstracts Co., Evanston, Ilinois, 1969, p123

20. S. Al-Madfai, Ph. D. Thesis, Univ. of Birmingham, 1969

21. P. E. Barker, "Preparative Gas Chromatography", A. Zlatkis, Ed., Wiley-Interscience, London, 1971, p325

22. J. H. Purnell, "Gas Chromatography", John Wiley and Sons, London, 1962

23. A. B. Littlewood, "Gas Chromatography", Academic Press, New York, 1962

24. J. C. Giddings, "Dynamics of Chromatography, Pt. 1 Principles and Theory", Edward Arnold Ltd., London, 1965

25. O. E. Schupp, "Techniques of Organic Chemistry, Vol XIII, Gas Chromatography", Wiley-Interscience, New York, 1969

26. D. H. James and C. S. G. Phillips, J. Chem. Soc., 1600 (1953)

27. J. H. Griffiths and C. S. G. Phillips, J. Chem. Soc., 3446 (1954)

28. E. Gluekauf, Trans. Farad. Soc., No.385, 51 (1), 34 (1955)

29. J. J. Van Deemter, F. J. Zuiderweg and A. Klinkenberg, Chem. Eng. Sci., 5, 271 (1956)

30. J. F. Young, "Gas Chromatography", Instrument Soc. Am. Symp. 1957, V. J. Coates, Ed., Academic Press, New York, 1958, p15

31. A. Klinkenberg and F. J. Sjenitzer, Chem. Eng. Sci., 5, 258 (1956)

32. J. J. Van Deemter, 2nd Informal Symp., G. C. Discussion Group, Cambridge, 1957

33. M. Golay, "Gas Chromatography 1958", D. H. Desty, Ed., Butterworths, London, 1958, p36

34. J. Bohemen and J. H. Purnell, J. Chem. Soc., p360 and 2630 (1961)

35. J. C. Giddings, J. Chem. Phys., 26,169 (1957)

36. J. M. Harper and E. G. Hammond, Anal. Chem., 37, 486 (1965)

37. R. M. Bethea and P. C. Bentsen, J. Chromatogr. Sci., 10, 575 (1972)

38. D. T. Sawyer and J. H. Purnell, Anal. Chem., 36, 457 (1964)

39. I. G. McWilliam and R. A. Dewar, "Gas Chromatography 1958", D. H. Desty, Ed., Butterworths, London, 1958, p142

40. J. C. Giddings, J. Gas Chromatogr., 1 (1), 12 (1963)

41. F. H. Huyten, W. Van Beersum and G. W. A. Rijinders, "Gas Chromatography 1960", R. P. W. Scott, Ed., Butterworths, London, 1960, p224

42. J. Pypker, "Gas Chromatography 1960", R. P. W. Scott, Ed., Butterworths, London, 1960, p240

43. M. Golay, 2nd Internat. Symp. Instr. Soc. Am., June 1959, p5

44. V. Pretorius and K.De Clerk, "Preparative Gas Chromatography", A. Zlatkis and V. Pretorius, Eds., Wiley-Interscience, 1971, p1

45. K-P. Hupe, U. Busch and K. Winde, J. Chromatogr. Sci., 7, 1 (1969)

46. J. C. Giddings, J. Gas Chromatogr., 1 (4), 38 (1963)

47. J. C. Giddings, Anal. Chem., 35, 439 (1963)

48. J. C. Giddings and G. E. Jensen, J. Gas Chromatogr., 2 (9), 290 (1964)

49. G. M. C. Higgins and J. F. Smith, "Gas Chromatography 1964", A. Goldup, Ed., Inst. of Petroleum, London, 1965, p94

50. G. W. A. Rijinders, "Advances in Chromatography Vol. 3", J. C. Giddings and R. A. Keller, Eds., Marcel Dekker, New York, 1966, p215

51. T. W. Smuts, D. Sc. Thesis, Univ. of Pretoria, 1967 (reported in reference 44)

52. E. Bayer, K-P. Hupe and H. Mack, Anal. Chem., 35, 492 (1963)

53. J. H. Knox, "Advances in Gas Chromatography", A. Zlatkis and L. Ettre, Eds., Preston Technical Abstract Co., Illinois, 1966

54. S. F. Spencer and P. Kuckorski, Facts and Methods Technical Paper, No.37

55. S. E. Charm, C. C. Matteo and R. A. Carlson, Chem. Eng. Prog. Symp. Ser., 64 (80), 9 (1968)

56. M. Verzele, J. Chromatogr., 15, 482 (1964)

57. M. Verzele, Planta. Medica Suppl. 38 (1967)

58. A. Sunal, Ph. D. Thesis, Univ. of Aston in Birmingham, 1973

59. J. R. Conder, "Advances in Analytical Chemistry and Instrumentation Vol.6, Progress in Gas Chromatography", J. H. Purnell, Ed., Wiley-Interscience, London, 1968, p209

60. J. R. Conder and J. H. Purnell, Trans. Farad. Soc., 64, 1505 (1968)

61. J. R. Conder and J. H. Purnell, Trans. Farad. Soc., 64, 3100 (1968)

62. J. R. Conder and J. H. Purnell, Trans. Farad. Soc., 65, 824 (1969)

63. J. R. Conder and J. H. Purnell, Trans. Farad. Soc., 65, 839 (1969)

64. F. Helfferich, J. Chem. Educ., 41, 410 (1964)

65. C. H. Bosanquet and G. D. Morgan, "Vapour Phase Chromatography", D. H. Desty, Ed., Butterworths, London, 1957, p35

66. C. H. Bosanquet, "Gas Chromatography 1958", D. H. Desty, Ed., Butterworths, London, 1958, p107

67. G. J. Krige and V. Pretorius, Anal. Chem., 37, 1186 (1965)

68. G. J. Krige and V. Pretorius, Anal. Chem., 37, 1191 (1965)

69. G. J. Krige and V. Pretorius, Anal. Chem., 37, 1195 (1965)

70. G. J. Krige and V. Pretorius, Anal. Chem., 37, 1202 (1965)

71. T. Johns, M. R. Burnell and D. W. Clarke, "Gas Chromatography", H. J. Noebels, R. F. Wall and N. Brenner, Eds., Academic Press, New York, 1961, p207

72. T. Johns, "Gas Chromatography, 1960", R. P. W. Scott, Ed., Butterworths, London, 1960, p242

73. J. D. McCallum, "Progress in Industrial Gas Chromatography Vol.1", H. A. Szymanski, Ed., Plenum Press, 1961, p125

74. E. M. Taft, Aeorograph Tech. Bull. W116, Varian Aeorograph, Walnut Creek, California, 1964

75. M. Verzele, J. Gas Chromatogr., 4, 180 (1966)

76. J. C. Giddings and E. N. Fuller, J. Chromatogr., 7, 255 (1963)

77. K. Kishimoto and Y. Yasumari, Japan. Analyst, 12, 125 (1963)

78. M. B. Mitzner and W. V. Jones, J. Gas Chromatogr., 3, 294 (1965)

79. J. L. Wright, J. Gas Chromatogr., 1 (1), 10 (1963)

80. R. W. Reiser, J. Gas Chromatogr., 4, 390 (1966)

81. M. B. Diximier, B. Roz and G. Guiochon, Anal. Chim. Acta, 38, 73 (1967)

82. M. J. Golay, "Gas Chromatography", H. J. Noebels, R. F. Wall and N. Brenner, Eds., Academic Press, New York, 1961

83. E. Bayer, K-P. Hupe and H. Mack, Anal. Chem., 35, 492 (1963)

84. G. J. Frisone, J. Chromatogr., 6, 97 (1961)

85. M. Verzele, J. Chromatogr., 9, 116 (1962)

86. A. B. Carel and G. Perkins, Anal. Chim. Acta, 34, 83 (1966)

87. U. S. Patents 3,354,619; 3,360,904; 3,398,512

88. A. B. Carel, R. E. Clement and G. Perkins, J. Chromatogr. Sci., 7, 218 (1969)

89. R. E. Pecsar, "Preparative Gas Chromatography", A. Zlatkis and V. Pretorius, Eds., Wiley-Interscience, London, 1971, p73

90. U. S. Patents 3,491,512; 3,250,058

91. J. M. Ryan, R. S. Timmins and J. F. O'Donnell, Chem. Eng. Prog. 64 (8), 53 (1968)

92. L. Mir, J. Chromatogr. Sci, 9., 436 (1971)

93. Anon, Chem. Eng. News, 46 (14), 62 (1968)

94. E. Bayer, "Gas Chromatography 1960", R. P. W. Scott, Ed., Butterworths, London, 1960, p236

95. C. L. Guillemin, J. Chromatogr., 12, 163 (1963)

96. C. L. Guillemin, J. Gas Chromatogr., 4, 104 (1966)

97. U. S. Patent 3,248,856

98. C. L. Guillemin, J. Chromatogr., 30, 222 (1967)

99. J. Albrecht and M. Verzele, J. Chromatogr. Sci., 8, 586 (1970)

100. A. Rose, D. J. Royer and R. S. Henly, Separation Sci., 2, 211 (1967

101. J. Albrecht and M. Verzele, J. Chromatogr. Sci., 9, 745 (1971)

102. J. H. Purnell, J. Chem. Soc., 1268 (1960)

103. M. Verzele, J. Bouche, A. DeByrne and M. Verstappe, J. Chromatogr., 18, 253 (1965)

104. M. Verzele and M. Verstappe, J. Chromatogr., 19, 495 (1965)

105. M. Verzele and M. Verstappe, J. Chromatogr., 19, 504 (1965)

106. M. Verzele, J. Gas Chromatogr., 3, 186 (1965)

107. M. Verzele, J. Gas Chromatogr., 4, 180 (1966)

108. M. Verzele, Planta Med. Suppl. 38 (1967)

109. P. V. Peurifoy, J. L. Ogilvie and I. Dvoretzky, J. Chromatogr., 5, 418 (1961)

110. J. R. Conder and J. H. Purnell, Chem. Eng. Prog. Symp. Ser., 91 (65), 1 (1969)

111. J. R. Conder and J. H. Purnell, Chem. Eng. Sci., 25, 353 (1970)

112. K. I. Sakodynskii and S. A. Volkow, J. Chromatogr., 49, 76 (1970)

113. S. A. Volkow and K. I. Sakodynskii, Chromatographia, 5, 327 (1972)

114. A. J. P. Martin, "Vapour Phase Chromatography 1956", D. H. Desty, Ed., Butterworths, London, 1957, pl

115. R. S. Porter and J. F. Johnson, Nature, 183, 391 (1959)

116. S. Sideman, Chem. Eng. Sci., 18, 95 (1963)

117. S. Sideman, Bull. Chem. Soc. Japan, 37, 1565 (1964)

118. K. I. Sakodynskii, S. A. Volkow, W. W. Brashnikow and N. M. Shaworonkow, "Gas Chromatography 1963", P. Angele and H. G. Struppe, Eds., Akademie Verlang GmbH, Berlin, 1964, p231

119. M. J. Golay, H. I. Hill and S. D. Norem, Anal. Chem., 35, 488 (1963)

120. Facts and Methods, F and M Scientific, Division of Hewlett-Packard, Pennsylvania, 6 (5), 1965

121. D. T. Sawyer and G. L. Hargrove, "Advances in Analytical Chemistry and Instrumentation Vol.6, Progress in Gas Chromatography", J. H. Purnell, Ed., Wiley-Interscience, London, 1968, p325

122. W. J.De Wet and V. Pretorius, Anal. Chem., 32, 169 (1960)

123. W. J.De Wet and V. Pretorius, Anal. Chem., 32, 1396 (1960)

124. S. M. Gordon and V. Pretorius, J. Gas Chromatogr., 2, 196 (1964)

125. S. M. Gordon, G. J. Krige and V. Pretorius, J. Gas Chromatogr., 2, 241 (1964)

126. S. M. Gordon, G. J. Krige and V. Pretorius, J. Gas Chromatogr., 2, 246 (1964)

127. S. M. Gordon, G. J. Krige and V. Pretorius, J. Gas Chromatogr., 2, 285 (1964)

128. S. M. Gordon, G. J. Krige and V. Pretorius, J. Gas Chromatogr., 3, 87 (1965)

129. K.De Clerk, T. W. Smuts and V. Pretorius, Sep. Sci., 1, 443 (1966)

130. K.De Clerk, and V. Pretorius, Sep. Sci., 6, 407 (1971)

131. D. A. Craven, J. Chromatogr. Sci., 8, 540 (1970)

132. J. R. Conder, presented at symposium on "Less Common Means of Separation", Inst. Chem. Eng., London, Nov. 1972

133. J. M. Ryan and G. L. Dienes, Drug Cosmetic Ind. 93 (1966)

134. K-P. Hupe, J. Chromatogr. Sci., 9, 11 (1971)

135. A. J. P. Martin, Discussions Farad. Soc., 7, 332 (1949)

136. J. C. Giddings, Anal. Chem., 34, 37 (1962)

137. D. Dinelli, S. Polezzo and M. Taramasso, J. Chromatogr., 7, 477 (1962)

138. U. S. Patent 3,187,486

139. S. Polezzo and M. Taramasso, J. Chromatogr., 11, 9 (1963)

140. M. Taramasso and D. Dinelli, J. Gas Chromatogr., 2, 150 (1962)

141. M. Taramasso, F. Sallusto and A. Guerra, J. Chromatogr., 20, 226 (1965)

142. M. Taramasso, J. Chromatogr., 49, 27 (1970)

143. U. S. Patent 3,078,647

144. U. S. Patent 3,503,712

145. M. V. Sussman, K. N. Astill, R. Rombach, A. Cerullo and S. S. Chen, Ind. Eng. Chem. Fund., 11 (2), 181 (1972)

146. E. J. Tuthill, J. Chromatogr. Sci., 8, 285 (1970)

147. H. Schultz, "Gas Chromatography 1962", M. Van Swaay, Ed., Butterworths, London, 1963, p225

148. G. R. Fitch, M. E. Probert and P. F. Tiley, J. Chem. Soc., 4875 (1962)

149. D. W. Pritchard, M. E. Probert and P. F. Tiley, Chem. Eng. Sci., 26, 2063 (1971)

150. R. P. W. Scott, "Gas Chromatography 1958", D. H. Desty, Ed., Butterworth, London, 1958, p189

151. U. S. Patent 2,869,672

152. U. S. Patent 2,893,955

153. D. Glasser, "Gas Chromatography 1966", A. B. Littlewood, Ed., Inst. of Petroleum, London, 1967, p119

154. U. S. Patent 3,016,107

155. Unidev information pamphlet on Sequential Separation, Unidev Ltd., Crawley, Sussex

156. P. J. Carr, paper presented at the '8th International Symposium on Advances in Chromatography', Toronto, Canada, 1973

157. P. E. Barker, S. A. Barker, B. W. Hatt and P. J. Sommers, Chem. and Proc. Eng., 52 (1), 64 (1971)

158. S. C. W. Wilkinson, Crane Packing Ltd., private communication

159. P. E. Barker and R. E. Deeble, presented at symposium on "Less Common Means of Separation", Inst. of Chem. Eng., London, Nov. 1972

160. P. E. Barker and R. E. Deeble, Anal. Chem., 45, 1121 (1973)

161. P. E. Barker and R. E. Deeble, British Patent Appl., 27786/72 and U. S. Patent Appl. 368,584

162. Instruction manual for Pye 104 Gas Chromatograph, Pye-Unicam Ltd., Cambridge

163. Gow-Mac Bulletin 5B-13, Gow-Mac, Shannon Airport, Ireland

164. In 'Effective Low-cost Cleaning with'Arklone'and 'Genklene', I.C.I. Ltd., Mond Division.

165. Chemical Engineers Handbook, J. H. Perry, Ed., McGraw Hill, New York, 1963 (4th edition)

166. N. I. Sax, "Dangerous Properties of Industrial Materials", van Nostrand Rheinhold,London, 1968

167. Jones Chromatography Ltd., Machen, Newport, Man., private communication

168. C. N. Reilley, G. P. Hildebrand and J. W. Ashley, Anal. Chem., 34, 1198 (1962)

169. J. C. Sternberg, "Advances in Chromatography Vol.2", J. C. Giddings and R. A. Keller, Eds., Edward Arnold, New York, 1966, p205

170. J. C. Giddings, Anal. Chem., 35, 1999 (1963)

171. M. R. Spiegel, "Theory and Problems of Statistics", Schaum Publishing Co., New York, 1961

172. A. J. Forsythe, T. A. Keenan, E. I. Organick and W. Stenberg, "Computer Science; BASIC Language Programming", John Wiley and Sons Inc., New York, 1970

173. H. J. Gold, Anal. Chem., 34, 175 (1962)

174. M. B. Evans and J. F. Smith, J. Chromatogr., 5, 300 (1961)

175. J. F. Smith, Nature, 193, 679 (1962)

176. R. Kaiser, "Gas Phase Chromatography Vol.3", transl. P. H. Scott, Butterworths, London, 1963, p51

177. E. R. Adlard, M.A. Khan and B. T. Whitham, "Gas Chromatography 1962", M. van Swaay, Ed., Butterworths, London, 1963, p84

178. R. P. W. Scott, Anal. Chem, 35, 481 (1963)

179. K-P. Hupe and E. Bayer, "Gas Chromatography 1964", A. Goldup, Ed., Inst. of Petr., London, 1965, p62

180. J. Peters and C. B. Euston, Anal. Chem., 37,657 (1965)

181. See, for example, K. Denbigh, "The Principles of Chemical Equilibrium", Cambridge University Press, 1964, p276

182. Dow Corning Ltd., Barry, Glamorgan, private communication

183. Phase-Sep Catalogue, Phase Separations Ltd., Deeside Industrial Estate, Queensferry, Flintshire

184. Instruction Manual for Perkin-Elmer F11 Gas Chromatograph, Perkin-Elmer Ltd., Beaconsfield, Bucks.

185. See, for example, Hewlett Packard Integrator Information Bulletin 3370B (March 1971), Hewlett Packard, Slough, Bucks.

186. L. Alders, "Liquid Liquid Extraction", Elsevier, Amsterdam, 1959 (2nd edition).

187. P. Rony, Sep. Sci., 3, 239 (1968)

188. P. Rony, Sep. Sci., 3, 357 (1968)

189. P. Rony, Sep. Sci., 5, 121 (1970)

190. P. Tiley, J. Appli. Chem., 17 (5), 131 (1967)

191. D. W. Pritchard, M. E. Probert and P. F. Tiley, Chem. Eng. Sci., 26, 2063 (1971)

192. C. T. Sciance and O. K. Crosser, A. I. Ch. E. Jnl., 12 (1), 100 (1966)

193. J. R. Conder and M. K. Shingari, J. Chromatogr. Sci., 11, 525 (1973)

APPENDIX 1

Calibration Charts

Figure A.1.1 Rotameter Calibration

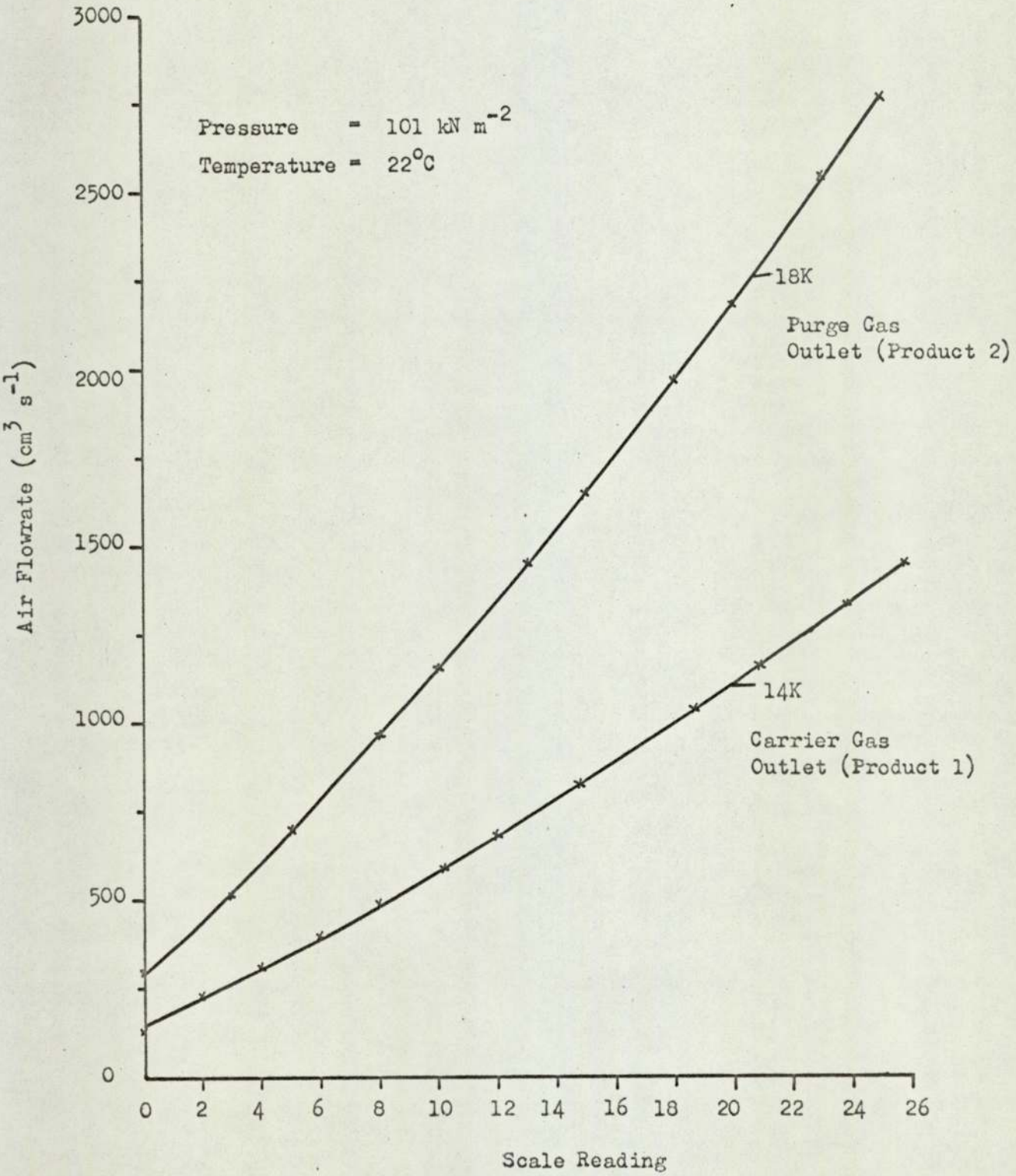

Figure A.1.2 Carrier Gas Flowrate at Mean Column Pressure (G_{mc}) versus Rotameter Scale for Various Column Inlet Pressures

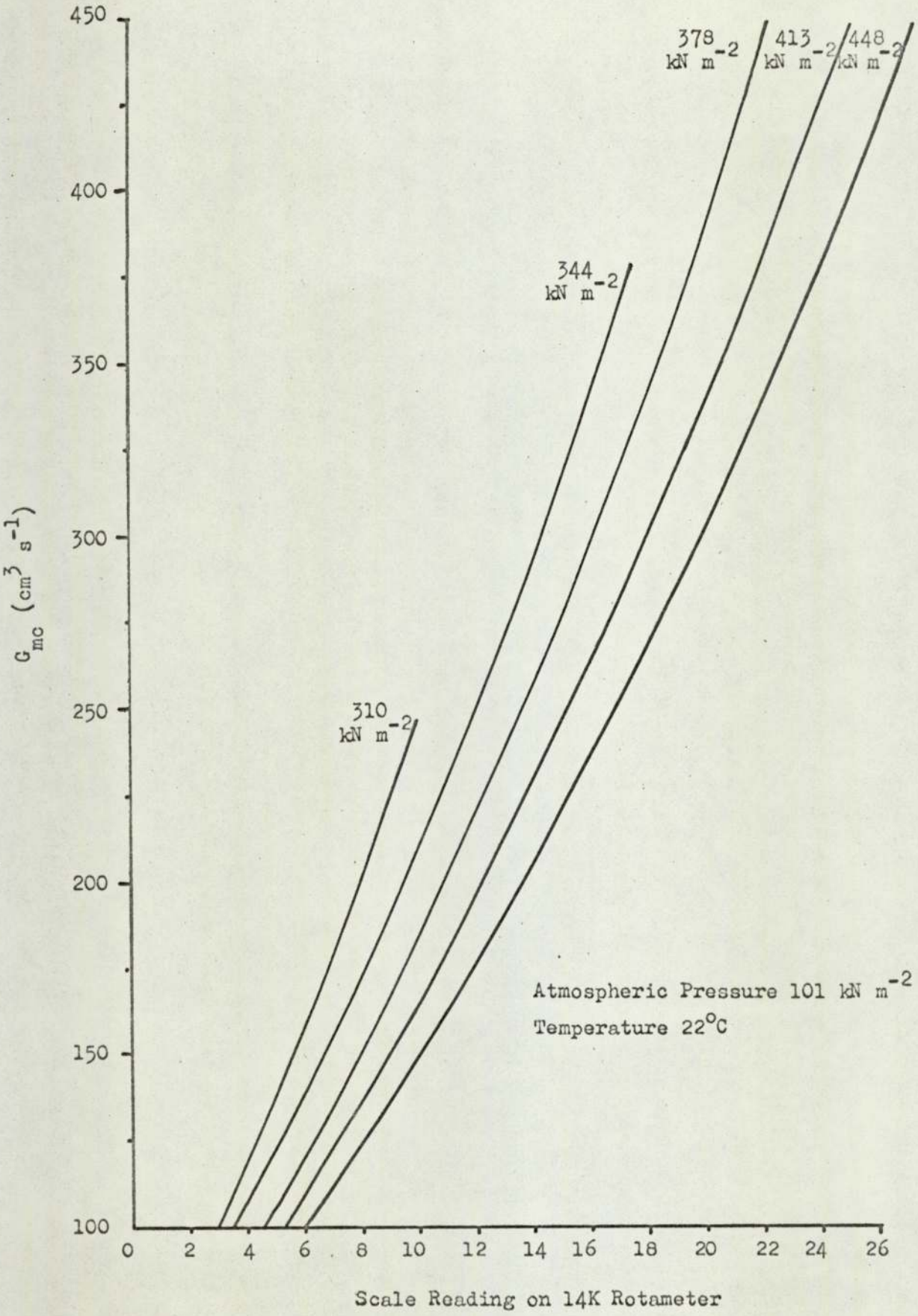

Figure A.1.3 Purge Gas Flowrate at Mean Column Pressure (S_{mc}) versus Rotameter Scale for Various Column Inlet Pressures

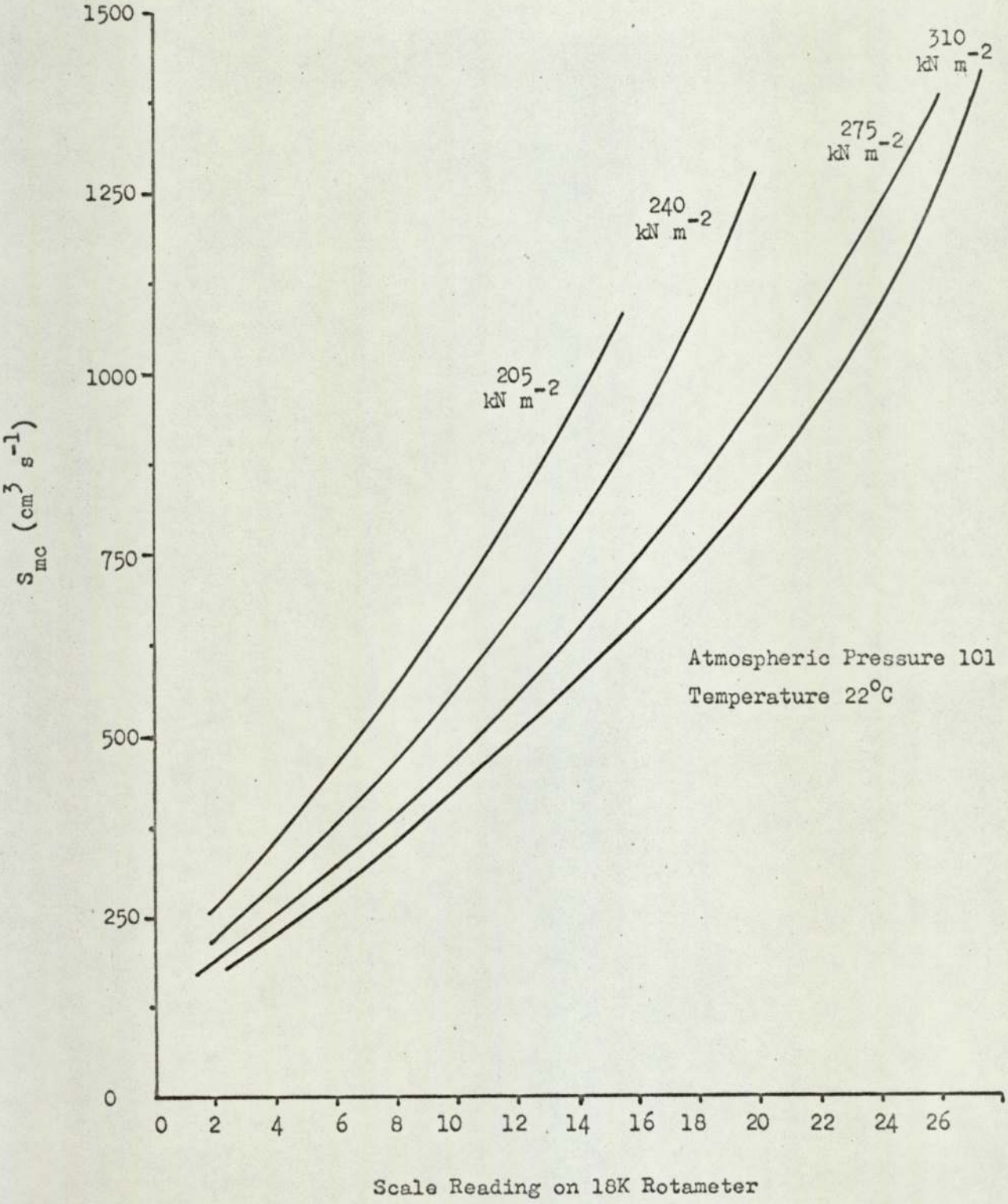

Figure A.1.4 Pressure Gauge Calibration

a) Carrier Gas Inlet

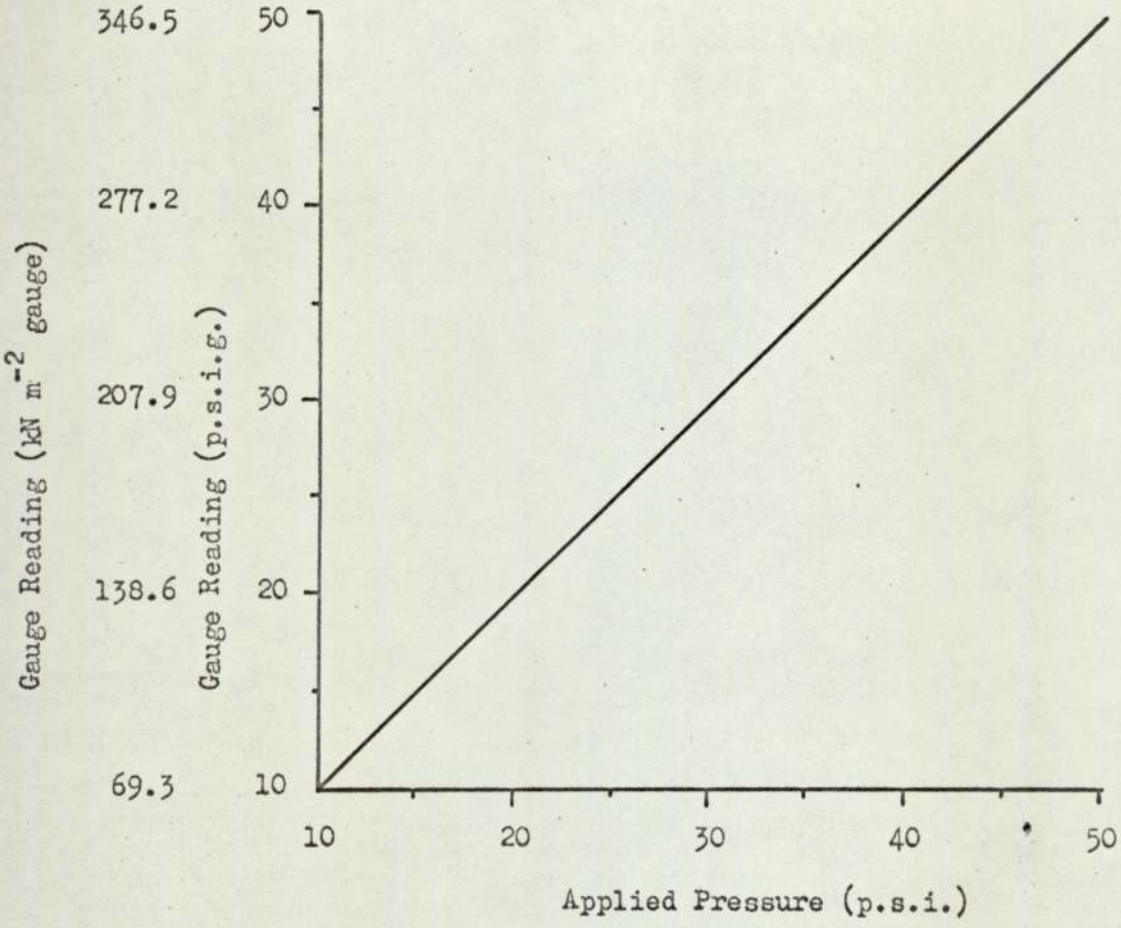

b) Carrier Gas Outlet

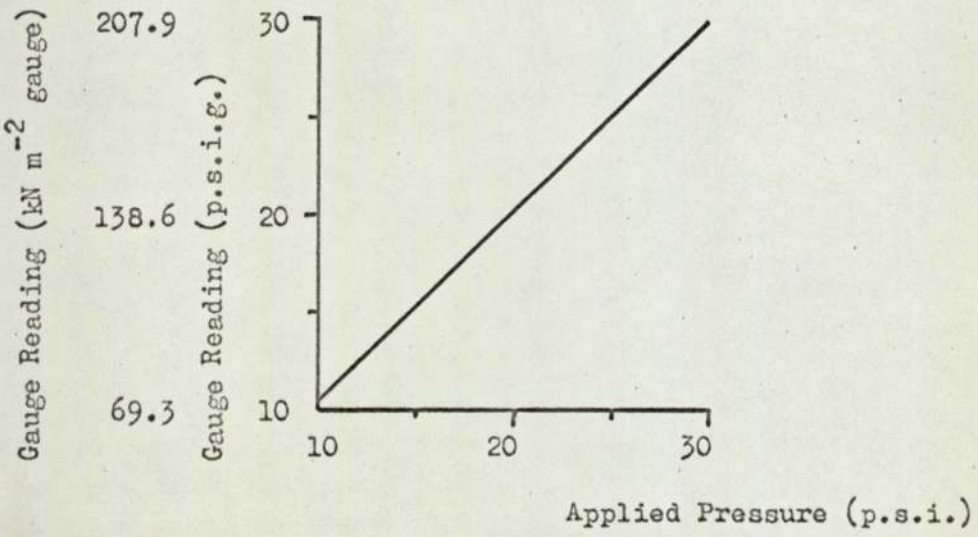

Figure A.1.4 (Cont'd.)

c) Purge Gas Inlet

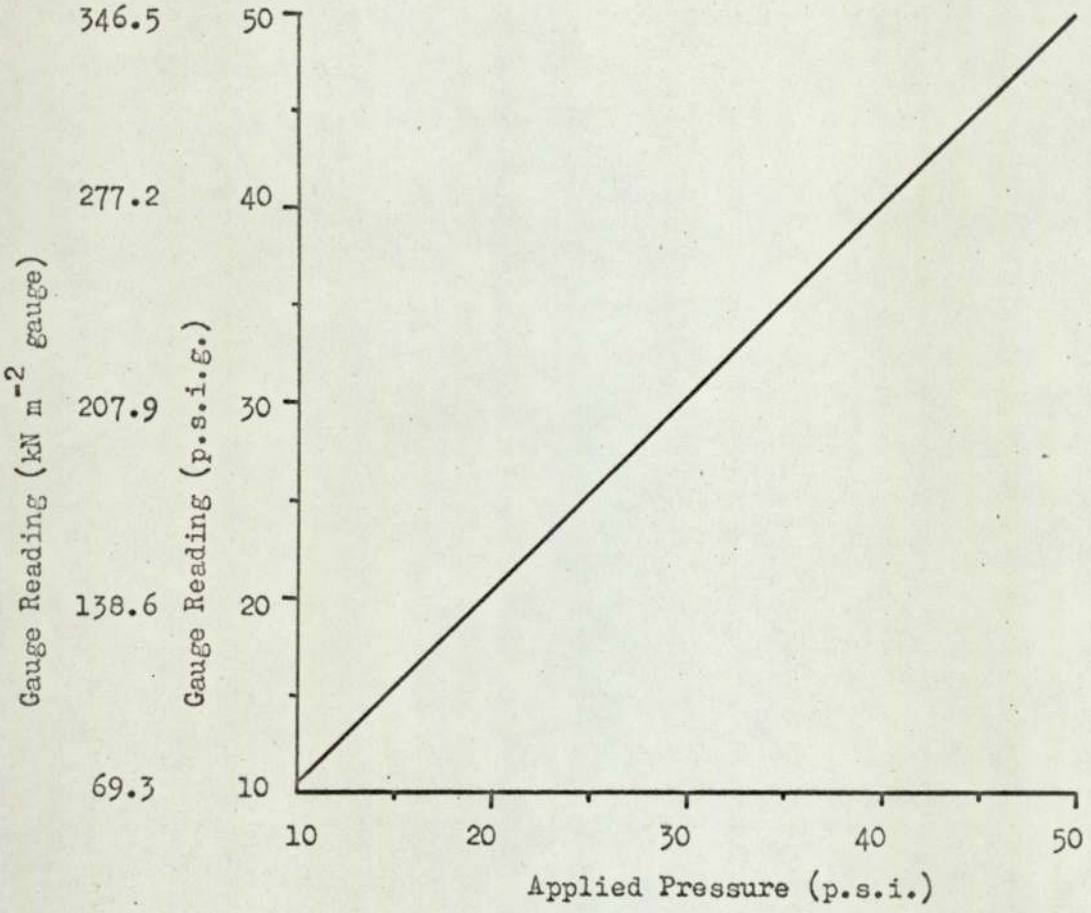

d) Purge Gas Outlet

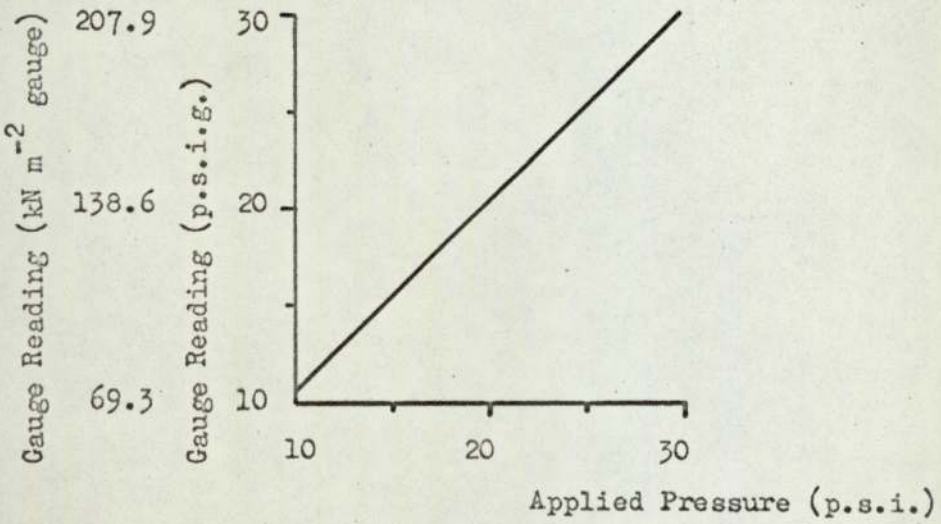

Figure A.1.4 (Cont'd.)

e) Floating Gauge for Point Pressure Measurements

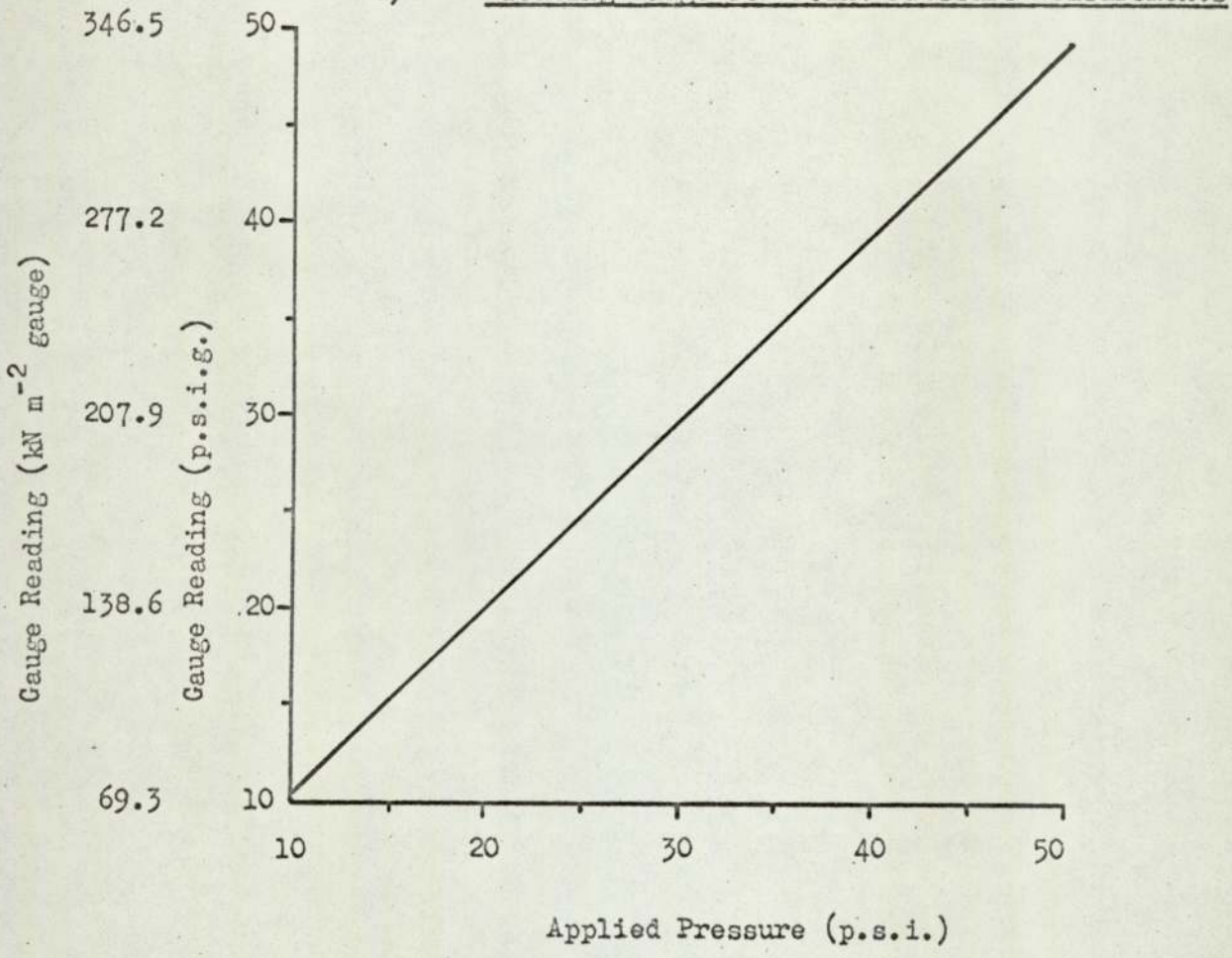

Figure A.1.5 Calibration of Solute Feed 'Micropump'

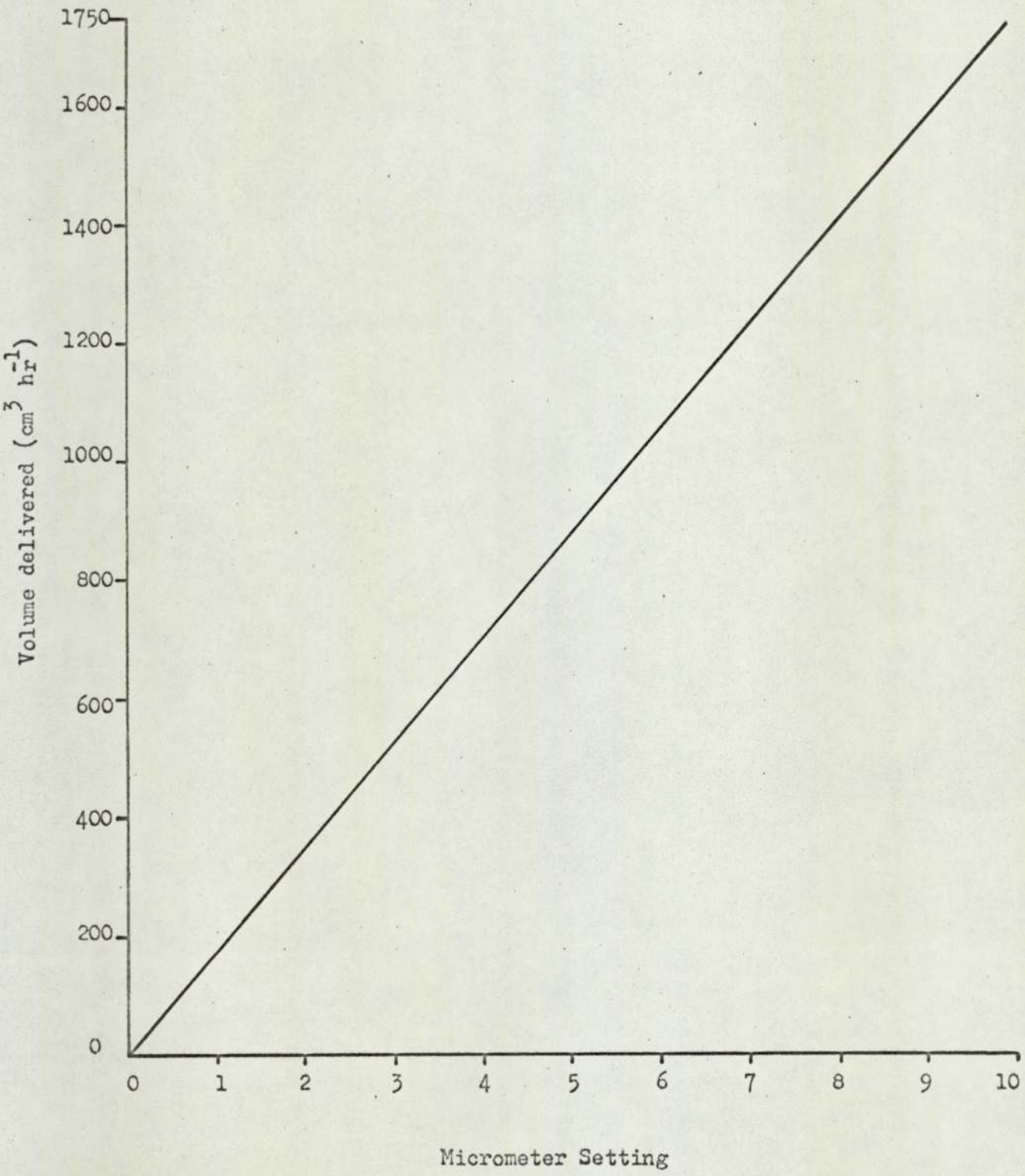

Figure A.1.6 Calibration of Automatic Timed Sequencing Unit

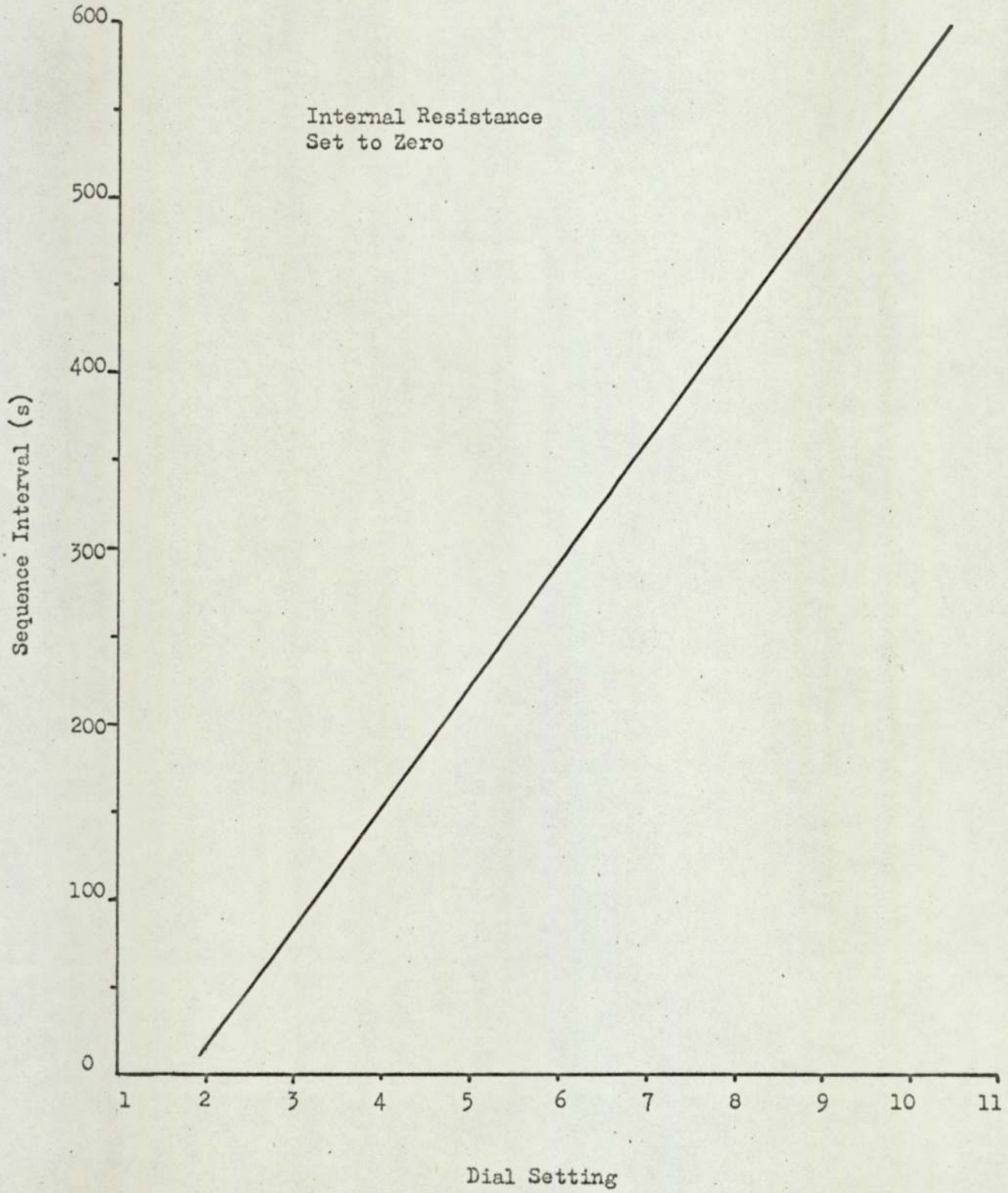

Figure A.1.7 Calibration of F11 Oven Temperature

(Injection block not heated)

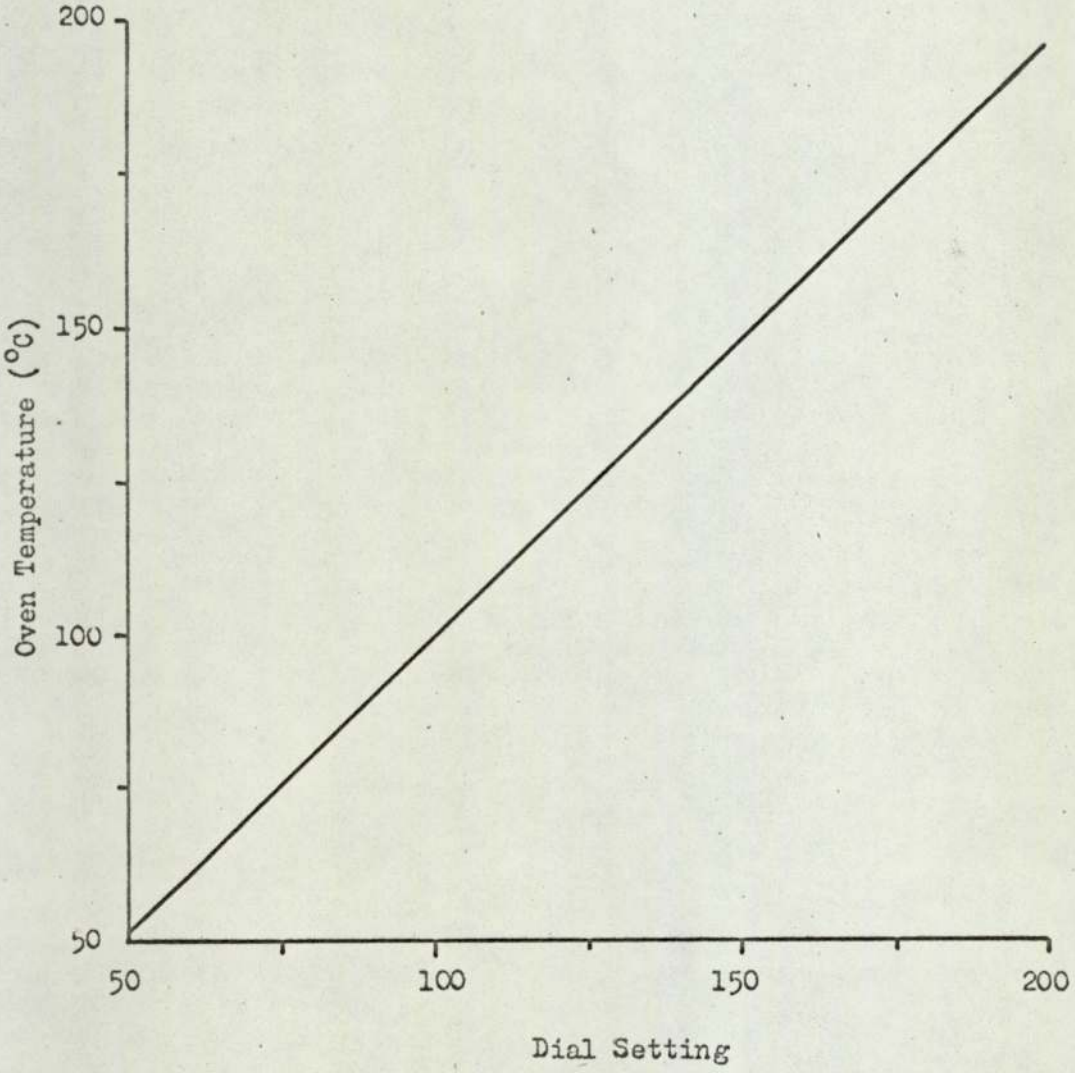

APPENDIX 2

Listings of Computer Programs Used for Calculation of Experimental Results

FIGURE A.2.1

(FLOWCHART GIVEN AS FIG.5.3)

```
10  PRINT "PROGRAM TO CALCULATE MEAN, STANDARD DEVIATION, SKEW,"
20  PRINT "KURTOSIS,N.T.P. AND H.E.T.P."
23  FOR A=1,2
24  IF A=1 GOTO 23
25  PRINT "CALC FOR COLUMN OUTLET PROFILE"
26  PRINT "================================="
27  GOTO 30
28  PRINT "CALC. FOR INJECTION PROFILE"
29  PRINT "============================"
30  DIM F(200)
35  PRINT "INPUT TIME TO START OF PROFILE OUTPUT(SECS.)"
36  INPUT T(A)
40  PRINT "NOS. OF DATA POINTS STORED ="
50  INPUT N
55  PRINT "TIME INTERVAL BETWEEN DATA POINTS STORED (SECS.)"
56  INPUT I
80  FOR J=1,N
90  READ F(J)
95  REM   F(J)=PROFILE HEIGHTS (CHART UNITS) AT INTERVAL I
100  NEXT J
110  S=0:S1=0:S2=0:S3=0:S4=0
155  PRINT "INPUT FRACTION OF DATA POINTS TO BE SAMPLED "
156  PRINT "ALL=1,HALF=2,THIRD=3 ETC."
157  INPUT N1
160  FOR J=1,N,N1
170  S=S+F(J)
180  S1=S1+I*J*F(J)
190  NEXT J
200  M1=S1/S
210  FOR J=1,N,N1
220  S2=S2+F(J)*(I*J-M1)↑2
230  S3=S3+F(J)*(I*J-M1)↑3
240  S4=S4+F(J)*(I*J-M1)↑4
250  NEXT J
260  M2=S2/S:D=M2↑.5:M3=S3/S:S9=M3/D↑3:K=M4/D↑4-3
310  PRINT "ARITHMETIC MEAN =",M1
320  PRINT "STANDARD DEVIATION =",D
325  PRINT "VARIANCE =",M2
330  PRINT "SKEW=",S9
340  PRINT "KURTOSIS =",K
361  M(A)=M1
362  V(A)=M2
365  NEXT A
366  PRINT "       "
367  PRINT " "
368  PRINT "NOW CALCULATION FOR N.T.P. AND H. E. T. P."
369  PRINT "=================================================="
370  PRINT "INPUT LENGTH OF PACKED SECTION IN CMS"
380  INPUT L
390  N9=((T(2)+M(2))-(T(1)+M(1)))↑2/(V(2)-V(1))
395  REM   THIS SI EQU. 5.2 FOR N.T.P.
400  H=L/N9
410  PRINT "N.T.P.=",N9
420  PRINT "H.E.T.P.=",H,"CMS"
430  END
```

?

FIGURE A.2.2

(FLOWCHART GIVEN AS FIG.5.5)

```
1   PRINT "PROGRAM TO CALCULATE INTERPARTICLE VOLUME, PACKING"
2   PRINT "VOLUME AND MEAN CARRIER GAS VELOCITY FOR COMPARISON"
3   PRINT "OF INDIVIDUAL COLUMN PROPERTIES"
5   DIM V(20),T(20),I(20),O(20),P(20),H(20),L(20)
6   DIM R(20),J(20),F(20),D(20),S(20),A(20),U(20)
7   DIM X(20),Y(20)
15   REM       L=COL.LEN(CMS), D=COL. DIAM(CMS),  N=NOS.OF RUNS
16   REM       V(J)=VOL.METER(FT↑3), T(J)=TIME VOL.MEASURED(SECS)
17   REM  I(J)=COL. INLET PRESS.(IN.HG), O(J)=COL. OUTLET PRESS.(IN.HG
18   REM  P(J)=ATMOS. PRESS.(CM.HG), H(J)=H2 RETENTION TIME(SECS.)
20   READ D,N,L
40   FOR J=1,N
50   READ V(J),T(J),I(J),O(J),P(J),H(J),L(J)
60   V(J)=V(J)*.23317E05/T(J)
65   REM  V(J)=CARRIER GAS FLOWRATE IN CM↑3/SEC.
70   I(J)=I(J)*2.54
80   O(J)=O(J)*2.54
85   REM  COLUMN PRESSURES NOW CONVERTED TO CM.HG
90   R(J)=(I(J)+P(J))/(O(J)+P(J))
100   J(J)=1.5*(R(J)↑2-1)/(R(J)↑3-1)
105   REM  J(J) = 'J'FACTOR
110   F(J)=V(J)*P(J)/(O(J)+P(J))*J(J)
115   REM  F(J)=MEAN COLUMN CARRIER GAS FLOWRATE
120   D(J)=F(J)*H(J)
125   REM  D(J) = RETENTION VOLUME FOR H2
130   S(J)=(L(J)*3.142*D↑2/4-D(J))*L/L(J)
135   REM  S(J) = PACKING VOLUME IN COLUMN
140   A(J)=D(J)/L(J)
150   U(J)=F(J)/A(J)
151   REM  U(J) = MEAN CARRIER GAS VELOCITY
155   X(J)=A(J)*L
156   REM  X(J)= TOTAL INTERPARTICLE VOLUME('DEAD VOLUME')
160   NEXT J
170   PRINT "    RUN        DEAD VOL       PACK VOL          VEL(CM/SEC)"
171   PRINT "    ===        ========       ========          ============"
175   FOR J=1,N
180   PRINT J,X(J),S(J),U(J)
190   NEXT J
200   STOP

?
```

FIGURE A.2.3

(FLOWCHART GIVEN AS FIG. 6.4)


```
1  PRINT "PROGRAM TO CALCULATE K V'S C AT A SERIES OF TEMPERATURES
10  READ D,M1,R
20  READ R1,C1,M9
30  READ N,X
35  REM  D=DENSITY OF SOLVENT,M1 =M.WT. OF SOLVENT
36  REM  R=GAS CONSTANT,RI=    ,C1=    ,M9=M.WT. OF SOLUTE
37  REM  N=NOS. OF TEMPS.,X=MAX. SOLUTE MOLE FRACTION IN LIQUID
40  I=1
50  READ T,P
55  REM  T=TEMPERATURE (K),P=SATURATED VAPOUR PRESSURE OF SOLUTE
67  PRINT "FOR TEMPERATURE =",T-273.2,"C"
63  PRINT "----------------"
69  PRINT "SATURATED VAPOUR PRESSURE =",P
70  PRINT "     X1           GAS CONC.          GAMMA          K"
71  PRINT "   ----         -----------    --------         ---"
80  X1=0
85  REM  X1=MOLE FRACTION OF SOLUTE IN LIQUID SOLVENT PHASE
100  X2=1-X1
105  REM  X2=MOLE FRACTION OF SOLVENT IN LIQUID SOLVENT PHASE
110  G=R1/(R1*X1+X2)*EXP(X2*(1-R1)/(R1*X1+X2)+C1*((X2/(R1*X1+X2))↑2
115  REM  G= Y ,---EQU. 6.23
120  K=R*T*D/(G*P*M1*X2)
125  REM  EQU. 6.24
130  C=X1*D*M9/(K*X2*M1)
135  REM  EQU. 6.25
140  PRINT X1,C,G,K
200  IF (X1+.1E-01)>X GOTO 263
205  REM  NOTE PRECAUTION AGAINST ROUND-OFF ERROR IN LINE 200
210  X1=X1+.5E-01
220  GOTO 100
263  PRINT
264  PRINT "=================================================
270  I=I+1
280  IF I>N GOTO 300
290  GOTO 50
300  STOP

?
```

FIGURE A.2.4

(FLOWCHART GIVEN AS FIG. 3.3)


```
1  PRINT "PROGRAM TO CALCULATE COLUMN CONCENTRATION PROFILES"
10  DIM I(100),P(100),V(100),A(100),G(100),W(100),B(100)
11  DIM C(100),H(100),K(100)
15  READ X
16  REM  X= NOS. OF SAMPLES PER SEQUENCING INTERVAL
20  READ N,P,S1,S2
21  REM  N=TOTAL NOS. OF SAMPLES
22  REM  S1 = SLOPE OF F.I.D. CALIBRATION CURVE FOR 'A'P
23  REM  S2 = SLOPE OF F.I.D. CALIBRATION CURVE FOR 'G'P
30  FOR J=1,N
40  READ I(J),P(J),V(J),A(J),G(J)
41  REM  I(J)=NOS. OF ISOLATED COLUMN WHEN SAMPLING COLUMN 2
42  REM  P(J) = SAMPLE POINT PRESS.,V(J)=SAMPLE VOLUME
43  REM  A(J)=AREA OF 'A'P PEAK (CHROMOLOG UNITS TO BASE 1*10↑2)
44  REM  G(J)=AREA OF 'G'P PEAK
70  W(J)=V(J)*(P(J)+P)/P
71  REM  W(J)=STANDARDISED SMPLE VOLUME
80  A(J)=A(J)*S1
81  REM  A(J)=WEIGHT OF 'A'P IN SAMPLE
90  G(J)=G(J)*S2
91  REM  G(J)=WEIGHT OF 'G'P IN SAMPLE
100  C(J)=A(J)/W(J)
101  REM  C(J)=STANDARDISED CONCENTRATION OF 'A'P
110  B(J)=A(J)/V(J)
111  REM  B(J)=COLUMN CONCENTRATION OF 'A'P
120  K(J)=G(J)/W(J)
121  REM  K(J)=STANDARDISED CONCENTRATION OF 'G'P
130  H(J)=G(J)/V(J)
131  REM  H(J)=COLUMN CONCENTRATION OF 'G'P
140  NEXT J
150  PRINT "FOR ARKLONE P"
160  PRINT "   BED              ST. VOL.      WT. INJ.      COL.CONC.
CONC."
165  Z=.5
170  FOR Y=1,X
175  FOR J=Y,N,X
177  IF Z>1 GOTO 185
180  PRINT I(J),W(J),A(J),B(J),C(J)
182  GOTO 190
185  PRINT I(J),W(J),G(J),H(J),K(J)
190  NEXT J
193  PRINT
194  PRINT
195  PRINT
196  PRINT "NEXT SAMPLING TIME AFTER SWITCHING"
197  PRINT
198  NEXT Y
200  PRINT
210  PRINT "FOR GENKLENE P"
220  PRINT "   BED              ST. VOL.      WT. INJ.      COL. CONC.
CONC."
225  IF Z>1 GOTO 260
240  Z=Z+1
250  GOTO 170
260  STOP
```

?

APPENDIX 3

Example Calculation of Weight of Solute Injected and Subsequent Calibration of Flame Ionisation Detector

Fig A.3.1 Example Calculation of the Weight of Solute Injected onto the Analytical Column

Solute - 'Arklone' P

1) Weight of solute initially injected into sealed flask = 0.015 g

Initial volume of flask at 20 °C and 101.3 kN m^{-2} = 1.2522 dm^3

Ambient temperature = 18.4 °C

Pressure in flask after solute injection = 101.5 kN m^{-2}

2) Initial solute concentration in flask

$$= \frac{0.0815}{1252.2 \times \frac{293.2}{291.6} \times \frac{101.5}{101.3}} = c_1 \text{ g cm}^{-3}$$

3) Volume of sample drawn from flask for injection onto column = 1.048 cm^3

Weight of solute injected

$$= 1.048 \times \frac{293.1}{291.6} \times \frac{101.5}{101.3} \times c_1$$

$$= 1.048 \times \frac{0.0815}{1252.2} = 0.682 \times 10^{-4} \text{ g}$$

4) Weight of solute remaining in flask

$$= 0.0815 - 0.682 \times 10^{-4} \text{ g} = 0.0814 \text{ g}$$

Return to (2) to recalculate solute concentration in the flask for next injection and so on.

Table A.3.1 Calibration of 1 cm^3 'Pressure-Lok' Syringe using Grooved Spacer Rods

Nominal Volume	Volume determined by weighing delivered distilled water
cm^3	cm^3
1.0	1.0479
0.9	0.9440
0.8	0.8365
0.7	0.7320
0.6	0.6252
0.5	0.5218
0.4	0.4168
0.3	0.3111
0.2	0.2046
0.1	0.1026

Table A.3.2 Example Flame Ionisation Detector Calibration

Initially injected 0.0815 g 'Arklone' P and 0.0688 g of 'Genklene' P by calibrated 100 µl syringe

Flask volume 1252.0 cm^3 at 20 °C

Lab. Pressure 99.9 kN m^{-2}

Lab. Temperature 18.5 °C

Injection Number	Flask Volume	Pressure in Flask above Ambient	Sample Volume	Amplifier Attenuation		Peak Height		Peak Area		Peak Height to base 1×10^2		Peak Area to Base 1×10^2		Weight of Solute injected	
				AP	GP	AP	GP	AP	GP	AP	GP	AP	GP	AP	GP
		kN m^{-2}	cm^3			chart units		'chromalog' units						10^{-4} g	10^{-4} g
1	1252.2	1.60	1.048	2×10^4	2×10^4	64.0	50.6	100	130	12800	20000	10120	26000	0.682	0.573
2	"	1.60	"	"	"	63.0	51.0	99	131	12600	19800	10200	26200	0.680	0.572
3	"	1.56	"	"	"	63.6	50.5	98	131	12660	19600	10100	26200	0.680	0.571
4	"	1.51	0.944	2×10^4	1×10^4	58.0	92.2	89	234	11600	17800	9220	23400	0.612	0.514
5	"	1.47	"	"	"	57.3	92.6	88	234	11460	17600	9260	23400	0.611	0.514
6	"	1.41	"	"	"	58.0	93.0	88	236	11600	17600	9300	23600	0.611	0.514
7	1252.1	1.31	0.837	2×10^4	1×10^4	54.2	84.0	79	210	10840	15800	8400	21000	0.541	0.455
8	"	1.23	"	"	"	53.6	82.9	78	208	10600	15600	8290	20800	0.541	0.454
9	"	1.16	"	"	"	53.6	83.5	78	209	10720	15600	8350	20900	0.540	0.453

Table A.3.2 Cont'd.

Injection Number	Flask Volume	Pressure in Flask above Ambient	Sample Volume	Amplifier Attenuation		Peak Height		Peak Area		Peak Height to base 1×10^2		Peak Area to base 1×10^2		Weight of Solute injected	
				AP	GP	AP	GP	AP	GP	AP	GP	AP	GP	AP	GP
		$kN\ m^{-2}$	cm^3			chart units		'chromalog' units						10^{-4} g	10^{-4} g
10	1252.1	1.11	0.732	1×10^4	1×10^4	93.9	72.1	138	182	9390	13800	7210	18200	0.472	0.397
11	"	1.00	"	"	"	94.1	71.3	140	180	9410	14000	7130	18000	0.472	0.396
12	"	0.93	"	"	"	92.6	71.5	138	183	9260	13800	7150	18300	0.471	0.396
13	"	0.89	0.625	1×10^4	1×10^4	75.9	61.3	118	154	7590	11800	6130	15400	0.402	0.338
14	"	0.85	"	"	"	75.2	61.9	117	156	7520	11700	6170	15600	0.402	0.338
15	"	0.80	"	"	"	75.2	62.1	117	155	7520	11700	6200	15500	0.402	0.338
16	"	0.75	0.522	1×10^4	1×10^4	64.1	50.5	98	128	6410	9800	5050	12800	0.335	0.282
17	"	0.67	"	"	"	64.9	50.9	97	129	6490	9700	5090	12900	0.335	0.282
18	"	0.59	"	"	"	64.2	51.1	99	129	6420	9900	5100	12900	0.335	0.282
19	"	0.53	0.417	1×10^4	50×10^2	52.8	86.2	78	214	5280	7800	4310	10700	0.268	0.225
20	"	0.52	"	"	"	52.1	85.7	78	212	5210	7800	4285	10600	0.267	0.225
21	"	0.49	"	"	"	52.0	86.8	77	214	5200	7700	4340	10700	0.267	0.225
22	"	0.45	"	"	"	51.3	84.4	77	210	5130	7700	4220	10500	0.267	0.225

Table A.3.2 Cont'd.

Injection Number	Flask Volume	Pressure in Flask above Ambient	Sample Volume	Amplifier Attenuation		Peak Height		Peak Area		Peak Height to base 1×10^2		Peak Area to base 1×10^2		Weight of Solute injected	
				AP	GP	AP	GP	AP	GP	AP	GP	AP	GP	AP	GP
		$kN\ m^{-2}$	cm^3			chart units		'chromalog' units						10^{-4} g	10^{-4} g
23	1252.1	0.40	0.311	50×10^2	50×10^2	76.2	61.6	116	157	3810	5800	3130	7850	0.199	0.168
24	"	0.39	"	"	"	76.0	63.8	114	156	3800	5700	3190	7800	0.199	0.168
25	"	0.37	"	"	"	75.4	61.0	115	153	3770	5750	3050	7650	0.199	0.168
26	"	0.36	"	"	"	74.8	62.2	115	153	3740	5750	3110	7650	0.199	0.168
27	"	0.32	0.205	50×10^2	50×10^2	72.8	42.0	80	103	3640	4000	2100	5150	0.131	0.110
28	"	0.28	"	"	"	73.7	42.2	79	105	3685	3950	2110	5250	0.131	0.110
29	"	0.27	"	"	"	74.0	41.2	79	102	3700	3950	2160	5100	0.131	0.110
30	"	0.26	"	"	"	72.4	40.8	78	104	3620	3900	2040	4200	0.131	0.110
31	"	0.26	0.103	20×10^2	20×10^2	61.0	50.4	96	123	1220	1920	1080	2460	0.066	0.056
32	"	0.24	"	"	"	61.5	50.5	97	120	1230	1940	1110	2400	0.066	0.056
33	"	0.21	"	"	"	63.0	50.2	97	119	1260	1940	1040	2380	0.066	0.056
34	"	0.19	"	"	"	61.4	50.4	96	119	1280	1920	1040	2380	0.066	0.056

APPENDIX 4

Detailed Results of Concentration Profile Analyses

Table A.4.1. Concentration Profile Analysis for Run 300 - 275 - 300

Notes: (i) $P_{std} = P_a = 102 kN\ m^{-2}$

(ii) All gas phase solute concentrations of less than 0.1×10^{-5} g cm^{-3} are given in first significant figure

(iii) Analysis recorded 6.25 hr after start-up

Column Isolated	Distance of sample point from Product 1 Outlet	P_{col} (at sample point)	$c_{i(col)}$		$c_{i(std)}$	
			AP	GP	AP	GP
	cm	$kN\ m^{-2}$	10^{-3} g cm^{-3}	10^{-3} g cm^{-3}	10^{-3} g cm^{-3}	10^{-3} g cm^{-3}
Sampling 100 s after sequencing action						
1	625	406	0.0002	0.209	0.00005	0.052
2	686	239	0.0001	0.016	0.00003	0.007
3	15	172	0.113	0.0004	0.067	0.0002
4	76	203	0.140	0.0003	0.070	0.0002
5	137	228	0.154	0.0005	0.068	0.0002
6	198	255	0.194	0.0004	0.077	0.0002
7	259	281	0.204	0.0004	0.073	0.0002
8	320	305	0.314	0.069	0.104	0.023
9	381	323	0.267	0.163	0.083	0.051
10	442	336	0.002	0.284	0.0006	0.085
11	503	366	0.001	0.232	0.0003	0.064
12	564	385	0.0008	0.234	0.0002	0.061
Sampling 250 s after sequencing action						
1	625	406	0.0001	0.220	0.00002	0.055
2	686	239	0.00004	0.0009	0.00002	0.0004
3	15	179	0.137	0.0005	0.077	0.0003
4	76	231	0.149	0.0005	0.073	0.0002
5	137	233	0.160	0.0005	0.070	0.0002
6	198	256	0.200	0.0004	0.079	0.0002
7	259	281	0.222	0.0005	0.080	0.0002
8	320	307	0.324	0.129	0.107	0.043
9	381	322	0.010	0.223	0.003	0.070
10	442	336	0.001	0.303	0.0003	0.091
11	503	366	0.001	0.204	0.0003	0.057
12	564	385	0.0006	0.222	0.0002	0.058

Table A.4.2 Concentration Profile Analysis for Run 500 - 275 - 300

Notes: (i) $P_{std} = P_a = 102 kN\ m^{-2}$

(ii) All gas phase solute concentrations of less than 0.1×10^{-5} g cm^{-3} are given in first significant figure

(iii) Analysis recorded 7.75 hrafter start-up

Column Isolated	Distance of sample point from Product 1 Outlet	P_{col} (at sample point)	$c_{i(col)}$		$c_{i(std)}$	
			AP	GP	AP	GP
	cm	kN m^{-2}	10^{-3} g cm^{-3}	10^{-3} g cm^{-3}	10^{-3} g cm^{-3}	10^{-3} g cm^{-3}
Sampling 100 s after sequencing action						
11	503	365	0.003	0.303	0.0007	0.085
12	564	380	0.002	0.286	0.0005	0.077
1	625	401	0.0006	0.297	0.0001	0.077
2	686	238	0.0002	0.063	0.00007	0.027
3	15	182	0.227	0.001	0.127	0.0007
4	76	210	0.270	0.001	0.128	0.0005
5	137	234	0.324	0.001	0.142	0.0006
6	198	262	0.377	0.0007	0.147	0.0003
7	259	281	0.434	0.0009	0.158	0.0003
8	320	306	0.507	0.060	0.170	0.020
9	381	323	0.461	0.144	0.146	0.046
10	442	349	0.034	0.301	0.010	0.088
Sampling 250s after sequencing action						
11	503	365	0.002	0.276	0.0006	0.077
12	564	390	0.001	0.280	0.0003	0.073
1	625	403	0.0002	0.288	0.00005	0.073
2	686	238	0.0002	0.005	0.00007	0.002
3	15	185	0.244	0.002	0.135	0.0008
4	76	213	0.300	0.0007	0.144	0.0004
5	137	240	0.364	0.0008	0.155	0.0003
6	198	261	0.404	0.0009	0.158	0.0003
7	259	282	0.467	0.0007	0.170	0.0003
8	320	307	0.561	0.145	0.187	0.048
9	381	325	0.177	0.191	0.056	0.060
10	442	351	0.004	0.356	0.001	0.104

Table A.4.3 Concentration Profile Analysis for Run 600 - 275 - 300

Notes: (i) $P_{std} = P_a = 101$ kN m^{-2}

(ii) All gas phase solute concentrations of less than 0.1×10^{-5} g cm^{-3} are given in first significant figure

(iii) Analysis recorded 5.75 hr after start-up

Column Isolated	Distance of sample point from Product 1 Outlet	P_{col} (at sample point)	$c_{i(col)}$		$c_{i(std)}$	
			AP	GP	AP	GP
	cm	kN m^{-2}	10^{-3} g cm^{-3}	10^{-3} g cm^{-3}	10^{-3} g cm^{-3}	10^{-3} g cm^{-3}
Sampling 100 s after sequencing action						
2	686	226	0.0002	0.065	0.00009	0.029
3	15	177	0.280	0.001	0.160	0.0007
4	76	201	0.344	0.0008	0.174	0.0004
5	137	228	0.424	0.0007	0.189	0.0003
6	198	254	0.507	0.0005	0.203	0.0002
7	259	280	0.601	0.0006	0.218	0.0002
8	320	302	0.714	0.066	0.240	0.022
9	381	324	0.648	0.140	0.203	0.044
10	442	340	0.414	0.201	0.124	0.060
11	503	364	0.011	0.341	0.003	0.095
12	564	380	0.003	0.429	0.0008	0.115
1	625	399	0.001	0.286	0.0003	0.073
Sampling 250 s after sequencing action						
2	686	225	0.0001	0.003	0.00006	0.001
3	15	183	0.307	0.001	0.170	0.0005
4	76	211	0.381	0.0007	0.183	0.0003
5	137	236	0.481	0.0006	0.207	0.0002
6	198	257	0.547	0.0005	0.216	0.0002
7	259	282	0.621	0.0005	0.224	0.0002
8	320	308	0.748	0.136	0.246	0.045
9	381	324	0.547	0.160	0.171	0.050
10	442	343	0.160	0.261	0.047	0.077
11	503	364	0.004	0.396	0.001	0.110
12	564	379	0.002	0.338	0.0006	0.090
1	625	400	0.0005	0.301	0.0001	0.076

Table A.4.4 Concentration Profile Analysis for Run 700 - 275 - 300

Notes: (i) $P_{std} = P_a = 100\ kN\ m^{-2}$

(ii) All gas phase solute concentrations of less than $0.1 \times 10^{-5}\ g\ cm^{-3}$ are given in first significant figure

(iii) Analysis recorded 5.50 hrafter start-up

Column Isolated	Distance of sample point from Product 1 Outlet	P_{col} (at sample point)	$c_{i(col)}$		$c_{i(std)}$	
			AP	GP	AP	GP
	cm	$kN\ m^{-2}$	$10^{-3}\ g\ cm^{-3}$	$10^{-3}\ g\ cm^{-3}$	$10^{-3}\ g\ cm^{-3}$	$10^{-3}\ g\ cm^{-3}$
Sampling 100 s after sequencing action						
3	15	170	0.334	0.001	0.196	0.0009
4	76	198	0.407	0.001	0.206	0.0007
5	137	225	0.507	0.0008	0.226	0.0003
6	198	252	0.621	0.0009	0.247	0.0003
7	259	277	0.694	0.0008	0.251	0.0003
8	320	295	0.788	0.054	0.268	0.018
9	381	322	0.821	0.224	0.256	0.070
10	442	349	0.681	0.229	0.202	0.068
11	503	362	0.013	0.313	0.004	0.087
12	564	379	0.004	0.785	0.001	0.207
1	625	386	0.002	0.629	0.0008	0.159
2	686	238	0.0003	0.058	0.0001	0.024
Sampling 250 s after sequencing action						
3	15	173	0.374	0.001	0.216	0.0007
4	76	198	0.447	0.0009	0.226	0.0005
5	137	227	0.567	0.0009	0.251	0.0004
6	198	253	0.648	0.0007	0.257	0.0003
7	259	279	0.721	0.0006	0.259	0.0002
8	320	301	0.834	0.184	0.278	0.061
9	381	321	0.774	0.234	0.241	0.073
10	442	337	0.434	0.282	0.129	0.084
11	503	362	0.013	0.402	0.004	0.111
12	564	379	0.003	0.772	0.0009	0.204
1	625	395	0.0006	0.345	0.0002	0.088
2	686	236	0.0003	0.004	0.0001	0.002

Table A.4.5 Concentration Profile Analysis for Run 200 - 275 - 400

Notes: (i) $P_{std} = P_a = 101$ kN m^{-2}

(ii) All gas phase solute concentrations of less than 0.1×10^{-5} g cm^{-3} are given in first significant figure

(iii) Analysis recorded 7.75 hrafter start-up

Column Isolated	Distance of sample point from Product 1 Outlet	P_{col} (at sample point)	$c_{i(col)}$		$c_{i(std)}$	
			AP	GP	AP	GP
	cm	kN m^{-2}	10^{-3} g cm^{-3}	10^{-3} g cm^{-3}	10^{-3} g cm^{-3}	10^{-3} g cm^{-3}
Sampling 150 s after sequencing action						
3	15	185	0.149	0.0002	0.082	0.0001
4	76	210	0.168	0.0008	0.081	0.0004
5	137	227	0.183	0.0008	0.081	0.0003
6	198	249	0.208	0.0007	0.084	0.0003
7	259	268	0.225	0.0007	0.085	0.0003
8	320	283	0.272	0.044	0.097	0.016
9	381	301	0.163	0.119	0.054	0.040
10	442	321	0.002	0.239	0.0005	0.075
11	503	338	0.002	0.163	0.0005	0.049
12	564	351	0.0009	0.175	0.0002	0.051
1	625	365	0.0003	0.163	0.00008	0.045
2	686	213	0.00003	0.008	0.00002	0.004
Sampling 350 s after sequencing action						
3	15	185	0.159	0.0009	0.082	0.0004
4	76	210	0.176	0.0008	0.084	0.0004
5	137	227	0.193	0.0008	0.083	0.0004
6	198	250	0.210	0.0007	0.084	0.0003
7	259	268	0.231	0.0007	0.087	0.0002
8	320	284	0.258	0.102	0.091	0.036
9	381	301	0.003	0.205	0.001	0.068
10	442	321	0.001	0.180	0.0004	0.056
11	503	339	0.001	0.70	0.0003	0.051
12	564	350	0.0006	0.172	0.0002	0.050
1	625	364	0.0001	0.161	0.0003	0.044
2	686	213	0.00005	0.0009	0.00002	0.0004

Table A.4.6 Concentration Profile Analysis for Run 300 - 275 - 400

Notes: (i) $P_{std} = P_a = 102$ kN m^{-2}

(ii) All gas phase solute concentrations of less than 0.1×10^{-5} g cm^{-3} are given in first significant figure

(iii) Analysis recorded 11.0 hr after start-up

Column Isolated	Distance of sample point from Product 1 Outlet	P_{col} (at sample point)	$c_{i(col)}$		$c_{i(std)}$	
			AP	GP	AP	GP
	cm	kN m^{-2}	10^{-3} g cm^{-3}	10^{-3} g cm^{-3}	10^{-3} g cm^{-3}	10^{-3} g cm^{-3}
Sampling 150 s after sequencing action						
3	15	185	0.201	0.0006	0.111	0.0003
4	76	206	0.255	0.0006	0.126	0.0003
5	137	227	0.278	0.0005	0.125	0.0002
6	198	247	0.325	0.0006	0.134	0.0002
7	259	268	0.359	0.0005	0.136	0.0002
8	320	282	0.426	0.030	0.154	0.011
9	381	298	0.241	0.114	0.083	0.039
10	442	319	0.003	0.192	0.001	0.062
11	503	338	0.002	0.285	0.0005	0.086
12	564	350	0.001	0.174	0.0003	0.051
1	625	365	0.0003	0.196	0.00008	0.055
2	686	208	0.0001	0.024	0.00005	0.012
Sampling 350 s after sequencing action						
3	15	192	0.225	0.0002	0.119	0.0001
4	76	212	0.272	0.0006	0.131	0.0003
5	137	232	0.309	0.0005	0.135	0.0002
6	198	254	0.322	0.0006	0.133	0.0002
7	259	271	0.382	0.0005	0.144	0.0002
8	320	285	0.396	0.098	0.142	0.035
9	381	302	0.138	0.117	0.046	0.039
10	442	322	0.002	0.252	0.0006	0.079
11	503	338	0.002	0.222	0.0005	0.067
12	564	350	0.0009	0.196	0.0003	0.057
1	625	364	0.0002	0.189	0.00005	0.053
2	686	205	0.00005	0.002	0.00001	0.001

Table A.4.7 Concentration Profile Analysis for Run 400 - 275 - 400

Notes: (i) $P_{std} = P_a = 102\ kN\ m^{-2}$

(ii) All gas phase solute concentrations of less than $0.1 \times 10^{-5}\ g\ cm^{-3}$ are given in first significant figure

(iii) Analysis recorded 8.67 hrafter start-up

Column Isolated	Distance of sample point from Product 1 Outlet	P_{col} (at sample point)	$c_{i(col)}$		$c_{i(std)}$	
			AP	GP	AP	GP
	cm	$kN\ m^{-2}$	$10^{-3}\ g\ cm^{-3}$	$10^{-3}\ g\ cm^{-3}$	$10^{-3}\ g\ cm^{-3}$	$10^{-3}\ g\ cm^{-3}$
Sampling 150 s after sequencing action						
2	686	239	0.0001	0.019	0.00005	0.008
3	15	186	0.187	0.003	0.103	0.0001
4	76	202	0.244	0.0005	0.124	0.0002
5	137	226	0.274	0.0005	0.124	0.0002
6	198	243	0.354	0.0005	0.149	0.0002
7	249	269	0.347	0.0004	0.132	0.0002
8	320	282	0.507	0.073	0.184	0.026
9	381	291	0.417	0.122	0.143	0.042
10	442	320	0.053	0.186	0.017	0.059
11	503	336	0.002	0.246	0.0006	0.075
12	564	352	0.002	0.288	0.0004	0.084
1	625	366	0.0004	0.225	0.0001	0.063
Sampling 350 s after sequencing action						
2	686	236	0.00007	0.0004	0.00003	0.0002
3	15	191	0.197	0.0007	0.105	0.0004
4	76	211	0.294	0.0006	0.143	0.0003
5	137	232	0.347	0.0005	0.153	0.0002
6	198	252	0.377	0.0005	0.153	0.0002
7	249	271	0.387	0.0005	0.146	0.0002
8	320	285	0.541	0.119	0.194	0.043
9	381	306	0.320	0.122	0.107	0.041
10	442	323	0.003	0.221	0.0009	0.070
11	503	337	0.002	0.328	0.0006	0.100
12	564	352	0.0009	0.204	0.0003	0.059
1	625	366	0.0002	0.238	0.0005	0.066

Table A.4.8 Concentration Profile Analysis for Run 500 - 275 - 400

Notes: (i) $P_{std} = P_a = 102$ kN m^{-2}

(ii) All gas phase solute concentrations of less than 0.1×10^{-5} g cm^{-3} are given in first significant figure

(iii) Analysis recorded 6.67 hrafter start-up

Column Isolated	Distance of sample point from Product 1 Outlet	P_{col} (at sample point)	$c_{i(col)}$		$c_{i(std)}$	
			AP	GP	AP	GP
	cm	kN m^{-2}	10^{-3} g cm^{-3}	10^{-3} g cm^{-3}	10^{-3} g cm^{-3}	10^{-3} g cm^{-3}
Sampling 150 s after sequencing action						
1	625	366	0.0008	0.356	0.0002	0.099
2	686	236	0.0001	0.019	0.00006	0.008
3	15	184	0.334	0.0002	0.186	0.0001
4	76	209	0.387	0.0005	0.198	0.0003
5	137	227	0.441	0.0005	0.199	0.0002
6	198	244	0.514	0.0004	0.216	0.0002
7	259	268	0.574	0.0006	0.219	0.0002
8	320	282	0.648	0.094	0.235	0.034
9	381	298	0.648	0.160	0.222	0.055
10	442	320	0.514	0.146	0.164	0.047
11	503	338	0.085	0.244	0.026	0.074
12	564	351	0.002	0.332	0.0006	0.097
Sampling 350 s after sequencing action						
1	625	366	0.0003	0.242	0.0008	0.076
2	686	232	0.00008	0.0003	0.00004	0.0001
3	15	197	0.357	0.0005	0.185	0.0002
4	76	213	0.414	0.0005	0.199	0.0002
5	137	235	0.467	0.0004	0.203	0.0002
6	198	254	0.541	0.0006	0.217	0.0002
7	259	273	0.607	0.0006	0.228	0.0002
8	320	287	0.681	0.150	0.198	0.054
9	381	308	0.594	0.156	0.198	0.052
10	442	324	0.347	0.165	0.110	0.052
11	503	339	0.006	0.290	0.002	0.088
12	564	352	0.001	0.364	0.0004	0.106

Table A.4.9 Concentration Profile Analysis for Run 600 - 275 - 400

Notes: (i) $P_{std} = P_a = 102$ kN m^{-2}

(ii) All gas phase solute concentrations of less than 0.1×10^{-5} g cm^{-3} are given in first significant figure.

(iii) Analysis recorded 7.5 hr after start-up

Column Isolated	Distance of sample point from Product 1 Outlet	P_{col} (at sample point)	$c_{i(col)}$		$c_{i(std)}$	
			AP	GP	AP	GP
	cm	kN m^{-2}	10^{-3} g cm^{-3}	10^{-3} g cm^{-3}	10^{-3} g cm^{-3}	10^{-3} g cm^{-3}
Sampling 150 s after sequencing action						
10	442	312	0.834	0.225	0.273	0.074
11	503	334	0.854	0.244	0.261	0.075
12	564	348	0.754	0.261	0.222	0.077
1	625	365	0.467	0.274	0.131	0.077
2	686	216	0.001	0.022	0.0006	0.010
3	15	176	0.314	0.0002	0.183	0.0001
4	76	198	0.434	0.0005	0.224	0.0003
5	137	215	0.534	0.0004	0.253	0.0002
6	198	240	0.607	0.0005	0.259	0.0002
7	259	261	0.714	0.0004	0.280	0.0002
8	320	280	0.741	0.119	0.271	0.043
9	381	296	0.801	0.212	0.277	0.073
Sampling 350 s after sequencing action						
10	442	318	0.848	0.215	0.273	0.069
11	503	338	0.821	0.257	0.249	0.078
12	564	348	0.654	0.265	0.192	0.078
1	625	365	0.220	0.309	0.062	0.087
2	686	213	0.0003	0.0007	0.0002	0.0003
3	15	187	0.424	0.0005	0.232	0.0003
4	76	209	0.474	0.0004	0.232	0.0002
5	137	228	0.567	0.0005	0.254	0.0002
6	198	247	0.648	0.0004	0.268	0.0002
7	259	268	0.734	0.0005	0.280	0.0002
8	320	283	0.814	0.194	0.294	0.070
9	381	298	0.788	0.191	0.270	0.066

Table A.4.10 Concentration Profile Analysis for Run 300 - 275 - 500

Notes: (i) $P_{std} = P_a = 101$ kN m^{-2}

(ii) All gas phase solute concentrations of less than 0.1×10^{-5} g cm^{-3} are given in first significant figure

(iii) Analysis recorded 6.0 h after start-up

Column Isolated	Distance of sample point from Product 1 Outlet	P_{col} (at sample point)	$c_{i(col)}$		$c_{i(std)}$	
			AP	GP	AP	GP
	cm	kN m^{-2}	10^{-3} g cm^{-3}	10^{-3} g cm^{-3}	10^{-3} g cm^{-3}	10^{-3} g cm^{-3}
Sampling 100 s after sequencing action						
3	15	172	0.005	0.0005	0.003	0.0003
4	76	197	0.324	0.0003	0.174	0.0004
5	137	210	0.344	0.0006	0.166	0.0003
6	198	226	0.401	0.0007	0.179	0.0003
7	259	241	0.421	0.0007	0.176	0.0003
8	320	257	0.541	0.037	0.213	0.015
9	381	273	0.547	0.145	0.202	0.054
10	442	288	0.060	0.155	0.021	0.054
11	503	305	0.002	0.311	0.0005	0.103
12	564	311	0.002	0.328	0.0006	0.106
1	625	325	0.0007	0.240	0.0002	0.075
2	686	208	0.0002	0.117	0.00008	0.057
Sampling 300 s after sequencing action						
3	15	181	0.290	0.0003	0.161	0.0002
4	76	147	0.344	0.0007	0.177	0.0004
5	137	213	0.360	0.0006	0.171	0.0003
6	198	228	0.411	0.0006	0.182	0.0003
7	259	244	0.494	0.001	0.205	0.0004
8	320	261	0.581	0.127	0.224	0.049
9	381	277	0.427	0.124	0.156	0.045
10	462	291	0.003	0.202	0.001	0.070
11	503	299	0.001	0.372	0.0004	0.123
12	564	312	0.002	0.311	0.0006	0.101
1	625	325	0.0002	0.248	0.00007	0.077
2	686	205	0.0001	0.002	0.00007	0.001
Sampling 450 s after sequencing action						
3	15	181	0.304	0.0005	0.169	0.0003
4	76	197	0.344	0.0007	0.177	0.0004
5	137	212	0.374	0.0006	0.178	0.0003
6	198	229	0.404	0.0006	0.178	0.0003
7	259	246	0.407	0.0006	0.167	0.0002
8	320	261	0.601	0.149	0.232	0.058
9	381	274	0.300	0.108	0.111	0.040
10	442	291	0.002	0.286	0.0007	0.099
11	503	299	0.001	0.358	0.0005	0.118
12	564	311	0.001	0.246	0.0004	0.080
1	625	325	0.0002	0.240	0.00006	0.075
2	686	203	0.0002	0.001	0.00008	0.0006

Table A.4.11 Concentration Profile Analysis for Run 400 - 275 - 500

Notes: (i) $P_{std} = P_a = 100 kN\ m^{-2}$

(ii) All gas phase solute concentrations of less than 0.1×10^{-5} g cm^{-3} are given in first significant figure

(iii) Analysis recorded 7.0 hr after start-up

Column Isolated	Distance of sample point from Product 1 Outlet	P_{col} (at sample point)	$c_{i(col)}$		$c_{i(std)}$	
			AP	GP	AP	GP
	cm	kN m^{-2}	10^{-3} g cm^{-3}	10^{-3} g cm^{-3}	10^{-3} g cm^{-3}	10^{-3} g cm^{-3}
Sampling 100 s after sequencing action						
3	15	175	0.007	0.001	0.004	0.0008
4	76	200	0.472	0.0008	0.216	0.0004
5	137	212	0.469	0.0006	0.221	0.0003
6	198	229	0.513	0.0006	0.224	0.0003
7	259	242	0.593	0.0007	0.245	0.0004
8	320	261	0.705	0.026	0.271	0.010
9	381	274	0.811	0.137	0.297	0.050
10	442	290	0.811	0.183	0.279	0.063
11	503	306	0.272	0.364	0.089	0.119
12	564	313	0.025	0.545	0.008	0.174
1	625	328	0.023	0.440	0.0007	0.134
2	686	210	0.0006	0.212	0.0003	0.101
Sampling 300 s after sequencing action						
3	15	183	0.350	0.0007	0.191	0.0004
4	76	201	0.422	0.0005	0.210	0.0003
5	137	214	0.469	0.0006	0.219	0.0003
6	198	230	0.524	0.0007	0.228	0.0003
7	259	245	0.628	0.001	0.257	0.0005
8	320	264	0.760	0.087	0.288	0.033
9	381	279	0.829	0.176	0.297	0.063
10	442	294	0.723	0.212	0.246	0.072
11	503	306	0.072	0.456	0.024	0.149
12	564	314	0.003	0.540	0.001	0.172
1	625	329	0.002	0.408	0.0005	0.124
2	686	209	0.0002	0.002	0.00008	0.001
Sampling 450 s after sequencing action						
3	15	183	0.386	0.0007	0.211	0.0004
4	76	201	0.468	0.0007	0.223	0.0004
5	137	214	0.479	0.0006	0.224	0.0003
6	198	231	0.561	0.0009	0.243	0.0004
7	259	247	0.659	0.002	0.267	0.0009
8	320	265	0.800	0.123	0.302	0.044
9	381	280	0.815	0.188	0.291	0.067
10	442	295	0.507	0.257	0.172	0.087
11	503	306	0.003	0.508	0.0009	0.166
12	564	314	0.002	0.506	0.0005	0.161
1	625	329	0.001	0.362	0.0004	0.110
2	686	209	0.00004	0.015	0.00002	0.007

Table A.4.12 Concentration Profile Analysis for Run 500 - 275 - 500

Notes: (i) $P_{std} = P_a = 102$ kN m^{-2}

(ii) All gas phase solute concentrations of less than 0.1×10^{-5} g cm^{-3} are given in first significant figure

(iii) Analysis recorded 7.67 hr after start-up

Column Isolated	Distance of sample point from Product 1 Outlet	P_{col} (at sample point)	$c_{i(col)}$		$c_{i(std)}$	
			AP	GP	AP	GP
	cm	kN m^{-2}	10^{-3} g cm^{-3}	10^{-3} g cm^{-3}	10^{-3} g cm^{-3}	10^{-3} g cm^{-3}
Sampling 100 s after sequencing action						
3	15.	178	0.009	0.001	0.005	0.0007
4	76	199	0.581	0.0008	0.298	0.0004
5	137	215	0.668	0.001	0.317	0.0005
6	198	228	0.701	0.0008	0.314	0.0004
7	249	249	0.901	0.0009	0.371	0.0004
8	320	262	0.968	0.025	0.377	0.010
9	381	281	0.868	0.170	0.316	0.062
10	442	294	1.135	0.429	0.394	0.149
11	503	311	1.285	0.492	0.426	0.163
12	564	324	1.180	0.913	0.373	0.289
1	625	336	0.567	0.753	0.173	0.229
2	686	203	0.004	0.362	0.002	0.182
Sampling 300 s after sequencing action						
3	15	196	0.521	0.0006	0.271	0.0003
4	76	199	0.554	0.001	0.285	0.0006
5	137	227	0.680	0.0009	0.298	0.0004
6	198	239	0.901	0.001	0.385	0.0004
7	249	256	0.851	0.0009	0.340	0.0004
8	320	268	0.885	0.073	0.337	0.028
9	381	281	0.935	0.297	0.341	0.108
10	442	296	1.355	0.483	0.469	0.167
11	503	310	1.001	0.841	0.331	0.278
12	564	324	0.901	0.766	0.285	0.242
1	625	336	0.254	0.673	0.077	0.205
2	686	203	0.0004	0.040	0.0002	0.020
Sampling 450 s after sequencing action						
3	15	196	0.567	0.0008	0.296	0.0004
4	76	199	0.581	0.001	0.299	0.0005
5	137	227	0.768	0.0007	0.346	0.0003
6	198	240	0.995	0.001	0.424	0.0005
7	259	256	0.901	0.0009	0.360	0.0004
8	320	268	0.818	0.101	0.312	0.039
9	381	282	1.051	0.379	0.381	0.137
10	442	296	1.285	0.492	0.444	0.170
11	503	310	0.918	0.925	0.303	0.306
12	564	324	1.048	0.707	0.331	0.224
1	625	336	0.090	0.601	0.026	0.178
2	686	203	0.0004	0.002	0.0002	0.001

Table A.4.13 Concentration Profile Analysis for Run 300 - 275 - 600

Notes: (i) $P_{std} = P_a = 101\ kN\ m^{-2}$

(ii) All gas phase solute concentrations of less than 0.1×10^{-5} g cm^{-3} are given in first significant figure

(iii) Analysis recorded 5.0 hrafter start-up

Column Isolated	Distance of sample point from Product 1 Outlet	P_{col} (at sample point)	$c_{i(col)}$		$c_{i(std)}$	
			AP	GP	AP	GP
	cm	$kN\ m^{-2}$	10^{-3} g cm^{-3}	10^{-3} g cm^{-3}	10^{-3} g cm^{-3}	10^{-3} g cm^{-3}
Sampling 100 s after sequencing action						
4	76	201	0.360	0.0007	0.182	0.0004
5	137	223	0.407	0.0007	0.185	0.0003
6	198	236	0.434	0.001	0.187	0.0006
7	259	255	0.474	0.0007	0.189	0.0003
8	320	267	0.601	0.024	0.229	0.009
9	381	281	0.601	0.166	0.217	0.060
10	442	295	0.059	0.180	0.020	0.062
11	503	312	0.002	0.360	0.0005	0.118
12	564	324	0.0009	0.427	0.0003	0.134
1	625	337	0.0004	0.393	0.0001	0.119
2	686	185	0.0001	0.121	0.00005	0.055
3	15	201	0.0005	0.0003	0.0003	0.0002
Sampling 300 s after sequencing action						
4	76	211	0.377	0.0007	0.182	0.0003
5	137	223	0.431	0.0007	0.197	0.0003
6	198	240	0.487	0.0005	0.206	0.0002
7	259	256	0.507	0.0007	0.202	0.0003
8	320	270	0.628	0.156	0.237	0.059
9	381	282	0.501	0.162	0.181	0.059
10	442	297	0.005	0.214	0.002	0.074
11	503	312	0.001	0.433	0.0005	0.142
12	564	327	0.0007	0.421	0.0002	0.131
1	625	338	0.0002	0.355	0.00006	0.107
2	686	224	0.00005	0.003	0.00002	0.001
3	15	196	0.250	0.0003	0.130	0.0002
Sampling 500 s after sequencing action						
4	76	212	0.387	0.0007	0.186	0.0003
5	137	227	0.431	0.0007	0.194	0.0003
6	198	241	0.447	0.0007	0.189	0.0003
7	259	256	0.501	0.0007	0.199	0.0003
8	320	269	0.581	0.168	0.219	0.064
9	381	283	0.278	0.146	0.100	0.053
10	442	297	0.001	0.368	0.0004	0.126
11	503	311	0.001	0.440	0.0005	0.144
12	564	324	0.0007	0.381	0.0002	0.124
1	625	338	0.00013	0.309	0.00004	0.093
2	686	225	0.00003	0.0005	0.00001	0.0002
3	15	196	0.321	0.001	0.167	0.0006

Table A.4.14 Concentration Profile Analysis for Run 400 - 275 - 600

Notes: (i) $P_{std} = P_a = 101\ kN\ m^{-2}$

(ii) All gas phase solute concentrations of less than $0.1 \times 10^{-5}\ g\ cm^{-3}$ are given in first significant figure

(iii) Analysis recorded 5.5 hr after start-up

Column Isolated	Distance of sample point from Product 1 Outlet	P_{col} (at sample point)	$c_{i(col)}$		$c_{i(std)}$	
			AP	GP	AP	GP
	cm	$kN\ m^{-2}$	$10^{-3}\ g\ cm^{-3}$	$10^{-3}\ g\ cm^{-3}$	$10^{-3}\ g\ cm^{-3}$	$10^{-3}\ g\ cm^{-3}$
Sampling 100 s after sequencing action						
3	15	186	0.0004	0.002	0.0002	0.001
4	76	205	0.535	0.0008	0.264	0.0004
5	137	222	0.603	0.0009	0.274	0.0004
6	198	232	0.688	0.0007	0.300	0.0003
7	259	251	0.800	0.0007	0.322	0.0003
8	320	266	0.913	0.0008	0.347	0.0003
9	381	280	0.845	0.105	0.305	0.038
10	442	295	0.868	0.167	0.297	0.057
11	503	309	0.857	0.172	0.280	0.056
12	564	323	0.618	0.201	0.193	0.063
1	625	338	0.138	0.253	0.042	0.076
2	686	233	0.0009	0.237	0.0004	0.103
Sampling 300 s after sequencing action						
3	15	198	0.436	0.0009	0.223	0.0005
4	76	213	0.547	0.0007	0.259	0.0004
5	137	226	0.637	0.0008	0.284	0.0003
6	198	240	0.744	0.0008	0.313	0.0003
7	259	256	0.845	0.0007	0.334	0.0003
8	320	268	0.947	0.036	0.356	0.014
9	381	282	0.879	0.135	0.315	0.048
10	442	296	0.935	0.172	0.319	0.059
11	503	310	0.812	0.188	0.264	0.061
12	564	324	0.458	0.237	0.143	0.074
1	625	337	0.013	0.351	0.004	0.105
2	686	227	0.0004	0.009	0.0002	0.004
Sampling 550 s after sequencing action						
3	15	199	0.528	0.0005	0.268	0.0003
4	76	215	0.603	0.0009	0.283	0.0004
5	137	228	0.705	0.0007	0.312	0.0003
6	198	240	0.767	0.0007	0.323	0.0003
7	259	256	0.890	0.0007	0.350	0.0003
8	320	268	0.879	0.099	0.330	0.037
9	381	282	0.913	0.153	0.327	0.055
10	442	297	0.919	0.194	0.312	0.066
11	503	310	0.699	0.192	0.228	0.063
12	564	313	0.293	0.225	0.091	0.070
1	625	336	0.002	0.413	0.0006	0.124
2	686	227	0.0005	0.002	0.0002	0.0008

Table A.4.15 Concentration Profile Analysis for Run 300 - 155 - 300

Notes: (i) $P_{std} = P_a = 101 kN\ m^{-2}$

(ii) All gas phase solute concentrations of less than 0.1×10^{-5} g cm^{-3} are given in first significant figure

(iii) Analysis recorded 7.0 h after start-up

Column Isolated	Distance of sample point from Product 1 Outlet	P_{col} (at sample point)	$c_{i(col)}$		$c_{i(std)}$	
			AP	GP	AP	GP
	cm	$kN\ m^{-2}$	10^{-3} g cm^{-3}	10^{-3} g cm^{-3}	10^{-3} g cm^{-3}	10^{-3} g cm^{-3}
Sampling 100 s after sequencing action						
4	76	189	0.218	0.0002	0.119	0.00009
5	137	210	0.295	0.0003	0.142	0.00009
6	198	226	0.364	0.0003	0.162	0.0001
7	259	242	0.474	0.0003	0.198	0.0001
8	320	257	0.654	0.021	0.257	0.008
9	381	274	0.507	0.119	0.187	0.044
10	442	288	0.620	0.121	0.218	0.042
11	503	307	0.668	0.143	0.220	0.047
12	564	313	0.634	0.169	0.204	0.055
1	625	326	0.661	0.175	0.205	0.054
2	686	190	0.005	0.024	0.003	0.013
3	15	172	0.107	0.0004	0.063	0.0002
Sampling 250 s after sequencing action						
4	76	196	0.275	0.0002	0.142	0.0001
5	137	211	0.339	0.0003	0.162	0.0001
6	198	228	0.427	0.0003	0.189	0.0001
7	259	246	0.561	0.0003	0.230	0.0001
8	320	260	0.654	0.106	0.254	0.041
9	381	275	0.541	0.114	0.199	0.042
10	442	291	0.654	0.136	0.227	0.047
11	503	307	0.681	0.156	0.224	0.051
12	564	314	0.641	0.157	0.206	0.050
1	625	326	0.329	0.101	0.102	0.031
2	686	187	0.0006	0.0008	0.0003	0.0004
3	15	172	0.226	0.0001	0.129	0.0001

Table A.4.16 Concentration Profile Analysis for Run 300 - 215 - 350

Notes: (i) $P_{std} = P_a = 100$ kN m^{-2}

(ii) All gas phase solute concentrations of less than 0.1×10^{-5} g cm^{-3} are given in first significant figure

(iii) Analysis recorded 8.5 hr after start-up

Column Isolated	Distance of sample point from Product 1 Outlet	P_{col} (at sample point)	$c_{i(col)}$		$c_{i(std)}$	
			AP	GP	AP	GP
	cm	kN m^{-2}	10^{-3} g cm^{-3}	10^{-3} g cm^{-3}	10^{-3} g cm^{-3}	10^{-3} g cm^{-3}
Sampling 150 s after sequencing action						
8	320	250	0.641	0.056	0.257	0.022
9	381	266	0.594	0.137	0.224	0.052
10	442	281	0.547	0.142	0.195	0.051
11	503	296	0.277	0.181	0.094	0.061
12	564	309	0.012	0.218	0.004	0.071
1	625	324	0.003	0.144	0.0009	0.045
2	686	227	0.0002	0.009	0.00007	0.004
3	15	157	0.292	0.0002	0.186	0.0002
4	76	175	0.345	0.0003	0.198	0.0002
5	137	196	0.384	0.0003	0.196	0.0002
6	198	213	0.437	0.0003	0.206	0.0002
7	249	238	0.567	0.0004	0.239	0.0002
Sampling 300 s after sequencing action						
8	320	252	0.621	0.105	0.247	0.042
9	381	269	0.587	0.137	0.220	0.051
10	442	283	0.481	0.137	0.170	0.049
11	503	294	0.103	0.203	0.034	0.068
12	564	310	0.004	0.184	0.001	0.060
1	625	324	0.0007	0.151	0.0002	0.047
2	686	224	0.0001	0.0007	0.00005	0.0003
3	15	167	0.312	0.0002	0.187	0.0001
4	76	182	0.352	0.0003	0.193	0.0002
5	137	203	0.391	0.0003	0.193	0.0002
6	198	223	0.481	0.0003	0.216	0.0001
7	259	238	0.594	0.0003	0.250	0.0001

Table A.4.17 Concentration Profile Analysis for Run 300 - 345 - 450

Notes: (i) $P_{std} = P_a = 98\ kN\ m^{-2}$

(ii) All gas phase solute concentrations of less than 0.1×10^{-5} g cm^{-3} are given in first significant figure

(iii) Analysis recorded 7.0 hr after start-up

Column Isolated	Distance of sample point from Product 1 Outlet	P_{col} (at sample point)	$c_{i(col)}$		$c_{i(std)}$	
			AP	GP	AP	GP
	cm	kN m^{-2}	10^{-3} g cm^{-3}	10^{-3} g cm^{-3}	10^{-3} g cm^{-3}	10^{-3} g cm^{-3}
Sampling 100 s after sequencing action						
4	76	187	0.195	0.0006	0.102	0.0003
5	137	199	0.203	0.0005	0.096	0.0002
6	198	233	0.248	0.0004	0.105	0.0002
7	259	249	0.278	0.0004	0.110	0.0002
8	320	261	0.335	0.064	0.127	0.024
9	381	287	0.369	0.132	0.127	0.045
10	442	306	0.002	0.311	0.0006	0.100
11	503	323	0.001	0.355	0.0004	0.108
12	564	338	0.0007	0.237	0.0002	0.069
1	625	355	0.0003	0.229	0.00007	0.064
2	686	206	0.0003	0.067	0.0001	0.032
3	15	166	0.154	0.0003	0.092	0.0002
Sampling 250 s after sequencing action						
4	76	194	0.201	0.0005	0.102	0.0003
5	137	215	0.211	0.0004	0.097	0.0002
6	198	235	0.255	0.0005	0.107	0.0002
7	259	251	0.299	0.0005	0.117	0.0002
8	320	274	0.359	0.123	0.129	0.044
9	381	290	0.188	0.132	0.064	0.045
10	442	307	0.002	0.368	0.0005	0.118
11	503	324	0.001	0.295	0.0004	0.091
12	564	338	0.0005	0.247	0.0002	0.072
1	625	355	0.0001	0.245	0.00004	0.068
2	686	204	0.00005	0.006	0.00002	0.003
3	15	173	0.181	0.0006	0.103	0.0003
Sampling 400 s after sequencing action						
4	76	194	0.211	0.0005	0.108	0.0003
5	137	215	0.221	0.0005	0.101	0.0002
6	198	236	0.288	0.0004	0.120	0.0002
7	259	261	0.292	0.002	0.110	0.0007
8	320	276	0.205	0.123	0.073	0.044
9	381	291	0.005	0.251	0.002	0.085
10	442	307	0.002	0.347	0.0005	0.111
11	503	323	0.0008	0.252	0.0002	0.077
12	564	338	0.0004	0.252	0.0001	0.073
1	625	356	0.0001	0.199	0.00003	0.055
2	686	201	0.00004	0.0006	0.00002	0.0003
3	15	172	0.188	0.0006	0.109	0.0003

Table A.4.18 Concentration Profile Analysis for Run 300 - 425 - 500

Notes: (i) $P_{std} = P_a = 99$ kN m^{-2}

(ii) All gas phase solute concentrations of less than 0.1×10^{-5} g cm^{-3} are given in first significant figure

(iii) Analysis recorded 8.67 hrafter start-up

Column Isolated	Distance of sample point from Product 1 Outlet	P_{col} (at sample point)	$c_{i(col)}$		$c_{i(std)}$	
			AP	GP	AP	GP
	cm	kN m^{-2}	10^{-3} g cm^{-3}	10^{-3} g cm^{-3}	10^{-3} g cm^{-3}	10^{-3} g cm^{-3}
Sampling 150 s after sequencing action						
3	15	181	0.131	0.0005	0.072	0.0003
4	76	208	0.143	0.030	0.068	0.014
5	137	230	0.163	0.038	0.070	0.016
6	198	251	0.205	0.056	0.081	0.022
7	259	275	0.196	0.080	0.071	0.029
8	320	291	0.265	0.130	0.090	0.044
9	381	315	0.204	0.182	0.065	0.058
10	442	333	0.0007	0.429	0.0002	0.127
11	503	349	0.0005	0.320	0.0001	0.091
12	564	365	0.0006	0.311	0.0002	0.084
1	625	380	0.0001	0.307	0.00003	0.080
2	686	206	0.00003	0.036	0.00002	0.017
Sampling 300 s after sequencing action						
3	15	187	0.117	0.025	0.062	0.013
4	76	209	0.154	0.032	0.073	0.015
5	137	232	0.169	0.043	0.072	0.018
6	198	252	0.191	0.060	0.075	0.024
7	259	278	0.220	0.090	0.078	0.032
8	320	293	0.399	0.160	0.135	0.054
9	381	310	0.006	0.248	0.002	0.079
10	442	333	0.0006	0.398	0.0002	0.118
11	503	349	0.0008	0.292	0.0002	0.083
12	564	365	0.0005	0.316	0.0001	0.086
1	625	380	0.0001	0.284	0.0003	0.074
2	686	203	0.00005	0.002	0.00002	0.001
Sampling 450 s after sequencing action						
3	15	187	0.143	0.030	0.075	0.016
4	76	208	0.149	0.035	0.071	0.017
5	137	230	0.188	0.048	0.081	0.020
6	198	253	0.193	0.068	0.076	0.027
7	259	278	0.240	0.107	0.086	0.038
8	320	293	0.344	0.164	0.116	0.055
9	381	311	0.001	0.393	0.0004	0.125
10	442	333	0.0005	0.320	0.0001	0.095
11	503	349	0.0007	0.288	0.0002	0.082
12	564	365	0.0003	0.303	0.00008	0.082
1	625	380	0.00007	0.200	0.00002	0.052
2	686	203	0.00003	0.0002	0.00002	0.0001

Table A.4.19 Concentration Profile Analysis for Run 300 - 205 - 300

Notes: (i) $P_{std} = P_a = 101$ kN m^{-2}

(ii) All gas phase solute concentrations of less than 0.1×10^{-5} g cm^{-3} are given in first significant figure

(iii) Analysis recorded 8.0 hr after start-up

Column Isolated	Distance of sample point from Product 1 Outlet	P_{col} (at sample point)	$c_{i(col)}$		$c_{i(std)}$	
			AP	GP	AP	GP
	cm	kN m^{-2}	10^{-3} g cm^{-3}	10^{-3} g cm^{-3}	10^{-3} g cm^{-3}	10^{-3} g cm^{-3}
Sampling 100 s after sequencing action						
1	625	361	0.414	0.088	0.116	0.025
2	686	233	0.001	0.049	0.0005	0.021
3	15	182	0.127	0.0004	0.071	0.0002
4	76	203	0.252	0.0003	0.128	0.0001
5	137	224	0.312	0.0002	0.141	0.0001
6	198	241	0.356	0.0002	0.149	0.00008
7	259	266	0.420	0.0002	0.160	0.00008
8	320	280	0.554	0.023	0.200	0.008
9	381	288	0.547	0.099	0.187	0.034
10	442	310	0.614	0.124	0.200	0.040
11	503	334	0.581	0.153	0.176	0.046
12	564	347	0.534	0.144	0.156	0.042
Sampling 250 s after sequencing action						
1	625	361	0.040	0.045	0.011	0.013
2	686	232	0.0003	0.001	0.0001	0.0005
3	15	187	0.225	0.0001	0.121	0.00005
4	76	210	0.278	0.0002	0.134	0.0001
5	137	224	0.292	0.0002	0.129	0.00008
6	198	241	0.379	0.0002	0.155	0.0001
7	259	266	0.501	0.0002	0.189	0.00008
8	320	280	0.554	0.076	0.199	0.027
9	381	295	0.514	0.096	0.172	0.032
10	442	310	0.594	0.127	0.189	0.040
11	503	334	0.567	0.152	0.170	0.046
12	564	347	0.467	0.093	0.136	0.027

Table A.4.20 Concentration Profile Analysis for Run 300 - 240 - 350

Notes: (i) $P_{std} = P_a = 101\ kN\ m^{-2}$

(ii) All gas phase solute concentrations of less than 0.1×10^{-5} g cm^{-3} are given in first significant figure

(iii) Analysis recorded 8.5 hrafter start-up

Column Isolated	Distance of sample point from Product 1 Outlet	P_{col} (at sample point)	$c_{i(col)}$		$c_{i(std)}$	
			AP	GP	AP	GP
	cm	kN m^{-2}	10^{-3} g cm^{-3}	10^{-3} g cm^{-3}	10^{-3} g cm^{-3}	10^{-3} g cm^{-3}
Sampling 100 s after sequencing action						
2	686	232	0.0002	0.037	0.00009	0.016
3	15	182	0.173	0.0006	0.096	0.0003
4	76	199	0.258	0.002	0.131	0.0007
5	137	223	0.319	0.0004	0.144	0.0002
6	198	239	0.356	0.0006	0.150	0.0003
7	259	260	0.411	0.0004	0.159	0.0002
8	320	279	0.474	0.035	0.172	0.013
9	381	295	0.407	0.116	0.140	0.040
10	442	311	0.100	0.140	0.032	0.070
11	503	333	0.003	0.231	0.001	0.070
12	564	341	0.002	0.130	0.0007	0.039
1	625	358	0.0009	0.158	0.0003	0.044
Sampling 250 s after sequencing action						
2	686	230	0.00008	0.0005	0.00003	0.0002
3	15	188	0.261	0.0003	0.142	0.0002
4	76	208	0.309	0.0006	0.150	0.0003
5	137	225	0.339	0.0004	0.152	0.0002
6	198	245	0.381	0.0004	0.157	0.0001
7	259	267	0.447	0.0004	0.169	0.0001
8	320	281	0.481	0.114	0.173	0.041
9	381	296	0.280	0.107	0.096	0.037
10	442	316	0.005	0.238	0.001	0.076
11	503	333	0.003	0.136	0.0008	0.041
12	564	345	0.001	0.143	0.0004	0.042
1	625	359	0.0002	0.138	0.00006	0.039

Table A.4.21 Concentration Profile Analysis for Run 300 - 310 - 450

Notes: (i) $P_{std} = P_a = 101$ kN m^{-2}

(ii) All gas phase solute concentrations of less than 0.1×10^{-5} g cm^{-3} are given in first significant figure

(iii) Analysis recorded 6.33 hr after start-up

Column Isolated	Distance of sample point from Product 1 Outlet	P_{col} (at sample point)	$c_{i(col)}$		$c_{i(std)}$	
			AP	GP	AP	GP
	cm	kN m^{-2}	10^{-3} g cm^{-3}	10^{-3} g cm^{-3}	10^{-3} g cm^{-3}	10^{-3} g cm^{-3}
Sampling 200 s after sequencing action						
3	15	187	0.215	0.00006	0.116	0.00003
4	76	208	0.252	0.0007	0.122	0.0003
5	137	226	0.272	0.0006	0.122	0.0003
6	198	241	0.319	0.0006	0.134	0.0003
7	259	266	0.317	0.0005	0.121	0.0002
8	320	281	0.391	0.078	0.141	0.028
9	381	294	0.347	0.128	0.120	0.044
10	442	312	0.002	0.212	0.0007	0.069
11	503	332	0.002	0.385	0.0005	0.118
12	564	346	0.0007	0.229	0.0002	0.067
1	625	359	0.0003	0.247	0.00009	0.070
2	686	204	0.0001	0.009	0.00005	0.004
Sampling 400 s after sequencing action						
3	15	190	0.215	0.0007	0.115	0.0004
4	76	209	0.252	0.0007	0.122	0.0003
5	137	229	0.292	0.0006	0.130	0.0003
6	198	246	0.322	0.0006	0.133	0.0002
7	259	267	0.327	0.0005	0.124	0.0002
8	320	281	0.421	0.137	0.152	0.049
9	381	295	0.047	0.157	0.016	0.054
10	442	316	0.002	0.356	0.0005	0.114
11	503	335	0.001	0.346	0.0003	0.105
12	564	345	0.0006	0.225	0.0002	0.066
1	625	359	0.0002	0.255	0.00005	0.072
2	686	201	0.00008	0.0006	0.00004	0.0003

Table A.4.22 Concentration Profile Analysis for Run 300 - 340 - 500

Notes: (i) $P_{std} = P_a = 99\ kN\ m^{-2}$

(ii) All gas phase solute concentrations of less than 0.1×10^{-5} g cm^{-3} are given in first significant figure

(iii) Analysis recorded 9.0 hrafter start-up

Column Isolated	Distance of sample point from Product 1 Outlet	P_{col} (at sample point)	$c_{i(col)}$		$c_{i(std)}$	
			AP	GP	AP	GP
	cm	kN m^{-2}	10^{-3} g cm^{-3}	10^{-3} g cm^{-3}	10^{-3} g cm^{-3}	10^{-3} g cm^{-3}
Sampling 150 s after sequencing action						
12	564	341	0.0006	0.227	0.0002	0.066
1	625	357	0.0003	0.225	0.00007	0.063
2	686	205	0.00008	0.046	0.00004	0.022
3	15	181	0.201	0.0002	0.110	0.0001
4	76	198	0.211	0.0006	0.106	0.0003
5	137	215	0.258	0.0003	0.118	0.0001
6	198	237	0.287	0.0005	0.121	0.0002
7	259	262	0.298	0.0006	0.113	0.0002
8	320	278	0.402	0.075	0.144	0.027
9	381	293	0.284	0.128	0.096	0.044
10	442	309	0.002	0.181	0.0005	0.058
11	503	327	0.001	0.309	0.0004	0.094
Sampling 300 s after sequencing action						
12	564	337	0.0005	0.229	0.0002	0.068
1	625	349	0.0001	0.234	0.00003	0.067
2	686	206	0.00005	0.005	0.00002	0.003
3	15	185	0.218	0.0005	0.117	0.0003
4	76	204	0.228	0.0007	0.111	0.0004
5	137	224	0.228	0.0006	0.101	0.0003
6	198	244	0.268	0.0005	0.107	0.0002
7	259	264	0.345	0.0005	0.130	0.0002
8	320	279	0.441	0.112	0.157	0.040
9	381	293	0.180	0.107	0.061	0.036
10	442	310	0.002	0.334	0.0005	0.107
11	503	329	0.001	0.278	0.0004	0.084
Sampling 450 s after sequencing action						
12	564	337	0.0004	0.233	0.0001	0.068
1	625	350	0.00007	0.234	0.00002	0.066
2	686	206	0.00005	0.0004	0.00003	0.0002
3	15	186	0.216	0.0007	0.115	0.0004
4	76	208	0.241	0.0006	0.116	0.0003
5	137	223	0.258	0.0006	0.115	0.0002
6	198	244	0.305	0.0006	0.124	0.0003
7	259	265	0.382	0.0005	0.143	0.0002
8	320	279	0.401	0.122	0.142	0.043
9	381	293	0.009	0.216	0.003	0.073
10	442	312	0.0003	0.338	0.0009	0.108
11	503	331	0.0009	0.257	0.0003	0.077

Table A.4.23 Concentration Profile Analysis for Run 300 - 370 - 550

Notes: (i) $P_{std} = P_a = 100$ kN m^{-2}

(ii) All gas phase solute concentrations of less than 0.1×10^{-5} g cm^{-3} are given in first significant figure

(iii) Analysis recorded 6.75 hrafter start-up

Column Isolated	Distance of sample point from Product 1 Outlet	P_{col} (at sample point)	$c_{i(col)}$		$c_{i(std)}$	
			AP	GP	AP	GP
	cm	kN m^{-2}	10^{-3} g cm^{-3}	10^{-3} g cm^{-3}	10^{-3} g cm^{-3}	10^{-3} g cm^{-3}
Sampling 100 s after sequencing action						
1	625	358	0.0002	0.295	0.00006	0.083
2	686	207	0.00005	0.070	0.00002	0.034
3	15	182	0.161	0.0005	0.089	0.0003
4	76	206	0.214	0.009	0.104	0.004
5	137	224	0.204	0.011	0.091	0.005
6	198	241	0.214	0.019	0.089	0.008
7	259	265	0.244	0.041	0.092	0.015
8	320	280	0.287	0.126	0.103	0.045
9	381	294	0.320	0.177	0.109	0.060
10	442	310	0.001	0.393	0.0004	0.127
11	503	332	0.0009	0.362	0.0003	0.109
12	564	344	0.0005	0.301	0.0002	0.088
Sampling 300 s after sequencing action						
1	625	358	0.0001	0.305	0.00004	0.085
2	686	202	0.00005	0.002	0.00003	0.001
3	15	198	0.195	0.003	0.104	0.002
4	76	209	0.187	0.009	0.090	0.004
5	137	226	0.204	0.013	0.100	0.006
6	198	245	0.244	0.023	0.092	0.009
7	259	265	0.244	0.056	0.143	0.021
8	320	281	0.401	0.177	0.059	0.063
9	381	289	0.175	0.154	0.0004	0.052
10	442	312	0.001	0.452	0.0004	0.145
11	503	334	0.0009	0.368	0.0003	0.111
12	564	345	0.0004	0.286	0.0001	0.083
Sampling 500 s after sequencing action						
1	625	358	0.0001	0.234	0.00004	0.065
2	686	202	0.00003	0.0003	0.00002	0.0002
3	15	198	0.208	0.007	0.111	0.004
4	76	209	0.197	0.010	0.095	0.005
5	137	226	0.210	0.016	0.093	0.007
6	198	245	0.267	0.033	0.109	0.013
7	259	266	0.277	0.094	0.104	0.035
8	320	281	0.344	0.178	0.123	0.063
9	381	289	0.003	0.320	0.001	0.108
10	442	312	0.001	0.478	0.0004	0.153
11	503	334	0.0007	0.318	0.0002	0.095
12	564	345	0.0003	0.301	0.00009	0.087

APPENDIX 5

Calculation of Partial Pressure of 'Arklone' P at Maximum Column Concentration

Calculation of the Partial Pressure of 'Arklone' P Corresponding to the Highest Recorded Standardised Concentration During the Study of Solute Feedrate

For an ideal gas

$$P_i = P_{col} \cdot y_i \qquad \text{A5.1}$$

where P_i = partial pressure of component i

Substituting for y from equation 8.4

$$P_i = \frac{P_{col} \cdot c_{i(std)} \cdot R_g \cdot T}{M_i \cdot P_{std}} \qquad \text{A5.2}$$

From Run 500 - 275 - 500 the maximum value of $c_{AP(std)}$ = 0.469×10^{-3} g cm^{-3} (Appendix 4). The corresponding sample point pressure was 296 kN m^{-2} and temperature 22°C.

Hence $$P_i = \frac{296 \times 0.469 \times 10^{-3} \times 0.896 \times 10^4 \times 295}{187.4 \times 102}$$

$$= \underline{18.0 \text{ kN m}^{-2}}$$

From Fig 6.5 the saturated vapour pressure of 'Arklone' P, P°_{AP}, at 22°C = 38.0 kN m^{-2}.

Therefore the gas phase was not saturated by 'Arklone' P.

APPENDIX 6

Listing of Program for the Simulation
of the Sequential Unit

```
C     FORTRAN PLATE TO PLATE SIMULATION OF SCCR 1
      DIMENSION C1(720),C2(720),P(720),X(60),Y(60)
      REAL MWT1,MWT2,MOLVOL
      DO 1 NN=1,720
      C1(NN)=0.0
      C2(NN)=0.0
      P(NN)=0.0
    1 CONTINUE
      DO 2 NN=1,60
      X(NN)=0.0
      Y(NN)=0.0
    2 CONTINUE
      READ(2,3)GFLOW,SFLOW,VG,VL,CFEED1,CFEED2,DT
    3 FORMAT(7F10.0)
      READ(2,4)NFEED,NNCOL,ITOTAL,IIINI,IITYPE,NNTYPE
    4 FORMAT(6I4)
      READ(2,5)PAMB,PING,POUTG,PINS,POUTS
    5 FORMAT(5F10.0)
      READ(2,6)A01,A11,A21,A31
    6 FORMAT(4E13.6)
      READ(2,15)A02,A12,A22,A32
   15 FORMAT(4E13.6)
      READ(2,14)MWT1,MWT2,MOLVOL,TAMB
   14 FORMAT(4F10.0)
      WRITE(1,7)GFLOW,SFLOW,VG,VL
    7 FORMAT(1H ,7HGFLOW= F8.3,4X,7HSFLOW= F8.3,4X,4HVG= F10.5,
     14X,4HVL= F10.5)
      WRITE(1,8)CFEED1,CFEED2,DT
    8 FORMAT(1H ,8HCFEED1= E13.6,4X,8HCFEED2= E13.6,4X,
     14HDT= F10.5)
      WRITE(1,9)NFEED,NNCOL,ITOTAL,IIINI,IITYPE,NNTYPE
    9 FORMAT(1H ,7HNFEED= I2,1X,7HNNCOL= I3,1X,8HITOTAL= I3,
     11X,7HIIINI= I4,1X,8HIITYPE= I3,1X,8HNNTYPE= I3)
      WRITE(1,10)PAMB,PING,POUTG,PINS,POUTS
   10 FORMAT(1H ,6HPAMB= F6.1,1X,6HPING= F6.1,1X,7HPOUTG= F6.1,
     11X,6HPINS= F6.1,1X,7HPOUTS= F6.1)
      WRITE(1,11)A01,A02
   11 FORMAT(1H ,5HA01= E13.6,10X,5HA02= E13.6)
      WRITE(1,16)A11,A12
   16 FORMAT(1H ,5HA11= E13.6,10X,5HA12= E13.6)
      WRITE(1,17)A21,A22
   17 FORMAT(1H ,5HA21= E13.6,10X,5HA22= E13.6)
      WRITE(1,18)A31,A32
   18 FORMAT(1H ,5HA31= E13.6,10X,5HA32= E13.6)
      WRITE(1,19)MWT1,MWT2,MOLVOL,TAMB
   19 FORMAT(1H ,6HMWT1= F6.2,2X,6HMWT2= F6.2,2X,8HMOLVOL= F6.0,
     12X,6HTAMB= F5.1)
      MOLVOL=MOLVOL*(TAMB/273.)*(100.3/PAMB)
      NNTOT=NNCOL*12
      NNELEV=NNCOL*11+1
      NNFEED=(NFEED-1)*NNCOL+NNCOL/2+1
      NNCOL1=NNCOL+1
      DO 20 NN=NNCOL1,NNTOT
      P(NN)=(PING-(((PING-POUTG)/FLOAT(NNCOL*11))
     1*(FLOAT(NN-NNCOL)-0.5)))/PAMB
   20 CONTINUE
      DO 30 NN=1,NNCOL
```

```
      P(NN)=(PINS-(((PINS-POUTS)/FLOAT(NNBED))*
     1(FLOAT(NN)-0.5)))/PAMB
   30 CONTINUE
      WRITE(1,12)
   12 FORMAT(1H ,2H I,5X,5H  II ,5X,3H N ,5X,5H  NN ,5X,
     1 14H      C1(NN)    ,5X,14H     C2(NN)     )
      IISUM=1
      DO 100 I=1,ITOTAL
      ISTII=IIINI*(I-1)+1
      LSTII=IIINI*I
      DO 200 II=ISTII,LSTII
      NNSUM=1
      DO 300 N=1,12
      IF(N.LE.(NFEED-I))GO TO 500
      NNFST=NNCOL*(N-1)+1
      NNLST=NNCOL*N
      DO 400 NN=NNFST,NNLST
      IF(N.EQ.1)GO TO 70
      IF((N.EQ.2).AND.(NN.EQ.NNFST))GO TO 40
      IF(NN.EQ.NNFEED)GO TO 50
      IF(C1(NN-1).LT.0.1E-10)C1(NN-1)=0.0
      IF(C2(NN-1).LT.0.0E-10)C2(NN-1)=0.0
      CSTAN1=C1(NN-1)
      CSTAN2=C2(NN-1)
      CINP1=C1(NN-1)
      CINP2=C2(NN-1)
      GO TO 60
   40 CINP1=0.0
      CINP2=0.0
      CSTAN1=C1(NN)
      CSTAN2=C2(NN)
      GO TO 60
   50 CINP1=CFEED1+C1(NN-1)
      CINP2=CFEED2+C2(NN-1)
      CSTAN1=CINP1
      CSTAN2=CINP2
   60 CCOL1=CSTAN1*P(NN)
      CCOL2=CSTAN2*P(NN)
      GFLOWC=GFLOW*(1.+MOLVOL*(CSTAN1/MWT1+CSTAN2/MWT2))
      A=GFLOWC*DT/P(NN)
      AA=EXP(-A/((VG/P(NN))+VL*(((A31*CCOL1+A21)*CCOL1+A11)*
     1CCOL1+A01)))
      BB=EXP(-A/((VG/P(NN))+VL*(((A32*CCOL2+A22)*CCOL2+A21)*
     1CCOL2+A02)))
      C1(NN)=(1.-AA)*CINP1+AA*C1(NN)
      C2(NN)=(1.-BB)*CINP2+BB*C2(NN)
      GO TO 150
   70 IF(NN.EQ.NNFST)GO TO 80
      IF(C1(NN-1).LT.0.1E-10)C1(NN-1)=0.0
      IF(C2(NN-1).LT.0.1E-10)C2(NN-1)=0.0
      CSTAN1=C1(NN-1)
      CSTAN2=C2(NN-1)
      CINP1=C1(NN-1)
      CINP2=C2(NN-1)
      GO TO 90
   80 CINP1=0.0
      CINP2=0.0
```

```
      CSTAN1=C1(NN)
      CSTAN2=C2(NN)
   90 CCOL1=CSTAN1*P(NN)
      CCOL2=CSTAN2*P(NN)
      SFLOWC=SFLOW*(1.+MOLVOL*(CSTAN1/MWT1+CSTAN2/MWT2))
      A=SFLOWC*DT/P(NN)
      AA=EXP(-A/((VG/P(NN))+VL*(((A31*CCOL1+A21)*CCOL1+A11)*
     1CCOL1+A01)))
      BB=EXP(-A/((VG/P(NN))+VL*(((A32*CCOL2+A22)*CCOL2+A12)*
     1CCOL2+A02)))
      C1(NN)=(1.-AA)*CINP1+AA*C1(NN)
      C2(NN)=(1.-BB)*CINP2+BB*C2(NN)
  150 IF((NN.EQ.(NNTYPE*NNSUM)).AND.(II.EQ.(IITYPE*IISUM)))
     1GO TO 160
      GO TO 170
  160 WRITE(1,161)I,II,N,NN,C1(NN),C2(NN)
  161 FORMAT(1H ,I2,5X,I5,5X,I3,5X,I5,5X,E14.6,5X,E14.6)
  170 IF(NN.EQ.(NNTYPE*NNSUM))NNSUM=NNSUM+1
  400 CONTINUE
      GO TO 300
  500 NNSUM=NNSUM+NNCOL/NNTYPE
  300 CONTINUE
      IF(II.EQ.(IITYPE*IISUM))GO TO 180
      GO TO 200
  180 IISUM=IISUM+1
      WRITE(1,185)
  185 FORMAT(1H ,32HNEXT TIME INTERVAL FOR PRINT OUT)
  200 CONTINUE
      WRITE(1,190)
  190 FORMAT(1H ,24HNEXT SEQUENCING INTERVAL)
      WRITE(1,195)
  195 FORMAT(1H ,2H I,5X,5H  HI ,5X,3H N ,5X,5H  NN ,
     114H      C1(NN)    ,5X,14H     C2(NN)     )
      DO 1500 NN=1,NNCOL
      X(NN)=C1(NN)
      Y(NN)=C2(NN)
 1500 CONTINUE
      DO 2000 NN=1,NNTOT
      IF(NN.GE.NNELEV)GO TO 2010
      NNADJ=NN+NNCOL
      C1(NN)=C1(NNADJ)
      C2(NN)=C2(NNADJ)
      GO TO 2000
 2010 NNADJ=NN+1-NNELEV
      C1(NN)=X(NNADJ)
      C2(NN)=Y(NNADJ)
 2000 CONTINUE
  100 CONTINUE
      END
  $0   0
END OF JOB
```

Supporting Publication

Published in Analytical Chemistry, 45, 1121 (1973)

and "Advances in Chromatography 1973", A. Zlatkis, Ed., "Proceedings of the 8th International Symp., Toronto, Canada", published by Chromatography Conference, Chem. Dept., Univ. of Houston, 1973, p33.

Production Scale Organic Mixture Separation Using a New Sequential Chromatographic Machine

P. E. Barker and R. E. Deeble

Chemical Engineering Department, University of Aston in Birmingham, England

A new twelve-column, 7.6-cm diameter production scale sequential chromatographic separator is described which is suitable for the separation of a wide range of organic mixtures. The mode of operation of the separator has been demonstrated by the separation of a binary halocarbon mixture into product purities in excess of 99.9% at liquid feed rates up to 500 ml/hr. The average chromatographic efficiency measured in terms of HETP of the 12 packed columns varied from 10.7 to 14.3 mm as liquid feed rates increased from 300 to 600 ml/hr. Lower HETP values and higher throughputs are anticipated by using improved packing techniques and different operating conditions.

Harnessing the high resolving power of analytical chromatography for a chemical separation process at commercially viable throughputs has provided a challenge to research workers. From an appreciation of the principle of chromatography, it can be seen why development work has concentrated on three modes of operation. These operating methods are characterized by the three principal ways mobile and solvent phases may be moved relative to each other; co-currently, cross-currently, and counter-currently.

The most direct approach to scale-up is to increase the size of the analytical column in diameter and/or length (*1*). Provided separating efficiency can be maintained at a reasonable level, resolution of the injected feed mixture into its multiple constituents is theoretically possible. Research and development work has concentrated on column design and packing techniques, so now acceptably low HETP's can be achieved (*2*).

The largest operational co-current type of equipment reported in the literature is a 1.2-m diameter liquid chromatography system having a production capacity of 0.9 million kg/year, which is installed in a pharmaceutical plant (*3*). However, in the same paper, some design and costing details are given for the separation of *m*-xylene and *p*-xylene at a combined production rate of 45 million kg/year. As a gas–liquid chromatographic system, a 4.3-m diameter column was proposed.

The cross-flow mode of operation appears very attractive. Theoretically, the movement of mobile and solvent phase at right angles to one another should enable the attainment of a continuous "spectrum" of products as a consequence of the differing resultant component velocities. Attempts to achieve this theoretical concept in practice have resulted in several novel designs although development work has tended to be carried out on a comparatively small scale (*4, 5*). The system proposed by Dinelli *et al.* (*6–8*), in which carrier fluid flows down laterally rotated columns, suffers from two major limitations when considering further scale-up. For efficient separation, the requirement of very well matched columns and of a reliable mechanical seal cannot easily be met.

The continuous fractionation of a feed mixture into two components or into two mixtures of different composition, can be achieved by a counter-current movement, within definable limits, of the mobile and solvent phases. The solute(s) with least affinity for the solvent will be carried to the mobile phase outlet while the solute(s) more strongly absorbed onto the solvent will move preferentially in the direction of the solvent. The attraction of the application of counter-current chromatography at the production scale is the prospect of higher throughputs for a given column dimension. The feed is continuous, utilizing all of the available separating power of the column. Further, within the column, the two fractions need only be partially resolved to permit collection of resolved products at the column exits, a feature which permits severe overloading by conventional chromatographic standards.

Development work by Barker *et al.* (*4*) at the 2.5-cm column diameter level has resulted in the construction of a compact pseudo-continuous system in which the solvent loaded support is held stationary in a moving column, the column itself being rotated past fixed inlet and outlet ports. The principle of operation is shown in Figure 1*a*.

In moving to larger column diameters it is evident that physical movement of the column would provide a substantial mechanical problem, not least in the provision of large moving face seals necessary for the above system. A new approach based on proved valves has, therefore, been pursued by the authors to facilitate scale-up of the counter-current chromatographic separation process.

Principle of Operation of the New Sequential Machine. From Figure 1*b* it can be seen that the counter-current movement of mobile and solvent phase can be simulated by the movement of the ports, co-current to the mobile phase, past a fixed column. Further, observations from previous systems suggested the desirability of a separate fluid stream for the purging of the more strongly sorbed component(s). Two main advantages result. The purging fluid rate can be increased to such a level as to ensure the complete removal of product from the isolated section without increasing pressure in the separating section. Also the mobile fluid entering the main separating section is not contaminated with product 2.

A research prototype embracing the system indicated by Figure 1*b* has been constructed at the 7.6-cm (3-in)

(1) R. E. Pecsar, "Preparative Gas Chromatography," A. Zlatkis and V. Pretorius, Ed., Wiley-Interscience, London, 1971, Chap. 3, p 73.
(2) (a) J. Albrecht and M. Verzele, *J. Chromatogr. Sci.*, **8**, 586 (1970); (b) *ibid.*, **9**, 745 (1971).
(3) R. S. Timmins, L. Mir, and J. M. Ryan, *Chem. Eng. (New York)*, **76** (10), 170 (1969).
(4) P. E. Barker, "Preparative Gas Chromatography," A. Zlatkis and V. Pretorius, Ed., Wiley-Interscience, London, 1971, Chap. 10, p 325.
(5) E. J. Tuthill, *J. Chromatogr. Sci.*, **8**, 285 (1970).
(6) D. Dinelli, S. Polezzo, and M. Taramasso, *J. Chromatogr.*, **7**, 447 (1962).
(7) D. Dinelli, M. Taramasso, and S. Polezzo, U.S. Patent 3,187,486 (1965).
(8) M. Taramasso and D. Dinelli, *J. Gas Chromatogr.*, **2**, 150 (1964).

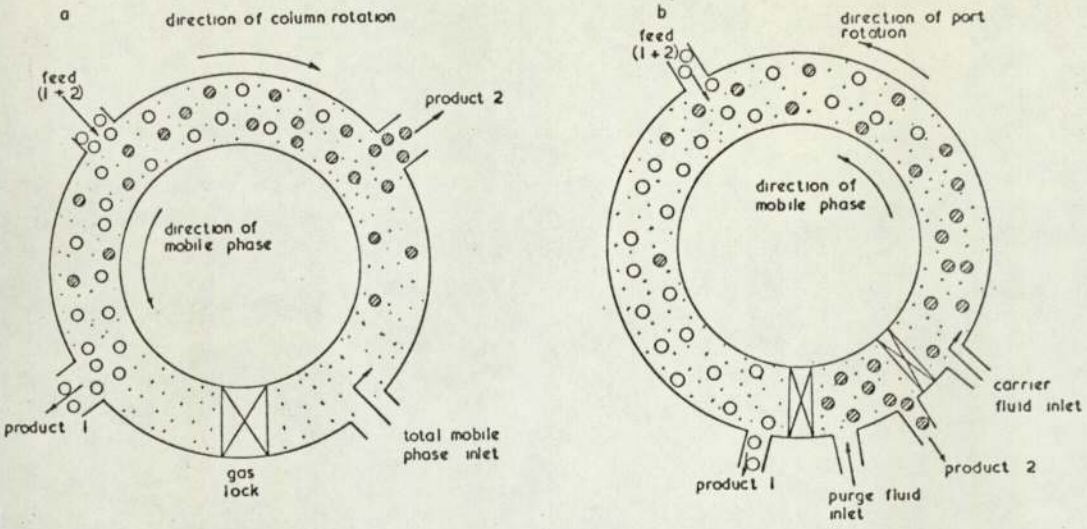

Figure 1. Diagrammatic representation of the principle of the counter-current chromatographic system

(*a*) Moving column past fixed ports, (*b*) moving ports past fixed column

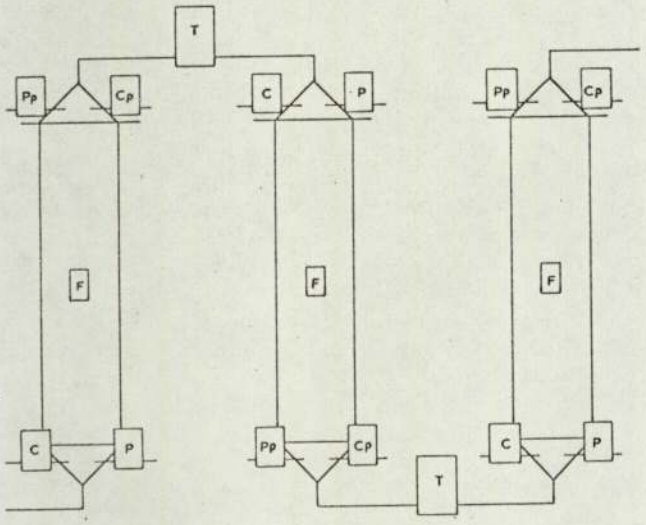

Figure 2. Schematic diagram of three columns showing relative position of solenoid valves

T = Transfer valve, F = feed valve, C = carrier fluid inlet valve, P = purge fluid inlet valve, Cp = carrier product outlet valve, Pp = purge product outlet valve

column diameter level. The form of chromatography chosen was gas–liquid.

EXPERIMENTAL

Design of the Unit (*9*). From Figure 1*b*, it can be seen that seven moving functions are required; feed inlet, carrier gas inlet and outlet, purge gas inlet and outlet, and two gas locks. The unit was therefore designed in discrete sections, *each* section being provided with the necessary functions by solenoid operated valves. Such a design enables the dimensions and materials of construction of the individual columns forming each stage to be variable over wide limits. However, the unit can no longer be termed "continuous."

Twelve 7.6-cm diameter copper columns of packed length 61-cm are linked alternatively at top and bottom to form a closed symmetrical ring (see Figure 2). On each "transfer" line between the columns is situated a "modified" 13-mm orifice, normally open, servo-acting solenoid valve (T).

Energizing a consecutive pair of these solenoids effectively isolates an individual column. The gas inlet and outlet ports, situated on the end cones of each column, are provided by four 6-mm orifice, normally closed, direct acting solenoid valves (C, C_p, P, P_p). A similar valve, but of 3-mm orifice, provides the inlet port for liquid feed (F). The 12 ports of each *type* are connected to an independent, centrally situated, distributor system. Lines from the gas distributors then pass to the relevant control and measuring devices while the feed distributor is connected to a positive displacement pump.

All valves are of brass bodies with Viton seats. It should be noted that careful selection of the direct operating valves was necessary as they must remain tightly closed when operating against a considerable back pressure.

The inlet and outlet solenoid valves are electrically connected, in the required combinations of 5, to 12 terminals. An additional rail of 12 terminals is provided for the transfer valves. The two terminal rails are interconnected, through a relay bank, such that when one terminal on the inlet/outlet valve rail is energized, then two terminals on the transfer valve rail are also energized. Each of these terminal combinations is energized in turn, for a selectable time interval of between 1 and 15 min, by an automatic electronic timing unit.

Assigning the numbers 1 to 12 to the individual columns; at a particular point in the cycle bed 2 would be isolated by energizing the solenoids on the transfer lines 1/2 and 2/3. The purge gas inlet and outlet solenoids on bed 2 are energized to open, effecting purging of the more strongly absorbed component. The carrier gas inlet solenoid on bed 3 is energized to open, carrier gas thus passing through 11 beds to exit from bed 1 as product 1, where the carrier gas outlet solenoid is energized. Feed is pumped into an appropriate bed lying between 3 and 1, say 8, through the energized centrally positioned valve. Within the column the feed is split into fourths by a simple cross distributor to assist even cross-sectional loading.

On sequencing, column 3 is isolated by energizing the solenoids on transfer lines 2/3 and 3/4. Purge gas now enters column 3 to purge product 2. Carrier flows from bed 4 round the unit to exit from the regenerated bed 2. Feed is now entering bed 9. Twelve sequences complete the cycle which then resumes.

The exact format of the switching arrangement for the solenoid valves is varied by rearranging the wiring to the 12 contact points on the timing unit. Hence, the feed point relative to carrier gas inlet can be easily repositioned as can the number of beds isolated for stripping.

The overall flow diagram of the system is given in Figure 3. As no carrier gas recycle system has been constructed, economics dictated the use of air. High pressure air (80 psig) passes through an initial filtering and drying stage followed by regulation to a lower pressure. Final clean-up and drying is achieved by passing through an interchangeable bed of silica gel 10 cm in diameter and 90 cm long. Total air inlet flow rate is monitored by a rotameter before being split into the respective carrier and purge streams. The inlet rotameter provides a means of checking for leaks. Accurate pressure control of the respective streams is established before the gas streams enter the separation unit. The flow rates of the outlet gas streams are regulated before being

(9) P. E. Barker and R. E. Deeble, Br. Patent Appl. 27786/72.

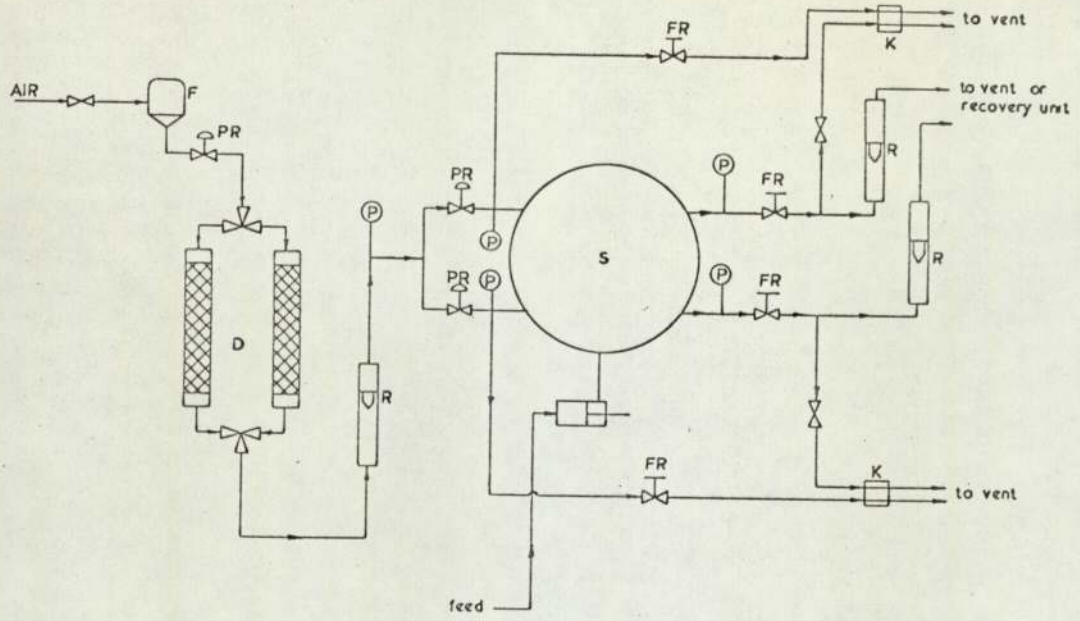

Figure 3. Line flow diagram for complete system (no detail of sequential unit is shown)

R = rotameter, P = pressure gauge, S = sequential unit, D = silica gel driers, PR = pressure regulator, FR = flow regulator, F = air filter, K = katharometer

measured by rotameters. As this is a research unit, no product recovery system has been constructed.

Continuous monitoring of the respective output profiles by a katharometer has been incorporated. A variable throughput positive displacement pump is used to control the liquid feed rate, the lines between the pump head and feed solenoids being maintained full throughout an experimental run. At least four gas sampling points are positioned on each column as well as one on the respective product lines. Quantitative analysis is performed on a Perkin Elmer F11 gas chromatograph in conjunction with a Kent Chromalog integrator.

Selection of a Chemical System for Separation Purposes. The chemical systems available for study on this prototype equipment are restricted by three factors: the use of air as a carrier, the lack of heating facilities, and the materials of construction of the equipment. Such halocarbons as 1,1,1,-trichloroethane (I.C.I. Ltd., Genklene P), 1,1,2,-trichloro-1,2,2,-trifluoroethane (I.C.I. Ltd., Arklone P), and methylene chloride on the phase silicone fluid D.C. 200/50 (Dow Corning) provide a combination of chemical mixtures of varying separation difficulty. The criteria of high volatility, noninflammability, comparatively low toxicity, and availability in bulk are met by these chemicals. For the initial work the mixture Arklone P and Genklene P was chosen, giving a separation factor of 2.9 at 21 °C.

The solid support selected was Chromosorb P, having a sieve range of 500–355 μ (30–44 B.S. mesh). A 25% loading on a total weight basis of the silicone fluid phase was applied to the packing. This approaches the highest loading which the support can hold without losing its "dry" properties, a high loading being consistent with the primary objective of throughput.

RESULTS AND DISCUSSION

Comparison of the Efficiency of the Packed Columns. Care was taken to approximately match the columns when packing. A combination of vigorous beating, tamping down with a heavy 30° cone (*10*), and the application of gas pressure was used to tightly pack each column.

To compare the chromatographic efficiency of the columns, HETP measurements were performed. Each column was isolated in turn and a constant inlet gas pressure applied. The outlet volumetric flowrate was also held constant. Thus any variation in column flow resistance resulted in a variation in the outlet pressure. While this did not ensure a constant gas velocity through the column, it was a more realistic comparison in terms of the subsequent operation of the unit in the separating mode. The injected sample was 1.0 ml of Arklone P injected directly into the inflowing gas stream. As such a technique results in an approximately exponential injection profile, the profile was monitored by a katharometer. Switching the katharometer to the column outlet stream enabled monitoring of the elution profile. The flow rate for the comparison study was, therefore, selected to permit complete recording of both traces for a common injection. A constant bleed flow to the katharometer was maintained by a flow regulator. The mean and variances of both the inlet and outlet profiles, which include a common contribution due to extracolumn dead volume, were computed by a simple program from the recorded details of trace height *vs.* time. Subtraction of these respective parameters gave the required retention time and variance attributable to the column (*11*) to enable the computation of HETP. In addi-

Table I. Comparison of Individual Column Properties[a]

Assigned column No.	Pressure drop across column, cm	Weight of packing, g	Dead volume, cm^3	Packed volume, cm^3	Velocity of carrier, cm/sec	HETP, mm
1	5.0	1635	1915	867	8.6	4.9
2	5.2	1650	2007	774	8.2	8.4
3	4.4	1650	1977	804	8.4	9.5
4	4.6	1635	1820	962	9.1	5.1
5	5.0	1650	1861	921	8.9	7.2
6	5.5	1635	1893	890	8.8	7.0
7	5.7	1650	1862	920	8.9	7.2
8	5.0	1650	1896	886	8.8	5.9
9	5.2	1650	2017	765	8.2	10.0
10	5.3	1635	1826	955	8.9	4.6
11	6.4	1650	2014	767	8.3	8.8
12	4.9	1650	1900	881	8.7	9.5

[a] Inlet pressure = 174.3 cm. Volumetric flow rate at column outlet = 610 cm^3/sec (760 mm, 20 °C).

(10) K.-P. Hupe, U. Busch, and K. Winde, *J. Chromatogr. Sci.*, **7**, 1 (1969).

(11) J. C. Sternberg in "Advances in Chromatography," Vol. 6, J. C. Giddings and R. A. Keller, Ed., Edward Arnold Ltd., London, 1968, Chap. 6, p 205.

Table II. Flow Settings for Separation Runs

Feed rate, ml/hr	Lab temp, °C	Partition coefficient: Arklone P	Partition coefficient: Genklene P	Average carrier gas flow rate at mean column conditions, l./min	Cycle time, min	"Apparent" liquid l./min	G/L	Average purge gas flow rate at mean column conditions, l./min	Purge gas / carrier gas
300	21	133	385	17.5	80	0.064	276	44.4	2.5
500	21	133	385	17.5	80	0.064	276	53.8	3.1
600	21	133	385	17.7	80	0.064	281	68.0	3.8

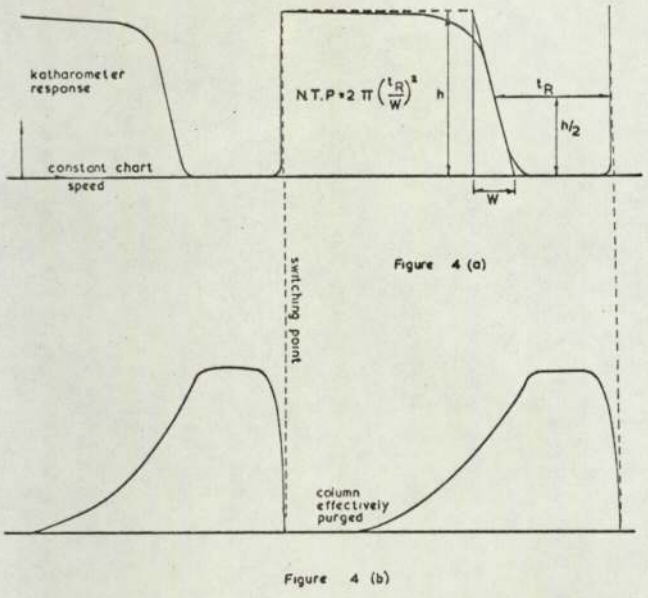

Figure 4 (a)

Figure 4 (b)

Figure 4. Form of product outlet profiles

(*a*) Carrier outlet (product 1), (*b*) purge outlet (product 2)

tion column dead volume and, hence, interparticle gas velocity were determined from the measurement of the retention time of a hydrogen sample.

From the results in Table I, the variation from column to column appears prohibitive to successful operation. However, it will be realized that 11 columns are linked to form the separating section. Thus, in sequencing through the cycle, the variation in the total number of plates in the separating section at any time is comparatively small. Further, as the unit is to be operated at high solute concentration, it is to be expected that in operation the column to column variation will diminish. Experimental observations substantiate both these points.

The computed values of the plate heights are high. This is in part attributable to the short length of column over which the measurements were made, coupled with a severe tailing contribution resulting from the substantial dead volume of the unpacked cones at the column ends. A reduction in HETP could be attained by an improved packing technique such as the shake, turn, and pressure method proposed by Albrecht and Verzele (2), coupled with packing of the cones with a suitable inert material (*12*).

Operation of the Sequential Unit in the Separation Mode. Details of three separation runs are given here. An equivolume mixture of Arklone P and Genklene P was the feedstock. The range of throughputs covered was 300–600 ml/hr. Selection of the gas flow rate through the separating section and the sequencing rate (apparent countercurrent liquid rate) was based on the simple theory outlined by Barker and Lloyd (*13*) for a truly continuous counter-current system. The partition coefficients used to estimate this gas-to-liquid ratio (G/L) were determined at the analytical level, no correction being made for finite concentrations. Table II gives details of the flow settings.

While the conditions for the separating section were held approximately constant throughout the experimental runs, it was necessary to increase the purge gas rate as feed rate and, hence, column concentration increased to ensure complete purging. This was taken as clear evidence of a nonlinear isotherm, the retention time of Genklene P increasing substantially with increasing concentration at the operating temperature (20–22 °C). Unpublished work performed in this department substantiates this observation.

The product output concentration profiles were continuously monitored by a katharometer on both product streams. These fulfilled a dual purpose. The build-up to a pseudo-steady state, necessary for the total system concentration profile analysis, as well as any variation in column-to-column product output profile shape could be observed.

The output profiles are akin to the leading (product 1) and tailing edged (product 2) of a frontal elution system in conventional chromatography (see Figure 4). An estimate of HETP was made from the carrier product profiles by the graphical technique proposed by Reilley *et al.* (*14*). The HETP values calculated and shown in Table III can only serve to indicate an order of the magnitude as the assumptions made in the techniques theoretical development are very tenuous when applied to the levels of concentration occurring in this unit. However, two clear trends are indicated by the results. They are the greater equivalence of the columns and a gradual decrease in the average value of plate height as the solvent concentration increases.

On the establishment of a reproducibly shaped outlet katharometer profile, the system concentration profile was

Table III. Comparison of HETP's Graphically Determined from Product 1 Output Profiles at Three Feed Rates

Product 1 exiting from column	HETP, mm: 300 ml/hr	500 ml/hr	600 ml/hr
1	8.4	10.9	14.2
2	10.9	11.7	12.4
3	13.7	16.9	17.9
4	13.7	13.6	15.3
5	9.1	11.1	16.5
6	11.1	11.3	13.0
7	9.4	11.7	13.3
8	9.4	10.0	12.4
9	12.0	13.6	14.9
10	10.2	12.0	12.4
11	12.0	15.3	16.5
12	11.5	12.2	13.0
Av	10.7	12.5	14.3

(12) W. M. Musser and R. E. Sparks, *J. Chromatogr. Sci.*, 9, 116 (1971).

(13) P. E. Barker and D. I. Lloyd, *J. Inst. Petrol., London*, 49, 73 (1963).

(14) C. N. Reilley, G. P. Hildebrand, and J. W. Ashley, *Anal. Chem.*, 34, 1198 (1968).

ascertained by quantitative analysis on the standard analytical chromatograph of samples taken from a fixed point in the unit during a complete sequencing cycle, two samples being taken at constant times within a switching interval. The calibration curve for the flame ionization detector was obtained from noted peak height and peak area responses to known concentration injections of a range of volumes of both Arklone P and Genklene P. The responses were analyzed to determine the linear range of the detector under the particular operating conditions. Within this range, a least squares fit was performed on the peak area *vs.* sample size data. The pressure at the time and point of sampling from the unit was also noted, utilizing a pressure gauge connected to a hypodermic needle. A plot of concentration against time in the cycle, for all but the two columns from which product is issuing, gives a profile which is equivalent to the concentration profile around the unit measured at a fixed point in time.

A limitation of the technique is that its accuracy only affords an order of magnitude estimate for the minor peak in the analysis of a near pure sample. Purities are quoted here strictly as a measured ratio of Arklone P to Genklene P.

The three concentration profiles from the separation runs reported here clearly show the effect of increasing concentration, Figure 5, *a–c*. Feeding at a rate of 300 ml/hr, this comparatively easy separation has been largely achieved within two columns. The remaining columns serve to marginally increase product purity of both products to a level in excess of 99.9%. The maximum concentration of Genklene occurs close to the feed point.

As the feed rate and, hence, concentration increases, both solutes increase their tendency toward the purge product exit, an observation consistant with the concentration isotherm. At 500 ml/hr, the Arklone P profile stretches into the fourth column following the feed point, the maximum Genklene P concentration also occurring in that column. While product 1 is still in excess of 99.9% Arklone P, product 2 is now at best 99.8% Genklene P.

Increasing the feed rate by a further 100 ml/hr results in a severe reduction in purity of the purged product, the Arklone P profile stretching the entire length of the separating section. The maximum feed rate in accordance with a good separation has been exceeded. However, this does not represent the maximum attainable throughput for the system. Moving the feed point closer to the carrier product offtake, together with an increase in the carrier gas flow rate, should permit throughputs approaching 1 l./hr.

CONCLUSION

The initial work clearly demonstrates the potential of the sequential valve process for production scale gas or liquid chromatographic separations. The mechanical reliability of the system is proved by virtually trouble-free research operation over the past year. Development work in column design and packing techniques can easily be incorporated, while a general increase in individual column size requires no increased complexity.

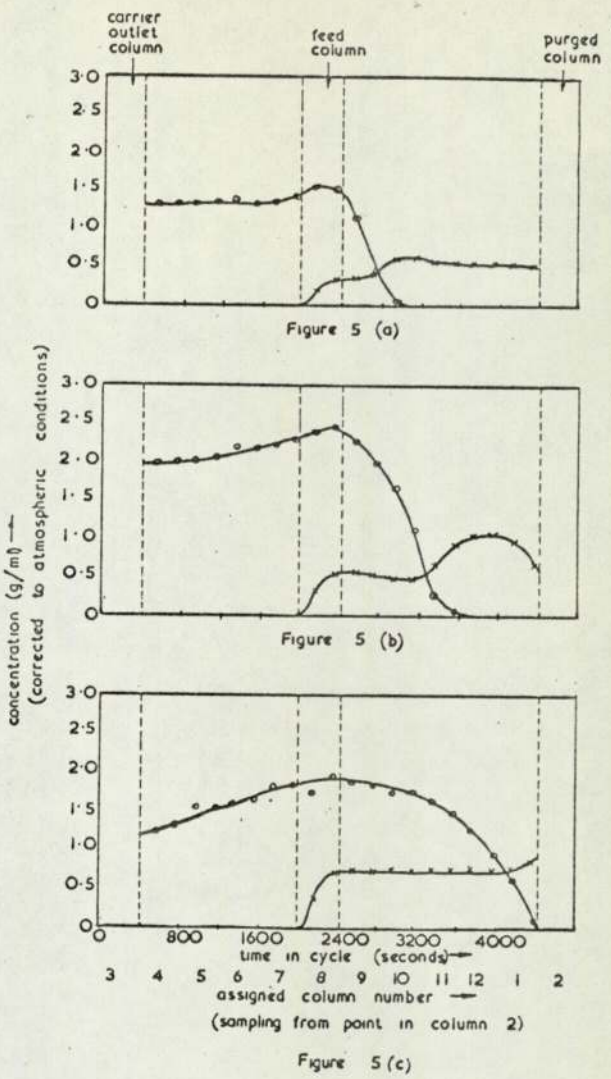

Figure 5. Concentration profiles around unit for three feed rates

(*a*) Feed rate = 300 ml/hr, O Arklone P × Genklene P, approximate time to steady state = 2 hr, time to start of analysis = 11 hr, carrier product > 99.9% Arklone P, purge product > 99.9% Genklene P.
(*b*) Feedrate = 500 ml/hr, O Arklone P × Genklene P, approximate time to steady state = 3.5 hr, time to start of analysis = 6.5 hr, carrier product > 99.9% Arklone P, purge product > 99.8% Genklene P.
(*c*) Feed rate = 600 ml/hr, O Arklone P × Genklene P, approximate time to steady state = 5.5 hr, time to start of analysis = 7.5, carrier product > 99.5% Arklone P, purge product-purity lost

Further work should give a better insight into the operating characteristics of the unit. In particular the effect of gas and "apparent" liquid rates on the throughput needs closer study.

Received for review November 22, 1972. Accepted February 5, 1973.